Mechanisms of Channel Arrest and Spike Arrest underlying metabolic depression and the remarkable anoxia-tolerance of the freshwater painted turtle (*Chrysemys picta bellii*)

by

Matthew Edward Malin Pamenter

A thesis submitted in conformity with the requirements

for the degree of Doctor of Philosophy

Graduate Department of Zoology

University of Toronto

Your file Votre référence
ISBN: 978-0-494-58067-7
Our file Notre référence
ISBN: 978-0-494-58067-7

Mechanisms of Channel Arrest and Spike Arrest underlying metabolic depression and the remarkable anoxia-tolerance of the freshwater painted turtle (*Chrysemys picta bellii*)

Doctor of Philosophy (2008). Matthew Edward Malin Pamenter

Department of Zoology, University of Toronto.

Abstract

Anoxia is an environmental stress that few air-breathing vertebrates can tolerate for more than a few minutes before extensive neurodegeneration occurs. Some facultative anaerobes, including the freshwater western painted turtle *Chrysemys picta bellii,* are able to coordinately reduce ATP demand to match reduced ATP availability during anoxia, and thus tolerate prolonged insults without apparent detriment. To reduce metabolic rate, turtle neurons undergo channel arrest and spike arrest to decrease membrane ion permeability and neuronal electrical excitability, respectively. However, although these adaptations have been documented in turtle brain, the mechanisms underlying channel and spike arrest are poorly understood. The aim of my research was to elucidate the cellular mechanisms that underlie channel and spike arrest and the neuroprotection they confer on the anoxic turtle brain. Using electrophysiological and fluorescent imaging techniques, I demonstrate for the first time that: 1) the α-amino-3-hydroxy-5-methyl-4-isoxazole propionic acid receptor undergoes anoxia-mediated channel arrest; 2) delta opioid receptors (DORs), and 3) mild mitochondrial uncoupling via mitochondrial ATP-sensitive K^+ channel opening result in an increase in cytosolic calcium concentration and subsequent channel arrest of the N-methyl-D-aspartate receptor, preventing excitotoxic calcium entry, and 4) reducing nitric oxide production; 5) the cellular concentration of reactive oxygen species (ROS) decreases with anoxia and ROS bursts do not occur during reoxygenation; and 6) spike arrest occurs in the anoxic turtle cortex, and that this is regulated by increased neuronal conductance to chloride and potassium ions due to activation of γ–amino-butyric acid receptors ($GABA_A$ and $GABA_B$ respectively), which create an inhibitory electrical shunt to dampen neuronal excitation during anoxia. These mechanisms are individually critical since blockade of DORs or GABA receptors induce excitotoxic cell death in anoxic turtle neurons. Together, spike and channel arrest significantly reduce neuronal excitability and individually provide key contributions to the turtle's long-term neuronal survival during anoxia. Since this turtle is the most anoxia-tolerant air-breathing vertebrate identified, these results suggest that multiple mechanisms of metabolic suppression acting in concert are essential to maximizing anoxia-tolerance.

Acknowledgements

Although this dissertation is an individual work, I could never have accomplished my goals or had so much fun along the way without the help/hindrance of many very wonderful people. First and foremost I must thank Dr. Les Buck, who has been both a supervisor and mentor for the past 5 years. I came into the lab with a general interest in neuroscience and he gave me the freedom and resources to carve my own path into the world of physiological research. Over the years we have engaged in many hearty debates (with or without the aide of pitchers of beer) on topics ranging from the cutting edge of comparative science to the most mundane of local political events or the vagaries of departmental red tape. He has dedicated his time to beating the artistic prose out of my writing style (when he could be cornered into actually getting some editing done) but otherwise generally let me follow my nose in my experimentation. I hope he agrees that this approach has paid off and that our time together has been very successful! For my part I am proud of what we have accomplished and I'm happy to say that I have achieved and surpassed the goals I set out for myself upon entering his lab.

Dr. Damian Shin taught me the terrible beauty of electrophysiology and the dangers of letting Les come near an experiment in progress, and I have tried to repay him by vastly increasing his volume of publications! Dame was a fast friend in the lab and I will always appreciate his inclusiveness, the tight friendship we formed, and the fact that it has lasted well beyond his leaving the lab. He helped me through a lot of work-related and personal problems and continues to do so, for which I am greatly appreciative. Here's to many more hazy nights of dubious activities! There were many other important people in the lab that helped me through my work, but none had quite the early or profound impact as Dame. Other lab members that meant a lot and made life more fun include Valeria Ramaglia, Youngwha Kwon (the nicest guy you'll

ever meet), Dr. Mike Wilkie (the most irritable guy you'll ever meet), and the many undergrads who either did my work for me or put up with my blasting music and asinine comments, particularly Mohan Cooray for spending a summer up to his elbows in turtle innards, Michael Richards for spending a summer in a lightless cave, George Zivkovic for spending a summer watching soccer, and Marki Sveen and Ciara O'Rielly for spending a summer being watched by all the guys.

A special thanks is due to all my friends in the department that made work more like a party on any given day, particularly at night when the caretakers were done! Specifically, Dame, Jake Ormond, David Hogg, Tanya Nock, and Marki Sveen. In various combinations we got up to a lot of trouble and that always made coming to work an adventure. Thanks to Dame, Dave and Aqsa Malik for many frank and frightening conversations about life and love. I also extend thanks to all the guys and girls I played basketball, softball or floor/street hockey with on weekday/weekend afternoons, particularly Paul Williams, Mike Dodd, Patrick James and Steve Walker. I would have been much more productive but much less happy without it!

Thank you to all my committee members, past and present. Particularly Dr. Stephen Tobe who was there from the beginning but due to his horrendous schedule could not be there in the end. Thank you also to Drs. Stephen Reid, Mike Salter, Melanie Woodin, Angela Lange, and Martin Wojtowicz for occasional or permanent service on my committee, for your time and attention to my work, for your thoughtful questions, and above all for making me sweat a bit during my exams. Without the challenge this wouldn't be half as much fun. Thanks also to Ian Buglass but not to Josie Valotta for helping me through the departmental side of life, to Norm and his friendly staff for all their loving care of my turtles, to Terry Hill for rambling rants about life, to Jim and Luu in shops for teaching me so many new curse words, to Mike Barrett for

always being such a great guy and always coming to me for the simplest of computing questions, to Marie and Tamar for spreading departmental gossip, to Nalini for dealing with me for 5 years, to Janet and Lisa for making my undergrad teaching labs run smoothly and to all the TAs who didn't resent me piling marking on their desk.

Outside of the department there are so many more who deserve my gratitude. Thanks to all my friends and family who listened to me describe my work with varying degrees of blankness on their faces, but with sincere interest in their hearts. To my best friends I owe much happiness: Craig and Vicki Bradley, Cathy Boscarino, Dame, Cait Dmitriev, Agnes Gozdzik, Rhain Louis, Josh Kirshenblat, Jeff and Ashley Pamenter, Mike and Jasmine Pritchard, and Will Sacks…you guys are my oldest and dearest friends and I appreciate the lifetime of love and support I've been lucky enough to receive from each of you, no matter how long I've known you. Particular recognition goes to Josh, my best friend and probably my soul mate in some twisted way. Good on us for making it this far!

Significantly I must thank the two wonderful ladies who filled my heart during the duration of my studies (although I don't think either ever really understood what I do). To Kate Busby who was there in the beginning I owe a great many thanks for love and support, and for many lessons in living with other people's messes (a valuable skill in any lab)! I'm glad we're still close and I wish you all the best. To Michelle Closson who made it almost all the way to the end I also owe a great deal of gratitude for always making me feel wise and capable of anything, both in the lab and in life. Although for periods you distracted me from my work for months at a time, your love was what got me out of bed every morning and gave me the courage to want to achieve more. More recently you have indirectly forced me to grow in many new ways and

directions and I thank you for that too. In the end you've made me a better person and I hope you are happy wherever you end up.

Finally, and most important, are my parents who have always supported me in all my decisions and offered no prejudice against any of my choices, no matter how silly they may have seemed. You gave me my brains, raised me right and then put me through school. I have all the thanks in the world for you but no volume of words can describe what you mean to me. You have always loved me unconditionally and your love and support have always lifted me up. To paraphrase Newton: in my life, you are the giants upon whose shoulders I have stood to see farther.

Table of Contents

Table of Figures

Table of Tables

Table 1. List of abbreviations

5HD	5-hydroxydecanoic acid
A_1R	adenosine A_1 Receptor
aCSF	artificial cerebrospinal fluid
AD	anoxic depolarization
AMPAR	α-amino-3-hydroxy-5-methyl-4-isoxazole propionic acid receptor
AP	action potential
AP_f	action potential frequency
ANT	adenine nucleotide translocator
APV	2-amino-5-phosphonopentanoic acid
ATP	adenosine triphosphate
BAPTA	1,2-bis(o-aminophenoxy)ethane-N,N,N',N'-tetraacetic acid
B_{max}	receptor binding affinity
$[Ca^{2+}]_c$	cytosolic calcium concentration
$[Ca^{2+}]_m$	mitochondrial calcium concentration
cAMP	cyclic adenosine monophosphate
CBF	cerebral blood flow
cGMP	cyclic adenosine monophosphate
CNS	central nervous system
CPA	N6-cyclopentyladenosine
DNP	dinitrophenol
DMSO	dimethyl sulfoxide
DOR	delta opioid receptor
DPCPX	8-cyclopentyl-1,3-dimethylxanthine
E_{ion}	reversal potential of specified ion
E_m	resting membrane potential
EAA	excitatory amino acid
ECD	excitotoxic cell death
EGTA	ethylene glycol tetraacetic acid
ERCA	ER calcium-ATPase
EPSC	excitatory post-synaptic current
$EPSP_f$	excitatory post-synaptic potential frequency
ETC	electron transport chain
EZA	6-ethoxy-2-benzothiazolesulfonamide
GABA	λ-amino butyric acid
G_i	inhibitory G protein
G_{ion}	conductance of specified ion
G_w	whole cell conductance
HCO_3^-	bicarbonate
HPC	hypoxic preconditioning
HPV	hypoxic pulmonary vasoconstriction
IAA	inhibitory amino acid
ICSF	intracellular cerebrospinal fluid
IMAC	inner membrane anion channel
IPC	Ischemic preconditioning

IPSP	inhibitory post-synaptic potential
KCC2	K^+-Cl^-co-transporter
LDH	lactate dehydrogenase
L-NAME	N-nitro-L-arginine methyl ester hydrochloride
MAD	mild anoxic depolarization
MCU	mitochondrial Ca^{2+} uniporter
MEQ	6-methoxy-N-ethylquinolinium iodide
MP7	Mastoparan
MPG	N-(2-mercapto-propionyl)-glycine
MPTP	mitochondrial permeability transition pore
mK_{ATP}	mitochondrial ATP-sensitive K^+ channel
mK_{Ca}	mitochondrial calcium-sensitive K^+ channel
NAC	N-acetyl-cysteine
NADH	nicotinamide adenine dinucleotide
NKCC1	$Na^+/K^+/2Cl^-$ co-transporter
NMDAR	N-methyl-D-aspartate receptor
NO	nitric oxide
NOS	nitric oxide synthase
nNOS	neuronal nitric oxide synthase
O_2^-	superoxide
OGD	oxygen-glucose deprivation
P_{open}	receptor open probability
pK_{ATP}	plasmalemmal ATP-sensitive K^+ channel
PKA	cAMP dependent protein kinase
PKC	protein kinase C
PKG	protein kinase G
PSD-95	post-synaptic density 95
PTX	Pertussis toxin
RCR	respiratory control ratio
R_a	access resistance
R_{in}	input resistance
ROS	reactive oxygen species
SDH	succinate dehydrogenase
SLE	seizure-like event
SNP	S-nitroso-N-acetylpenicillamine
TEA	tetraethylammonium
TTX	tetrodotoxin
VDAC	voltage-dependant anion channel
Ψ_m	mitochondrial inner membrane potential

1. General introduction to anoxic stress and mechanisms of anoxia-tolerance

1.1. The anoxic challenge: unavoidable depression in ATP supply

Glycolysis is the primary energy-producing pathway in both aerobic and anaerobic organisms, producing 2 molecules of ATP from the conversion of glucose into pyruvate (3 molecules of ATP from glycogen). During aerobic conditions, these end products are further catabolized via oxidative phosphorylation to produce 30 to 32 ATP molecules per glucose molecule, including glycolytic production (Hochachka and Dunn, 1983). During anoxia however, oxidative phosphorylation ceases, and as a result only 2-3 ATP are produced from the catabolism of each glycogen molecule. Thus, to maintain ATP supplies, the rate of glycolysis must increase by at least 10-fold. An increase in glycolytic rate to produce additional ATP is known as the Pasteur effect (Ainscow and Brand, 1999), and is not an efficient long-term protective mechanism since it is generally not possible to increase glycolytic rates sufficiently to maintain normoxic ATP consumption rates for more than a few minutes. As a result, cellular ATP stores decrease during anoxia unless ATP utilization is decreased to match ATP supply (Buck and Pamenter, 2006; Hochachka, 1986). Therefore, hypoxic or anoxic environments provide a unique set of challenges to organisms since reduced environmental oxygen significantly impacts cellular energy production. Most vertebrates and all mammals are minimally tolerant of anoxic stress and rapidly undergo cellular injury (necrosis and apoptosis) when exposed to low oxygen environments (Siesjo, 1989). Anoxic cell death occurs via a variety of mechanisms (see below), but the primary cause of anoxic cell death is a failure to meet cellular ATP demands. Furthermore, this anoxic cell mortality is proportional to the cells' reliance on oxidative metabolism.

Based on oxygen consumption, the brain is known to be the body's single greatest consumer of ATP. Although brain comprises only ~ 2% of total body mass, its metabolism utilizes 20% of the body's total energy (Schmidt-Nielson, 1984). Furthermore, the brain is highly aerobic, producing 95% of its ATP via oxidative metabolism, and the brain does not store significant quantities of glycogen or oxygen (Erecinska and Silver, 1989). Therefore, the brain is both the largest user of ATP and the first tissue to suffer cell damage as a result of oxygen deprivation. In the brain, ATP is consumed for the functioning of numerous transmembrane pumps, which maintain electrochemical gradients across cell membranes, a requirement for neuronal signaling and survival. The largest single consumer of ATP is the Na^+/K^+ ATPase, which uses 50-60% of the total energy consumed by the brain (Schmidt-Nielson, 1984). This pump maintains Na^+ and K^+ concentrations for the maintenance of resting membrane potential (E_m). In addition, this gradient facilitates the regulation of cytosolic calcium ($[Ca^{2+}]_c$) via the Na^+/Ca^{2+} exchanger and also for the proper functioning of voltage-sensitive glutamatergic receptors/ion channels (N-methyl-D-aspartate receptors (NMDARs) and α-amino-3-hydroxy-5-methyl-4-isoxazole propionic acid receptors (AMPARs)). Since a decrease in ATP production during anoxia is unavoidable, it is essential that ATP demand be reduced to match ATP supply in order to sustain pump activity and exclude excessive Ca^{2+} entry, thus avoiding anoxic cellular injury. Most vertebrates have not evolved endogenous mechanisms to rapidly and sufficiently depress cellular metabolism during anoxia to avoid cell death.

The remainder of this chapter will focus on a general introduction to the mechanisms of ischemic injury and rescue in mammals and endogenous ischemia tolerance in facultative anaerobes. Since each chapter in this thesis examines a functionally distinct aspect of the turtle's anoxia-tolerance, specific introductions and discussions of the mechanism examined in each set

of experiments are included in their respective chapters below and a general summation/integration of the key findings and pathways is included in chapter 7.

1.1.1. Excitotoxic cell death in mammalian neurons

In anoxia-intolerant organisms, oxygen deprivation induces elevations in the excitatory amino acid glutamate primarily by the reversed operation of glutamate transporters, which leads to over-excitation of AMPARs and NMDARs, subsequent excessive Ca^{2+} influx, neuronal depolarization and electrical hyper-excitability (Abele et al., 1990; Andine et al., 1991; Bosley et al., 1983; Crepel et al., 1993a; Lyubkin et al., 1997; Michaels and Rothman, 1990; Rossi et al., 2000). These excitatory events result in significant ion movement and require compensation by ATP-dependent pump activity to restore ionic gradients and neuronal homeostasis. However, the anoxic cell suffers an ~ 90% reduction in ATP availability due to the failure of oxidative phosphorylation, and combined with greatly increased ATP demand due to heightened neuronal excitability, ATP stores rapidly decline (Kopp et al., 1984; Santos et al., 1996). Depletion of ATP results in the abolishment of ATP-dependent pump activity, triggering a further depolarization of E_m, termed 'anoxic depolarization' (AD), that is irreversible by reoxygenation (Anderson et al., 2005; Lundberg and Oscarsson, 1953). Extended neuronal depolarization chronically over-activates voltage-sensitive channels and deleterious concentrations of Ca^{2+} and Na^+ enter the cell, furthering the neuronal depolarization and up-regulating excitatory events. Mitochondrial Ca^{2+} concentration ($[Ca^{2+}]_m$) is drastically increased, triggering the formation of the mitochondrial permeability transition pore (MPTP) and the release of mitochondrial apoptotic factors (Kannurpatti et al., 2004). Collectively these processes lead to excitotoxic cell death (ECD: Fig. 1) and underlie the sensitivity of mammalian neurons to ischemic insults (Choi, 1994; Siesjo, 1988).

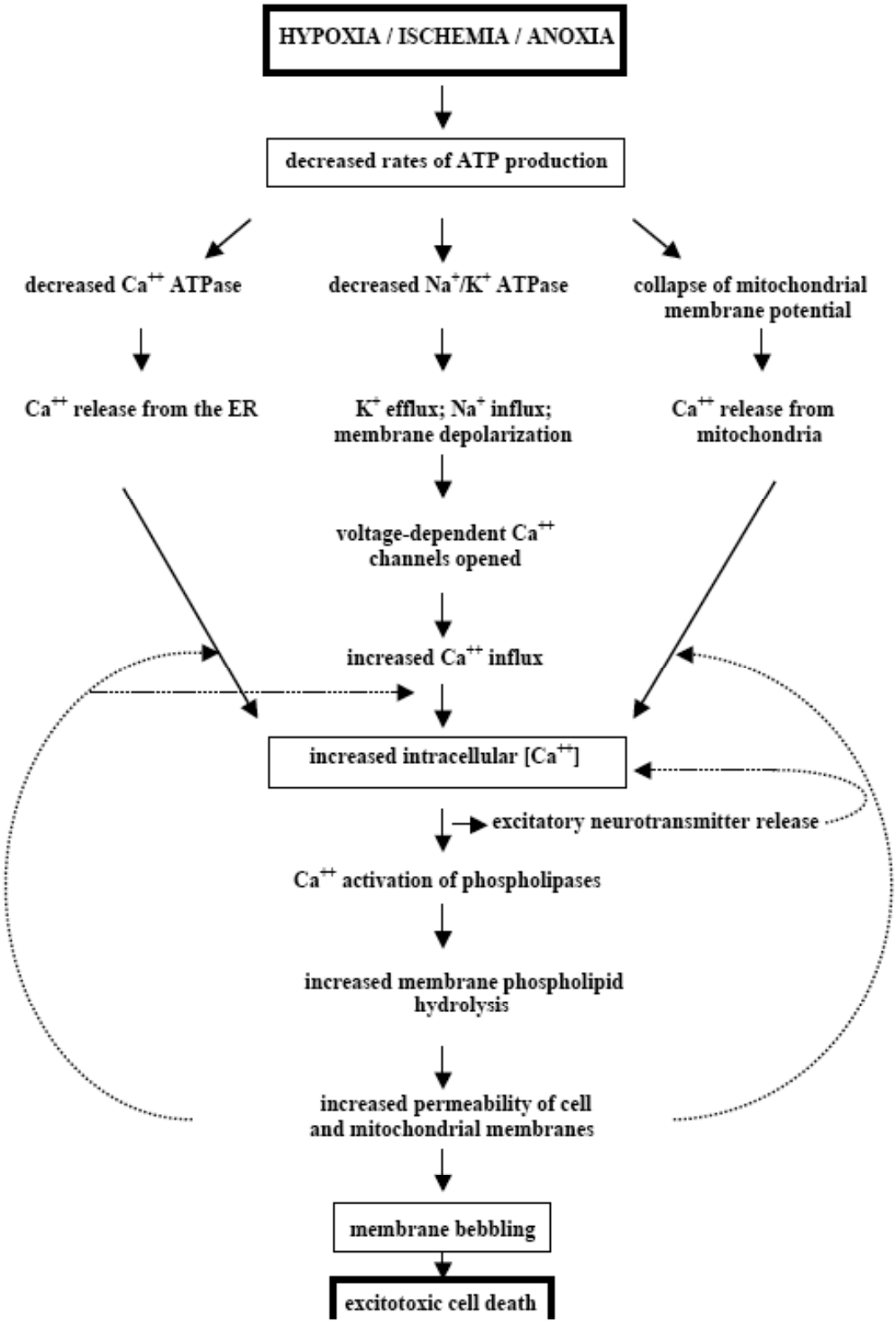

Figure 1. Schematic of neuronal mechanisms of ECD.

1.2. Solving the anoxic challenge: matching ATP demand with supply

Not all air-breathing organisms are intolerant to prolonged anoxic exposure. Facultative anaerobes are a class of organisms that are able to adjust their metabolism sufficiently to handle anoxic stress without apparent detriment. To date, a handful of air-breathing vertebrate facultative anaerobes have been identified and studied intensively. These "anoxia-tolerant" organisms include some species of freshwater turtle (*Chrysemys picta bellii, Trachemys scripta elegans*), the crucian carp (*Carassius carassius*), and the less anoxia-tolerant common goldfish (*Carassius auratius*) (Bickler and Buck, 2007; Buck and Pamenter, 2006). In addition, a number of "hypoxia-tolerant" organisms have been identified including the pond snail (*Lymnaea stagnalis*), the Australian epaulette shark (*Hemiscyllium ocellatum*), and the annual killifish (*Austrofundulus limnaeus*) (Cheung et al., 2006; Nilsson and Renshaw, 2004; Podrabsky et al., 2007).

The freshwater turtles listed above are the most anoxia-tolerant vertebrate species identified. In the laboratory, these turtles can survive anoxic episodes lasting days at 25ºC to six months at 3ºC without apparent detriment (Musacchia, 1959; Ultsch and Jackson, 1982). These turtles, along with carp and goldfish have evolved mechanisms to withstand prolonged anoxia while over-wintering under the frozen surfaces of lakes and ponds in North America and northern Europe, respectively (Nilsson, 2001; Ultsch et al., 1999). Like mammals, these organisms rely entirely on glycolytic energy production during periods of anoxic stress but unlike mammals, they survive anoxic episodes without significant depletion of ATP supplies (Buck, 1998; Chih et al., 1989a; Johansson and Nilsson, 1995; Johansson et al., 1995). Therefore, they must logically achieve a coordinated reduction in both ATP producing and utilizing pathways since ATP levels do not change despite an estimated 90% reduction in ATP

synthesis due to anoxic inhibition of oxidative phosphorylation. Indeed energy metabolism is decreased by 49 to > 90% in the anoxic turtle, indicating metabolism is depressed during anoxia sufficiently to meet decreased ATP availability (Buck et al., 1993; Doll et al., 1994; Jackson, 1968; Sick et al., 1984).

Turtles simultaneously employ a wide range of protective mechanisms across all organs and cell types in response to low oxygen environments; however, an explicit review of these responses is beyond the scope of this paper and has been reviewed extensively elsewhere (Bickler and Buck, 2007; Hochachka et al., 1996). Briefly, on the ATP-supply side of the equation, glycolysis is augmented by numerous mechanisms up- and down-stream of the metabolizing cell in order to maximize anaerobic ATP production. Turtle liver is 15% glycogen by mass and freshwater turtles possess livers that are proportionally larger than those of anoxia-intolerant organisms, providing an abundant long-term source of glycolytic substrate (Clark, 1973). Mobilization of glycogen from liver increases blood glucose levels and provides fuel to tissues with lower glycogen stores such as the brain; indeed turtle blood glucose levels rise 10-fold after four hours of forced submergence (Ramaglia and Buck, 2004). In addition, cerebral blood flow (CBF) is increased during anoxia, a mechanism that would enhance the delivery of glycolytic substrate to the brain as well as the removal of acidic anaerobic end products (Bickler, 1992b; Hylland et al., 1994). Finally, turtle tissue has a very high buffering capacity that allows it to sequester acidic anaerobic end products that accumulate during prolonged anoxia (Jackson, 1983). In particular, turtle bone and carapace sequesters H^+ ions to prevent extreme tissue acidification (Jackson et al., 2000a; Jackson et al., 2000b). However, although maximizing glycolytic throughput is important, the critical factors underlying the turtle's anoxia-tolerance are

likely mechanisms of metabolic arrest. Two such mechanisms have been characterized in the anoxic turtle: channel arrest and spike arrest.

1.2.1. Critical adaptations to anoxia: (a) channel arrest

As discussed above, ion pumping consumes the majority of neuronal ATP during normoxia. Ion pumps work to maintain gradients that are dissipated by passive leak of ions and by large-scale ionic shifts following excitatory events (e.g. the role of the Na^+/K^+ ATPase in E_m recovery following action potential (AP) firing. In the brain and liver of the anoxic turtle, Na^+/K^+ ATPase activity decreases ~ 40-90% without a reduction in E_m or [ATP] (Buck and Hochachka, 1993; Hylland et al., 1997; Lutz, 1984). Since Na^+/K^+ ATPase activity is directly related to membrane ion permeability, membrane permeability must decrease in order to facilitate the reduced workload of ion pumps. Membrane ion permeability can be decreased in two ways: (1) by reducing the conductance of individual leakage channels, or (2) by reducing the concentration of these channels in the membrane itself. A mechanism whereby ion channel conductance decreases to support a decrease in ion pumping is termed "ion channel arrest" (Hochachka, 1986). Several studies support the occurrence of channel arrest in the anoxic turtle brain, including 50-65% decreases in whole-cell NMDAR currents, NMDAR P_{open}, NMDAR-mediated Ca^{2+} influx, and whole-cell K^+ leakage (Buck and Bickler, 1995; Buck and Bickler, 1998a; Chih et al., 1989b; Shin and Buck, 2003). Furthermore, in addition to decreased ion conductance, both NMDAR and Na^+ channel density decrease during prolonged anoxia (Bickler et al., 2000; Perez-Pinzon et al., 1992c).

1.2.2. Critical adaptations to anoxia: (b) spike arrest

In addition to channel arrest-mediated reductions in ion leakage, turtle neurons demonstrate significant electrical quiescence during anoxia, a phenomenon known as 'spike arrest' (Perez-Pinzon et al., 1992a). Evidence for spike arrest in the anoxic turtle brain includes measurements of depolarized transmembrane potentials and Na^+ spike thresholds, and decreased action potential frequency (AP_f), field potentials, and EEG activity with anoxia (Fernandes et al., 1997; Perez-Pinzon et al., 1992a; Perez-Pinzon et al., 1992b). Depressed excitatory electrical activity preserves ATP supplies by reducing the workload of pumps responsible for neuronal ion re-equilibration during and following excitation (Perez-Pinzon et al., 1992a). The mechanism of spike arrest is unknown but is likely due to changes in excitatory and inhibitory amino acids (EAAs and IAAs) that are conducive to depressed electrical activity. Concentrations of the primary EAA glutamate decrease 40% in the first 1.5 hours of anoxia in turtle brain, and glutamate release and re-uptake mechanisms remain active (Milton et al., 2002). During longer duration anoxic exposures (up to 5 hours), glutamate levels decrease further to 30% of control levels (Thompson et al., 2007). Glutamate is the primary activating ligand of AMPARs and NMDARS and decreased [glutamate] would reduce the activity of both of these excitatory receptors. The overall depression of glutamatergic activity may substantially reduce excitatory activity in the anoxic turtle cortex and contribute to spike arrest and thus ATP conservation.

Conversely, anoxia causes rapid and prolonged elevations of γ-amino butyric acid (GABA) (Hitzig et al., 1985; Nilsson et al., 1990; Nilsson and Lutz, 1991). GABA is the predominant inhibitory neurotransmitter in the mature CNS, and mediates wide-spread electrical depression in most neurons (Lutz and Milton, 2004; Martyniuk et al., 2005; Turner and Whittle, 1983). GABA mediates three specific receptors: $GABA_A$ and $GABA_C$ receptors, which contain a

membrane-spanning Cl^- channel that is also conductive to bicarbonate (HCO_3^-), and $GABA_B$ receptors, which act on a K^+ channel via an associated G protein (Kaila et al., 1993). Activation of these receptors is electrically inhibitory in most mature mammalian neurons since the reversal potentials of K^+ and Cl^- (E_K and E_{Cl}) are near E_m. Therefore, increased membrane conductance to either of these ions (G_K and G_{Cl}) opposes neuronal depolarization away from E_K and E_{Cl} during excitatory events. Thus greater excitatory input is required to depolarize the neuron to threshold, resulting in decreased neuronal activity overall. In neurons, the Cl^- gradient is determined by the balance of extrusion of Cl^- through K^+-Cl^- co-transporters (KCC2), Cl^--bicarbonate exchangers, ATP-driven Cl^- pumps and voltage-sensitive Cl^- channels; with the accumulation of Cl^- through $Na^+/K^+/2Cl^-$ co-transporters (NKCC1) (for review see (Delpire, 2000; Kaila, 1994). The difference in expression of these opposing transporters determines neuronal E_{Cl} (Ben-Ari, 2002; Ben-Ari et al., 2007). If NKCC1 expression is higher, as in the developing mammalian brain, E_{Cl} is depolarizing with regard to E_m and $GABA_A$ receptor activation becomes excitatory (Fig. 2). Conversely, in the mature mammalian CNS, higher expression of KCC2 results in an E_{Cl} that is near E_m. Thus increased G_{Cl} results in an inward Cl^- flux and membrane hyperpolarization, and $GABA_A$ receptor activation is inhibitory under these circumstances. Therefore, in most mature neurons GABA is ideally situated as a mediator of spike arrest since [GABA] is rapidly elevated during anoxic insults in facultative anaerobes, and since activation of both GABAergic receptors opposes electrical hyper-excitability in the mature CNS.

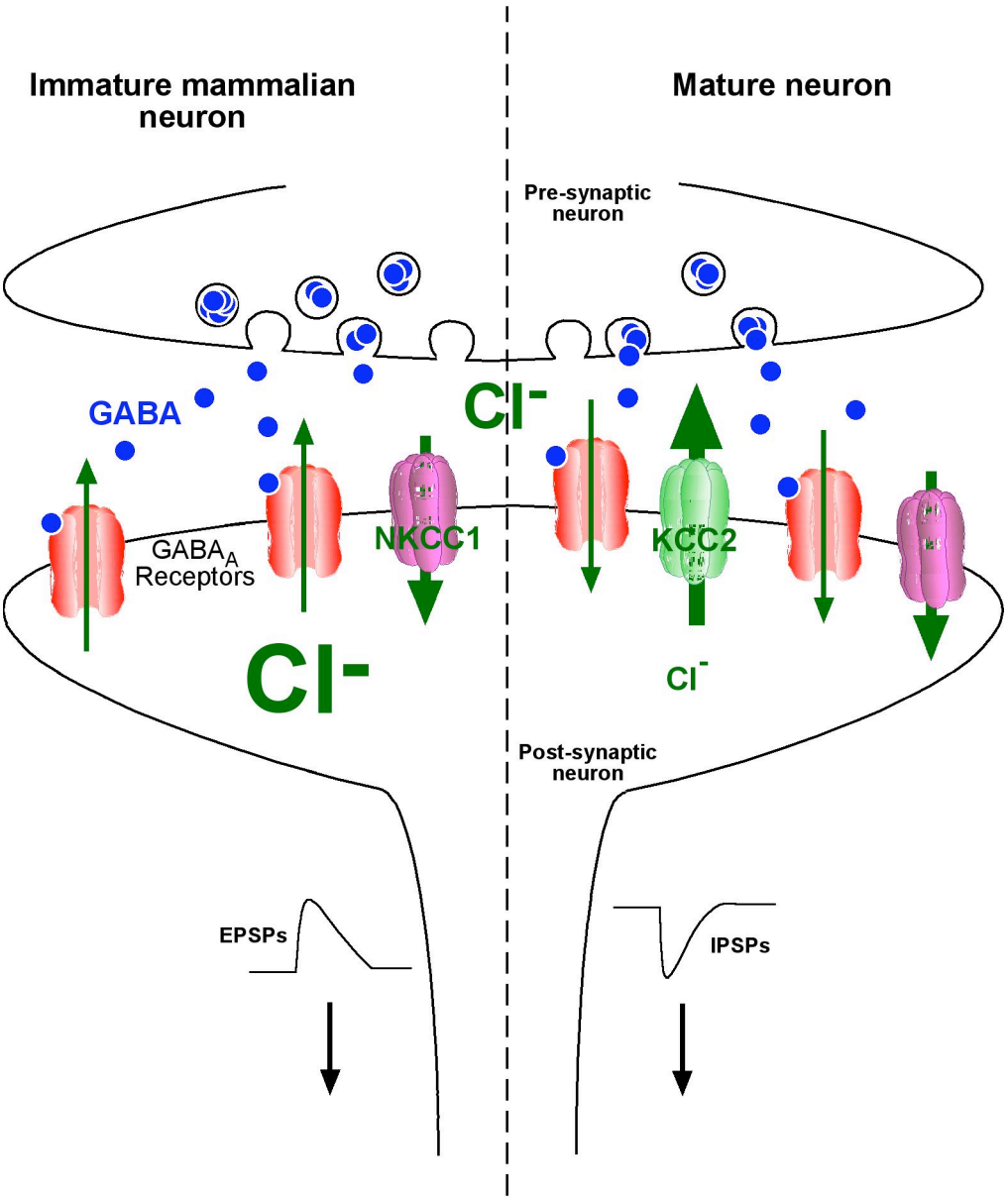

Figure 2. Cl^- gradients determine whether GABAergic signaling is inhibitory or excitatory in immature and mature mammalian neurons.

In immature mammalian neurons (left side), $Na^+/K^+/Cl^-$ (NKCC1) is expressed but the K+/Cl co-transporter (KCC2) is not and intracellular Cl^- (green) is high. Pre-synaptic GABA release (blue) leads to activation of post-synaptic $GABA_A$ receptors and passive extrusion of Cl^- ions out of the cell. This movement is depolarizing and results in the propagation of excitatory post-synaptic potentials (EPSPs) and increased neuronal excitation. In mature mammalian and facultative anaerobe neurons (right side), KCC2 expression is increased and intracellular Cl^- is low. Here, $GABA_A$ receptor activation results in the passive influx of Cl^- ions into the cell. This movement is hyperpolarizing and results in the propagation of inhibitory post-synaptic potentials (IPSPs) and decreased electrical excitability.

Together, channel arrest and spike arrest significantly depress electrical excitability and thus ATP demand in anoxic freshwater turtle neurons. These adaptations likely contribute significantly to the metabolic arrest that allows turtle brain to survive months of anoxia at low temperatures. However, although these phenomena have been identified and described in the anoxic turtle brain, the mechanisms underlying these changes are only beginning to be elucidated. Interestingly, as the mechanisms are examined, it is becoming apparent that the endogenous neuroprotective pathways employed in the anoxic turtle utilize the same underlying mechanisms as inducible neuroprotective systems in otherwise anoxia-sensitive mammalian brain, which will be discussed next.

1.3. Preconditioned protection: ischemic cell death and rescue via ischemic preconditioning

1.3.1. Anoxic neuroprotection in mammals: failure of direct receptor modulation

Although facultative anaerobes such as the western painted turtle are able to survive anoxic exposure, most aerobic organisms do not possess endogenously activated mechanisms to protect them completely from low-oxygen stress. Indeed even among turtle species our model is remarkably anoxia-tolerant, with some turtle species (e.g. soft shell turtles) being as sensitive to oxygen availability as most mammals (Ultsch, 2006). In general, mammalian cell death due to stroke can be minimized or in some cases abolished by mechanisms aimed at decreasing cellular excitability during anoxic stress. For example, activation of inhibitory $GABA_A$ receptors with partial or complete agonists following ischemic insult is neuroprotective against cell death in mature gerbil brain (Hall et al., 1997; Hall et al., 1998; Schwartz-Bloom et al., 1998; Schwartz-Bloom et al., 2000). However, although GABA perfusion, specific activation of GABA receptors or prevention of GABA catabolism via inhibition of the GABA transaminase provide moderate

neuroprotection against ischemic insult in gerbil brain, the degree of neuroprotection provided by enhanced GABAergic signaling is considerably less than that provided by inhibition of excitatory neuronal signaling mechanisms (Grabb et al., 2002; Inglefield et al., 1995; Sternau et al., 1989). More specifically, glutamate receptor antagonism (AMPARs or NMDARs) is neuroprotective against ischemic insults and toxic elevations in cellular Ca^{2+} are prevented (Rader and Lanthorn, 1989; Sheardown et al., 1990). However, glutamate receptors are critical to a variety of neuronal functions including memory formation, and clinical stroke interventions targeting glutamate receptors have produced severe psychotic and psychomimetic side-effects (Ikonomidou and Turski, 2002). Furthermore, glutamate receptor blockade does not prevent AD due to stroke or spreading depression in the penumbra (Anderson et al., 2005; Jarvis et al., 2001). Thus, direct modulation of excitatory receptors as a treatment against anoxic insults poseS significant shortcomings in terms of cellular or whole-organism viability, and therefore alternative mechanisms of inducible neuroprotection based on indirect regulation of these receptors may offer more viable treatment options for anoxic insults in a clinical setting.

1.3.2. Ischemic preconditioning and the 'mild uncoupling' hypothesis

Although direct manipulations of glutamatergic and GABAergic receptors during anoxia fail to completely ameliorate cell death, anoxia-sensitive tissues can be conditioned in such a manner so as to reduce the cellular damage suffered during ischemic insults. Ischemic preconditioning (IPC) is a phenomenon whereby a non-lethal period of ischemia protects tissues against subsequent, otherwise lethal ischemic insults (Murry et al., 1986; Schurr et al., 1986). This mechanism is both cardioprotective and neuroprotective in numerous organisms including dog, rabbit and rat heart and rat brain (Heurteaux et al., 1995; Liu and Downey, 1992; Murry et al., 1986; Schurr et al., 1986). Preconditioning significantly reduces infarct size in two distinct

windows of protection. The first occurs 1-2 hours after the initial ischemic insult and lasts for 2-4 hours. The second window occurs ~ 24 hours after the initial insult and provides protection for 12-48 hours and is thought to be a result of an up-regulation of the synthesis of neuroprotective proteins (Gidday, 2006). The underlying mechanisms of IPC-mediated protection are not well understood but a complicated picture involving interactions between numerous kinases, 2^{nd} messengers and ion channels is emerging (Downey et al., 2007; Gidday, 2006). Generally, mechanisms of preconditioning appear to function via some form of mitochondrial uncoupling. Mitochondrial uncoupling alters ATP production rates, reactive oxygen species (ROS) production and mitochondrial Ca^{2+} buffering and since all three of these molecules are key to regulating mechanisms of anoxia-tolerance, the mitochondrion is well positioned as a regulator of neuroprotective mechanisms. In order to understand the impact of mild mitochondrial uncoupling, it is important to first discuss the structure and function of mitochondrial membranes and their associated proteins.

1.3.3. Mitochondrial ion homeostasis

Morphologically, two membranes functionally divide the mitochondrion. In turn, these two membranes define two sub-mitochondrial compartments: the intermembrane space located between the inner and outer membranes, and the mitochondrial matrix located within the inner membrane. The outer membrane contains a number of proteins that make it permeable to molecules up to 10 kDa in size. Conversely, the inner membrane is composed of a higher percentage of specialized proteins and is the primary permeability barrier between the cytosol and the mitochondrial matrix. There is a large voltage gradient across the inner membrane, with the matrix being -180 mV with regard to the outside of the cell (O'Rourke, 2000; O'Rourke, 2007). The membrane is impermeable to protons, and thus the gradient is maintained, allowing

the energy of protons traveling back along their concentration gradient to be harnessed to move other ions across the membrane against their own concentration gradients. The mitochondrial membrane potential (Ψ_m) is generated primarily by the pumping of K^+ ions out of the matrix via a H^+/K^+ antiporter, which is powered by this proton gradient. The combination of the concentration and electrical gradients results in a proton-motive force, which energizes the phosphorylation of ADP to ATP via the ATP synthetase (O'Rourke, 2000; O'Rourke, 2007). Thus the H^+ gradient is tightly coupled to ATP production, and any mechanism that dissipates the gradient for physiological purposes other than ATP production is termed an uncoupling mechanism.

Opening of mitochondrial ion channels allows ions to flow across the mitochondrial inner membrane along their concentration gradient. In particular, increases in G_K lead to a depolarization of Ψ_m. Increased K^+ influx is partially countered by increasing the activity of the K^+/H^+ exchanger, which pumps K^+ ions out of the matrix at the expense of the H^+ gradient. The loss of available H^+ ions to compensate for the flux of K^+ ions results in a partial or "mild" uncoupling of the proton gradient and a depolarization of Ψ_m. A mild uncoupling causes a small depolarization of Ψ_m that is not sufficient to abolish mitochondrial functions driven by Ψ_m, but is sufficient to alter their rate of activity. Mitochondrial calcium ($[Ca^{2+}]_m$) buffering and ROS generation are two key functions of the mitochondria that are driven by this electrochemical gradient and both are significantly affected by mild uncoupling (O'Rourke, 2000; O'Rourke, 2007).

1.3.4. Effects of mild uncoupling: (a) calcium buffering

A balance between mitochondrial Ca^{2+} uptake and Ca^{2+} efflux mechanisms determine $[Ca^{2+}]_m$, and these mechanisms are dependent on the mitochondrial H^+ gradient. Ca^{2+} uptake into

the mitochondria occurs electrophoretically via the activity of the mitochondrial Ca^{2+} uniporter (MCU), which is driven by the large negative potential generated by the inwardly directed proton gradient. Patch-clamp experiments on the inner mitochondrial membrane of mitoplasts demonstrate that the uniporter has a high affinity for Ca^{2+} (2 nM) (Kirichok et al., 2004), suggesting that this channel functions at a resting rate under normal physiological conditions and increases the rate of Ca^{2+} uptake into the mitochondria under pathological conditions when $[Ca^{2+}]_c$ is elevated. Conversely, mitochondrial Ca^{2+} efflux occurs via a Na^+/Ca^{2+} exchanger and its associated Na^+/H^+ antiporter, as well as a Ca^{2+}/H^+ exchanger (for a review of mitochondrial Ca^{2+} cycling see (Gunter et al., 1998; O'Rourke, 2007).

Maintenance of $[Ca^{2+}]_m$ during anoxia is critical to surviving ischemic insults in mammals. During periods of prolonged anoxia, neuronal $[Ca^{2+}]_c$ slowly elevates due to progressive AD and the associated activation of voltage-gated cation channels. As $[Ca^{2+}]_c$ rises, $[Ca^{2+}]_m$ increases concomitantly, opposed by the activity of the mitochondrial Ca^{2+}/H^+ exchanger. When $[Ca^{2+}]_c$ reaches ~ 4-500 nM, the ability of the Ca^{2+}/H^+ exchanger to oppose mitochondrial Ca^{2+} uptake is overwhelmed and $[Ca^{2+}]_m$ begins to rise rapidly. This is termed the 'set point' and $[Ca^{2+}]_m$ becomes overloaded at 1-3 μM $[Ca^{2+}]_c$ (Nichols, 1978). Toxic elevations in $[Ca^{2+}]_m$ lead to formation of the mitochondrial permeability transition pore (MPTP), a junctional complex that is currently thought to be formed between the adenine nucleotide translocase (ANT) protein of the inner mitochondrial membrane and the voltage dependant anion channel (VDAC) protein of the outer mitochondrial membranes (for review see (Crompton, 2000). Many labs have shown that prevention of MPTP formation is critical to preventing neuronal apoptosis and necrosis following ischemic damage. For example, in neo-natal rat myocytes, ischemia-reperfusion results in apoptotic events that are abolished by cyclosporine A,

an inhibitor of the MPTP (Xu et al., 2001). Furthermore, pharmacological stimulation of MPTP formation abolished the protective effects of IPC, suggesting that cytoprotection induced by IPC opening also prevents MPTP formation (Cao et al., 2005). Therefore, maintenance of $[Ca^{2+}]_m$ is critical to IPC-mediated prevention of MPTP formation, release of apoptotic factors and inducible neuroprotection.

Since MCU-mediated mitochondrial Ca^{2+} uptake is driven by the mitochondrial proton gradient, dissipation of this gradient as occurs due to activation of mitochondrial K^+ channels, would reduce the rate of Ca^{2+} uptake into the mitochondria. Several studies have linked mild mitochondrial uncoupling to attenuated mitochondrial Ca^{2+} accumulation during anoxia. In rat heart, mildly uncoupling mitochondria by activating mitochondrial K^+ channels was neuroprotective against subsequent ischemic insults and prevented anoxia-mediated MPTP formation (Cao et al., 2005; Holmuhamedov, 1999). Mild uncoupling decreased the rate of Ca^{2+} uptake into isolated rat heart mitochondria and also increased the rate of Ca^{2+} release from isolated mitochondria that had been pre-loaded with Ca^{2+}. Both of these responses to uncoupling were linked to decreases in Ψ_m. Furthermore, in intact cardiomyocytes activation of mitochondrial K^+ channels decreased Ψ_m and reduced $[Ca^{2+}]_m$ accumulation during anoxia (Murata, 2001; Sato et al., 2005; Wang et al., 2001). Taken together, these data suggest IPC-mediated neuroprotection may be due to prevention of mitochondrial Ca^{2+} accumulation resulting from mild mitochondrial uncoupling.

1.3.5. Effects of mild uncoupling: (b) altered ROS production

Mitochondria are a major source of ROS production under normal physiological conditions. The production of ATP by oxidative phosphorylation is regulated partially by Ψ_m, and reverse electron flow in the electron transport chain (ETC) during oxidative phosphorylation

results in incidental ROS generation (St-Pierre et al., 2002). The rate of ROS generation by the mitochondria is associated with the rate of ATP production via the ETC, which in turn is regulated by the mitochondrial H^+ gradient. Therefore, a partial uncoupling of mitochondrial respiration will alter the rate of ROS production (Moroney et al., 1984). ROS in large quantities are highly deleterious to the cell, however ROS are constantly being produced by the mitochondria and alterations in the rate of radical formation may act as a redox signaling mechanism, potentially regulating downstream messengers such as PKC that may regulate neuroprotective mechanisms against ischemic insult (Oldenburg et al., 2003). There is evidence that redox signaling plays a role in ischemia tolerance, since ROS production is increased during IPC protocols (Vanden Hoek et al., 1998). Furthermore, in ischemic rabbit heart, IPC-mediated protection was abolished by inclusion of free radical scavengers, suggesting IPC triggers cardioprotection via the regulation of free radical generation (Vanden Hoek et al., 1998).

1.3.6. mK_{ATP} channels: mediators of uncoupling-mediated neuroprotection

Since K^+ flux determines Ψ_m, mitochondrial K^+ channels are likely candidates to mildly uncouple mitochondria and underlie IPC-based cytoprotection. Mitochondrial ATP-sensitive K^+ channels (mK_{ATP}) are presently favored as the mitochondrial uncoupling mechanism that underlies IPC in mammalian heart and brain (Auchampach et al., 1991; Kis et al., 2004; Oldenburg et al., 2003). Activation of mK_{ATP} channels partially dissipates the mitochondrial H^+ gradient, reducing the driving force of the MCU and subsequently decreasing mitochondrial accumulation of Ca^{2+} during ischemia, MPTP formation, and cytochrome C loss from the mitochondria. Conversely, blockade of mK_{ATP} abolishes IPC-mediated neuroprotection ubiquitously (Grover, 1997; Korge, 2002; Murata, 2001; Takashi et al., 1999; Yoshida et al., 2004). mK_{ATP} are located on the inner membrane of the mitochondria and although their specific

structure is unknown, it is thought to be similar to plasmalemmal K_{ATP} channels, which are composed of four pore-forming inward-rectifying K^+ channel subunits ($K_{IR}6.1$, 6.2) and four modulatory sulfonylurea receptors (SUR-1, 2) (Aguilar-Bryan and Bryan, 1999; Karschin et al., 1998). Physiologically these channels are mediated by several cellular messengers including PKC, adenosine, superoxide (O_2^-), and nitric oxide (NO) (Korge, 2002; Sasaki et al., 2000).

mK_{ATP} are not the only channels whose activation may provide neuroprotection against ischemic insult. Mitochondrial Ca^{2+}-sensitive K^+ channels (mK_{Ca}) are similar to plasmalemmal BK channels: they are multi-conductance state channels whose P_{open} is both voltage and $[Ca^{2+}]$ dependent and whose activity increases with Ψ_m depolarization (Siemen et al., 1999). In addition, mK_{Ca} currents in mitoplast-attached patches increased when the $[Ca^{2+}]$ outside the pipette was increased, suggesting that the Ca^{2+} sensor of the channel is located on the matrix side of the mitochondrial membrane (Xu et al., 2002). Therefore, the channels' activity increases as $[Ca^{2+}]_m$ rises due to sequestration of $[Ca^{2+}]_c$. Such an accumulation of Ca^{2+} occurs during ischemia and indeed mK_{Ca} channels are activated by hypoxia (Gu et al., 2007). Ca^{2+}-mediated increases in mK_{Ca} under hypoxic conditions would dissipate the mitochondrial H^+ gradient, partially uncouple the mitochondria, reduce MCU activity, and slow the cytotoxic accumulation of $[Ca^{2+}]_m$. Since activation of either mK_{Ca} or mK_{ATP} channels should have the same effect on cells (increased mG_K), it is not surprising that activation of mK_{Ca} channels in cardiac myocytes confers protection during global ischemia and reperfusion experiments that is similar in magnitude to the protection afforded by activation of mK_{ATP} channels or IPC (Cao et al., 2005; Xu et al., 2002). Furthermore, cytoprotection due to the activation of mK_{ATP} channels was not impaired by blockade of mK_{Ca} channels, or vice versa. These results suggest that the two channels function independently although their mechanism of action is similar: increased

mitochondrial G_K. Together, these data independently confirm the central role of K^+ influx into the mitochondrial matrix in IPC-mediated protection against ischemic injury that has been suggested by mK_{ATP} channel experiments.

1.3.7. Uncoupling and neuronal electrical inhibition

There is considerable evidence supporting mild mitochondrial uncoupling as critical to IPC-mediated neuroprotection against ischemic insults. However, although mild uncoupling attenuates both mitochondrial Ca^{2+} uptake and ROS production, the specific mechanisms of neuroprotection have not yet been elucidated. IPC-mediated mechanisms of neuroprotection in mammals may function upon the same principles as those underlying the turtles' anoxia-tolerance: minimizing ATP usage to prevent AD by limiting neuronal excitability via channel and spike arrest. Indeed, forms of both channel and spike arrest have been demonstrated in IPC-mediated neuroprotection by an interesting study that examined the binding affinity of glutamatergic and GABAergic receptors in ischemic hippocampal CA1 neurons. IPC-pretreatment with a 2.5-min period of ischemia significantly reduced cell death induced by a subsequent 5-min ischemic insult compared to non-pretreated neurons. In cells that survived ischemia the binding affinity (B_{Max}) of excitatory AMPA and NMDA receptors decreased and that of the inhibitory $GABA_A$ receptor increased. In addition, $GABA_A$ receptor B_{Max} increased progressively from 30 minutes to 48 hours after recirculation before decreasing (Sommer et al., 2002; Sommer et al., 2003). Furthermore, in rat cortical slices exposed to IPC treatment [GABA] was considerably elevated and glutamate release and cell death were decreased compared to control ischemic slices in which glutamate increased 5-fold and [GABA] did not change (Dave et al., 2005; Johns et al., 2000).

It is interesting to note that IPC renders mammalian neurons more anoxia-tolerant by mimicking endogenous changes observed in the anoxic turtle cortex: decreased [glutamate], elevated [GABA], increased $GABA_A$ receptor $B_{Max,}$ reduced NMDAR membrane density, reduced neuronal excitation, and prevention of AD and subsequent toxic cytosolic accumulation of calcium.

1.4. Hypotheses and organization of thesis

Turtles are considerably more anoxia-tolerant than mammals although they have the same basic dependency on oxygen for cellular metabolism. Mechanisms employed by the turtle, if properly understood, may be adapted to mammalian models and provide insight into enhancing mammalian tolerance to ischemic insults due to stroke. To date, the majority of research into the turtle's anoxia-tolerance has focused on observations of critical differences between mammals and turtles. Indeed there are many clear and obvious differences in gross physiology between mammals and reptiles. However, there is a limited degree of evolutionary divergence neurologically in terms of basic brain function and the underpinnings of an AP (neurotransmitters, receptors and ion channels). Therefore, differences in anoxia-tolerance are likely due to differential activation or expression of signaling pathways and mechanisms otherwise common to both mammals and facultative anaerobes. In fact, it is highly likely that many of the mechanisms and pathways of neuroprotection utilized in the anoxic turtle are expressed but are functionally inactive in mammals. As such, anoxia-tolerant organisms and IPC-treated mammalian models may offer complimentary models for researchers where one model offers endogenous mechanisms of protection that are mechanistically similar to inducible mechanisms in the other.

The overarching aim of my research was to elucidate the mechanisms that regulate electrical quiescence in the anoxic turtle cortex. This entailed examination of glutamatergic and GABAergic receptor function as well as ROS and nitric oxide, which can also contribute to cellular excitability. Specifically I aimed to test the following hypotheses:

(1) The AMPAR will exhibit channel arrest with the transition to anoxia (Chapter 2).

(2) Anoxia will result in 'mild uncoupling' of turtle mitochondria via the activation of mitochondrial K^+ channels (Chapter 3).

(3) The anoxic change in $[Ca^{2+}]_c$ observed by others is mediated by mitochondrial uncoupling, and underlies the anoxic decrease in NMDAR activity (Chapter 3).

(4) The anoxia-mediated spike arrest that occurs in turtle cortex is mediated by the previously determined increase in extracellular [GABA] (Chapter 4).

(5) [ROS] and [NO] will decrease with the transition to anoxia (Chapters 3, 5).

Note regarding organization of thesis: The bulk of my thesis has been published in peer-reviewed journals. For the sake of simplicity, these papers are presented as chapters or subchapters in this thesis. These chapters have been edited for redundancy, repetition, and uniformity. Abstracts are presented un-edited from their published form. Finally, the materials and methods section from all papers have been amalgamated into a single methods section placed following the research chapters as chapter 8. All the research chapters use the same basic preparation with variations on whole-cell recording or cellular fluorescence measuring techniques. The reader may refer to this chapter while reading the research chapters.

2. AMPARs undergo channel arrest in the anoxic turtle cortex

Preface

A modified version of this chapter was published as: Pamenter ME, Shin DS and Buck LT (2008). AMPARs undergo channel arrest in the anoxic turtle cortex. *Am. J. Physiol.* 294:R606-613.

The idea to explore channel arrest in the AMPAR came from L Buck and was based on whole-cell NMDA receptor experiments by L Buck. D Shin initiated the project and performed 10% of the whole-cell ligand-induced AMPAR current experiments. I performed the remainder of ligand experiments, IV curve, EPSC and EPSP experiments and wrote the paper with editing by L Buck.

Abstract

NMDAR activity is related to the activity of another glutamate receptor, the α-amino-3-hydroxy-5-methylisoxazole-4-propionic acid receptor (AMPAR). AMPAR blockade is neuroprotective against anoxic insult in mammals but the role of AMPARs in the turtle's anoxia-tolerance has not been investigated. To determine if AMPAR activity changes during hypoxia or anoxia in the turtle cortex, whole-cell AMPAR currents, AMPAR-mediated excitatory postsynaptic potentials (EPSPs) and excitatory postsynaptic currents (EPSCs) were measured. The effect of AMPAR blockade on normoxic and anoxic NMDAR currents was also examined. During 60 mins of normoxia, evoked peak AMPAR currents and the frequencies and amplitudes of EPSPs and EPSCs did not change. During anoxic perfusion: evoked AMPAR peak currents decreased 59.2 ± 5.5 and 60.2 ± 3.5% at 20 and 40 mins, respectively, $EPSP_f$ and amplitude decreased 28.7 ± 6.4% and 13.2 ± 1.7% respectively, and $EPSC_f$ and amplitude decreased 50.7 ± 5.1% and 51.3 ± 4.7%, respectively. In contrast, hypoxic (PO_2 = 5%) AMPAR peak currents were potentiated 56.6 ± 20.5 and 54.6 ± 15.8% at 20 and 40 mins, respectively. All changes were reversed by re-oxygenation. AMPAR currents and EPSPs were abolished by 6-cyano-7-nitroquinoxaline-2,3-dione (CNQX). In neurons pre-treated with CNQX, anoxic NMDAR currents were reversibly depressed by 49.8 ± 7.9%. These data suggest that AMPARs may undergo channel arrest in the anoxic turtle cortex.

2.1. Introduction: AMPARs and excitotoxicity

Glutamate activation of post-synaptic AMPARs produces excitatory post-synaptic potentials (EPSPs) that induce neuronal depolarization, Mg^{2+} exclusion from the pore of the NMDAR, and subsequent activation of NMDARs in the post-synaptic cell (Conti and Weinberg, 1999; Nowak et al., 1984). AMPAR-mediated currents are therefore rapid upstream signals that induce downstream NMDAR-mediated Ca^{2+} influx. AMPAR blockade thus decreases excitability earlier than NMDAR blockade and is neuroprotective following oxygen deprivation due to cardiac arrest or following severe global, focal, or repeated ischemic insults (Diemer et al., 1992; Iwasaki et al., 2004; Sheardown et al., 1990; Sheardown et al., 1993; Siesjo et al., 1991). AMPAR blockade is also neuroprotective in preventing cell death due to Parkinsonism and seizures (Klockgether et al., 1991; Ohmori et al., 1994). Perhaps the most compelling evidence for a role of AMPA in ECD is that transgenic mice expressing high levels of AMPARs are more susceptible to focal ischemia then wild type mice (Le et al., 1997). Despite this evidence, research into the role of AMPARs in anoxia-tolerance has been overlooked in favor of extensive research into NMDAR-mediated cell death.

Since AMPARs play an important role in activating NMDARs during normoxia, it follows then to ask if they play a role in the anoxic regulation of NMDARs. Anoxia-mediated depression of AMPAR activity may contribute to depression of NMDAR activity, decreased electrical excitability, reduced energy expensive Na^{+}/K^{+} ATPase activity and thus reduced metabolic demand. Since the channel arrest hypothesis has not been investigated in AMPARs, the aim of this study was to determine whether AMPAR activity changes in the hypoxic or anoxic turtle brain and to examine interactions between AMPA and NMDA receptors in anoxic turtle cortical neurons.

2.2. Results: AMPAR activity decreases with anoxia

Normoxic and anoxic whole-cell AMPAR activity. AMPA dose-response curves are shown in Fig. 3. The current voltage curve of AMPA-elicited currents had a slope conductance of 11.9 ± 0.8 pS and a reversal potential of 3.4 ± 2.9 mV (n = 8, Fig. 4), similar to mammalian AMPARs (Maruo et al., 2006). Summary data of whole-cell current traces following AMPA application are shown in Fig. 5A. Whole-cell AMPAR currents did not change significantly over 80 mins of normoxic perfusion. AMPA currents ranged from 1146 ± 180 pA at t = 10 min to 1122 ± 193 pA at t = 80 mins (n = 9, Fig. 5B). Under hypoxic conditions, AMPAR currents were significantly increased in 6 of 7 patches (P<0.001). AMPAR currents increased on average 30.9 ± 6.1 and 37.9 ± 12.1% at 20 and 40 mins of treatment, respectively, and returned to control levels following 40 mins of reoxygenation (n = 7, Fig 5C). Under anoxic conditions AMPAR currents decreased significantly in all patches by an average of 59.2 ± 5.5 and 60.2 ± 3.5% at 20 and 40 mins of anoxic perfusion, respectively (P<0.001). Following 40 mins of normoxic reperfusion, AMPAR current magnitude was not significantly different from normoxic controls (n = 11, Fig. 5D). AMPA-induced currents were reduced by 93 ± 1.8 % by the AMPAR specific blocker CNQX in normoxia and anoxia (n = 9, Fig. 5B).

The average normoxic EPSC frequency was 4.12 ± 1.14 Hz and this frequency decreased ~50% with anoxic perfusion to 2.03 ± 0.42 Hz (n = 12, Figs. 6A, D-E). The average normoxic EPSC amplitude was 21.8 ± 3.4 pA and this also decreased ~50% with anoxic perfusion to 10.5 ± 1.2 pA (n = 6, Figs. 6A-C). The average normoxic excitatory postsynaptic potential (EPSP) frequency was 1.8 ± 0.4 Hz and this frequency was significantly decreased in all patches by 28.7 ± 6.4% with anoxic perfusion (n = 11, Figs. 7A, C). The average EPSP amplitude was 4.3 ± 0.1 mV and this also decreased significantly during anoxic perfusion in all patches by 13.2 ± 1.7%.

CNQX abolished EPSP firing under normoxic conditions (99.6 ± 0.7% reduction, n = 6, Fig. 7B), suggesting EPSPs are primarily mediated by AMPARs. During anoxia, CNQX significantly depressed EPSP firing by 95.3 ± 2.4% (n = 4). Perfusion of the NMDAR antagonist APV had no effect on EPSP frequency (n = 4, data not shown).

Normoxic and Anoxic whole-cell NMDAR activity. Summary data of whole-cell NMDAR currents are shown in Fig. 8A. NMDAR currents did not change during 80 mins of normoxia, ranging from 1853.7 ± 696 to 1894.5 ± 856 pA at t =0 and 50 mins, respectively (n = 11, Fig. 8B). The anoxic depression in NMDAR activity is well documented (Bickler et al., 2000; Buck and Bickler, 1995; Buck and Bickler, 1998a; Shin and Buck, 2003; Shin et al., 2005), but for the purpose of statistical comparisons was repeated for this paper. NMDAR currents decreased significantly in all patches by an average of 48.6 ± 4.4 % and 54.0 ± 4.3 % following 20 and 40 mins of anoxic perfusion, respectively (P<0.001, n = 5, Fig. 8C). Currents recovered to control levels following 40 mins of reoxygenation. NMDAR currents were abolished by APV (n = 5, Fig. 8B). The anoxic decrease in NMDAR currents was unaffected by AMPAR blockade: NMDAR currents were significantly decreased in all patches by an average of 49.8 ± 7.9 and 48.8 ± 6% at 20 and 40 mins of anoxic perfusion when both the normoxic and anoxic aCSF contained CNQX throughout the experiment (P<0.03, n = 5, Fig. 8E).

2.3. AMPA Figures

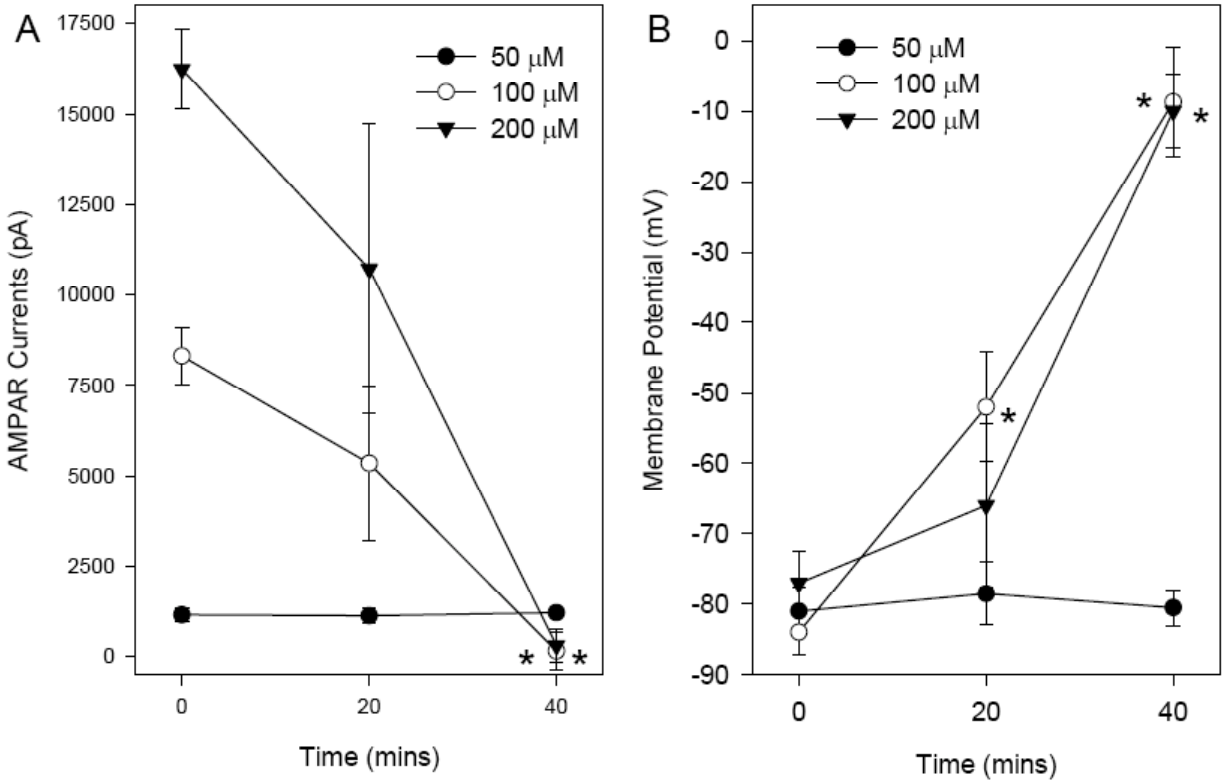

Figure 3. Dose mortality curve of AMPA-elicited peak current.

[AMPA] > 50 μM resulted in diminished AMPA-evoked currents and loss of membrane potential consistent with cell death. (A) Peak current magnitude at 0, 20 and 40 mins of recordings. **(B)** Change in E_m of cells treated with various AMPA doses in Fig. 1A. Asterisks (*) represent values significantly different from corresponding normoxic values ($P<0.05$). Data are represented as mean and standard error of mean (SEM) from 4 to 6 separate experiments.

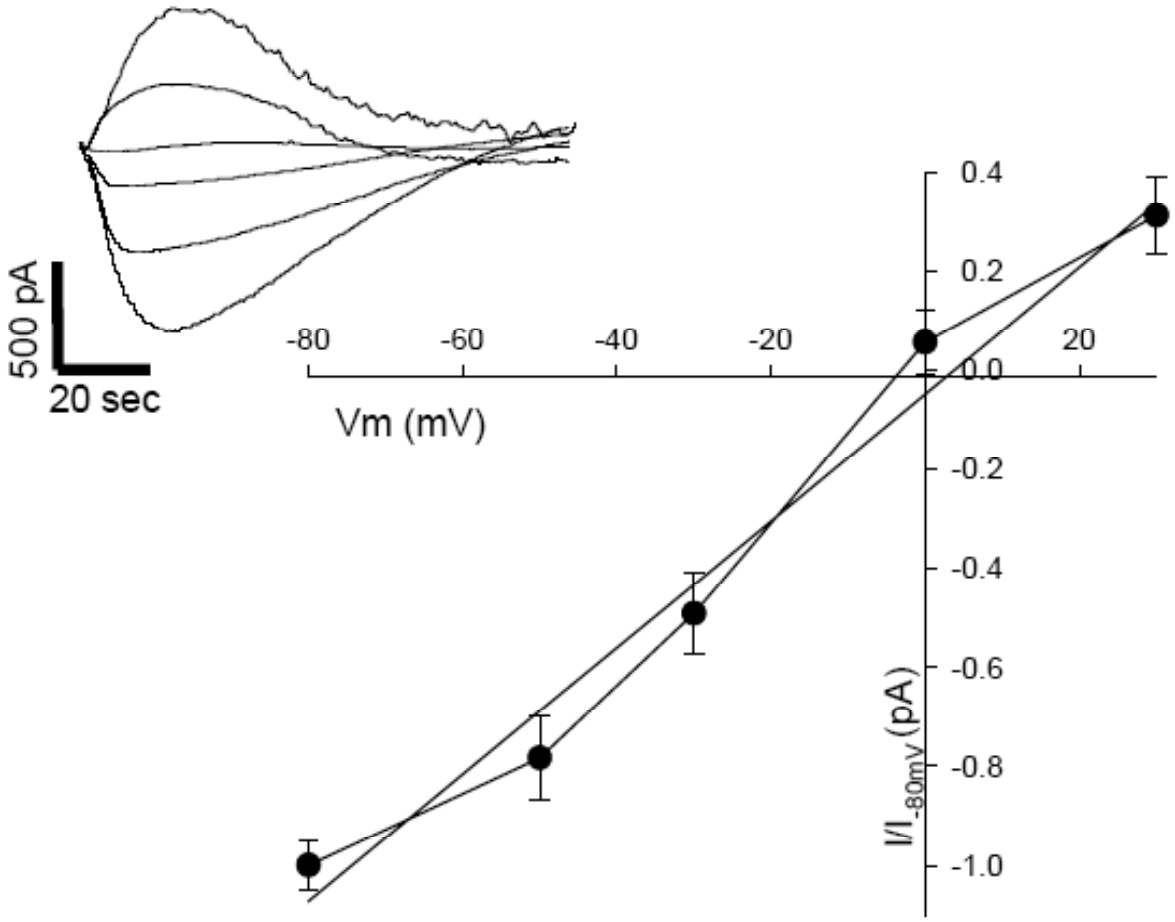

Figure 4. Normoxic current-voltage relationship of AMPA-elicited currents.

Cells were voltage-clamped in 20 or 30 mV steps from -80 to +30 mV and normalized to recordings at -80 mV. All cells were perfused with TTX and APV to prevent APs and NMDAR contamination. Data are represented as mean and standard error of mean (SEM) from 8 separate experiments. The slope conductance was 11.9 ± 0.8 pS.

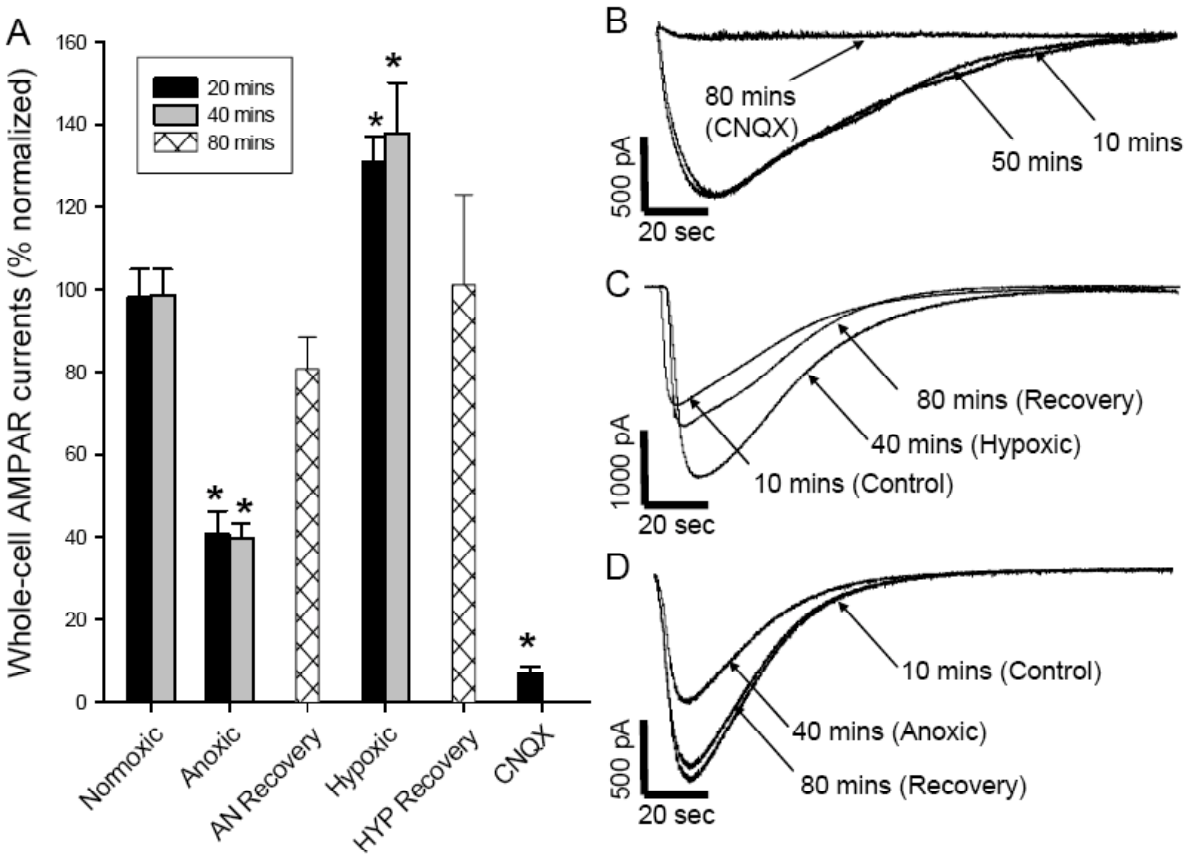

Figure 5. AMPAR whole-cell currents are reversibly decreased by anoxia.

(A) Raw whole-cell AMPA (50 μM) -evoked currents recorded from a single cell undergoing the following treatments **(B)** normoxic perfusion and with and without CNQX, **(C)** normoxic to anoxic transition and recovery, **(D)** normoxic to hypoxic (5% O_2) transition and recovery. All cells were perfused with APV to prevent currents from NMDARs. Asterisks (*) represent values significantly different from corresponding normoxic values ($P<0.05$). Data are represented as mean and standard error of mean (SEM) from 7 to 14 separate experiments.

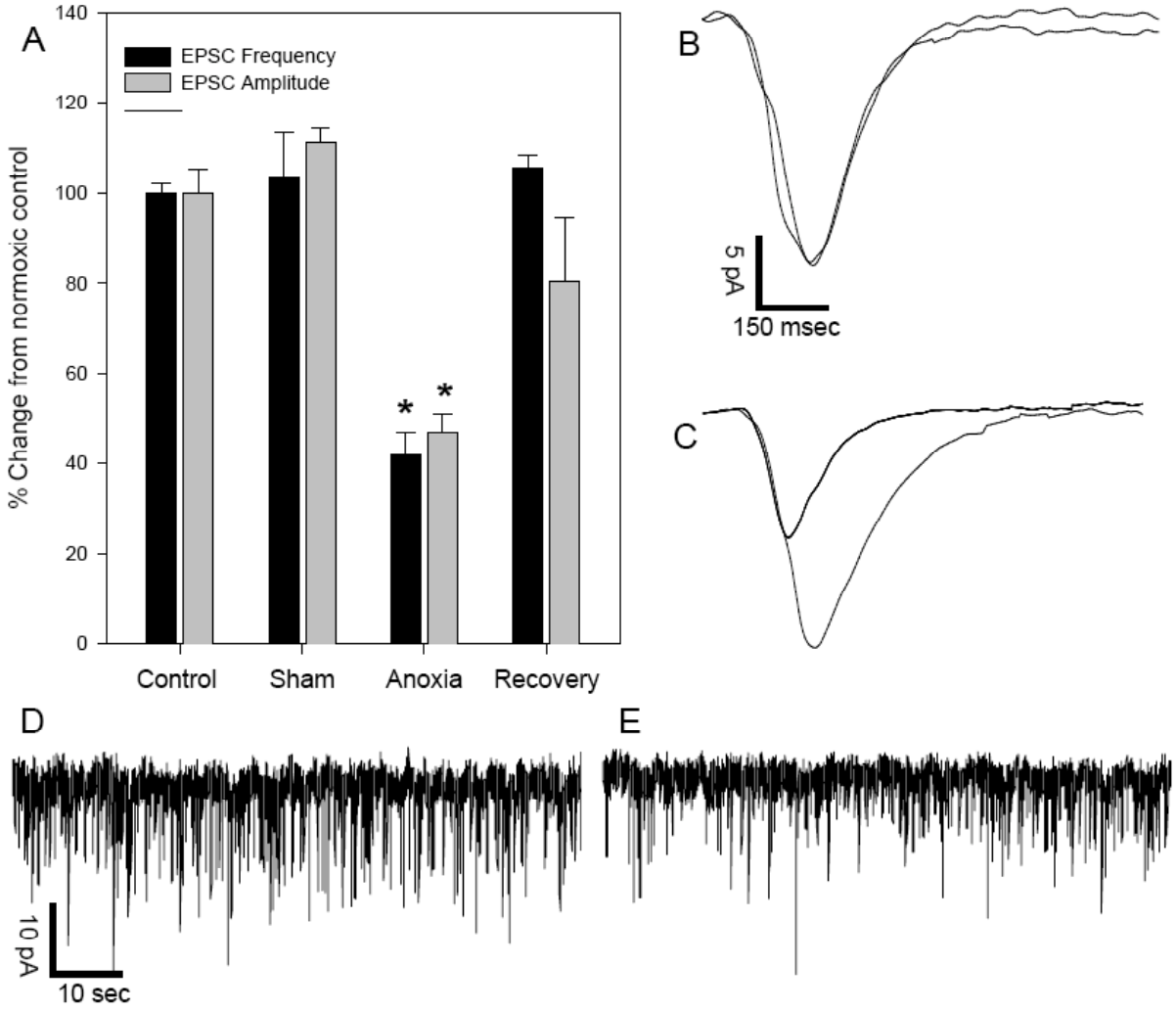

Figure 6. Spontaneous EPSC frequency and amplitude are decreased by anoxia (A).

(B-C) Composite EPSC averages (50 events each) during sham normoxic to normoxic **(B)** and normoxic to anoxic **(C)** transitions in the same cell. **(D-E)** Sample raw EPSC activity from the same neuron under normoxia **(D)** and anoxia **(E)**. Asterisks (*) represent values significantly different from corresponding normoxic values ($P<0.05$). Experiments were conducted in the presence of APV to abolish NMDAR-mediated contributions. Data are represented as mean and standard error of mean (SEM) from 7 separate experiments.

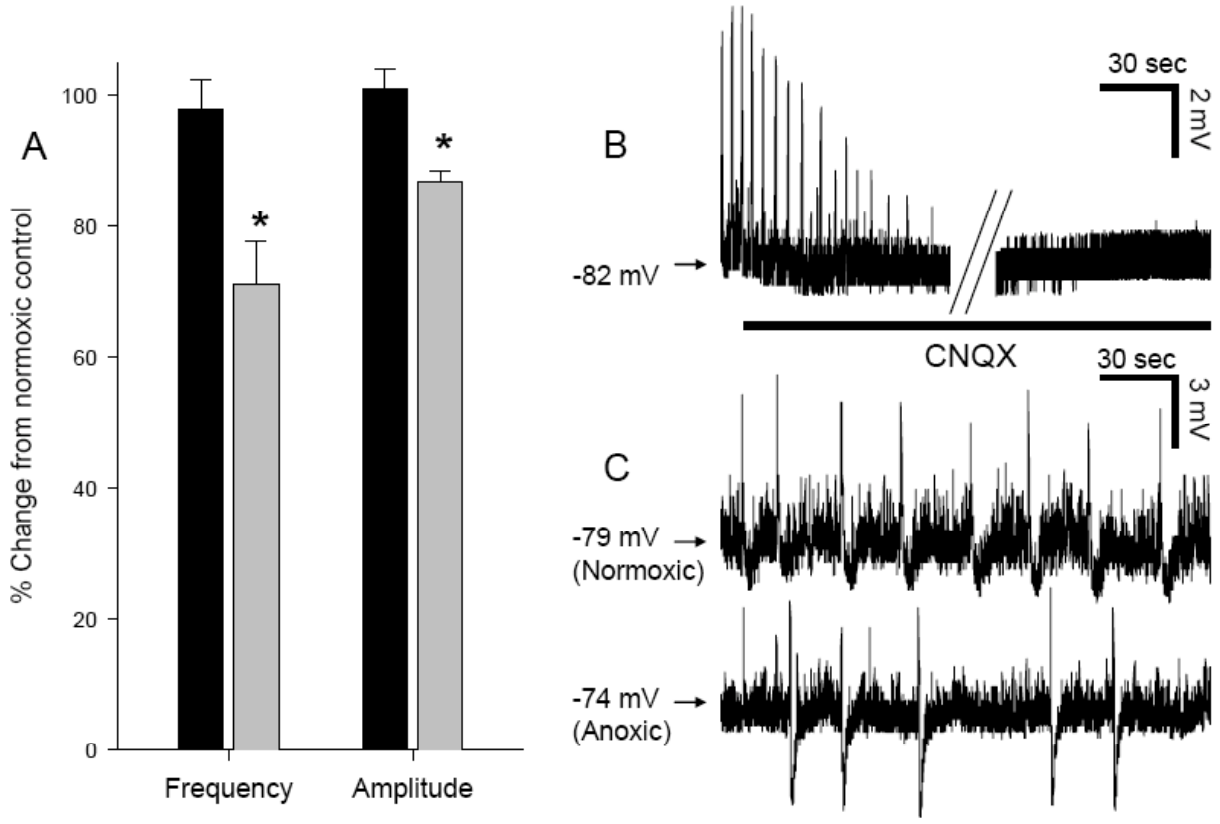

Figure 7. EPSP frequency and amplitude decrease with anoxia.

(A) Summary of normalized EPSP frequencies and amplitudes from cortical neurons 30 mins following sham normoxic to normoxic (black bars) or normoxic to anoxic (grey bars) transitions. **(B)** CNQX abolishes spontaneous EPSP activity (solid line represents duration of CNQX exposure. Note: break represents 5 mins of CNQX perfusion. **(C)** Raw spontaneous EPSP activity from a single cell during a normoxic to anoxic transition. APV was perfused throughout experiments to prevent NMDAR-mediated contamination. Asterisks (*) represent values significantly different from corresponding normoxic values ($P<0.05$). Data are represented as mean and standard error of mean (SEM) from 5 to 11 separate experiments.

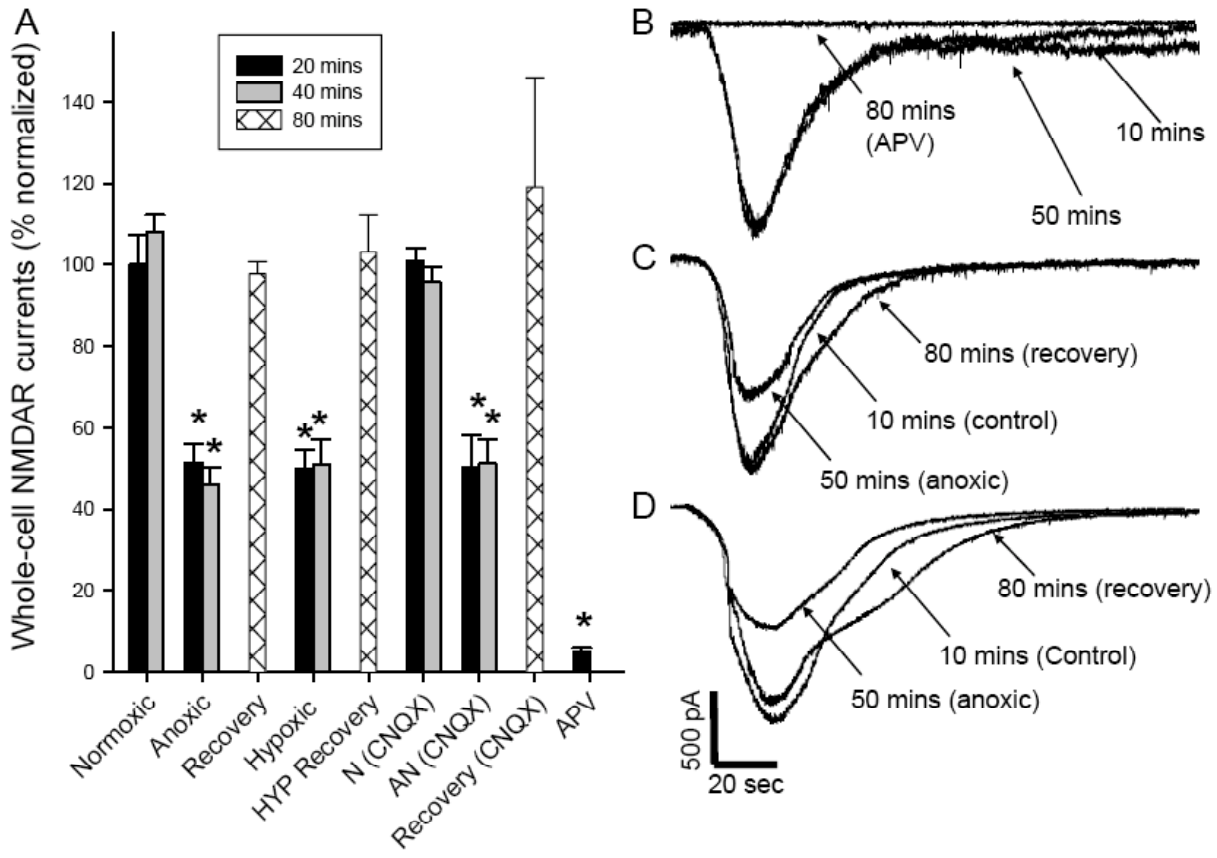

Figure 8. The effect of AMPAR blockade on NMDAR currents.

(A) Summary of normalized NMDA receptor whole-cell currents from turtle cortical neurons undergoing various treatments. Raw whole-cell NMDAR currents recorded from a single cell undergoing the following treatments: **(B)** normoxic perfusion and with APV, **(C)** normoxic to anoxic transition, **(D)** normoxic to anoxic transition with CNQX perfusion throughout the experiment. Asterisks (*) represent values significantly different from corresponding normoxic values ($P<0.05$). Data are represented as mean and standard error of mean (SEM) from 4 to 12 separate experiments.

2.4. Discussion: Anoxic channel arrest of AMPARs

I demonstrate that in the hypoxic (5% O_2) turtle cortex AMPAR currents are significantly potentiated. This potentiation is completely reversed by reoxygenation. Similar responses to hypoxia have been reported in rat hippocampal AMPARs where AMPAR currents isolated from NMDAR-mediated contributions (2 mM Mg^{2+}) have been shown to potentiate 25-80% during short-term hypoxia in rat neurons (Lyubkin et al., 1997; Quintana et al., 2006). However, during prolonged hypoxia, potentiation of AMPAR currents is not observed, suggesting AMPA activity may become suppressed during prolonged oxygen deprivation in mammals (Arai et al., 1990).

Increased AMPAR activity during hypoxia contributes to the hypoxic reorganization of synapses, including the appearance of AMPAR-mediated events at previously silent synapses and increased synthesis of excitatory receptor subunits (Jourdain et al., 2002; Quintana et al., 2006). However, synaptogenesis in this context is not associated with the normal "healthy" function of mammalian neurons during hypoxia and may permanently lower seizure thresholds. Neonatal rats are moderately tolerant to hypoxia compared to adult rats and survive brief periods of hypoxia without cell death (Jensen, 1995). However, in neonatal rats exposed to hypoxia, seizures occur and following the hypoxic episode susceptibility to seizures is permanently increased. Furthermore, cell death occurs following subsequent, previously sub-lethal hypoxic insults (Jensen, 1995; Koh and Jensen, 2001). Blockade of AMPARs but not NMDA receptors prior to the hypoxic insult prevented seizures and the long-term increase in seizure susceptibility (Jensen et al., 1995). If enhanced AMPAR activity leads to formation of new synapses during hypoxia, and mammalian AMPAR blockade prevents permanent hypoxia-mediated decreases in seizure thresholds, then it is logical that the synaptic connections formed during hypoxia may

underlie the permanent reorganization towards a state of increased seizure susceptibility following hypoxic insult in rat brain.

Contrary to mammals, my observation that potentiation of turtle AMPAR currents during hypoxia was not suppressed is intriguing. The turtle is an oxygen conformer: that is, it adapts its metabolic rate in a graded fashion to match available oxygen concentrations and does not simply switch cellular functions on and off (Buck and Pamenter, 2006). Behaviorally, turtles are frequently submerged in normoxic water for prolonged periods in their natural environment. At the tissue level, hypoxic exposure mimics prolonged submergence of the animal in normoxic water during foraging, feeding and to escape predation. Indeed, turtles are able to extract oxygen from water while they are submerged via oxygen diffusion across exposed skin surfaces (primarily the cloacae), and thus during prolonged dives or while over-wintering they likely undergo long periods of falling oxygen levels as the oxygen content of ice-covered ponds slowly dissipates (Ultsch and Jackson, 1982).

A number of the protective systems utilized by the turtle brain to survive anoxia are also up- or down-regulated during hypoxia to a different degree, including elevations in the rate of glycolysis and the putative O_2 sensor neuroglobin, and decreases in Ca^{2+} uptake and metabolic rate (Bickler et al., 2004; Costanzo et al., 2001; Hicks and Wang, 1999; Hochachka et al., 1996; Kelly and Storey, 1988; Milton et al., 2006). This suggests the turtle is able to respond rapidly and appropriately to various oxygen tensions and unlike most mammals, is able to match its energy demand to supply under metabolically compromising hypoxic conditions. For the turtle, prolonged submergence is likely a very common situation, and tolerance of intermittent hypoxia may not require deep depression of neural functions compared to the metabolically challenging anoxic environment. Therefore, it is possible that the continued potentiation of turtle AMPAR

activity during hypoxia serves a specific signaling mechanism to activate systems that will later be protective against anoxia, and that this potentiation is sustainable without detriment to the turtle brain.

During anoxia, it is beneficial to reduce energy demands to a low level. Therefore, it is logical that turtle AMPAR activity is reduced during anoxia to decrease general electrical excitability and energetically expensive protein synthesis associated with synaptogenesis. My experiments support this hypothesis. Anoxia decreased evoked peak AMPAR currents and spontaneous AMPA-mediated EPSC amplitude significantly, and these currents recovered to control levels following reoxygenation. Spontaneous AMPAR-mediated EPSP activity was also depressed by anoxia. Decreases in the frequency and amplitude of EPSPs and EPSCs reduce the overall excitability of a neuron; therefore reduced EPSP activity and magnitude due to decreased AMPAR currents may contribute to electrical depression in the anoxic turtle cortex (Perez-Pinzon et al., 1992a). Channel arrest of AMPARs and subsequent electrical depression preserve cellular energy stores as they reduce ion leakage across the membrane and thus reduce the workload of energetically expensive ion pumps. It is not surprising that AMPARs would undergo channel arrest in the anoxic turtle cortex as numerous studies have identified incidences of channel arrest in this organism, including NMDARs, K^+ channels and the Na^+/K^+ ATPase, whose activity decreases 31-34% in the anoxic turtle brain (Buck and Bickler, 1995; Chih et al., 1989b; Hylland et al., 1997).

AMPAR activity may also decrease the activity of NMDARs in the anoxic turtle cortex. There is some evidence to suggest that NMDARs and AMPARs communicate via a mechanism separate from the voltage-based removal of the NMDAR Mg^{2+} block. In rat hippocampal slices, modulation of AMPARs results in *inverse* changes in NMDAR currents via a mechanism that is

voltage and Ca^{2+} independent (Bai et al., 2002). These authors suggested that since both receptors are stimulated by the same endogenous ligand (glutamate), it is beneficial for the receptors to regulate each other's activity such that a large potentiation of AMPAR currents, as occurs under hypoxic conditions, subsequently decreases NMDAR currents or vice-versa. In the hypoxic turtle brain where I observed enhanced AMPAR activity, such a mechanism might initially depress NMDAR currents until broader second messenger-based systems are initiated. To determine if AMPARs mediate the previously reported depression of NMDAR activity I exposed cells to a normoxic to anoxic transition under constant CNQX application. NMDAR currents were reversibly depressed by anoxia and the magnitude of this depression was not different from that observed in anoxic experiments without CNQX. Although decreased AMPAR activity does not appear to directly regulate NMDAR excitability, depressed AMPAR currents would nonetheless reduce NMDAR activity. Since AMPAR-mediated depolarization removes the Mg^{2+} block from the pore of the NMDAR, a reduction in AMPAR current, $EPSP_f$ and amplitude would reduce NMDAR activity in the anoxic turtle cortex. NMDAR activity is reduced by up to 65% following 20 mins of anoxic perfusion (Buck and Bickler, 1998a), and 60% of the receptors are reversibly removed from the cell membrane during weeks of anoxia (Bickler et al., 2000). Therefore under prolonged anoxia, NMDAR activity may be reduced by >85%. A reduction in the AMPAR-mediated excitation of neuronal membranes upstream of NMDAR activation would likely enhance the turtle's already substantial suppression of NMDA receptors and subsequent avoidance of glutamate-receptor mediated ECD during anoxia.

In summary, my data indicate that turtle AMPARs undergo channel arrest during anoxic episodes. Other than the NMDA receptor, this in the only channel in which channel arrest has been measured directly in any organism. Decreased AMPAergic excitability may help to prevent

ECD in the cortex of the anoxia-tolerant freshwater turtle as well as in the anoxia-intolerant mammal. Therefore, understanding how the turtle cortex is able to regulate AMPARs during anoxia may provide insight into neuroprotective mechanisms of AMPAR regulation in mammalian models of stroke.

3. Regulation of NMDARs

3.1. Mitochondrial ATP-sensitive K^+ channels regulate NMDAR activity in the cortex of the anoxic turtle

Preface

A modified version of this chapter was published as: Pamenter ME, Shin DS, Cooray M and Buck LT (2008). Mitochondrial ATP-sensitive K^+ channels regulate NMDAR activity in the cortex of the anoxic turtle. *J. Physiol.* 586:1043-1058.

I hypothesized that mK_{ATP} channels and mitochondrial uncoupling underlie the anoxic changes in Ca^{2+} and NMDAR activity in the turtle cortex and designed the experiments for this work. D Shin performed 10% of the whole-cell NMDAR experiments and assisted with confocal microscope imaging of fixed turtle brain sheets. M Cooray and L Buck performed all experiments on isolated mitochondria. I performed the remainder of the whole-cell experiments, all live-cell imaging experiments and tissue fixation and imaging. I wrote the paper with editing by L Buck.

Abstract

The freshwater turtle's anoxic survival is possibly mediated by a decrease in NMDAR activity and maintenance of cellular calcium concentrations ($[Ca^{2+}]_c$) within a narrow range during anoxia. In mammalian ischemic models, activation of mitochondrial ATP-sensitive K^+ channels (mK_{ATP}) partially uncouples mitochondria resulting in a moderate increase in $[Ca^{2+}]_c$ and neuroprotection. The aim of this study was to determine the role of mK_{ATP} in anoxic turtle NMDAR regulation and if mitochondrial uncoupling and $[Ca^{2+}]_c$ underlie this regulation. In isolated mitochondria, the K_{ATP} channel activators diazoxide and levcromakalim increased mitochondrial respiration and decreased ATP production rates, indicating mitochondria were 'mildly' uncoupled by 10-20%. The mK_{ATP} antagonist 5-hydroxydecanoic acid (5HD) blocked these changes. During anoxia, $[Ca^{2+}]_c$ increased 9.3 ± 0.3% and NMDAR currents decreased 48.9 ± 4.1%. These changes were abolished by: K_{ATP} blockade with 5HD or glibenclamide, $[Ca^{2+}]_c$ chelation with 1,2-bis(o-aminophenoxy)ethane-N,N,N',N'-tetraacetic acid (BAPTA) or by activation of the MCU with spermine. Similar to anoxia, diazoxide or levcromakalim increased $[Ca^{2+}]_c$ 8.9 ± 0.7% and 3.8 ± 0.3%, while decreasing normoxic whole-cell NMDAR currents by 41.1 ± 6.7% and 55.4 ± 10.2%, respectively. These changes were also blocked by 5HD or glibenclamide, BAPTA, or spermine. Blockade of mitochondrial Ca^{2+}-uptake decreased normoxic NMDAR currents 47.0 ± 3.1% and this change was blocked by BAPTA but not by 5HD. Taken together, these data suggest mK_{ATP} activation in the anoxic turtle cortex uncouples mitochondria and reduces mitochondrial Ca^{2+} uptake via the uniporter, subsequently increasing $[Ca^{2+}]_c$ and decreasing NMDAR activity.

3.1.1. Introduction: the 'mild uncoupling' hypothesis

There is growing consensus that IPC-induced protection is mediated by the partial uncoupling of the mitochondrial H^+ gradient following the activation of mK_{ATP} channels. In particular, mK_{ATP}-mediated neuroprotection has been shown in cultured rat cortical neurons exposed to glutamate toxicity (Kis et al., 2004; Kis et al., 2003); following cerebral artery occlusion in rats (Shimizu et al., 2002); in rat hippocampal and cortical neurons following anoxia/reperfusion injury (Heurteaux et al., 1995; Semenov, 2000); and in anoxic juvenile mouse brainstem (Muller et al., 2002). Opening of mK_{ATP} increases mitochondrial G_K, mildly uncoupling Ψ_m (Holmuhamedov, 1999). This potential drives the MCU and thus mitochondrial Ca^{2+} uptake. In rat cortical slices blockade of the MCU decreases NMDAR activity and reduces glutamate-induced Ca^{2+} influx (Kannurpatti, 2000). Thus NMDAR activity has been linked to mitochondrial Ca^{2+} uptake and mK_{ATP} to the regulation of this uptake.

In the anoxic turtle cortex a small increase in $[Ca^{2+}]_c$ attenuates turtle NMDAR activity and prevents larger lethal increases in $[Ca^{2+}]_c$ (Bickler et al., 2000). Similarly, a mild elevation in rat hippocampal $[Ca^{2+}]_c$ was neuroprotective against subsequent ischemic insults, preventing toxic accumulation of $[Ca^{2+}]_c$ and reducing cell death (Bickler and Fahlman, 2004). I hypothesize that activation of mK_{ATP} channels partially uncouples the mitochondrial H^+ gradient, decreases the activity of the MCU and subsequently impairs mitochondrial Ca^{2+} uptake, mildly elevates $[Ca^{2+}]_c$ and attenuates NMDAR activity in the turtle cortex. The aims of this chapter are to determine 1) whether mK_{ATP} are present in turtle mitochondria, 2) if activation of these channels uncouples mitochondria, 3) if mK_{ATP} can regulate NMDA receptor activity in the normoxic turtle cortex, 4) if mK_{ATP} activity underlies the anoxic decrease in NMDA receptor activity, and 5) whether effects of mK_{ATP} activity on NMDA receptor currents are Ca^{2+}-dependent.

3.1.2. Results: mK_{ATP} channels regulate $[Ca^{2+}]_c$ and NMDARs via "mild uncoupling" of mitochondria

mK_{ATP} channels are present in the anoxic turtle cortex. Turtle cortical sheets were stained using the live-cell fluorophores BODIPY-glibenclamide (K_{ATP} probe, Figs. 9C, F) and mitotracker deep red (mitochondrial probe, Figs. 9D, G). Pyramidal cells were visualized on a confocal microscope. Overlays of the two stains are shown in Figs. 9E, H. To my knowledge this is the first time that mK_{ATP} channels have been imaged in an intact brain slice from any organism.

Activation of mK_{ATP} channels 'mildly' uncouples mitochondria. K^+ channel openers increase mitochondrial G_K, mildly uncoupling the mammalian mitochondrial inner membrane potential and accelerating O_2 respiration (Garlid et al., 1997). The effects of K^+ channel openers have not been previously studied in turtle mitochondria. I measured O_2 consumption as an indicator of mitochondrial activity and to evaluate the specificity of the pharmacological treatments used in the whole-cell experiments to mitochondrial ion channels. For mitochondrial experiments the average respiratory control ratio (RCR) was 10.8 ± 0.7. Activation of mK_{ATP} channels with the general K_{ATP} channel agonist levcromakalim (100 μM) or the mK_{ATP} channel specific agonist diazoxide (100 μM) increased O_2 respiratory rate 21.6 ± 4.0% and 88.6 ± 9.3% respectively (n = 6 and 23 respectively, Figs. 10A, B, E). These effects were blocked by 100 μM 5-hydroxydecanoic acid (5HD: a mK_{ATP}-specific antagonist) (n = 10 for diazoxide + 5HD; n = 5 for levcromakalim + 5HD, Figs. 10C, F).

The K^+ channel ionophore valinomycin (5 μM) was added to the mitochondrial preparation to artificially increase mG_K. Valinomycin addition resulted in a 413.9 ± 61.1%

increase in respiration rate (n = 8, Fig. 10D). Subsequent application of diazoxide to cells treated with valinomycin did not further increase respiration rate (n = 6, Fig. 10D). Since the effects of valinomycin and diazoxide were not additive, diazoxide and valinomycin likely caused mitochondrial uncoupling via a similar mechanism, which is increased mitochondrial G_K. NS1619 (50 μM), which opens mK_{Ca} channels was applied to further examine the role of increased mitochondrial G_K in uncoupling mitochondria. NS1619 increased the respiration rate by 73.8 ± 13.9% (n = 6, Fig. 10G). As a positive control, complete uncoupling of the mitochondria with the protonophore dinitrophenol (DNP: 10 mM) resulted in a 760.2 ± 135.1% increase in respiration rate (data not shown, n = 8). If DNP is considered to completely uncouple mitochondrial respiration then the uncoupling effect of mK_{ATP} activation with diazoxide is about 9.7% of the overall rate of O_2 consumption.

Activation of mK_{ATP} channels reduces the rate of mitochondrial ATP production. The rate of mitochondrial ATP production was used as a second measure of mitochondrial uncoupling. ADP was added to isolated mitochondria to initiate state III respiration and the sample was allowed to respire until state IV respiration was achieved. Once a new steady state had been reached, diazoxide was added to the mitochondria to open mK_{ATP} channels and a second amount of ADP was added to the mitochondria (Fig. 11A). Results were compared to double ADP addition experiments without the addition of diazoxide between substrate additions. In mitochondria with diazoxide, oxygen consumption rates decreased by 22.6 ± 1.6% while the time required for the mitochondria to utilize the available ADP for ATP production increased by 50.4 ± 20.5% (n = 9, Fig. 11B).

Activation of mK_{ATP} channels alters $[Ca^{2+}]_c$. A small elevation of $[Ca^{2+}]_c$ is central to the anoxic attenuation of turtle NMDAR activity, but its source is not known (Bickler et al., 2000;

Shin et al., 2005). Mitochondrial Ca^{2+} uptake occurs primarily via the MCU, which is driven by the electrochemical gradient across the mitochondrial inner membrane. Therefore, uncoupling of mitochondria should impair mitochondrial Ca^{2+} handling by reducing the driving force on the MCU. Since mitochondria are major Ca^{2+} buffers in the cell, decreases in mitochondrial Ca^{2+} uptake should cause elevations in $[Ca^{2+}]_c$. In turtle cortical slices $[Ca^{2+}]_c$ did not change during normoxia, but increased during anoxic perfusion by 9.4 ± 0.3% (*n* = 5, 7, Figs. 12A-C). This effect was reversed by reperfusion with normoxic aCSF. The anoxic increase in $[Ca^{2+}]_c$ was blocked by 5HD (*n* = 4, Figs. 12A, E). Furthermore, normoxic perfusion of diazoxide or levcromakalim induced elevations in $[Ca^{2+}]_c$ of 8.9 ± 0.7% and 3.8 ± 0.3%, respectively (*n* = 3 for each, Figs. 12A, F, H). These increases were reversed by drug washout and prevented by simultaneous perfusion with 5HD (*n* = 3 for each, Figs. 12A, G, I). To determine if the source of the $[Ca^{2+}]_c$ was intra- or extracellular, slices were perfused with anoxic aCSF with 0 $[Ca^{2+}]$ and 5 mM EGTA. In these experiments anoxia resulted in an increase in $[Ca^{2+}]_c$ of 10.5 ± 0.7%, indicating the source of the anoxic elevation of $[Ca^{2+}]_c$ is cellular and not due to Ca^{2+} entry from extracellular sources (*n* = 4, Figs. 12A, D).

mK_{ATP} channels underlie the anoxic change in NMDAR currents. I examined the role of both mitochondrial and plasmalemmal K_{ATP} (pK_{ATP}) and mK_{Ca}^{2+} channels in regulating NMDAR activity using whole-cell voltage-clamp recordings from turtle cortical pyramidal neurons. During 50 mins of normoxic perfusion turtle NMDAR currents did not change, but decreased 48.9 ± 4.1 and 54 ± 5.2% at 30 and 50 mins of anoxia, respectively (*n* = 10 for each, Figs. 13A, C-D). During normoxia, activation of mK_{ATP} channels with the levcromakalim decreased whole-cell NMDAR currents 39.4 ± 3.1 and 49.7 ± 6.7% at 30 and 50 mins, respectively (*n* = 9, Figs. 13A, E). Diazoxide (350 μM) perfusion resulted in a similar decrease in NMDAR activity of

43.8 ± 10.0 and 41.1 ± 6.7% at 30 and 50 mins, respectively (n = 7, Figs. 13A, F). Similar results were seen at lower concentrations of diazoxide (100 μM), which decreased NMDAR currents 40.5 ± 10% after 50 mins perfusion (n = 10, Fig. 13B). At 10 μM, diazoxide had no effect on NMDAR currents (n = 4). The diazoxide-mediated decreases were not statistically different from the anoxic decrease in NMDAR activity (P>0.001). The effect of both levcromakalim and diazoxide was abolished by perfusion of the general K_{ATP} antagonist glibenclamide or by 5HD (n = 8, 6 respectively, Figs. 13A, G). During anoxia, the decrease in NMDAR currents was abolished by mK_{ATP} channel blockade with glibenclamide or 5HD (n = 10, 8 respectively, Figs. 13A, H, I).

Diazoxide can also inhibit succinate dehydrogenase (SDH) activity at high concentrations (Busija et al., 2005; Schafer et al., 1969). To determine whether SDH inhibition decreased NMDAR activity the effect of the specific SDH inhibitor malonate on NMDAR activity was examined. Perfusion of 5 mM malonate during normoxic recording did not alter NMDAR activity (n = 7, Fig. 13J). In another experiment, cells were initially exposed to malonate and subsequently to diazoxide. In these experiments malonate had no effect on NMDAR currents but diazoxide application reduced normoxic NMDAR currents by 47.1 ± 16.1% (n = 5, Fig. 13A). As an additional control, isolated mitochondria were perfused with malonate. Malonate did not significantly change mitochondrial respiration rate in state IV mitochondria (n = 6), but significantly decreased the rate of O_2 consumption by 74.8 ± 8.1% in state III mitochondria (n = 10, data not shown). Diazoxide also decreased state III respiration rates by 37.3 ± 2.1% (n = 7, data not shown) and this decrease was not blocked by 5HD (n = 5, data not shown). Taken together, these data suggest that the inhibition of SDH by diazoxide occurs primarily during state III respiration and does not affect the regulation of coupled mitochondria.

Mitochondrial K_{ATP} and not plasmalemmal K_{ATP} channels underlie the anoxic change in NMDAR currents. To examine the role of pK_{ATP} channels on NMDAR currents, I dialyzed ATP out of the cytosol to a nominal concentration using patch electrodes filled with ISCF containing 0 [ATP]. Over the course of several hours (data shown up to 50 mins), ATP dialysis did not alter NMDAR activity during normoxic perfusion, nor did it affect the anoxic-mediated decrease in NMDAR activity (n = 7, 8 respectively, Fig. 14). Importantly, application of diazoxide to ATP-dialyzed cells resulted in a decrease in NMDAR activity of 40.8 ± 6.2% (n = 6, Fig. 14). This decrease was statistically similar to the pharmacological activation of mK_{ATP} at normal $[ATP]_c$.

To confirm that the mK_{ATP}-mediated decrease of NMDAR activity was due to a change in mitochondrial G_K, I studied the effect of mK_{Ca}^{2+} modulation on normoxic NMDAR activity. Activation of these channels increased mitochondrial G_K in a similar fashion to mK_{ATP} activation. Administration of the mK_{Ca}^{2+} agonist NS1619 caused a decrease in NMDAR activity of 51.7 ± 8.4 and 50.0 ± 6.5% at 30 and 50 mins of NS1619 perfusion, respectively, similar to mK_{ATP} activation (n = 11, Fig. 15). The mK_{Ca}^{2+}-mediated decrease in NMDAR currents was blocked by the K_{Ca}^{2+} antagonist paxilline (1 μM), but not by 5HD (n = 4, 3 respectively, Fig. 15). In addition, the mK_{ATP}-mediated decrease in NMDAR activity due to diazoxide application was not prevented by mK_{Ca}^{2+} blockade with paxilline (n = 3, Fig. 15). To confirm the role of K^+ channels in this response, a set of experiments were performed using the general K^+ channel blocker cesium (1.2 mM). Cesium perfusion had no effect on normoxic NMDAR activity, but did prevent the anoxic decrease in whole-cell NMDAR currents supporting the hypothesis that increased mitochondrial G_K underlies the anoxic regulation of NMDAR activity (n = 7, 8 respectively, Fig. 15).

Other Ca^{2+} sources. Chelation of $[Ca^{2+}]_c$ with 5 mM BAPTA prevented the anoxic decrease in NMDAR currents, confirming that the anoxic decrease in NMDAR activity is mediated by Ca^{2+} (n = 8, Fig. 16). The primary cellular sources of Ca^{2+} are the endoplasmic reticulum (ER) and mitochondria. To examine the role of Ca^{2+} from ER stores in NMDAR regulation ER Ca^{2+} release was blocked by inhibiting the ryanodine receptor (with 10 μM ryanodine, n = 7) or the ER Ca^{2+}-ATPase (ERCA: with 1 μM thapsigargin, n = 10). In both cases, inhibition had no effect on normoxic NMDAR currents. Furthermore, this blockade did not prevent the anoxic decrease in NMDAR activity (n = 3 for each). To determine if mitochondrial uncoupling affects normoxic NMDAR activity by Ca^{2+} modulation, diazoxide was co-applied in the presence of BAPTA. Chelation of $[Ca^{2+}]_c$ prevented the diazoxide-mediated decrease of normoxic NMDAR currents (n = 8, Fig. 16), implicating mitochondrial Ca^{2+} handling as a regulatory link between anoxic activation of mK_{ATP} channels and subsequent reductions in NMDAR activity.

The MCU underlies anoxic changes in $[Ca^{2+}]_c$. Mitochondrial uncoupling inhibits the MCU and direct blockade of the MCU with 40 nM ruthenium red resulted in a decrease in normoxic NMDAR currents of 44.4 ± 5.3 and 47.1 ± 9.1% at 30 and 50 mins, respectively (n = 7, Fig. 17). This decrease was blocked by BAPTA but not by 5HD, indicating the decrease is Ca^{2+}-mediated and downstream of mK_{ATP} activation (n = 6 for each, Fig. 17). Spermine (500 μM) is a known activator of the MCU. Perfusion of this polyamine had no effect on peak normoxic NMDAR currents but abolished the anoxic and diazoxide-mediated decreases in NMDAR activity (n = 5 for each, Fig. 17).

Spermine is both an activator of the MCU (Sparagna et al., 1995; Zhang et al., 2006) and, at higher concentrations, a potentiator of NMDAR currents (Takano et al., 2005). To ensure that

spermine was not involved in NMDAR potentiation I performed normoxic control experiments with 500 μM and 2.5 mM spermine. At the lower concentration I found no significant potentiation of NMDAR activity (Fig. 17). At the higher concentration, only two out of 9 recorded neurons showed potentiation. Since potentiation was rarely seen, even at higher spermine concentrations, I can exclude the possibility that spermine directly potentiated NMDAR activity in my experiments.

3.1.3. Figures

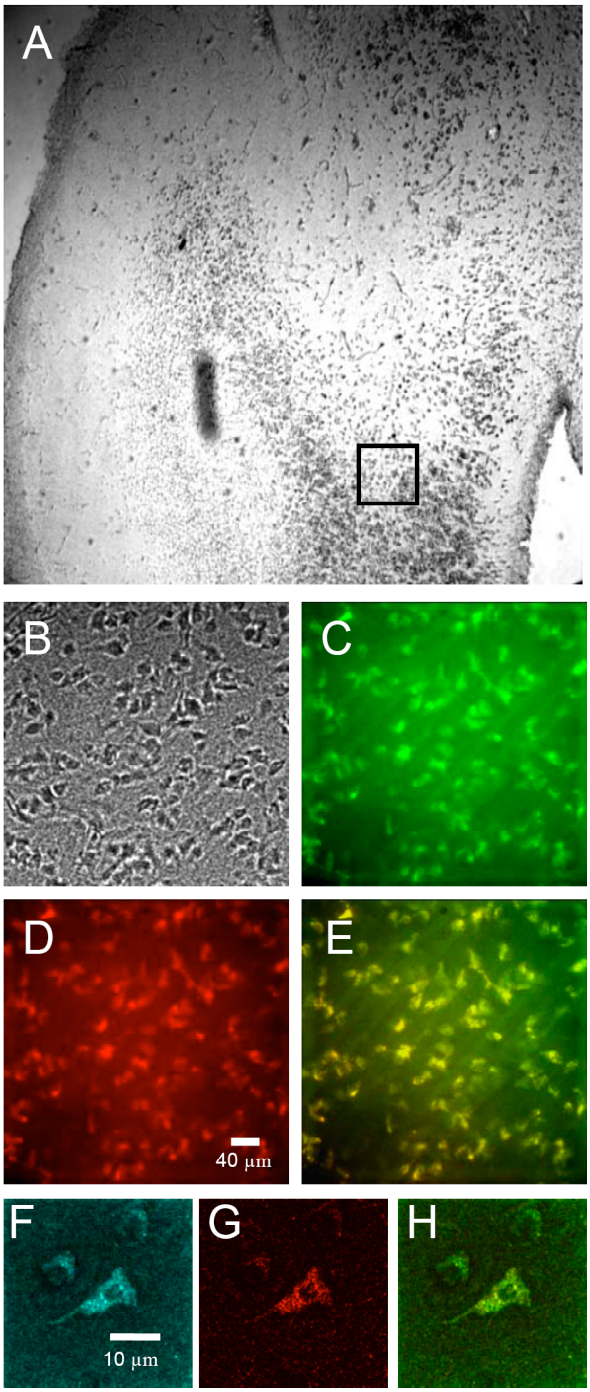

Figure 9. K_{ATP} channels in the turtle cortex.

(**A**) Turtle cortical sheet (4x magnification). (B-E) are boxed region in (A) at 40x magnification. **(F-H)** are a single neuron at 100x magnification. **(B)** shows a bright field image of the cortical sheet. **(C and F**) show BODIPY-glibenclamide staining to visualize K_{ATP} channels, **(D and G)** show MitoTracker Deep Red to stain mitochondria. Images were overlaid to show colocalization between mitochondria and mK_{ATP} channels **(E and H)**.

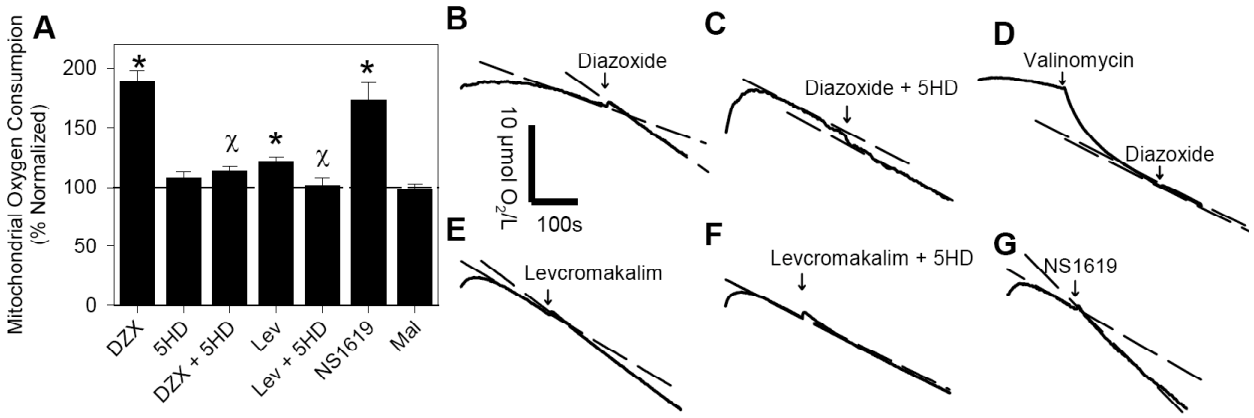

Figure 10. K_{ATP} activation uncouples state IV mitochondrial respiration.

(A) Percent normalized mitochondrial respiration rates following treatment. Dashed line represents control rate of oxygen consumption before drug application. Symbols indicate data significantly different from normoxic controls (*) or drug treatment controls (χ). Data are expressed as mean +/- SEM. **(B-G)** Sample oxygen consumption curves. Arrows indicate the addition of pharmacological treatments to state IV respiring mitochondria. Dotted lines represent the slopes used to determine changes in rate before and after treatment. Abbreviations: diazoxide (DZX), levcromakalim (Lev), malonate (Mal), 5-hydroxydecanoic acid (5HD).

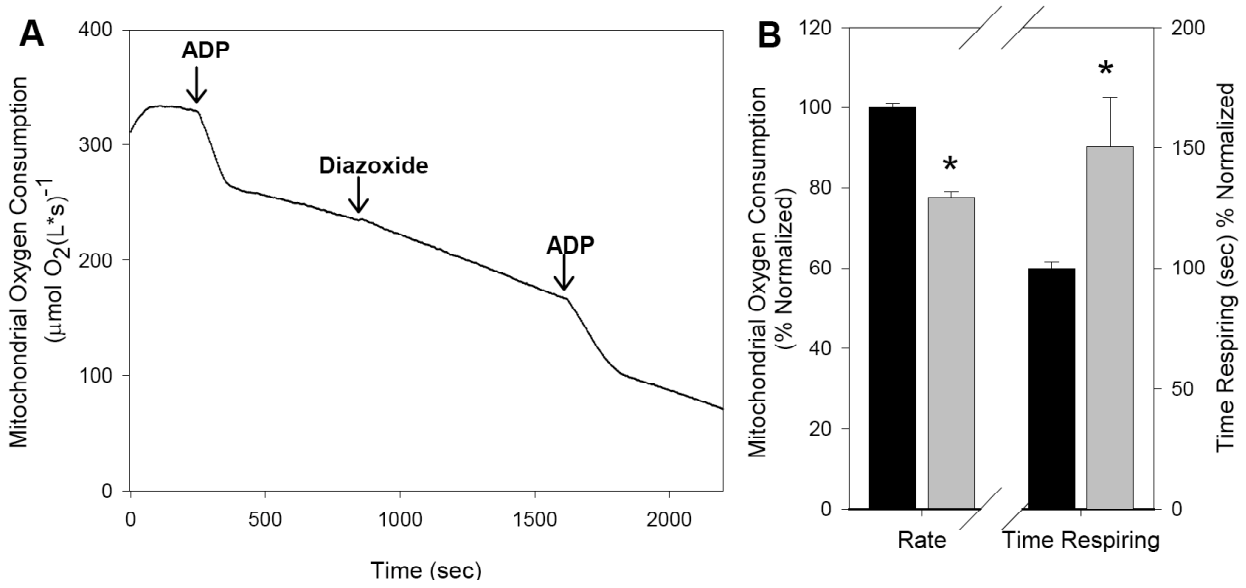

Figure 11. mK_{ATP}-mediated mitochondrial uncoupling decreases ATP production.

(A) A representative experiment. Arrows indicate addition of substrate (ADP) or diazoxide. The resulting change in rate and the time before respiration returns to baseline was measured and compared to experiments without diazoxide addition. **(B)** Graph showing mean changes in oxygen consumption rates and total state III respiration time. Black bar represents control without diazoxide, grey bar represents oxygen consumption with diazoxide. (*) indicates data significantly different from control values. Data are presented as mean +/- SEM.

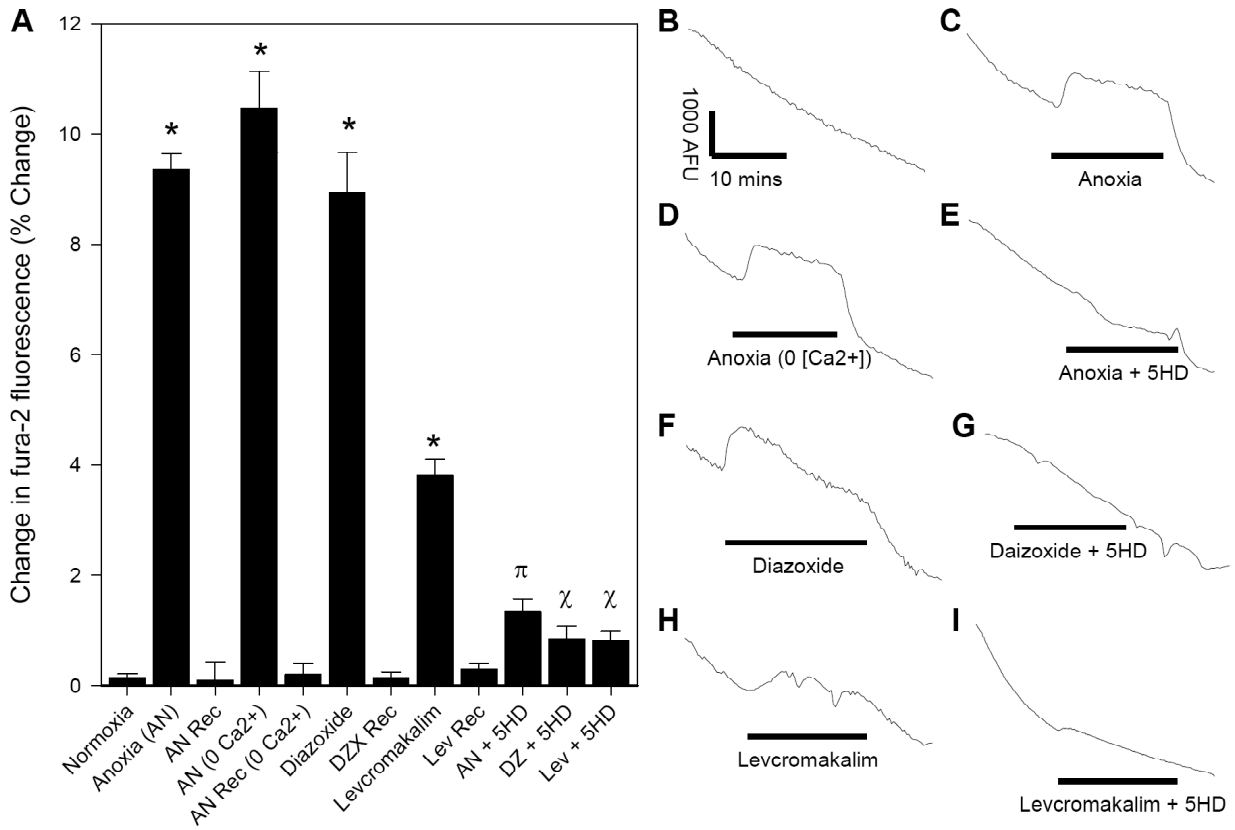

Figure 12. $[Ca^{2+}]_c$ increases during anoxia and following mitochondrial uncoupling.

(A) Percent normalized changes in fura-2 calcium fluorescence at 1 min post-treatment. Symbols indicate data significantly different from normoxic control (*), anoxic control (π), or drug treatment control (χ). Data are expressed as mean +/- SEM. **(B-I)** Raw data traces of fura-2 calcium fluorescence $[Ca^{2+}]_c$ from neurons treated as indicated. AFU = Arbitrary Fluorescence Units. Abbreviations: diazoxide (DZX), levcromakalim (Lev), anoxia (AN), 5-hydroxydecanoic acid (5HD).

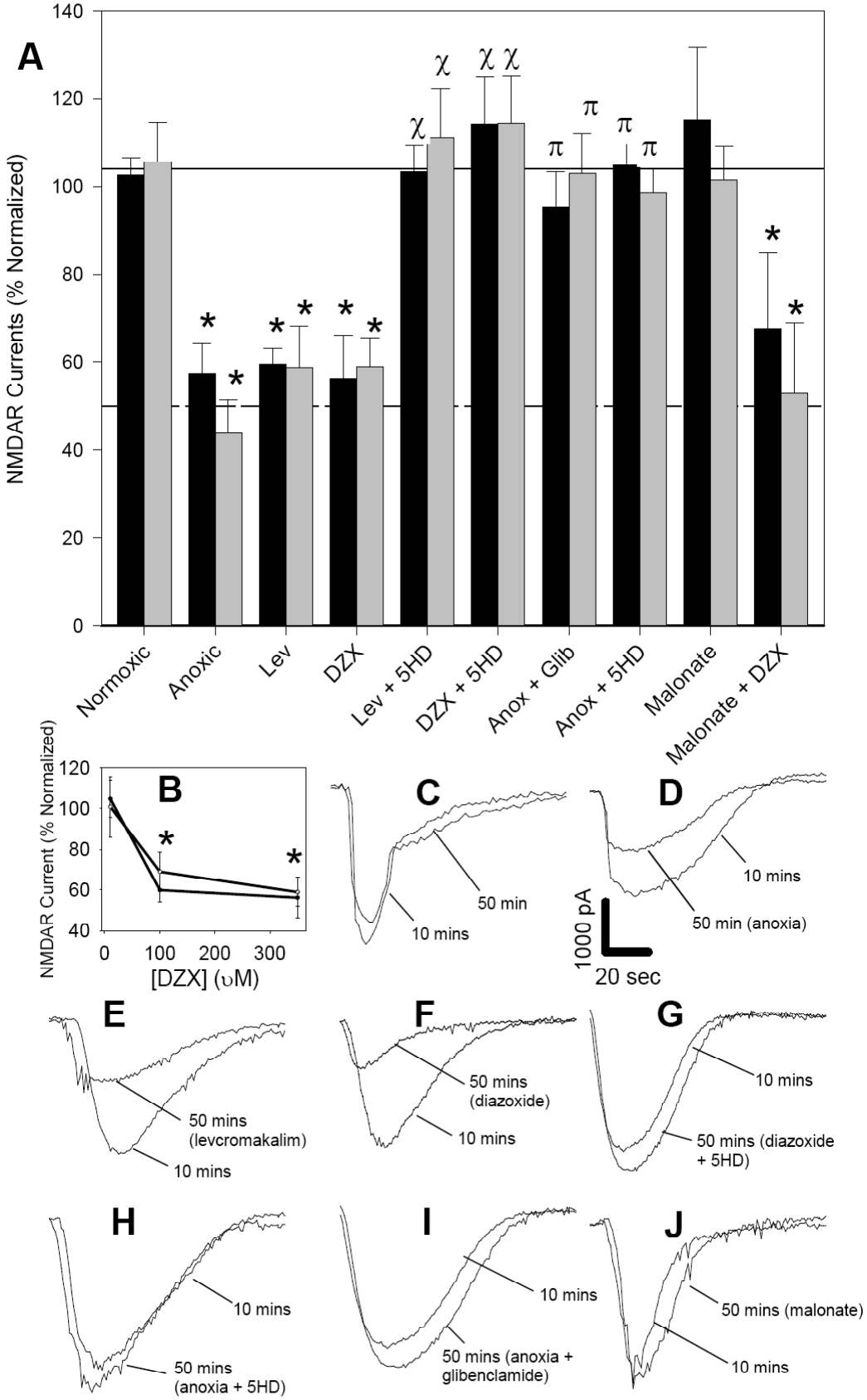
A
NMDAR Currents (% Normalized)
140
120
100
80
60
40
20
0
Normoxic
Anoxic
Lev
DZX
Lev + 5HD
DZX + 5HD
Anox + Glib
Anox + 5HD
Malonate
Malonate + DZX
B
NMDAR Current (% Normalized)
[DZX] (υM)
C
50 min
10 mins
D
10 mins
50 min (anoxia)
1000 pA
20 sec
E
50 mins
(levcromakalim)
10 mins
F
50 mins
(diazoxide)
10 mins
G
10 mins
50 mins (diazoxide
+ 5HD)
H
10 mins
50 mins
(anoxia + 5HD)
I
10 mins
50 mins (anoxia +
glibenclamide)
J
50 mins (malonate)
10 mins

Figure 13. K^+ channel openers reduce whole-cell NMDAR currents.

(A) Percent normalized NMDAR currents at *t* = 30 (black bars) and 50 (grey bars) mins of treatment. Solid line represents normoxic controls, dashed line represents anoxic controls. **(B)** Dose response curve of normalized paired normoxic NMDAR currents vs. [diazoxide]. Symbols indicate data significantly different from normoxic control (*), anoxic control (π), or drug treatment control (χ). Data as mean +/- SEM. **(C-I)** Paired sample NMDAR currents at *t* = 10 mins (control) and following 40 mins of treatment exposure (*t* = 50 mins). Abbreviations: diazoxide (DZX), levcromakalim (Lev), glibenclamide (Glib), 5-hydroxydecanoic acid (5HD), anoxia (anox).

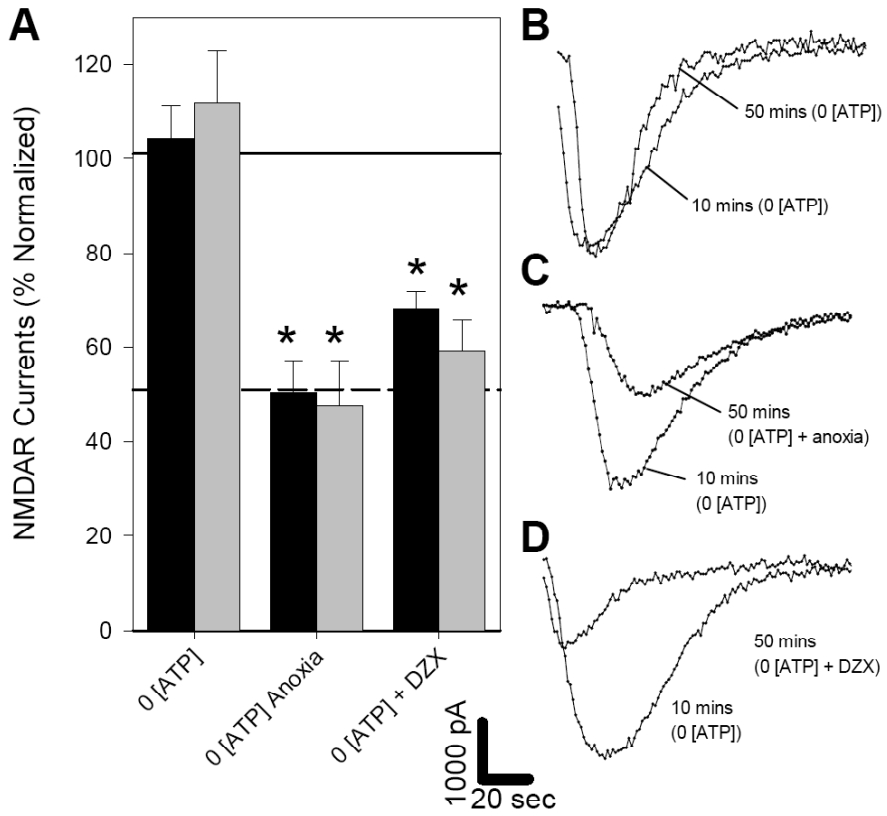

Figure 14. $[ATP]_c$ and pK_{ATP} channels do not alter NMDAR currents.

(A) Percent normalized NMDAR currents at t = 30 (black bars) and 50 (grey bars) mins of treatment. Solid line represents normoxic controls, dashed line represents anoxic controls Symbols indicate data significantly different from normoxic controls. Data are expressed as mean +/- SEM. Experiments are normoxic except where indicated. **(B-D)** Paired sample NMDAR currents at *t* = 10 mins (control) and following 40 minutes of treatment exposure (*t* = 50 mins). Experiments are normoxic except where indicated. Abbreviations: diazoxide (DZX).

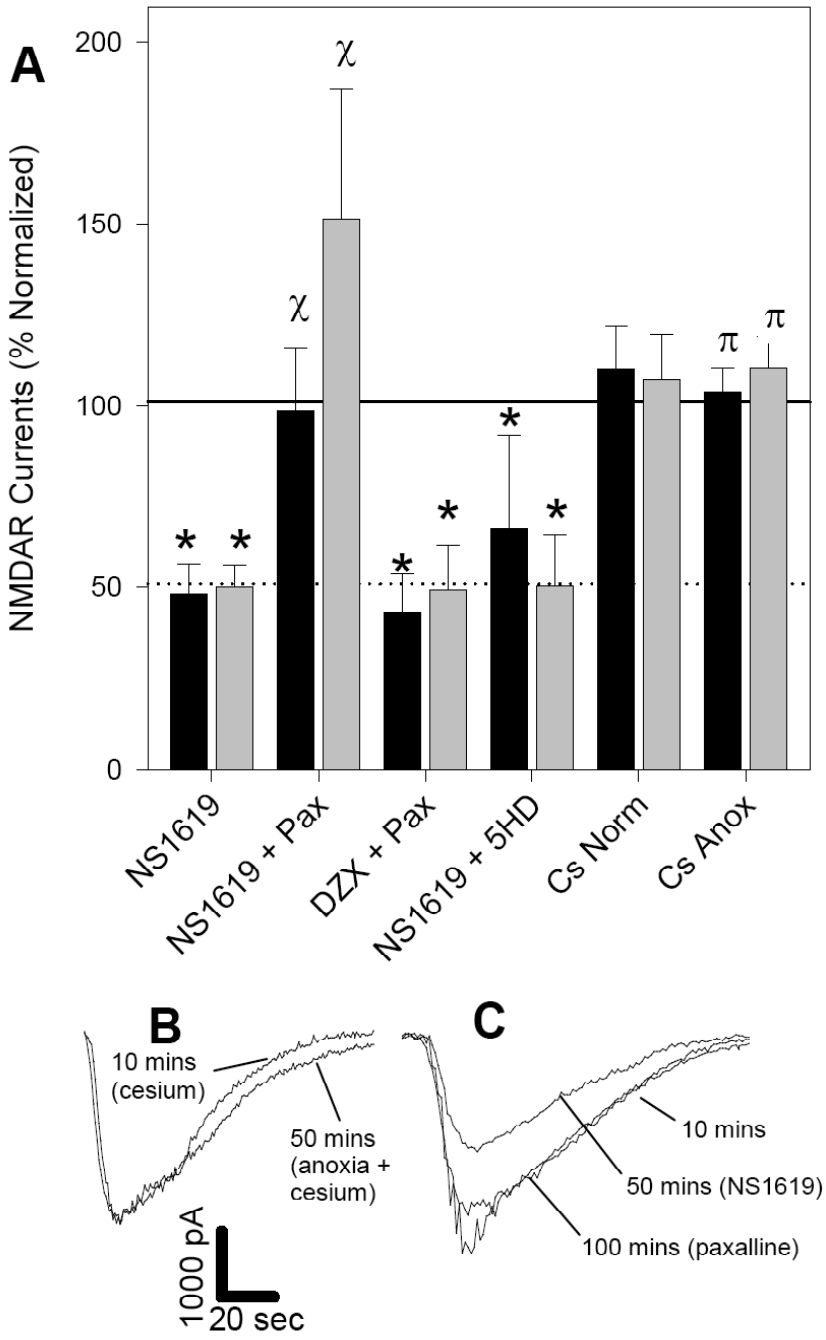

Figure 15. Increased mitochondrial K^+ conductance reduces NMDAR currents.

(A) Percent normalized NMDAR currents at *t* = 30 (black bars) and 50 (grey bars) mins of treatment. Solid line represents normoxic controls, dashed line represents anoxic controls. Symbols indicate data significantly different from normoxic control (*), anoxic control (π), or drug treatment control (χ). Data are expressed as mean +/- SEM. **(B-C)** Paired sample NMDAR currents at *t* = 10 mins (control) and following 40 minutes of treatment exposure (*t* = 50 mins). Abbreviations: diazoxide (DZX), paxallin (Pax), cesium (Cs) normoxia (norm), anoxia (anox).

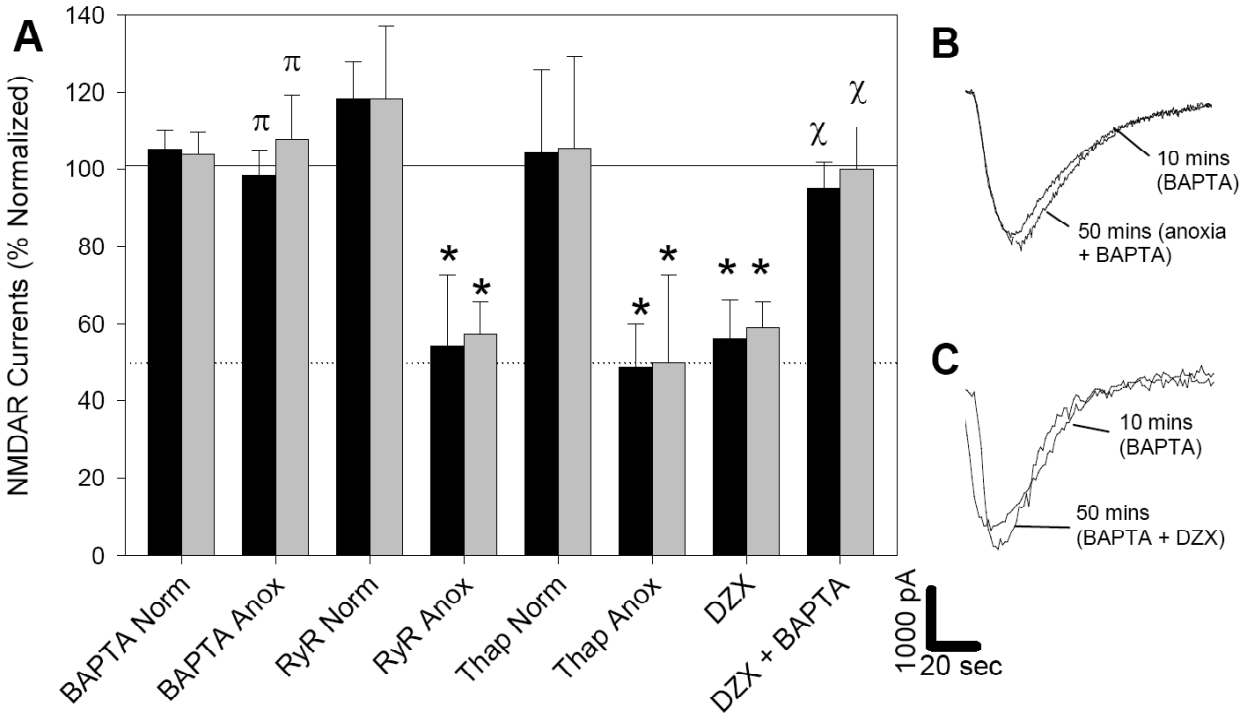

Figure 16. Role of cellular Ca^{2+} modulators on whole-cell NMDAR currents.

(A) Percent normalized NMDAR currents at *t* = 30 (black bars) and 50 (grey bars) mins of treatment. Solid line represents normoxic controls, dashed line represents anoxic controls Symbols indicate data significantly different from normoxic control (*), anoxic control (π), or drug treatment control (χ). Data are expressed as mean +/- SEM. **(B-C)** Paired sample NMDAR currents at *t* = 10 mins (control) and following 40 minutes of treatment exposure (*t* = 50 mins). Abbreviations: ryanodine (RyR), thapsigargin (Thap)., diazoxide (DZX), normoxia (norm), anoxia (anox).

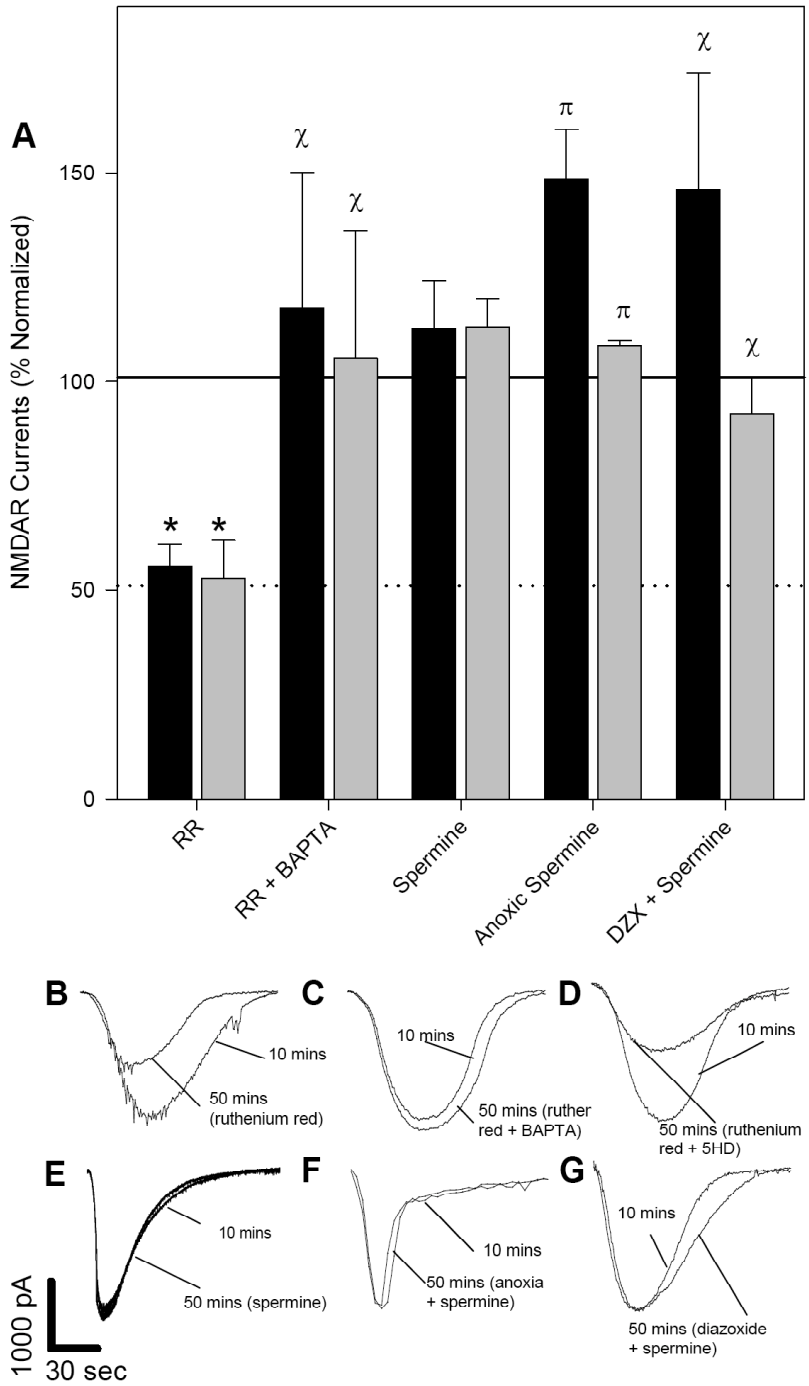

Figure 17. MCU activity underlies the anoxic decrease of NMDAR currents.

(A) Percent normalized NMDAR currents at *t* = 30 (black bars) and 50 (grey bars) mins of treatment. Solid line represents normoxic controls, dashed line represents anoxic controls Symbols indicate data significantly different from normoxic control (*), anoxic control (π), or drug treatment control (χ). Data are expressed as mean +/- SEM. **(B-G)** Paired sample NMDAR currents at *t* = 10 mins (control) and following 40 minutes of treatment exposure (*t* = 50 mins). Abbreviations: diazoxide (DZX), ruthenium red (RR).

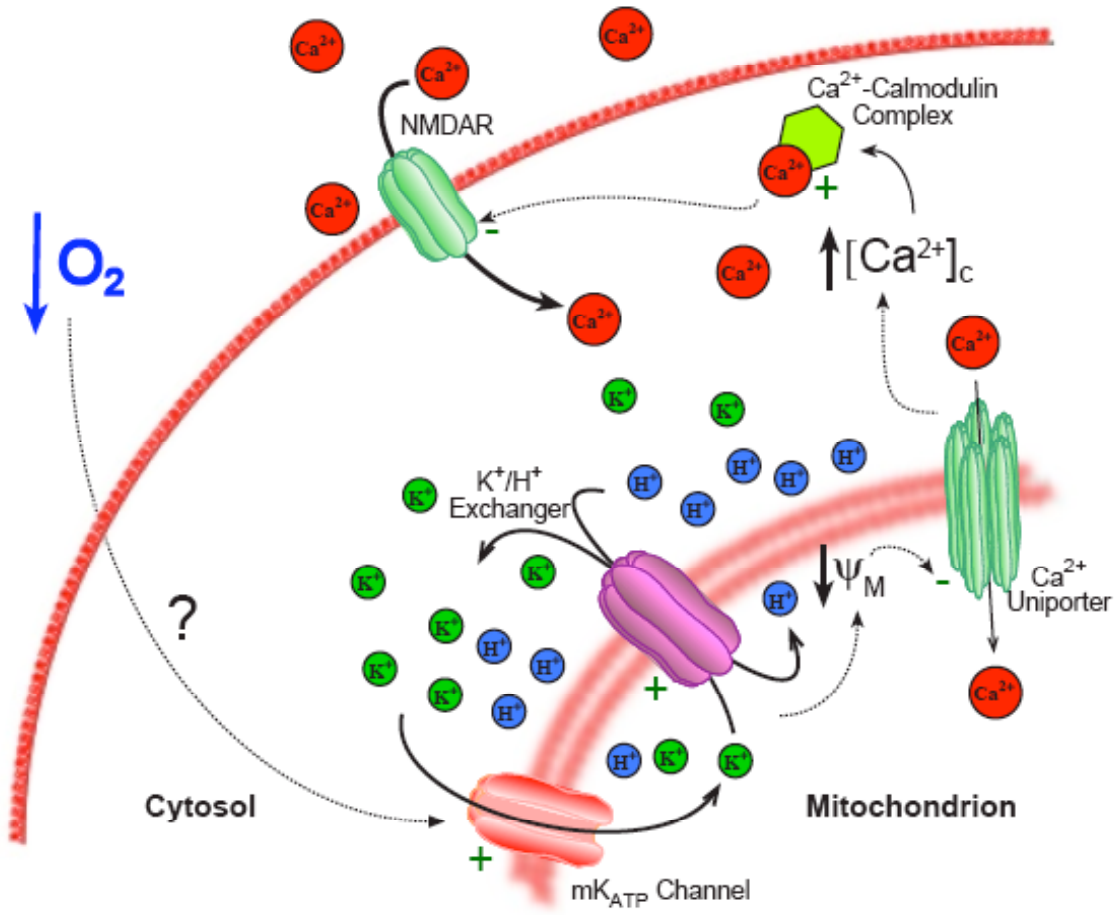

Figure 18. Schematic: mechanism of mK_{ATP}-mediated NMDA receptor channel arrest.

Dotted lines represent direction of pathway progression in a counter-clockwise direction commencing with decreased oxygen availability. The signal via which oxygen availability is transmitted to the mitochondria is unknown. During anoxia, increased opening of mK_{ATP} channels augments K^+ efflux from the mitochondria. Increased K^+ influx leads to futile K^+/H^+ cycling and mildly decreases ψ_m. This mild uncoupling reduces the driving force on the MCU, slowing mitochondrial Ca^{2+} uptake and subsequently raising $[Ca^{2+}]_c$. Mildly elevated $[Ca^{2+}]_c$ complexes with calmodulin and decreases the influx of ions through the NMDAR via a mechanism also involving protein kinases and phosphatases, see (Shin et al., 2005).

3.1.4. Discussion: the role of mK_{ATP} channels in NMDAR channel arrest

I proposed that in the turtle brain, mild mitochondrial uncoupling leads to changes in Ca^{2+} homeostasis and alters NMDAR function. Indeed, I demonstrate that mitochondrial uncoupling by the opening of mK_{ATP} channels with diazoxide increases $[Ca^{2+}]_c$ and decreases NMDAR currents during normoxia. Similarly, during anoxia $[Ca^{2+}]_c$ increases and NMDAR currents are reduced. The diazoxide or anoxia-mediated changes were blocked by the inclusion of the mK_{ATP} blockers 5HD or glibenclamide. Opening of mK_{ATP} uncouples mitochondria by increasing mitochondrial G_K (Fig. 18). This specificity of action was confirmed by increasing mG_K independently of mK_{ATP}: activation of mK_{Ca} also decreased normoxic NMDAR currents, mimicking the effects of mK_{ATP} activation or anoxia. Blocking mK_{Ca} during anoxic perfusion did not abolish the decrease in NMDAR activity however, confirming the specific action of mK_{ATP} on the anoxic regulation of NMDARs.

In isolated mitochondria, mK_{ATP} activation caused mild uncoupling of Ψ_m. Increased O_2 consumption and decreased ATP production following mK_{ATP} activation indicated mitochondria were uncoupled 10-20%. These measurements are similar to the 12-14% uncoupling of Ψ_m observed with similar drug application in mammalian mitochondria (Holmuhamedov, 1998; Murata, 2001). Furthermore, the effects of diazoxide and valinomycin on mitochondrial respiration rate were not cumulative: valinomycin induced maximum mitochondrial G_K and diazoxide had no additional effect on mitochondria already partially uncoupled by valinomycin. This suggests that the uncoupling action of diazoxide occurs via an increase in K^+ conductance.

The regulatory link between mK_{ATP} channel-mediated uncoupling and NMDARs is a decrease in MCU activity. Mitochondrial uncoupling dissipates the H^+ gradient that drives the activity of this pump, reducing Ca^{2+} uptake into the mitochondria (Fig. 18). Therefore, blockade

of the MCU with ruthenium red mimics the effect of uncoupling on mitochondrial Ca^{2+} uptake. Mitochondria are a major calcium sink in the cell, thus a decrease in mitochondrial Ca^{2+} uptake results in an elevation of $[Ca^{2+}]_c$. In my experiments, antagonism of the MCU reduced normoxic NMDAR currents similarly to anoxia and diazoxide or levcromakalim application. Secondly, chelation of $[Ca^{2+}]_c$ abolished the anoxic-, diazoxide- and ruthenium red-mediated decreases in NMDAR activity suggesting changes in $[Ca^{2+}]_c$ occur downstream of each of these components. Finally, activation of the MCU abolished both the anoxic- and diazoxide-mediated decreases in NMDAR currents, thus pharmacological activation of the MCU overcomes the indirect inhibition of the pump mediated by mK_{ATP} activation. Together these data indicate mK_{ATP} uncouple mitochondria, reducing the activity of the MCU, limiting mitochondrial Ca^{2+} uptake, subsequently elevating $[Ca^{2+}]_c$ and decreasing NMDAR activity.

In mammalian neurons, ischemic insults cause complete depolarization of Ψ_m and formation of mitochondrial permeability transition pores (MPTPs), which are associated with the release of apoptotic activators and cell death. IPC causes mK_{ATP} channels to open, inducing a mild uncoupling of Ψ_m, which leads to neuroprotective effects including prevention of: further mitochondrial depolarization, MPTP formation and cell death (Ishida, 2001; Murata, 2001). Although the exact mechanisms that underlie this neuroprotection remain unidentified, many aspects of the pathway have been elucidated and are remarkably similar to the mechanism of NMDAR arrest in turtle brain identified here. In mammals, IPC induces mK_{ATP}-mediated mitochondrial uncoupling, which prevents mitochondrial Ca^{2+} overload by limiting Ca^{2+} uptake via the MCU (Holmuhamedov, 1998; Rousou et al., 2004; Saotome et al., 2005) and by activating cyclosporin-sensitive Ca^{2+} release from the mitochondria (Holmuhamedov, 1999). In rat hearts exposed to ischemia, $[Ca^{2+}]_c$ was elevated 4-fold while $[Ca^{2+}]_m$ rose 10-fold and tissue

death ensued. Treatment with diazoxide caused further elevation of $[Ca^{2+}]_c$ by ~50%, but $[Ca^{2+}]_m$ elevation was reduced by 80% and survival was improved (Wang, 2001). These authors concluded that ischemia-induced elevations in $[Ca^{2+}]_m$ are toxic in rats and that lowering $[Ca^{2+}]_m$ overload is an underlying protective mechanism in IPC. In another study ruthenium red was used to block mitochondrial Ca^{2+} uptake via the MCU. Just as ruthenium red mimicked anoxia-mediated NMDAR decrease in the turtle, it also mimics the protective effects of IPC in rat hearts: reducing infarct size, lactate dehydrogenase (LDH) leakage and mitochondria MPTP formation. Furthermore, activation of the MCU with spermine prevented IPC-mediated cardio-protection and induced MPTP formation (Zhang et al., 2006). Thus activation of mK_{ATP} during ischemia compromises MCU activity and prevents toxic elevation of $[Ca^{2+}]_m$.

Although the importance of preventing mitochondrial Ca^{2+} accumulation has been demonstrated, a potential link between mK_{ATP} and NMDARs has received little attention in mammalian models. One study found that diazoxide enhanced glutamatergic currents in hippocampal neurons (Crepel et al., 1993b). However, these changes were likely due to secondary effects of diazoxide on SDH activity since these authors used a high concentration of diazoxide (600 μM), and their findings were neither blocked by the K_{ATP} antagonists glibenclamide or tolbutamide, nor mimicked by other K_{ATP} agonists. A few studies have indicated a potential protective mechanism involving mK_{ATP} and NMDARs. In rat hippocampal cultures ECD was prevented in neurons treated with K^+ channel activators. This protection was reversed by glyburide, a general K_{ATP} channel antagonist (Abele and Miller, 1990). One study of interest demonstrated that inhibition of mitochondrial Ca^{2+} uptake desensitized NMDAR activity (Kannurpatti, 2000). While this study did not involve mK_{ATP} channels, it demonstrated a link between mitochondrial Ca^{2+} handling and NMDAR function.

My results suggest that mK_{ATP}, and not pK_{ATP} channels mediate changes in NMDAR activity. K_{ATP} channels are activated by decreases in [ATP] on the inside of the membrane the channel is spanning. Thus pK_{ATP} and mK_{ATP} channels are regulated by changes in cytosolic and mitochondrial [ATP], respectively (Matsuo et al., 2005; Zhang et al., 2001). Even though neuronal [ATP] decreases 23% with anoxia in the turtle (Buck, 1998), it is unlikely that pK_{ATP} are involved in NMDAR regulation because ATP dialysis did not alter NMDAR activity during either normoxic or anoxic perfusion, nor did it prevent the effect of diazoxide application on NMDAR activity. These results, combined with the actions of the specific mK_{ATP} modulators on whole-cell NMDAR currents and $[Ca^{2+}]_c$ provide evidence that mitochondrial and not plasmalemmal K_{ATP} channels regulate NMDAR during anoxia. It should be noted that the anoxic decrease in $[ATP]_c$ in turtle cortex may have limited effects on the activity of pK_{ATP} channels. The cytosol is compartmentalized, particularly near the plasma membrane and the activity of ATP-dependent channels is related to change in adenylate concentrations in these membrane localized sub-compartments and not necessarily to $[ATP]_c$ as a whole (Babenko et al., 1998).

Glibenclamide binding density studies indicate K_{ATP} channels are distributed throughout the turtle brain (Jiang et al., 1992); however, research into their role in the anoxia-tolerance of turtle brain is sparse and conflicting. For example, Jiang et al. reported that K_{ATP} blockade with glibenclamide had no effect on anoxic K^+ efflux, however others have reported that K_{ATP} blockade reduces K^+ efflux during early anoxia (Pek-Scott and Lutz, 1998). These authors blocked K_{ATP} channels with glibenclamide in the first hour and with 2,3-butanedione monoxime (BDM) during 2-4 hours of anoxia. Unfortunately, the use of BDM limits the conclusions that can be drawn from these data regarding the role of K_{ATP} channels. In brain, BDM has been shown to inhibit L-type calcium channels and glycine-gated chloride currents and to increase

GABAergic currents (Allen et al., 1998; Brightman et al., 1995; Ye and McArdle, 1996). More importantly regarding K^+ currents, BDM has been shown to directly regulate K^+ flux via inhibition of Kv2.1 channels (Lopatin and Nichols, 1993). There is also evidence that K_{ATP} activation may decrease glutamate release and maintain dopamine release in the anoxic turtle cortex (Milton and Lutz, 1998; Milton et al., 2002; Thompson et al., 2007). While experiments with diazoxide in those studies offer some support for a role of mK_{ATP} channels in the normoxic regulation of dopamine and glutamate release, conclusions regarding the role of K_{ATP} channels in the anoxic regulation of these metabolites is also based on treatment of cells with BDM.

In the anoxic turtle brain, $[Ca^{2+}]_c$ is mildly elevated and NMDAR activity is decreased within 20 mins of anoxic perfusion, and during prolonged anoxia (6 weeks) $[Ca^{2+}]_c$ remains slightly elevated and the decrease in NMDAR activity is maintained (Bickler and Buck, 1998). Over the same time period, extracellular $[Ca^{2+}]$ increases 6-fold, highlighting the importance of NMDAR down-regulation to prevent toxic intracellular calcium accumulation. Conversely, in rats $[Ca^{2+}]_c$ becomes elevated 10-fold within minutes of anoxia and this Ca^{2+} influx is entirely mediated by NMDARs (Bickler and Hansen, 1994).

In conclusion, my study provides evidence that mK_{ATP} channel activation uncouples turtle mitochondria and subsequently decreases NMDAR activity. Mitochondrial uncoupling decreases Ca^{2+} uptake via the MCU, raising cytosolic calcium levels and decreasing both normoxic and anoxic NMDAR currents (Fig. 18). mK_{ATP} channels are currently considered a primary mediator of IPC-mediated protection, however the end-mediators of this protection are undetermined in mammals. To my knowledge, this is the first study that demonstrates mK_{ATP} channel regulation of NMDARs and may represent a common mechanism between the prevention of excitotoxic cell death and preconditioned neuroprotection from ischemic insult.

3.2. Adenosine mediates NMDA receptor activity in a pertussis toxin-sensitive manner during normoxia but not anoxia in turtle cortex

Preface

A modified version of this chapter was published as: Pamenter ME, Shin DS and Buck LT (2008). Adenosine A1 receptor activation mediates NMDA receptor activity in a pertussis toxin-sensitive manner during normoxia but not anoxia in turtle cortical neurons. *Brain Res.* 1213:27-34.

The impetus to examine the role of A1 receptors in NMDAR tolerance was L Buck's and the idea to examine the role of G proteins was mine. D Shin conducted 50% of control adenosine receptor experiments. I performed the remainder of these experiments and all G protein experiments and wrote the paper with editing by L Buck.

Abstract

Adenosine is a defensive metabolite that is critical to anoxic neuronal survival in the freshwater turtle. Channel arrest of the N-methyl-D-aspartate receptor (NMDAR) is a hallmark of the turtle's remarkable anoxia-tolerance and adenosine receptor (A_1R)-mediated depression of normoxic NMDAR activity is well documented in turtle brain. However, experiments examining the role of A_1Rs in depressed NMDAR activity during anoxia have yielded inconsistent results. The aim of this study was to examine the role of A_1R in the normoxic and anoxic regulation of turtle brain NMDAR activity. Mechanisms downstream of A_1R activation were also examined. Whole-cell NMDAR currents were recorded for one-hour at 20-min intervals from turtle cortical pyramidal neurons exposed to pharmacological adenosine receptor modulation or G_i protein modulation during normoxia (95% O_2/5% CO_2) and anoxia (95% N_2/5% CO_2). NMDAR currents were unchanged during normoxia and decreased 51.3 ± 3.9% following anoxic exposure. Normoxic agonism of adenosine A_1 receptors (A_1R) with adenosine or N6-cyclopentyladenosine (CPA) decreased NMDAR currents 57.1 ± 11.3% and 59.4 ± 5.9%, respectively. The A_1R antagonist 8-cyclopentyl-1,3-dimethylxanthine (DPCPX) had no effect on normoxic NMDAR currents and prevented the adenosine and CPA but not the anoxia-mediated decrease in NMDAR activity. Pre-treating cortical slices with the G_i protein inhibitor pertussis toxin (PTX) prevented both the CPA and anoxia-mediated decreases in NMDAR currents. The CPA-mediated decreases were also prevented by calcium chelation or by blockade of mitochondrial ATP-sensitive K^+ channels. My results suggest the anoxic decrease in NMDAR activity is activated by a PTX-sensitive mechanism that is independent of A_1R activity.

3.2.1. Introduction: adenosine and the anoxic turtle

Adenosine has been termed a retaliatory metabolite because its concentration is rapidly elevated during periods of cell stress, such as anoxia, and because adenosine generally up-regulates cytoprotective mechanisms against anoxic insults and during seizures (Buck, 2004; Downey et al., 2007; Pagonopoulou et al., 2006). Freshwater turtles (*Chrysemys picta bellii* and Trachemys *scripta elegans*) are the most anoxia-tolerant vertebrates known and within 2 hours of anoxic exposure brain adenosine concentration increases 10-fold (Buck and Pamenter, 2006; Nilsson and Lutz, 1992). Furthermore, turtle brain adenosine receptor abundance is maintained while receptor binding affinity increases 2.5-fold during prolonged anoxic exposure (Lutz and Kabler, 1997; Lutz and Manuel, 1999). Elevation in [adenosine] and subsequent activation of the adenosine A_1R receptor are critical in surviving anoxic insults in turtle cortex since blockade of these receptors during anoxia leads to increases in K^+ efflux, ROS production, glutamate release and cell death (Milton et al., 2007; Pek and Lutz, 1997; Perez-Pinzon et al., 1993; Thompson et al., 2007). However, despite considerable evidence supporting a role for adenosine in the turtle's anoxia-tolerance, the mechanisms underlying this protection are poorly understood.

One potential mechanism of adenosine-mediated neuroprotection may be down-regulation of NMDAR activity. However, while there is considerable evidence supporting anoxic channel arrest of this receptor, the mechanism(s) underlying this phenomenon have not been fully elucidated and may involve adenosine. There is some evidence for adenosine involvement in the regulation of NMDAR activity in the turtle cortex. During normoxia, adenosine perfusion or activation of the A_1R receptor leads to a depression in NMDAR-mediated Ca^{2+} influx and a ~50% reduction in NMDAR P_{open} (Buck and Bickler, 1995; Buck and Bickler, 1998a). Anoxia induces similar changes in NMDAR-mediated Ca^{2+} entry and NMDAR P_{open}, but concomitant

perfusion of adenosine during anoxia does not induce synergistic increases in these two variables; suggesting the adenosine-mediated and the anoxia-mediated NMDAR regulatory mechanisms function via the same pathway (Bickler et al., 2000; Buck et al., 1998; Buck and Bickler, 1995). However, while the normoxic adenosine and A_1R agonist-mediated changes were blocked by an A_1R antagonist, the effects of A_1R blockade on the anoxic changes were inconsistent: NMDAR-mediated Ca^{2+} entry remained depressed by anoxia, however the decrease in NMDAR P_{open} was prevented (but see further discussion below) (Buck and Bickler, 1995; Buck and Bickler, 1998a). Thus while support for normoxic regulation of NMDAR activity by adenosine is strong, data on the anoxic interaction between these receptors is inconclusive.

Other labs have also reported similarly dichotomous results regarding the role of adenosine in normoxia versus anoxia in the facultative anaerobes. For example, in the anoxic freshwater turtle brain, extracellular glutamate levels decrease due to reductions in synaptic vesicular glutamate release (Milton et al., 2002; Nilsson et al., 1990). During normoxia, adenosine perfusion reduces synaptic glutamate release, however A_1R blockade during anoxia with theophylline does not prevent the anoxic decrease in synaptic glutamate release (Milton et al., 2002). Another example comes from the hypoxia-tolerant coral reef epaulette shark, which can survive severe hypoxia for hours (Wise et al., 1998). Anoxia or adenosine induce significant and similar decreases in aortic blood pressure and heart rate; however adenosine receptor blockade prevents only the adenosine-mediated changes and not the anoxia-mediated changes (Stenslokken et al., 2004).

An explanation for these results may be derived from the mechanism of adenosine receptor activity. A_1Rs are G-protein coupled receptors and adenosine binding results in dissociation of an inhibitory G_i subunit, which interacts with adenylyl cyclase and depresses

cAMP production. However, in addition to adenosine receptors there are other G protein-coupled receptors in neurons that may underlie responses to anoxia, including decreased NMDAR activity. Therefore, many signaling pathways may converge on a common G_i-based pathway to regulate NMDAR activity during normoxia and anoxia. Changes in [cAMP] alter the activity of numerous downstream kinases and phosphatases (Domanska-Janik et al., 1993); and in the anoxic turtle brain [cAMP] is decreased and the anoxic decrease in NMDAR activity involves protein phosphatases (Pamenter et al., 2007; Shin et al., 2005). In addition, I have recently shown that mK_{ATP} channels control the anoxic decrease in NMDAR activity (Pamenter et al., 2008d), which are also sensitive to regulation by PKC and PKG via mechanisms that may involve G protein cascades (Costa et al., 2005; Kis et al., 2003). Thus, anoxic turtle NMDAR activity may be regulated by changes in G protein signaling cascades that occur independently of adenosine receptor activation.

The aims of this paper are to examine: (1) the effects of adenosine and A_1R manipulation on whole-cell NMDAR peak currents during normoxia and a normoxic to anoxic transition; (2) the role of inhibitory G_i proteins in the adenosine- and anoxia-mediated change in NMDAR peak currents; and (3) whether or not the adenosine-mediated change in NMDAR activity act via the same pathway as mK_{ATP} activation.

3.2.2. Results: adenosinergic regulation of whole-cell NMDA receptor activity

Changes in NMDAR currents during normoxic to anoxic transitions have been described previously but are repeated here for statistical comparison. NMDAR currents did not change in magnitude during 40 mins of normoxic recordings, ranging from 850.4 ± 87.5 to 937.3 ± 74.8 pA (Figs. 19A-B, *n* = 8). Conversely, currents were decreased by 45.5 ± 8.6 and 51.3 ± 3.9% at 20 and 40 mins of anoxia respectively (Fig. 20A-B, *n* = 8). Anoxic NMDAR currents recovered to control magnitude following 20 mins of re-oxygenation (data not shown).

During normoxic conditions, application of 250 μM adenosine resulted in an anoxic-like decrease in NMDAR currents of 47.2 ± 6.2 and 57.1 ± 11.3% following 20 and 40 mins of adenosine perfusion, respectively (Figs. 19A, C, *n* = 8). Similarly, perfusion of the A_1R agonist CPA also induced decreases in NMDAR currents of 45.6 ± 11.7 and 59.4 ± 5.9% at 20 and 40 mins of CPA perfusion, respectively (Figs. 19A, D, *n* = 8). The specificity of these responses to A_1R activation was confirmed by the inclusion of the A_1R antagonist DPCPX, which blocked the effect of the two agonists (Figs. 19A, F-G, *n* = 8 for ADO plus DPCPX, n = 7 for CPA plus DPCPX). DPCPX perfusion alone had no effect on normoxic NMDAR currents (Figs. 19A, E, *n* = 4).

To examine the role of adenosine in the anoxic decrease in NMDAR activity, I treated cells with anoxia concomitant with either adenosine or CPA. The anoxic decrease in NMDAR activity with simultaneous adenosine or CPA application did not differ from anoxic treatment alone (Figs. 20A, C-D, *n* = 5 for each). In addition, blockade of A_1Rs with DPCPX during anoxia did not abolish the anoxia-mediated decrease in NMDAR currents, which were depressed by 28.6 ± 6.8 and 53.4 ± 10.2% at 20 and 40 mins of anoxic perfusion, respectively (Figs. 20A, D, *n* = 5 for each). Adenosine receptors are G protein-coupled receptors and adenosine-ligand

binding results in dissociation of an inhibitory G_i protein subunit. In another set of experiments cortical sheets were incubated overnight at 4°C in 400 nM pertussis toxin (PTX), an inhibitor of G_i protein activation. In tissues pretreated with PTX the anoxic decrease in NMDAR activity was not observed (Figs. 20A, E, *n* = 5). Incubation of sheets in normoxic saline for 24 and 48 hours at 4°C has no effect on peak NMDAR currents (data not shown).

Since G proteins, mK_{ATP} channels and changes in $[Ca^{2+}]_c$ mediate the decrease in turtle NMDAR activity during anoxia (Bickler et al., 2000; Pamenter et al., 2008d), I hypothesized that adenosine or activation of the A_1R during normoxia may increase the activity of G proteins and trigger anoxia-like reductions in NMDAR currents during normoxia via mK_{ATP} channels and changes in $[Ca^{2+}]_c$. Similar to the anoxic decrease, the CPA-mediated decrease in NMDAR activity was prevented by PTX pre-incubation (Figs. 21A-B, *n* = 5). Furthermore, the effects of both adenosine (*n* = 13) and CPA (*n* = 11) were reversed by the mK_{ATP} antagonist 5HD (Figs. 21A, C-E). Finally, in recordings with the Ca^{2+}-chelator BAPTA in the recording electrode the CPA-mediated decrease in NMDAR activity was not observed (Figs. 21A, F, *n* = 3).

3.2.3. Figures

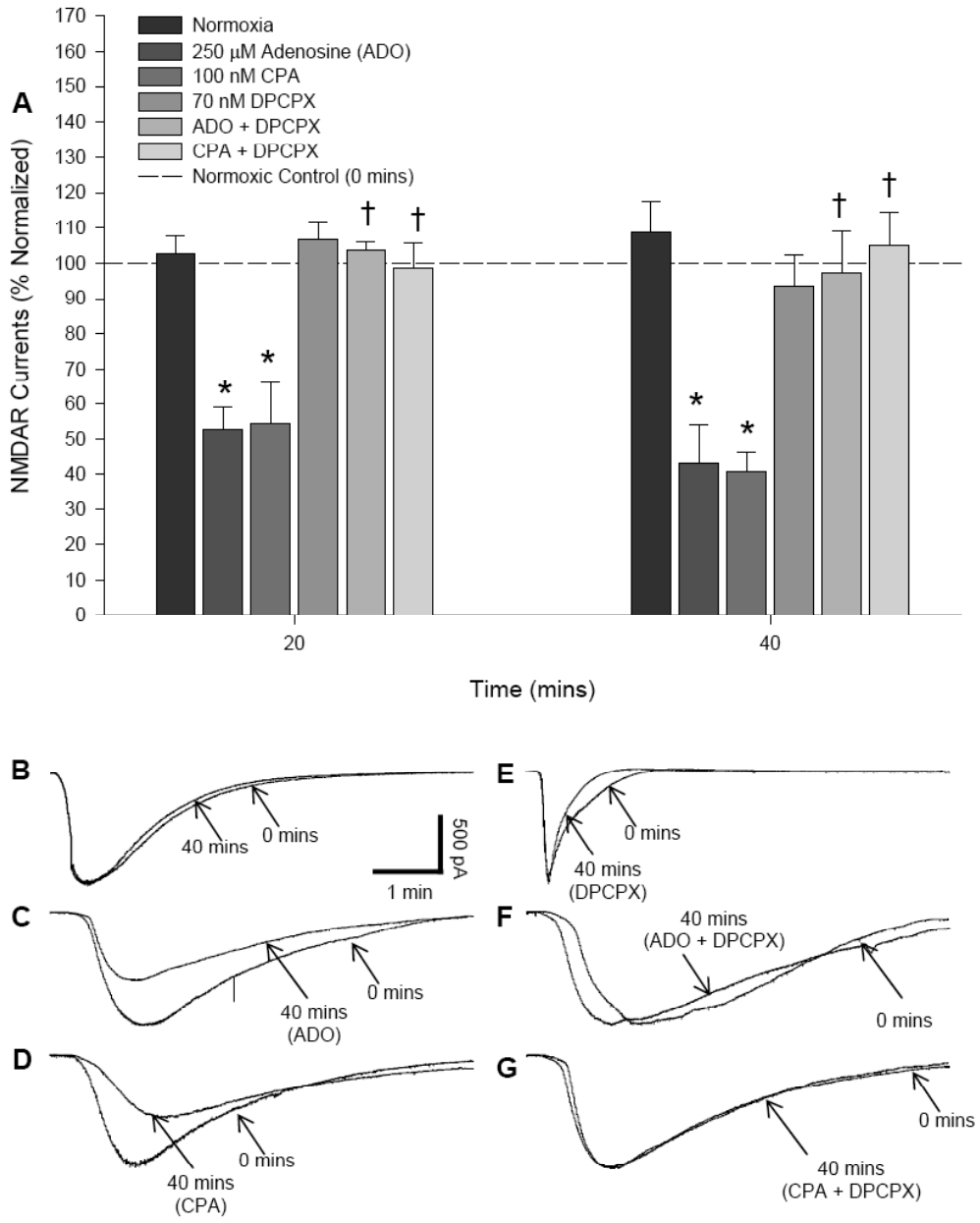

Figure 19. A_1 receptors regulate normoxic NMDAR currents.

(A) Summary of changes in peak NMDAR currents during normoxia and following treatment with adenosine receptor modulators. NMDAR currents following treatment (t = 20, 40 mins) were normalized to control recordings from the same cell (t = 0 mins, shown as dashed line). Data are expressed as mean ± SEM. Asterisks indicate data significantly different from normoxic controls. Daggers indicate significant difference from ADO or CPA perfusion alone. Significance was assessed at $P < 0.05$. **(B-G)** Raw data traces of whole-cell NMDAR currents during treatment with **(B)** a sham switch, **(C-D)** the adenosine receptor (A_1R) agonists adenosine (ADO) or N6-cyclopentyladenosine (CPA), **(E)** the A_1R antagonist 8-cyclopentyl-1,3-dimethylxanthine (DPCPX), or **(F-G)** combined application of A_1R agonists and DPCPX.

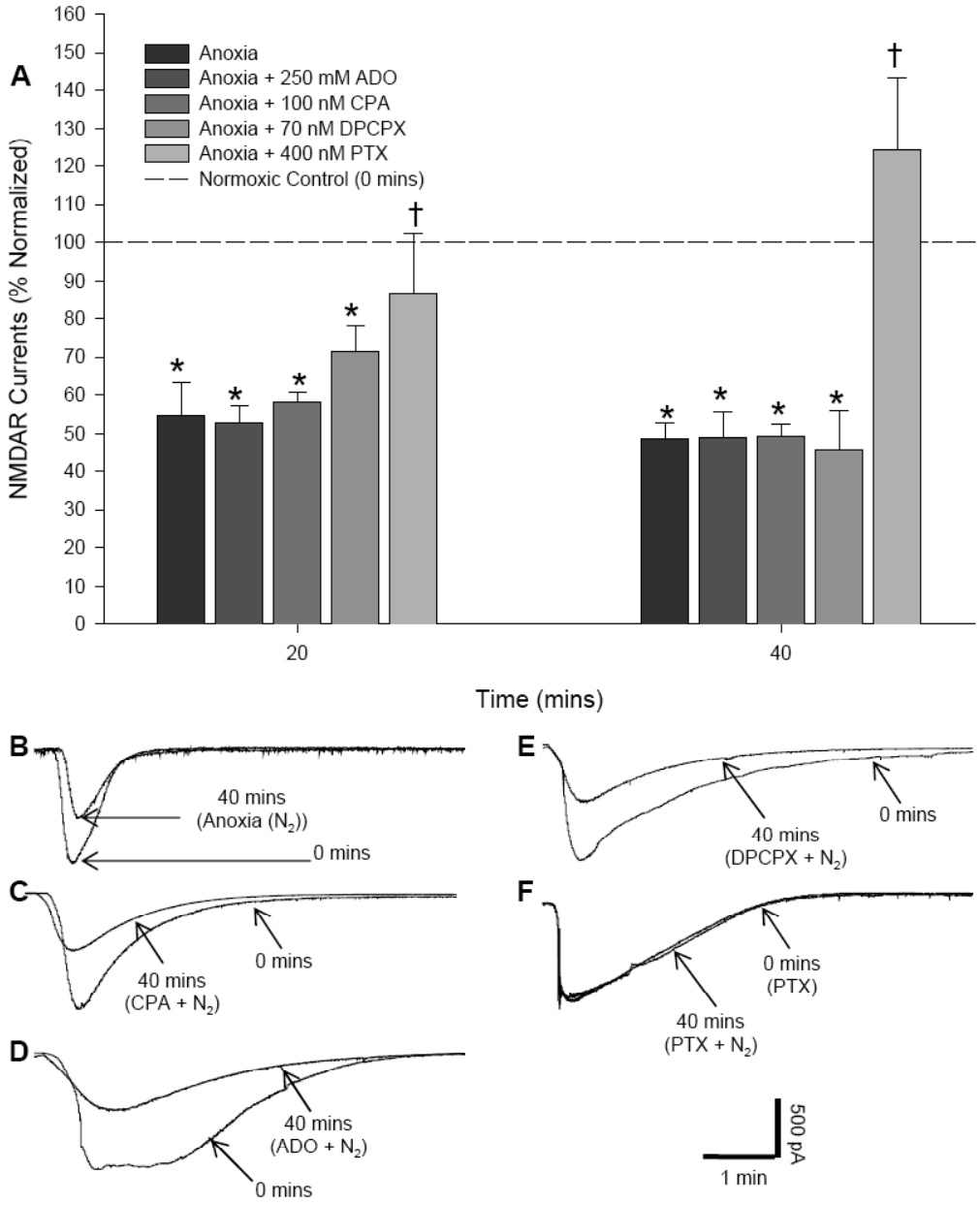

Figure 20. G_i proteins but not A_1 receptors mediate the anoxic decrease in NMDAR currents.

(A) Summary of changes in peak NMDAR currents during normoxia and following treatment with adenosine receptor modulators or following pre-incubation with the G_i protein inhibitor pertussis toxin (PTX). Anoxic NMDAR currents following treatment (t = 20, 40 mins) were normalized to control recordings from the same cell (t = 0 mins, shown as dashed line). Data are expressed as mean ± SEM. Asterisks indicate data significantly different from normoxic controls. Daggers indicate significant difference from anoxic controls. Significance was assessed at $P < 0.05$. **(B-G)** Raw data traces of whole-cell NMDAR currents following normoxic to anoxic transitions **(B)** or anoxic treatment combined with **(C-D**) CPA or ADO, **(E)** DPCPX, or **(F)** PTX.

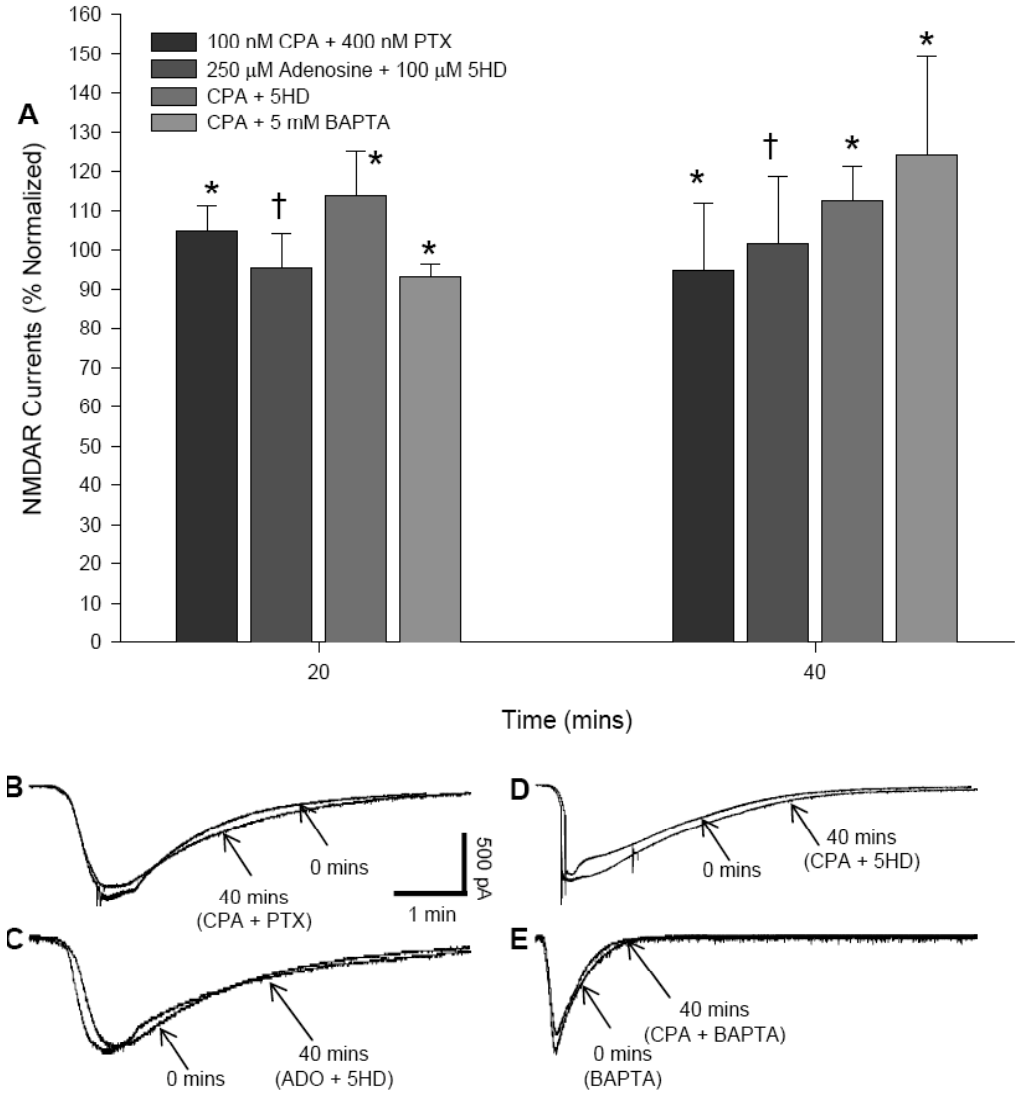

Figure 21. A_1 receptor-mediated NMDAR depression functions via the same pathway as the anoxic NMDAR depression.

(A) Summary of changes in peak NMDAR currents during normoxia and following treatment with adenosine receptor activators and co-treatment with G_i or ATP-sensitive K^+ channel (mK_{ATP}) inhibitors or with Ca^{2+} chelation. NMDAR currents following treatment (t = 20, 40 mins) were normalized to control recordings from the same cell (t = 0 mins). Data are expressed as mean ± SEM. Asterisks indicate data significantly different from normoxic CPA controls (see Fig. 1). Daggers indicate data significantly different from normoxic adenosine controls (see Fig. 1) ($P < 0.05$). **(B-E)** Raw data traces of whole-cell NMDAR currents following co-perfusion of adenosine agonists and **(B)** PTX, **(C-D)** the mK_{ATP} agonist 5-hydroxydecanoic acid, or **(E)** BAPTA.

Discussion: G_i proteins but not adenosine regulate anoxic NMDAR activity

Previous results examining the role of adenosine receptors in the regulation of anoxic turtle cortical NMDAR activity are conflicting as only the anoxic change in NMDAR P_{open} and not the anoxic change in NMDAR-mediated Ca^{2+} flux was prevented by adenosine receptor antagonism (Buck and Bickler, 1995; Buck and Bickler, 1998a). This discrepancy may be explained by experimental design. In examining P_{open}, Buck and Bickler (1995) pre-incubated tissue in the A_1R antagonist 8-phenyltheophylline (8PT) and then exposed cortical slices to either anoxia or adenosine perfusion. Changes in P_{open} were not observed in either of these experiments; however, examination of the mean P_{open} of these treatment groups indicates P_{open} was depressed prior to the start of experiments in pre-incubated tissues. Indeed the observed average P_{open} of pre-incubated tissue prior to the commencement of experiments was similar to values recorded from either anoxic or adenosine perfused neurons (Buck and Bickler, 1998a). My present experimental design offers a direct comparison of the effect of A_1R blockade during anoxia because I used a paired design and measured control and treatment recordings from the same cell. In this study, adenosine was found to attenuate NMDAR currents via activation of the A_1R and this effect was prevented by A_1R blockade, G_i protein inhibition, mK_{ATP} blockade, or by chelation of intracellular Ca^{2+}. During anoxia however, A_1R blockade failed to abolish the anoxia-mediated decrease in NMDAR activity, while G_i protein inhibition, mK_{ATP} blockade, and Ca^{2+} chelation did abolish it (see chapter 3.1). These data support a role for adenosine-mediated NMDAR regulation during normoxia but not during anoxia, and indicate that the normoxic and anoxic pathways are different but converge at some point on a common pathway such as G protein-coupled cascades.

It may be that the anoxic decrease in NMDAR activity observed in the turtle cortex is regulated in part by changes in a G_i-mediated mechanism independent of A_1Rs. If this were the case, then activation of adenosine-mediated G_i protein mechanisms during normoxia would up-regulate the endogenous mechanism of NMDAR suppression that is otherwise activated by anoxia, and thus adenosine would depress normoxic NMDAR activity. Conversely, blockade of A_1Rs during anoxia would have no effect on NMDAR currents if the G_i protein-based mechanism initiated during anoxia were triggered by other G_i-coupled receptors. My results from cortical sheets pre-incubated in the G_i inhibitor PTX support this hypothesis. I report that both the anoxic and CPA-mediated decrease in NMDAR currents are prevented by PTX pre-incubation, suggesting both mechanisms rely on G_i protein signaling cascades. Since PTX but not DPCPX abolished the anoxic decrease in NMDAR activity, it is logical that the anoxic depression must involve the activity of G_i protein-coupled receptors other than A_1Rs. There are numerous such receptors in neurons and one receptor in particular, the delta opioid receptor, is a strong candidate for involvement in this mechanism.

Interestingly, a mechanism linking adenosine receptors and mK_{ATP} may have also evolved in oxygen-sensitive mammalian brain. There is significant evidence supporting adenosine and mK_{ATP} involvement in models of IPC in mammals (Kis et al., 2004; Kis et al., 2003; Murry et al., 1986; Reshef et al., 2000a; Reshef et al., 2000b). However, adenosine receptor blockade does not prevent neuroprotection, while mK_{ATP} blockade does (Heurteaux et al., 1995; Yoshida et al., 2004). Thus the role of adenosine in mammalian preconditioned protection appears to occur via activation of mK_{ATP}-mediated pathways similar to those that occur in the turtle. Also similar to the turtle cortex, the role of adenosine in IPC appears to be feed-forward: conferring protection if actively upregulated prior to ischemic insults, but

adenosine does not appear to be critical to IPC-mediated mechanisms of neuroprotection in mammals.

Although adenosine receptors do not appear to be involved in the anoxic regulation of NMDAR activity in the turtle cortex, adenosine still plays a critical neuroprotective role in the anoxic turtle brain. Blockade of adenosine receptors during anoxia results in increased neuronal death in turtle brain (Milton et al., 2007; Perez-Pinzon et al., 1993), so adenosine must regulate other critical mechanisms of anoxia-tolerance. Adenosine receptors regulate glutamate release during prolonged anoxia, and reductions in glutamate release reduce both AMPAR and NMDAR activity independent of post-synaptic receptor modulation, thereby decreasing neuronal susceptibility to excitotoxic events. (Milton and Lutz, 2005; Milton et al., 2002; Thompson et al., 2007). Alternatively, adenosine may depress electrical activity independently of glutamatergic regulation (Materi et al., 2000; Mei et al., 1994; Obrietan et al., 1995; Rezvani et al., 2007). For example, adenosine receptor activity prevented increased excitatory synaptic events in the turtle basal optic nucleus (Ariel, 2006).

Adenosine also plays a role in the regulation of CBF during anoxic episodes. Adenosine causes vasodilation of cerebral blood vessels, resulting in increased blood flow and enhanced delivery of glycolytic substrate (Collis, 1989). In the anoxic turtle brain, CBF increases nearly 2-fold, while adenosine perfusion during normoxia increases CBF nearly 4-fold. Furthermore, both these increases were prevented by adenosine receptor blockade (Hylland et al., 1994). Turtle brains undergo a remarkable suppression of energy-utilizing mechanisms during anoxia, however they do not completely shut off function and are thus dependant on glycolytic metabolism for energy production (Chih et al., 1989a; Doll et al., 1994; Doll et al., 1993; Edwards, 1989; Feng et al., 1988). Inhibition of glycolysis during anoxia induces cell death in

turtle neurons despite their enormous reduction in energy expenditures, therefore an increase in CBF may be critical in supplying adequate glycolytic substrate to anoxic turtle brains.

In conclusion, I demonstrate that stimulation of adenosine receptors during normoxia depresses turtle cortical NMDAR currents via a PTX-sensitive mechanism that also involves mK_{ATP} channels and changes in $[Ca^{2+}]_c$. During anoxia, similar decreases in NMDAR activity are observed that are mediated by the same down stream signaling components but appear to occur independently of A_1R activation. These data resolve previous discrepancies regarding the role of adenosine in NMDAR regulation in the anoxic turtle cortex and indicate the mechanisms of anoxic neuroprotection mediated by adenosine likely do not involve direct regulation of NMDAR activity.

3.3. Delta opioid receptor antagonism potentiates NMDA receptor currents and induces extended neuronal depolarization in anoxic turtle cortex

Preface

A modified version of this chapter was published as: Pamenter ME and Buck LT (2008). Delta opioid receptor antagonism potentiates NMDA receptor currents and induces extended neuronal depolarization in anoxic turtle cortex. *J. Exp. Biol.* 211:3512-3517.

I designed and performed all experiments in this study and wrote the paper with editing by L. Buck.

Abstract

Delta-opioid receptor (DOR) activation is neuroprotective against short-term anoxic insults in mammalian brain. This protection may be conferred by inhibition of N-methyl-D-aspartate receptors (NMDARs), whose over-activation during anoxic insult otherwise leads to deleterious accumulation of cytosolic calcium ($[Ca^{2+}]_c$), severe membrane potential (E_m) depolarization, and excitotoxic cell death (ECD). Conversely, NMDAR activity is decreased by ~ 50% with anoxia in the cortex of the painted turtle and large elevations of $[Ca^{2+}]_c$, severe E_m depolarization, and ECD are avoided. DORs are expressed in high quantity throughout turtle brain relative to mammalian brain; however, the role of DORs in anoxic NMDAR regulation has not been investigated in turtles. We examined the effect of DOR blockade with naltrindole (1-10 μM) on E_m, NMDAR activity, and $[Ca^{2+}]_c$ homeostasis in turtle cortical neurons during normoxia and the transition to anoxia. Naltrindole potentiated normoxic NMDAR currents by 78 ± 5% and increased $[Ca^{2+}]_c$ 13 ± 4%. Anoxic neurons treated with naltrindole were strongly depolarized, NMDAR currents were potentiated 70 ± 15%, and $[Ca^{2+}]_c$ increased 5-fold compared to anoxic controls. Following naltrindole washout, E_m remained depolarized and $[Ca^{2+}]_c$ became further elevated in all neurons. The naltrindole-mediated depolarization and increased $[Ca^{2+}]_c$ were prevented by NMDAR antagonism or by perfusion of the G_i protein agonist mastoparan 7, which also reversed the naltrindole-mediated potentiation of NMDAR currents. Together, these data suggest DORs mediate NMDAR activity in a G_i-dependent manner and prevent deleterious NMDAR-mediated $[Ca^{2+}]_c$ influx during anoxic insults in the turtle cortex.

3.3.1. Introduction: Delta opioid receptors and ischemic preconditioning

Delta opioid receptors (DORS) are a class of G_i coupled receptors whose activation is neuroprotective against hypoxic or ischemic insults in mammalian neurons (Chao et al., 2007b; Zhang et al., 2002; Zhang et al., 2000). Recently, DORs have been linked to IPC-mediated neuroprotective mechanisms: in IPC-treated animals, DOR mRNA and protein titers are elevated concomitantly with increased neuroprotection, while a DOR antagonist prevents this increase in DOR expression and abolishes neuroprotection. In addition, DOR antagonism induces cell death in normoxic rat cortical neurons and accelerates anoxia-induced cell death (Zhang et al., 2002). This finding is particularly important since it suggests that a tonic background level of DOR activation is critical to neuronal survival. Despite strong evidence supporting a role for DORs as neuroprotective against anoxic insults, the mechanism of neuroprotection is unclear. Interestingly, research into the effects of NMDAR pharmacological agents on the mechanism of opioid dependency provided evidence for a cross-talk mechanism between DORs and NMDARs such that activation of DORs reduces NMDAR activity and vice-versa (Cao et al., 1997; Wang and Mokha, 1996). Since NMDAR over-activity is central to ECD and AD following ischemic insult, and since DOR activation provides neuroprotection against such insults, it is reasonable to suspect that DOR-mediated regulation of NMDAR activity is neuroprotective.

Given the emerging role for DORs in mammalian IPC models, it is noteworthy that turtle brain expresses very high endogenous levels of DORs in comparison to rat brain and that unlike rat, DORs are abundantly distributed throughout all regions of the turtle brain (Xia and Haddad, 2001). Given the functional connection between DORs and NMDARs in mammalian brain and the widespread distribution of DORS in turtle brain, I hypothesized that DOR activity may be involved in the regulation of turtle cortical NMDAR activity during anoxia. The aim of this study

was to examine the effect of DOR blockade on turtle cortical neuron electrical activity, whole-cell NMDAR peak current activity, and $[Ca^{2+}]_c$ during normoxia and during transition to anoxia.

3.3.2. Results: Delta opioid receptor-mediated regulation of NMDA receptor activity

During normoxia, E_m did not change significantly over 1 hour of recording in any neuron (Figs. 22A&23, *n* = 8), while anoxic perfusion resulted in a rapid depolarization of ~ 8 mV that was reversed following reoxygenation (Figs. 22B&23, *n* = 15). The anoxic changes in turtle NMDAR activity and $[Ca^{2+}]_c$ homeostasis are well-documented but these experiments were repeated here for statistical comparisons (Bickler et al., 2000; Pamenter et al., 2008d; Shin and Buck, 2003). During 90-mins of control recordings, normoxic NMDAR peak currents did not change significantly, ranging from 986 ± 120 to 1087 ± 73 pA, and $[Ca^{2+}]_c$ was determined to be 142 ± 8 nmol•L^{-1} (Figs. 22A, 24&25, *n* = 5 for each). Anoxic perfusion induced 50 ± 7% and 53 ± 9% reductions in NMDAR activity at 20 and 40 mins of anoxia, respectively (Figs. 22B&24, *n* = 8). $[Ca^{2+}]_c$ increased with anoxia by ~ 40% to 199 ± 15 nmol•L^{-1} (Figs. 22B&25, *n* = 5). Following normoxic reperfusion NMDAR currents and $[Ca^{2+}]_c$ returned to control levels .

Naltrindole perfusion during normoxia did not lead to significant sustained E_m depolarization, however large discrete depolarizing events were observed at a frequency of 0.06 ± 0.01 Hz (Figs. 22C (inset) &23, *n* = 20). Perfusion of the NMDAR antagonist APV abolished these depolarizing currents suggesting they are mediated by NMDARs. Naltrindole potentiated normoxic NMDAR peak currents by 49 ± 6 and 78 ± 4% following 20- and 40-mins, respectively (Figs. 22C&24, *n* = 6), and increased $[Ca^{2+}]_c$ 13 ± 4% (Figs. 22C&25, *n* = 6). Both these changes were reversed by washout of naltrindole. APV also abolished the naltrindole-mediated increase in $[Ca^{2+}]_c$, indicating the increase was due to NMDAR-mediated Ca^{2+} influx (Fig. 8A&B, *n* = 5).

During anoxia, naltrindole resulted in hyper-excitability, extended depolarization, and in 7 out of 23 experiments (31%), terminal loss of E_m (Figs. 22D&23, *n* = 23). In all 23 neurons, the extended depolarization was not reversed by reoxygenation, suggesting impaired neuronal viability following anoxia. The depolarization may have been due to increased NMDAR activity since naltrindole prevented the anoxic decrease in NMDAR peak currents. In fact, naltrindole potentiated NMDAR currents by 44 ± 19 and 70 ± 15% following 20 and 40 mins of anoxic perfusion, respectively (Figs. 22D&24, *n* = 6). This increase resembles the potentiation of turtle NMDAR currents by naltrindole during normoxia but is striking compared to the ~ 50% *decrease* in NMDAR activity normally observed in anoxic cortical neurons. Concomitant with the increase in NMDAR current magnitude and enhanced depolarization, naltrindole treatment during anoxia resulted in significantly greater increases in $[Ca^{2+}]_c$ compared to anoxic controls. In these neurons $[Ca^{2+}]_c$ increased 212 ± 16% to 302 ± 22 nmol•L^{-1}; and unlike in control anoxic recordings, $[Ca^{2+}]_c$ continued to increase following washout with normoxic naltrindole-free saline to 544 ± 56 nmol•L^{-1}, a 382% increase over control $[Ca^{2+}]_c$ and ~ 350% greater than $[Ca^{2+}]_c$ in control anoxic experiments following reoxygenation (Figs. 22D&25, *n* = 5).

I hypothesized that the electrical hyper-excitability and loss of E_m observed in most anoxic turtle cortical neurons treated with naltrindole may be due to over-activation of NMDARs and subsequent NMDAR-mediated excitotoxic elevations in $[Ca^{2+}]_c$. Blockade of NMDARs with APV prevented whole-cell NMDA-evoked currents (Fig. 22E), and had no effect on $[Ca^{2+}]_c$ or E_m (data not shown). Perfusion of APV during anoxia prevented naltrindole-mediated electrical hyper-excitability and extended depolarization (Figs. 22E&23, *n* = 7). The electrical response of anoxic neurons treated with naltrindole and APV resembled that of the response to anoxia alone and not that of anoxic/naltrindole neurons. Perhaps more importantly, in anoxic/naltrindole-

treated cells already undergoing electrical hyper-excitability, APV perfusion both abolished the excitation and enhanced E_m depolarization (Fig. 26). APV also prevented $[Ca^{2+}]_c$ increases beyond changes observed in anoxic controls and $[Ca^{2+}]_c$ decreased significantly following reoxygenation (Figs. 22E&25, $n = 4$).

Blockade of DORs with naltrindole prevents DOR-mediated G_i cascades. Mastoparan-7 (MP7) is a direct stimulator of G_i proteins and perfusion of MP7 should relieve the naltrindole-mediated DOR blockade as it acts downstream of DORs and thus of naltrindole. Therefore, I co-perfused cortical sheets with MP7 and naltrindole during anoxia. MP7 prevented the naltrindole-mediated electrical hyper-excitability and severe depolarization was not observed (Figs. 22F&23 $n = 6$). Furthermore, the anoxic decrease in NMDAR activity was restored and NMDAR activity decreased (Fig. 22F&23, $n = 6$). Finally, large increases in $[Ca^{2+}]_c$ were not observed and cells behaved like control anoxic cells: $[Ca^{2+}]_c$ increased 46 ± 3% with anoxia to 208 ± 25 nmol•L^{-1} and this change was reversed by reoxygenation (Fig. 22F&25, $n = 5$).

3.3.3. Figures

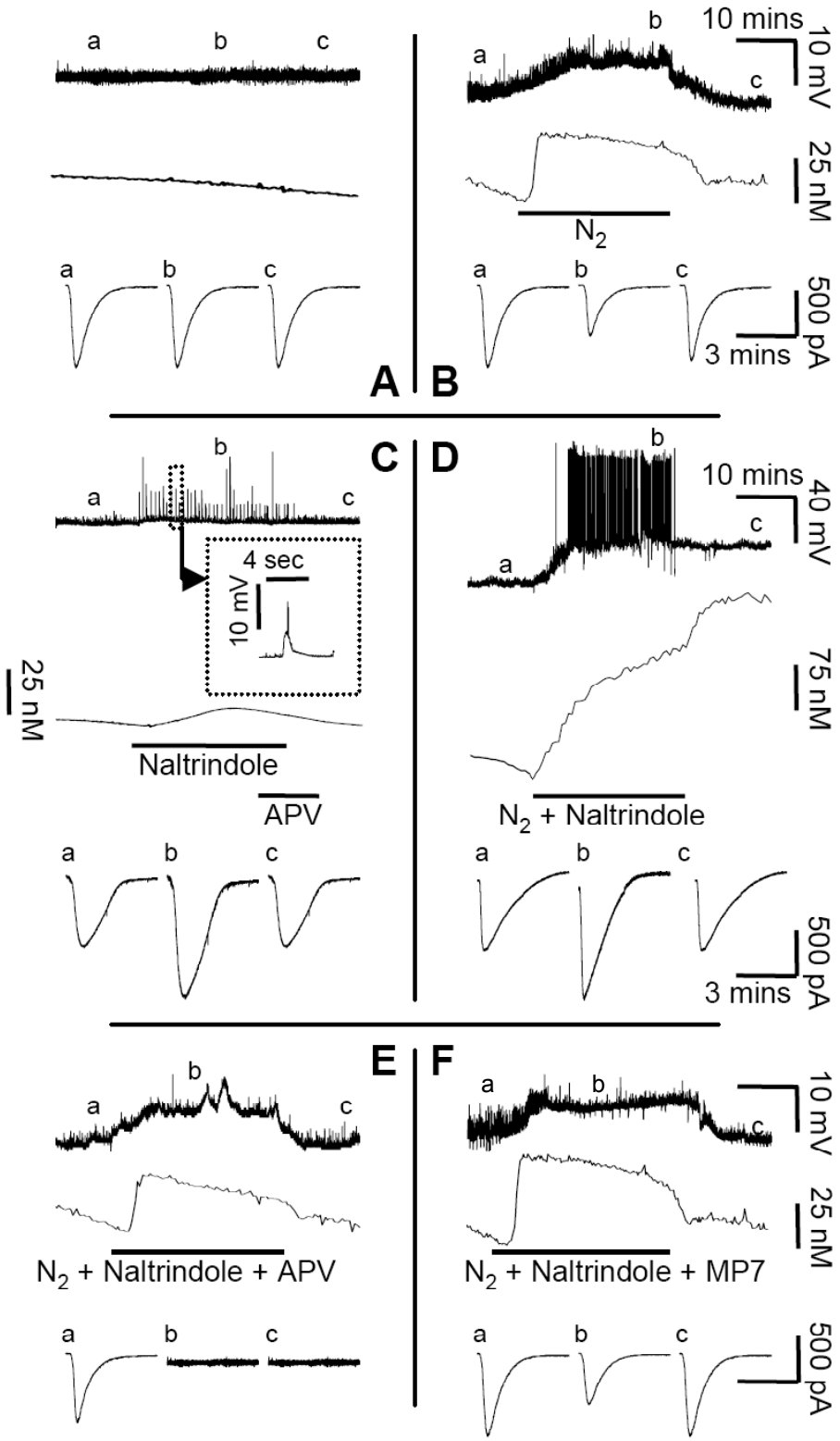
a
b
c
10 mins
10 mV
25 nM
N2
500 pA
3 mins
A
B
C
D
4 sec
10 mV
25 nM
Naltrindole
APV
40 mV
75 nM
N2 + Naltrindole
E
F
N2 + Naltrindole + APV
N2 + Naltrindole + MP7

Figure 22. Neuronal responses to naltrindole during anoxia.

For each panel the top trace (E_m) and the middle trace ($\Delta[Ca^{2+}]_c$) correspond to the same treatment regime as indicated by the solid black bars. The whole cell NMDAR currents (bottom trace) were recorded at the time-points indicated by a, b or c on the E_m trace within the same panel. All experiments were conducted on individual cortical sheets exposed to **(A)** normoxia, **(B)** anoxia, **(C)** normoxia plus naltrindole, **(D)** anoxia plus naltrindole, **(E)** anoxia plus naltrindole in the presence of the NMDAR antagonist APV, or **(F)** anoxia plus naltrindole in the presence of the G_i agonist MP7.

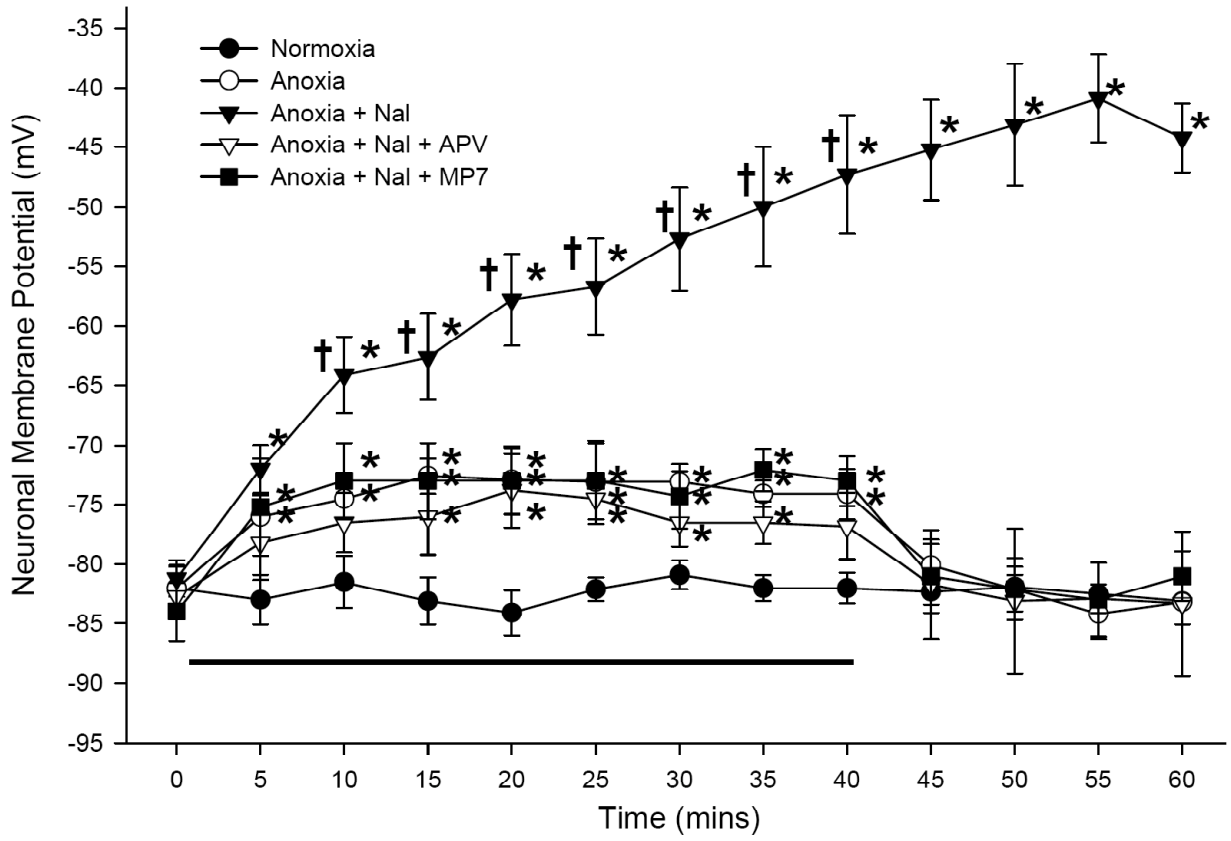

Figure 23. Naltrindole enhances anoxic neuronal depolarization via Gi protein inhibition.

Summary of E_m changes from cortical neurons during treatment as indicated in figure legend. E_m was assessed as the mean of sequential 5-min recording segments. Data are expressed as mean ± SEM. Asterisks (*) indicate data significantly different from normoxic controls. Daggers (†) indicate data significantly different from anoxic controls. Significance was assessed at $P < 0.05$. The bar indicates duration of treatment as specified in the figure legend.

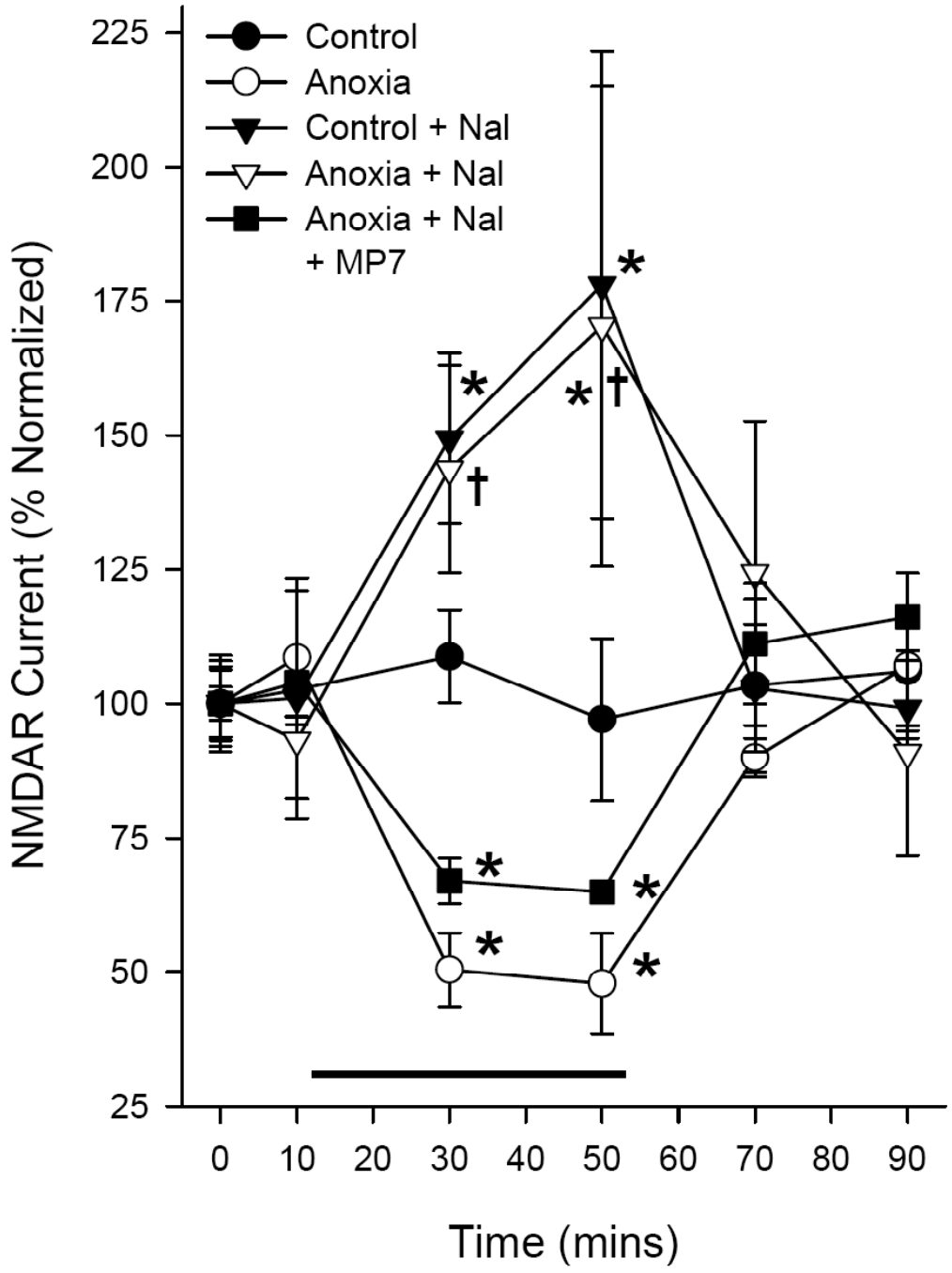

Figure 24. Naltrindole potentiates normoxic NMDAR currents and reverses the anoxic decrease in NMDAR currents via Gi protein inhibition.

Summary of changes in NMDAR currents during treatment as indicated in figure legend. Data are expressed as mean ± SEM. Asterisks (*) indicate data significantly different from normoxic controls. Daggers (†) indicate data significantly different from anoxic controls. Double daggers (‡) indicate data significantly different from anoxic neurons treated with naltrindole. Significance was assessed at $P < 0.05$. The bar indicates duration of treatment as specified in the figure legend.

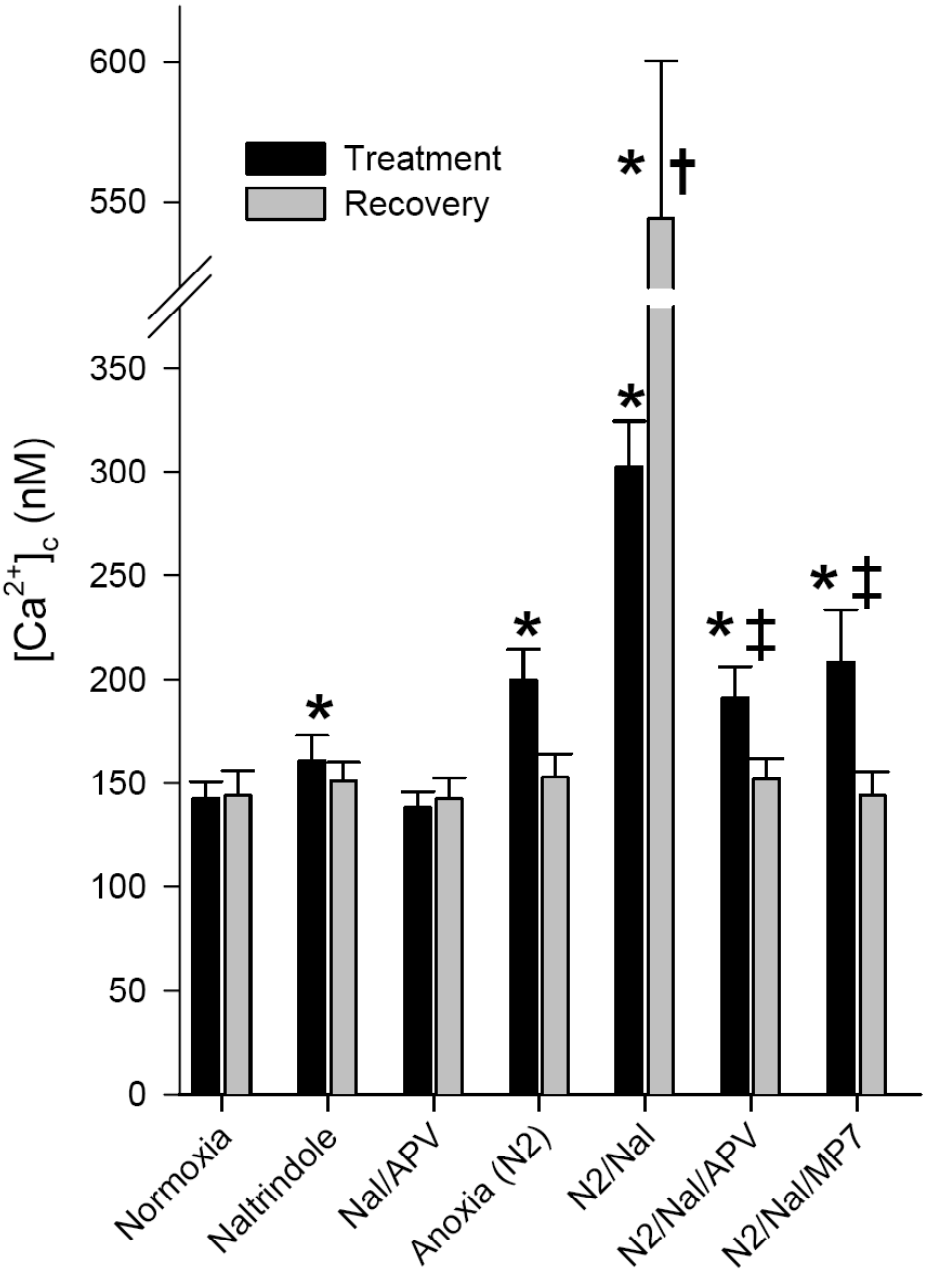

Figure 25. Naltrindole induces severe NMDAR-mediated calcium influx.

Summary of changes in $[Ca^{2+}]_c$ during normoxia and anoxia with and without the DOR antagonist naltrindole alone or in the presence of APV or MP7. Data are expressed as mean ± SEM. Asterisks (*) indicate data significantly different from normoxic controls. Daggers (†) indicate data significantly different from anoxic controls. Double daggers (‡) indicate data significantly different from anoxia plus naltrindole treatment. Significance was assessed at $P < 0.05$. The bar indicates duration of treatment as specified in the figure legend.

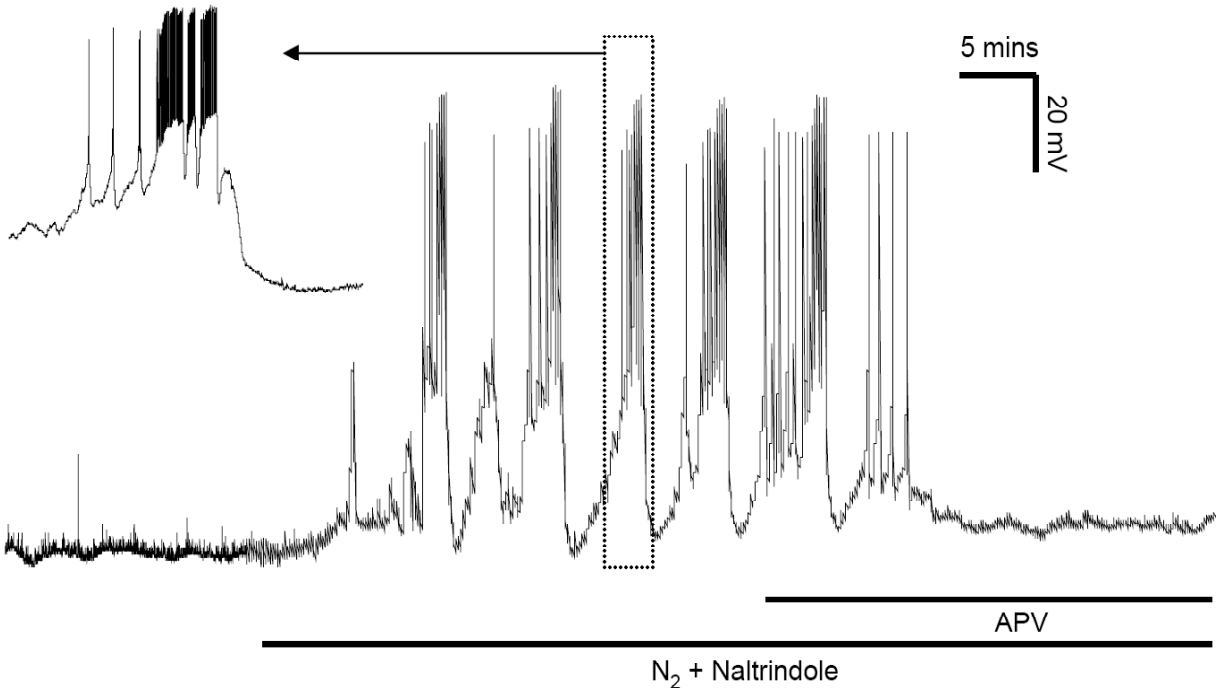

Figure 26. NMDAR blockade abolishes excitatory events in anoxia + naltrindole neurons.

3.3.4. Discussion: DOR regulation is critical to survival in the anoxic cortex

In this chapter I demonstrate that DORs inhibit NMDAR-dependent Ca^{2+} influx during both normoxia and anoxia via a G_i-sensitive mechanism in turtle cortical neurons. DOR antagonism with naltrindole potentiated normoxic NMDAR currents and Ca^{2+} influx, suggesting that a basal level of DOR activity is critical to regulating NMDARs and $[Ca^{2+}]_c$. In anoxic neurons treated with naltrindole, terminal depolarization occurred in 31% of our experiments and a large depolarization of E_m was observed in all neurons that was not reversed by reperfusion of normoxic naltrindole-free aCSF. Concomitantly, anoxic elevations in $[Ca^{2+}]_c$ were greatly increased by naltrindole and were further increased following reoxygenation. This is contrary to control anoxia-alone experiments in which both the E_m depolarization and the increase in $[Ca^{2+}]_c$ were significantly smaller in magnitude and reversed following reoxygenation (Bickler, 1992a; Bickler et al., 2000; Pamenter and Buck, 2008; Pamenter et al., 2008d). These deleterious events are likely dependent on NMDAR-mediated Ca^{2+}influx since naltrindole-mediated electrical hyper-excitability, severe prolonged depolarization, and enhanced Ca^{2+} influx were abrogated in cortical slices pre-treated with the NMDAR antagonist APV. Furthermore, in cells exhibiting seizure-like events during anoxic naltrindole perfusion, APV application abolished hyper-excitability and E_m recovered following reoxygenation.

Turtle neurons employ numerous mechanisms to limit glutamatergic hyper-excitability during anoxia, including: depressed NMDAR activity and receptor abundance, reduced glutamate release, and decreased AMPAR activity (Bickler et al., 2000; Milton et al., 2002; Pamenter et al., 2008c). As a result, NMDAR-mediated damage due to toxic $[Ca^{2+}]_c$ accumulation and deleterious NO production are avoided in the anoxic turtle cortex (Bickler, 1992a; Pamenter et al., 2008a). In previous studies examining turtle cortical NMDAR activity,

neurons were voltage-clamped and perfused with TTX to prevent action potentials. As a result, the true importance of NMDAR regulation on anoxic neuronal survival could not be determined. In the present study, I directly correlate enhanced NMDAR activity with excessive $[Ca^{2+}]_c$ accumulation and terminal depolarization in cortical neurons, highlighting the critical role of NMDAR depression in the turtles' anoxia-tolerance. Indeed turtle neurons exposed to naltrindole during anoxia responded in a fashion similar to mammalian neurons exposed to glutamate toxicity or ischemia. In such neurons, excessive NMDAR-mediated Ca^{2+} influx is observed along with severe depolarization (Coulter et al., 1992; Garthwaite and Garthwaite, 1986; Garthwaite et al., 1986). Furthermore, upon reoxygenation mammalian E_m remains depolarized, and as in our experiments, these effects could be prevented by perfusion of an NMDAR antagonist prior to the onset of severe depolarization (Limbrick et al., 2003).

The mechanism via which DORs and NMDARs interact is poorly understood, but since DORs are coupled to G_i proteins, the pathway likely involves G_i activation. There is some indirect evidence to support a role for G protein-mediated responses in the turtle's anoxia-tolerance. Whole-brain [cAMP] decreases significantly in the anoxic cortex, and since cAMP is directly mediated by G_i activity this data suggests anoxia-induced changes in G_i signaling occur in turtle brain (Pamenter et al., 2007). Furthermore, we have recently shown that the anoxic depression in turtle NMDAR activity is blocked by pertussis toxin, a G_i inhibitor (Pamenter et al., 2008b). Combined with our present report that the G_i activator MP7 depressed NMDAR currents and prevented extended depolarization and large accumulations of $[Ca^{2+}]_c$ following anoxic/naltrindole perfusion, there is now mounting evidence that G_i signaling is critical to the regulation of NMDARs in the anoxic cortex. G proteins are well suited to act as anoxic messengers since they mediate numerous downstream mechanisms in neurons. Of particular

interest are mK_{ATP}, whose activity can be directly regulated by binding of G protein subunits to the sulfonylurea subunit of the mK_{ATP} channel (Wada et al., 2000). Recently we demonstrated mK_{ATP} channels mediate the anoxic decrease in turtle NMDAR activity; such that activation of mK_{ATP} during anoxia partially uncouples mitochondria, decreasing the mitochondrial Ca^{2+} buffering capacity and subsequently elevating $[Ca^{2+}]_c$, which regulates NMDARs via a phosphatase-dependent process (Bickler et al., 2000; Pamenter et al., 2008d; Shin et al., 2005). Although mK_{ATP} activation is critical to anoxic decreases in NMDAR activity, these channels are not oxygen sensitive and are thus unlikely to be the primary detector of low oxygen that initiates downstream NMDAR depression. Therefore, the pathway upstream of mK_{ATP} activation in turtle cortical NMDAR depression remains of interest.

Interestingly, just as anoxic turtle neurons treated with naltrindole resemble ischemic mammalian neurons, mammalian mechanisms of inducible neuroprotection may parallel the endogenous mechanism of NMDAR regulation in the anoxic turtle cortex. In mammals, DOR and mK_{ATP} activation are both critical to HPC-induced neuroprotection and agonists of either receptor are neuroprotective in a range of ischemia-tolerance models, including HPC (Chao et al., 2007a; Kis et al., 2003; Yoshida et al., 2004; Zhang et al., 2000). Since targeted blockade of either receptor prevents HPC-mediated neuroprotection in mammals and NMDAR depression in turtle, it is logical that the two receptors must function at separate but critical points in the same pathway. Indeed there is evidence supporting this hypothesis: blockade of K_{ATP} channels abolishes DOR-blockade induced neuroprotection in ischemic mammalian heart and brain (Lim et al., 2004; Patel et al., 2002). The mechanism of DOR/mK_{ATP}-induced neuroprotection in mammalian brain remains unresolved, however regulation of NMDAR activity as occurs in the turtle is an attractive possibility as this regulation is critical to preventing ECD in mammalian

neurons (Arundine and Tymianski, 2003; Pamenter et al., 2008d). This hypothesis is supported indirectly by the inverse relationship between NMDAR activity and DOR activation observed in mammalian brain whereby increases in DOR activity suppress NMDAR activity (Cao et al., 1997; Wang and Mokha, 1996). Therefore, the final mediator of neuroprotection in DOR-mediated HPC models may be a reduction in NMDAR current.

DOR protein expression in the turtle brain is high relative to rat brain tissue (Xia and Haddad, 2001), and this difference in receptor expression could partly explain the turtle's remarkable innate anoxia tolerance relative to mammalian brain, despite their apparent reliance on similar neuroprotective mechanisms. Greater receptor expression may confer a higher sensitivity to opioid-mediated signaling, allowing turtle brain to rapidly decrease NMDAR activity in response to decreasing environmental oxygen while long-term mechanisms of metabolic depression are being activated (e.g. removal of channels from neuronal membranes (Bickler et al., 2000; Perez-Pinzon et al., 1992c). Conversely, mammalian brain requires HPC pre-treatment to upregulate DOR protein expression and 'prime' the brain against subsequent low-oxygen insults. Thus turtle brain is better able to respond quickly to low-oxygen insults than murine brain. Conversely, the role of DOR-mediated signaling in long-term anoxia-tolerance in the turtle remains undetermined, however NMDAR activity remains depressed during at least the first six weeks of anoxia in turtle brain and DOR-mediated pathways may regulate this depression (Bickler, 1998).

The metabolic state of the anoxic turtle brain is very tightly regulated and any significant deviation from this state that increases electrical activity may quickly overcome the turtle neurons' ability to match its metabolic depression to decreased energy availability during anoxia. This may explain why naltrindole is neurotoxic in turtles during anoxia but not normoxia, despite

potentiating NMDAR currents in both experiments. During normoxia, the Na^+/Ca^{2+} exchanger and the associated Na^+/K^+ ATPases that maintain the Na^+ gradient counter excessive NMDAR-mediated Ca^{2+} influx. However, during anoxia turtle ATPase activity is decreased to match decreased ATP production (Buck and Hochachka, 1993; Buck and Pamenter, 2006; Hylland et al., 1997). Thus an increase of Na^+/Ca^{2+} exchanger activity to counter NMDAR-mediated Ca^{2+} influx would deplete the Na^+ gradient more rapidly then the ATPase can match in its' reduced activity state, leading to rundown of E_m and deleterious $[Ca^{2+}]_c$ accumulation.

In conclusion, I show that blockade of DORs potentiates normoxic NMDAR currents and not only prevents but reverses the anoxic decrease in NMDAR activity, leading to excitotoxic events, increased Ca^{2+} influx, and terminal depolarization in a significant percentage of anoxic neurons. Our results offer a strong hypothesis to researchers examining mammalian models of HPC-mediated neuroprotection against ischemic insults. DOR activation is neuroprotective in mammalian models of stroke, and in both the turtle and mammals DORs regulate NMDAR activity. As in turtle neurons, depression of NMDAR activity is critical to ischemic survival in mammalian neurons since blockade of NMDARs reduces $[Ca^{2+}]_c$ accumulation and prevents ECD following ischemic insult in mammals. However, direct blockade of NMDARs results in sedative or psychomimetic side effects (Ikonomidou and Turski, 2002). DOR-mediated inhibition of NMDARs, as occurs in turtle cortex, may offer an indirect mechanism of NMDAR depression that is independent of direct pharmacological NMDAR blockade.

3.4. Endogenous reductions in N-methyl-D-aspartate receptor activity inhibit nitric oxide production in the anoxic freshwater turtle cortex

Preface

A modified version of this chapter was published as: Pamenter ME, Hogg DW and Buck LT (2008). Endogenous reductions in N-methyl-D-aspartate receptor activity inhibit nitric oxide production in the anoxic freshwater turtle cortex. *FEBS Lttrs.* 582:1738-1742.

I conceived of and designed the experiments. DW Hogg and I each performed 50% of the experiments and I wrote the paper with editing by L Buck.

Abstract

Increased nitric oxide (NO) production from hypoxic mammalian neurons increases cerebral blood flow (CBF) but also glutamatergic excitotoxicity and DNA fragmentation. Anoxia-tolerant freshwater turtles have evolved NO-independent mechanisms to increase CBF; however, the mechanism(s) of NO regulation are not understood. In turtle cortex, anoxia or NMDAR blockade depressed NO production by 27 ± 3 and 41 ± 5%, respectively. NMDAR antagonists also reduced the subsequent anoxic decrease in NO by 74 ± 6%, suggesting the majority of the anoxic decrease is due to endogenous suppression of NMDAR activity. Prevention of NO-mediated damage during the transition to and from anoxia may be incidental to natural reductions of NMDAR activity in the anoxic turtle cortex.

3.4.1. Introduction: hypoxic nitric oxide (NO) production

CBF is generally elevated with hypoxia or hypercapnea in human and murine models (Ioroi et al., 1998; Van Mil et al., 2002). Increased CBF is considered neuroprotective since it allows greater delivery of glycolytic substrate and rapid removal of acidic anaerobic end products from sensitive brain regions. NO is a signaling metabolite that plays a critical role in the regulation of CBF in adult mammalian brain such that: (1) CBF increases coordinately with increased NO production in response to hypoxia and also following reoxygenation; (2) NO scavengers or inhibition of nitric oxide synthases (NOS) decrease CBF and abolish the hypoxic increase in CBF; and (3) NO promoters increase CBF in normoxia and during hypoxia (Namiranian et al., 2005). In murine models, ischemia induces rapid elevations in cerebral NO, increases NOS activity and elevates NOS gene expression, and all of these events contribute to neuroprotective increases in CBF (Iadecola et al., 1995; Kader et al., 1993).

Although NO promotes enhanced CBF, there is considerable debate as to whether NO production is neurotoxic or neuroprotective in ischemic mammalian neurons (Iadecola, 1997). For example, in rat, mouse, gerbil and neonatal piglet brain, NO scavengers or inhibition of neuronal or inducible NOS provide significant neuroprotection and prevent DNA fragmentation and release of apoptotic factors (Fang et al., 2006; Haga et al., 2003; van den Tweel et al., 2005; Zubrow et al., 2002). Furthermore, decreased NO formation has been linked to improved behavioral testing performance and neuroprotection in gerbils (Li et al., 2004). However, others have reported that NO donors provide neuroprotection against global and focal models of ischemia in adult rat brain, reduce the extent of ischemic infarct damage in neo-natal rat brain and reduce ROS-mediated neurotoxicity (Banerjee et al., 2007; Kakizawa et al., 2007; Martinez-Murillo et al., 2007; Serrano et al., 2007). These conflicting reports may be due to the interaction

of NO with numerous cellular systems simultaneously. For example, NO can act as a free radical scavenger, ameliorating the deleterious effects of ROS (Wink et al., 1994); however, NO can also interact with superoxide to produce peroxynitrate, leading to DNA fragmentation and cell degradation via apoptotic pathways (Bonfoco et al., 1995).

In mammals, the neurotoxic effects of NO are primarily mediated by excessive glutamatergic receptor activity. Ischemic insults promote elevated glutamate release and over-activation of NMDARs, which is the primary entry point of Ca^{2+} during ischemia and whose activation leads to ECD in ischemic mammalian neurons (Choi, 1994). Neuronal NOS (nNOS) is associated with the NMDAR scaffold protein – postsynaptic density 95 (PSD-95), and NMDAR activation leads to cytosolic Ca^{2+} accumulation and stimulation of nNOS-dependent NO production (Ishii et al., 2006; Scorziello et al., 2004). NO is a powerful intra and intercellular signaling molecule and it enhances glutamate release from pre-synaptic neurons, contributing significantly to the acceleration of ECD (Katchman and Hershkowitz, 1997; Montague et al., 1994). Therefore, although enhanced NO production promotes CBF and provides neuroprotection during ischemic insults, the side effects of this mechanism are complex and may lead to ECD or apoptotic events in afflicted neurons.

Facultative anaerobes such as the turtle and the crucian carp rely solely on glycolytic metabolism during anoxic episodes and are thus dependent on maintained delivery of glycolytic substrate (Chih et al., 1989a; Johansson and Nilsson, 1995; Johansson et al., 1995). Changes in CBF during anoxia and recovery have been reported in both the red-eared slider and the crucian carp, but changes in NO production have not been measured in any facultative anaerobic species. In turtle, CBF increases from 1.7 to 2.6-fold within the first hour of anoxia before returning to pre-anoxia levels, presumably due to the onset of a deeper metabolic depression which limits the

need for enhanced glycolytic substrate delivery (Davies, 1989; Hylland et al., 1994). Furthermore, secondary increases in CBF of up to 80% were observed upon reoxygenation, which may contribute to the removal of acidic anaerobic end products. During normoxia, turtle CBF can be mediated by adenosine or by acetylcholine via the activity of NO; however during anoxia, adenosine alone affects the anoxic increase in CBF while inhibition of NO synthesis or an NO donor have no effect on anoxic CBF (Bickler, 1992b; Hylland et al., 1994). Similarly, in the anoxic crucian carp CBF is increased by anoxia and this increase is not prevented by NOS blockade. NO synthesis has an absolute requirement for oxygen, thus the inability of NO drugs to block the anoxic increase in CBF in these organisms is not surprising.

Although inhibition of NO synthesis during anoxia did not alter turtle CBF, NOS inhibition during normoxia led to a complete cessation of CBF that recovered to control flow rates within 15-20 mins (Hylland et al., 1994). These authors concluded that turtles possess a CBF tonus that is NO-mediated similar to the constant vasodilatory tonus observed in mammals (Fernandez et al., 1993), but that upon suppression of this tonus, secondary CBF-regulating mechanisms take over. This secondary mechanism may be responsible for anoxic increases in CBF, which are not susceptible to NO-mediated signaling. Indeed, since these facultative anaerobes survive for months in a zero-oxygen environment, NO-mediated regulation of CBF would be impossible and thus the development of a non NO-based mechanism is an evolutionary necessity. However, in their natural environment turtles undergo frequent prolonged periods of intermittent hypoxia while foraging or diving during which surges in NO production may occur.

As discussed above, increased CBF is neuroprotective but there is debate as to whether increases in NO production are neuroprotective or neurotoxic during anoxic insult and following reoxygenation in mammals. Thus the mechanism of CBF regulation in the anoxic turtle is of

interest because CBF is greatly elevated during anoxia and following reoxygenation independently of NO production, and because CBF becomes effectively immune to NO signaling during anoxia. It is currently not known how the response of turtle brain to NO is down-regulated during the transition to anoxia and this response could be due to changes in the production of NO, either via direct down-regulation of NOS or as a result of decreased NMDAR-mediated Ca^{2+} influx during anoxia in the turtle cortex. The aims of this chapter were to (1) determine the changes in NO production from turtle cortex during normoxia and during a normoxic to anoxic transition followed by reoxygenation recovery. Furthermore, (2) I examined the ability of the NOS inhibitor N^{G}-nitro-L-arginine methyl ester (L-NAME: 0.5 - 5.0 mM) to decrease NO production during normoxia (Rees et al., 1990). Finally, (3) I examined the role of NMDAR activity in NO production by blocking NMDARs with 60 μM APV during normoxia and during normoxic to anoxic transitions.

3.4.2. Results and discussion

For up to two hours of normoxic recording DAF-FM fluorescence (a measure of [NO]) decreased steadily at a low rate due to photo bleaching or dye leakage but the rate of DAF-FM fluorescence decrease was unchanging (n = 4, Figs. 27A&B). The specificity of the dye for NO was confirmed by perfusion of either sodium nitroprusside (SNP: 0.1 - 10.0 mM) or L-NAME onto normoxic cortical sheets. Perfusion of the general NOS inhibitor L-NAME resulted in slow and small reduction in NO production of 5.8 ± 1.1% (n = 5, Figs. 27A&C), consistent with a low rate of endogenous NOS activity in the turtle cortex. The NO-donor SNP induced rapid and repeatable increases in DAF-FM fluorescence of 22.6 ± 3.7% (n = 4, Figs. 27A&D). These responses to SNP or L-NAME are consistent with similar control experiments in mammalian brain (Kojima et al., 2001).

In cortical sheets exposed to anoxic aCSF, NO production rapidly decreased 27.1 ± 3.1% with decreasing oxygen and recovered to baseline levels immediately upon reoxygenation (n = 5, Figs. 27A&E). These changes were rapid and repeatable in contrast to NO changes in ischemic mammalian brain where low oxygen induces rapid increases in NO, likely due to increases in glutamatergic-connected nNOS activity associated with excitotoxic Ca^{2+} entry and eventual apoptotic cell death (Peeters-Scholte et al., 2002). Since inhibition of inducible and neuronal NOS is generally neuroprotective in mammals, I hypothesized that NOS activity is naturally depressed in the anoxia-tolerant turtle brain. To examine this hypothesis I pre-incubated cortical sheets with anoxic aCSF for 30 mins and then treated them simultaneously with L-NAME and anoxia. In these experiments, no significant change in DAF-FM fluorescence was observed after L-NAME perfusion, suggesting NOS activity is depressed in the anoxic turtle cortex (n = 4, Figs. 27A&F).

The decrease in NO formation during the transition to anoxia may be related to glutamatergic receptor activity in the anoxic turtle cortex. In mammals, the toxic effects of NO are mediated by NMDARs, which induce NO formation in a manner dependent on NMDAR-mediated Ca^{2+}-influx. Furthermore, the surge of NO observed in ischemic murine brain is abolished by glutamatergic receptor antagonists (Garthwaite et al., 1988; Lin et al., 1996). The turtle brain expresses a number of adaptations that limit excitotoxic glutamatergic Ca^{2+} entry during anoxia, including reduced glutamate release, depressed NMDAR and AMPAR currents and removal of NMDARs from the neuronal membrane with prolonged anoxia (Bickler et al., 2000; Milton et al., 2002; Pamenter et al., 2008c). As a result of these mechanisms, toxic accumulations of cytosolic Ca^{2+} and ECD are avoided during prolonged anoxia. Therefore, regulation of NMDAR-mediated Ca^{2+} entry may underlie the reduced NO production observed during the transition to anoxia in turtle cortex.

To examine the role of NMDAR activity in the regulation of NO production during anoxic transitions, I treated cortical sheets with the NMDAR antagonist APV during normoxia and then subsequently recorded DAF-FM fluorescence during a normoxic to anoxic transition in the presence of APV. In normoxic sheets, APV resulted in a 41.2 ± 4.9% depression of NO production (n = 4, Figs. 28A-B). Subsequent anoxic exposure of the same tissue resulted in a further small decrease in NO production of 7.1 ± 2.3 % that was ~75% smaller than the regular anoxia-alone decrease in NO production ($P < 0.01$, n = 4, Figs. 28A-B). These data suggest that the decrease in NO production during the transition to anoxia is due largely to depressed NMDAR activity in the cortex. The observation that the magnitude of the decrease of NO production with APV was greater than with anoxia alone is likely due to complete NMDAR

inhibition by APV compared to the ~ 50% endogenous reduction in NMDAR activity in the anoxic cortex (Bickler et al., 2000).

The primary neuroprotective mechanism mediated by depressed glutamatergic activity is the prevention of toxic Ca^{2+} accumulation (Bickler and Buck, 1998), but it is interesting to note that in the anoxic turtle cortex, depressed NMDAR activity may preclude neuronal damage via a second mechanism: by limiting NO accumulation and associated DNA fragmentation. In mammals, NO contributes to detrimental feed-forward mechanisms that accelerate ECD: NO production is promoted by NMDAR-mediated Ca^{2+} entry and then acts as a retrograde signal to enhance glutamate release and increase the over-activation of NMDARs (Katchman and Hershkowitz, 1997; Montague et al., 1994). Therefore, the evolution of NO-independent mechanisms to increase CBF in the turtle cortex allows neuroprotective increases in CBF without deleterious elevations in NO and NMDAR activity that occur concomitantly in mammals. In the anoxic turtle brain, changes in CBF are regulated by an adenosine-based mechanism since adenosine perfusion mimics the anoxic increase in CBF and blockade of adenosine A_1R receptors abolishes both the adenosine- and anoxia-mediated increases in CFB (Hylland et al., 1994).

In summary, some facultative anaerobes utilize increased CBF to enhance neuronal survival during anoxic exposure. Enhanced CBF is also neuroprotective in mammals where it is NO-dependent, however increased NO production leads to elevated glutamate release and DNA fragmentation. Here I measured for the first time in a facultative anaerobe changes in NO production in response to anoxic perfusion and reoxygenation and NOS or NMDAR inhibition. The evolution of NO-independent mechanisms of increased CBF allows these organisms to suppress the production of NO and thus reduce free radical damage and NO-dependent glutamate

release without compromising increased blood flow during the transition to and from anoxia. Furthermore, an NO-independent mechanism would allow for regulation of CBF during prolonged anoxia when oxygen is not available and NO cannot be formed.

3.4.3. Figures

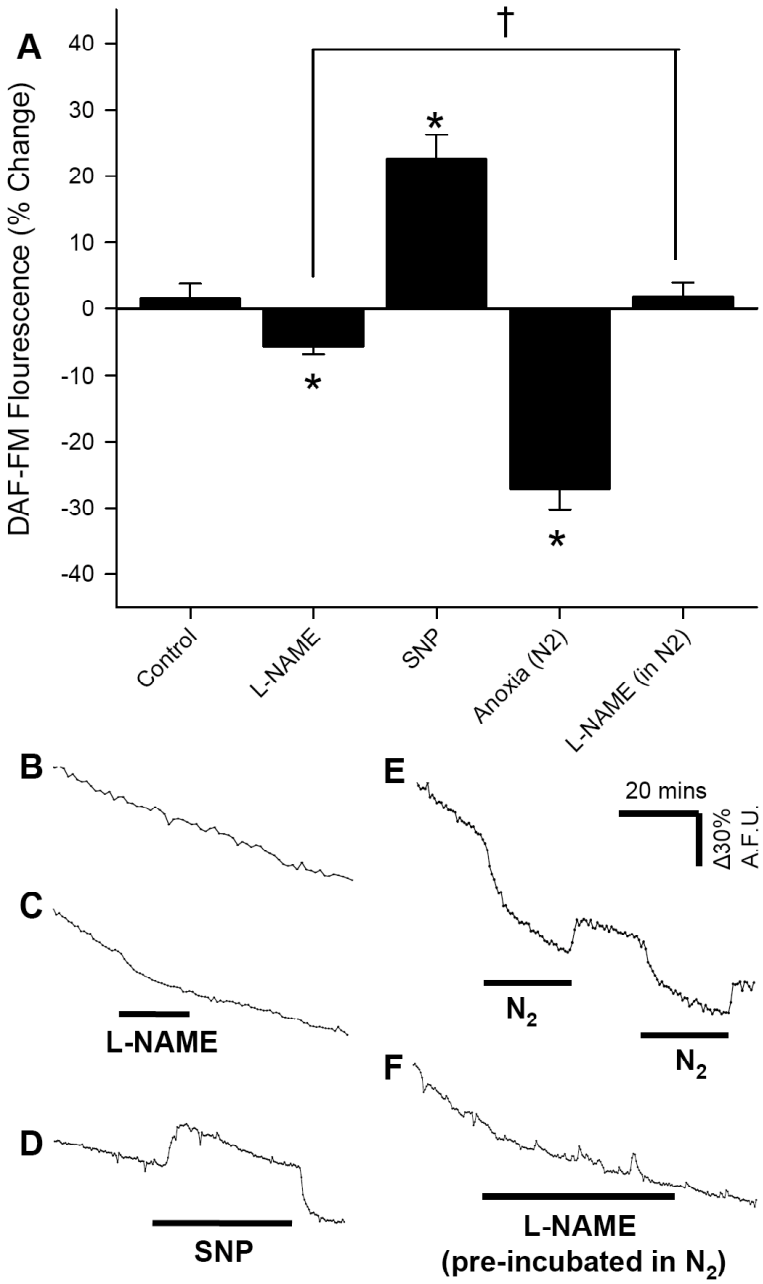

Figure 27. NO production and NOS activity decrease with anoxia in cortical sheets.

(A) Normalized changes in normoxic DAF-FM fluorescence (NO production) from cortical sheets undergoing a normoxic to anoxic transition or treatment with the general NOS inhibitor L-NAME (0.5-5 mM) or the NO donor SNP (0.1-10 mM). Data are expressed as mean ± SEM. Asterisks indicate significant changes from control baseline following treatment onset. Dagger indicates significant difference ($P < 0.05$). **(B-F)** Raw data traces of DAF-FM fluorescence changes from cortical sheets undergoing treatments as specified by the solid bars under the individual traces. Each trace represents the average of > 25 neurons from a single cortical sheet.

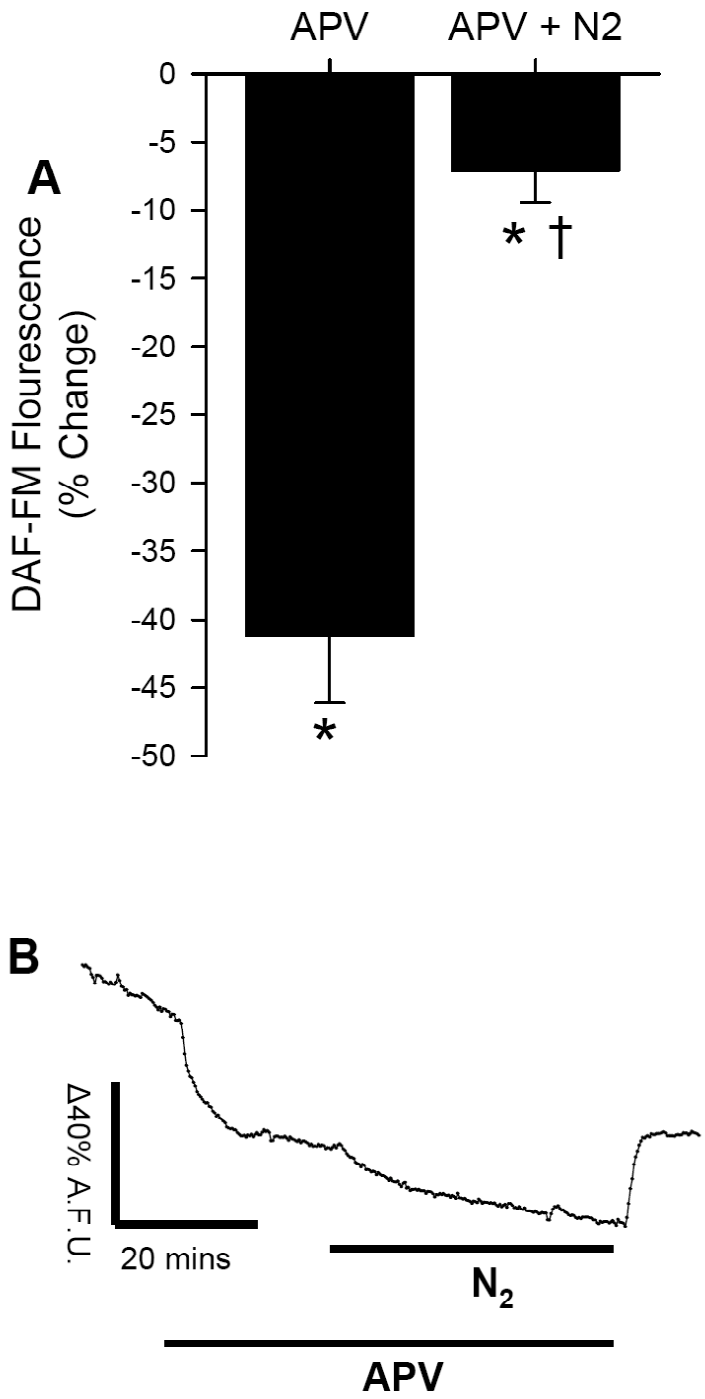

Figure 28. Anoxic changes in NO production and NOS activity in cortical sheets.

(A) Normalized changes in DAF-FM fluorescence from cortical sheets undergoing NMDAR blockade with APV (60 μM) or a normoxic to anoxic transitions in the presence of APV. Data are expressed as mean ± SEM. Asterisks indicate significant changes from control baseline following treatment onset. Dagger indicates data significantly different from anoxic control (see Fig. 1, $P < 0.05$). **(B)** Raw data trace of DAF-FM fluorescence changes from a cortical sheet undergoing treatments as specified by the solid bars under the individual traces. Each trace represents the average of > 25 neurons from a single cortical sheet.

4. GABA receptor-mediated spike arrest prevents seizures and cell death in anoxic turtle cortex

Preface

I designed and performed all experiments in this study except for the perforated patch experiments, which were performed by J Ormond. D Hogg performed 40% of the MEQ imaging experiments. I wrote the paper with editing by L Buck.

Abstract

Ischemic insults cause hyper-excitability and cell death in mammalian neurons. In the painted turtle, neurons survive prolonged anoxic exposure by suppressing electrical excitability through a poorly understood mechanism. We asked whether the inhibitory neurotransmitter GABA, which becomes elevated in anoxic turtle brain, might underlie this suppression. We found that the effects of GABA application, including increased whole-cell conductance and action potential threshold and decreased action potential frequency mimicked those of anoxia. GABA receptor blockade under anoxic conditions prevented the suppression, leading to seizures, anoxic depolarization, deleterious calcium influx, and cell death. Neurons could be rescued by blocking voltage-sensitive sodium channels and associated action potential-mediated hyper-excitability. Our results indicate that during anoxia, widespread GABA release and the resulting large, sustained inhibitory conductance prevents hyper-excitability via a shunt-like mechanism. The critical nature of GABA-mediated electrical depression to the survival of turtle cortical neurons during anoxia indicates a potential site for therapeutic intervention against anoxic insults in mammalian brain.

4.1. Introduction to inhibitory GABAergic signaling

It has been more than 20 years since Peter Hochachka first published his concept of channel arrest, which predicts a decrease in membrane ion conductance to reduce metabolic energy expenditure as an adaptation to oxygen-limiting environments (Hochachka, 1986). This hypothesis is supported by experiments on anoxia-tolerant freshwater turtles (*C. picta*, *T. scripta*) and fish (*C. auratius*, *C. carassius*), which demonstrate decreased neuronal conductance to excitatory Na^+ and Ca^{2+} ions with anoxia, along with decreased channel density, pump activity, and energy consumption (Bickler et al., 2000; Buck and Bickler, 1995; Hylland et al., 1997; Pamenter et al., 2008c; Pamenter et al., 2008d; Perez-Pinzon et al., 1992c; Wilkie et al., 2008). However, while channel arrest of excitatory ion channels undoubtedly contributes to anoxic energy conservation, increased conductance to inhibitory ions may play a more pivotal role in anoxia-tolerance. Indeed, we now demonstrate in the case of inhibitory GABA receptors, ion channel conductance also increases under oxygen limiting circumstances in turtle cortex.

GABA is the primary inhibitory neurotransmitter in the mature mammalian CNS (Krnjevic, 1997), and anoxia-tolerant species collectively exhibit rapid and prolonged elevations in [GABA] when deprived of oxygen (Hitzig et al., 1985; Hylland and Nilsson, 1999; Nilsson and Winberg, 1993). The role of GABAergic signaling during anoxia has not been directly examined in any facultative anaerobe; however in most mature mammalian neurons, increases in GABA-mediated conductance to inhibitory Cl^- (G_{Cl}) and K^+ (G_K) clamp membrane potential (E_m) near the reversal potentials of these ions. Excitatory electrical inputs are thus dampened by an opposing flow of negative current due to chronically activated GABA receptors, limiting AP generation, neuronal excitability, and thus conserving energy supplies (Ben-Ari, 2002).

Failure to limit neuronal hyper-excitability in low oxygen environments leads to dire consequences for mammalian neurons, which are unable to sustain sufficient ATP production to meet cellular demands. As a result, the Na^+/K^+ pump fails and E_m runs down rapidly. This anoxic depolarization (AD) leads to neuronal hyper-excitability, deleterious Ca^{2+} influx through chronically activated NMDARs, ECD, and spreading depression in the penumbra (Anderson et al., 2005; Lundberg and Oscarsson, 1953; Yao et al., 2007). While glutamate receptor blockade can prevent ECD in mammals (Sattler and Tymianski, 2000), it does not prevent AD-mediated injury or post-insult apoptotic cell death (Anderson et al., 2005; Jarvis et al., 2001). Furthermore, spike arrest occurs in anoxic Purkinje neurons from turtle cerebellum, a brain region which does not express functional glutamatergic NMDARs in mature mammals (Albin and Gilman, 1992; Audinat et al., 1992; Crepel et al., 1983; Perez-Pinzon et al., 1992a; Perkel et al., 1990). Since electrical depression is observed in the absence of glutamatergic receptors in these neurons, and since ischemic insults in mammalian neurons are not ameliorated by glutamatergic blockade, examination of alternative mechanisms of limiting electrical excitability during ischemic insults is of pressing interest. The purpose of this paper was to test the hypothesis that increased GABAergic conductance mediates electrical suppression in the anoxic turtle cortex.

4.2. Results: the role of GABA in anoxic electrical inhibition

Turtle cortical neurons undergo electrical depression during anoxia. In control experiments with normoxic perfusion we observed no significant changes in E_m, AP frequency (AP_f), whole cell conductance (G_w), AP threshold (AP_{th}), cytosolic Cl^- concentration ($[Cl^-]_c$), or $[Ca^{2+}]_c$,, (*n* = 15, Figs. 29A-B, D-F, H-I, K-L). However, neurons exposed to acute anoxia underwent a significant depression in electrical activity. ECD did not occur in anoxic turtle neurons and hyper-excitability and AD were not observed (*n* = 19). Instead, AP_f decreased ~ 75%, E_m was mildly depolarized by ~ 8 mV, and G_w and AP_{th} increased 25-35% (Figs. 1A, C-E, G). $[Cl^-]_c$ decreased and $[Ca^{2+}]_c$ was moderately elevated with no evidence of excitotoxic increase in $[Ca^{2+}]_c$ or electrical activity characteristic of ischemic mammalian neurons (*n* = 5 and 7 respectively, Figs. 29H, J, K, I). Upon reperfusion with normoxic aCSF, electrical depression was rapidly reversed and AP_f, G_w, AP_{th}, $[Cl^-]_c$, and $[Ca^{2+}]_c$ returned to normoxic levels. All turtle neurons survived anoxic experiments without apparent detriment.

Increased normoxic GABAergic signaling mimics anoxic 'spike arrest'. The effect of GABA perfusion (0.25 – 2.0 mM) on neuronal electrical activity was examined in normoxic neurons using both perforated patch and whole-cell patch-clamp techniques. In gramicidin perforated-patch experiments, E_m was -91.0 ± 1.0 mV and E_{GABA} was slightly depolarizing at -87.4 ± 1.3 mV (*n* = 10, Figs. 30A&B). Perfusion of GABA resulted in an ~ 75% decrease in input resistance (R_{in}), which was not blocked by perfusion of either $GABA_A$ or $GABA_B$ antagonists (*n* = 3 for each, Fig. 30C). All GABA-mediated changes were reversed by GABA washout.

In whole-cell experiments, GABA perfusion induced electrical depression in cortical neurons that mimicked anoxic spike arrest, characterized by decreased AP_f and increased G_w and

AP_{th}, (n = 10, Figs. 31A-C). GABA also induced moderate Cl^- efflux (n = 4, Fig. 31D). None of these changes were significantly different from anoxic changes ($P < 0.001$) and all changes were reversed by GABA washout. Blockade of $GABA_A$ receptors (with gabazine, n = 7) or $GABA_B$ receptors (with CGP55845, n = 8) each increased electrical excitability in normoxic neurons: AP_f was increased 20-fold by gabazine and 5-fold by CGP55845 (Fig. 31A). Furthermore, with blockade of either GABA receptor, G_w increased by ~ 20% (data not shown). This increase was likely due to increased channel opening during excitatory events since co-treatment with TTX abolished AP firing and also prevented the increase in G_w attributable to antagonism of either receptor (n = 8 for each, Fig. 31B). Finally, GABA perfusion induced an efflux of Cl^- (n = 4, Fig. 32D), which was abolished by co-perfusion of gabazine but not CGP55845 (data not shown). Individual GABA receptor blockade had no effect on normoxic $[Cl^-]_c$ (n = 3 for each, Fig. 32D).

GABA receptors mediate anoxic 'spike arrest'. GABA perfusion during anoxia induced similar changes in each of the parameters measured compared to anoxia-alone or GABA-alone treated neurons (n = 10, Fig 31A-D). In neurons treated with anoxia plus a single GABA receptor antagonist, electrical excitability was moderately increased relative to anoxic control experiments, including increased AP_f and smaller increases in AP_{th} and G_w. Anoxic neurons treated with individual GABA receptor antagonists were quieter electrically than control neurons treated with either GABA receptor antagonist during normoxia; however, simultaneous blockade of both $GABA_A$ and $GABA_B$ receptors entirely prevented the anoxic increase in G_w and depolarization of AP_{th}, AP_f increased 2831.5 ± 271.1% (n = 15, Figs. 31A-C), and $[Cl^-]_c$ was unchanged (n = 5, Fig. 31D). Furthermore, these neurons exhibited seizure-like events (SLEs) and 67% of patched neurons underwent terminal depolarization of E_m (as assessed by a sustained

loss of E_m to > -10 mV and an inability to fire APs) despite reoxygenation (Figs. 32A-B). Finally, $[Ca^{2+}]_c$ became elevated 4-fold with co-perfusion of gabazine and CGP55845 during anoxia and was elevated further to > 1 uM during reperfusion (*n* = 4, Figs. 32D-E).

Na^+ channel blockade abolishes neurotoxicity induced by anoxic GABA receptor antagonism. Since blockade of inhibitory GABAergic signaling during anoxia resulted in SLEs and terminal depolarization, we hypothesized that hyper-excitation in these neurons resulted in chronic depletion of ATP supplies, failure of neuronal ATPases, loss of E_m, and subsequent cell death. To test this hypothesis, we prevented ATP production by inducing chemical ischemia (blocking glycolysis with iodoacetate while simultaneously blocking oxidative phosphorylation with NaCN). Simulated ischemia resulted in SLEs, terminal depolarization of E_m, deleterious $[Ca^{2+}]_c$ influx and rapid cell death that were all statistically similar to neurons treated with GABAergic antagonists during anoxia (*n* = 5, Figs. 32A&D). If hyper-excitation leads to energy depletion and terminal depolarization, then prevention of AP firing with the voltage-gated Na^+ channel antagonist tetrodotoxin (TTX) should limit electrical excitability and prevent terminal depolarization during anoxic insults. Indeed, treatment of GABA antagonist-treated anoxic neurons with TTX inhibited APs and prevented SLEs and deleterious $[Ca^{2+}]_c$ accumulation (*n* = 6, Figs. 32A, C-D, F). Furthermore, TTX also prevented terminal depolarization upon reperfusion in these neurons. TTX had no effect on G_w in normoxic experiments or on the increase in G_w in control anoxic experiments (*n* = 5, raw data not shown).

4.3. Figures: GABA

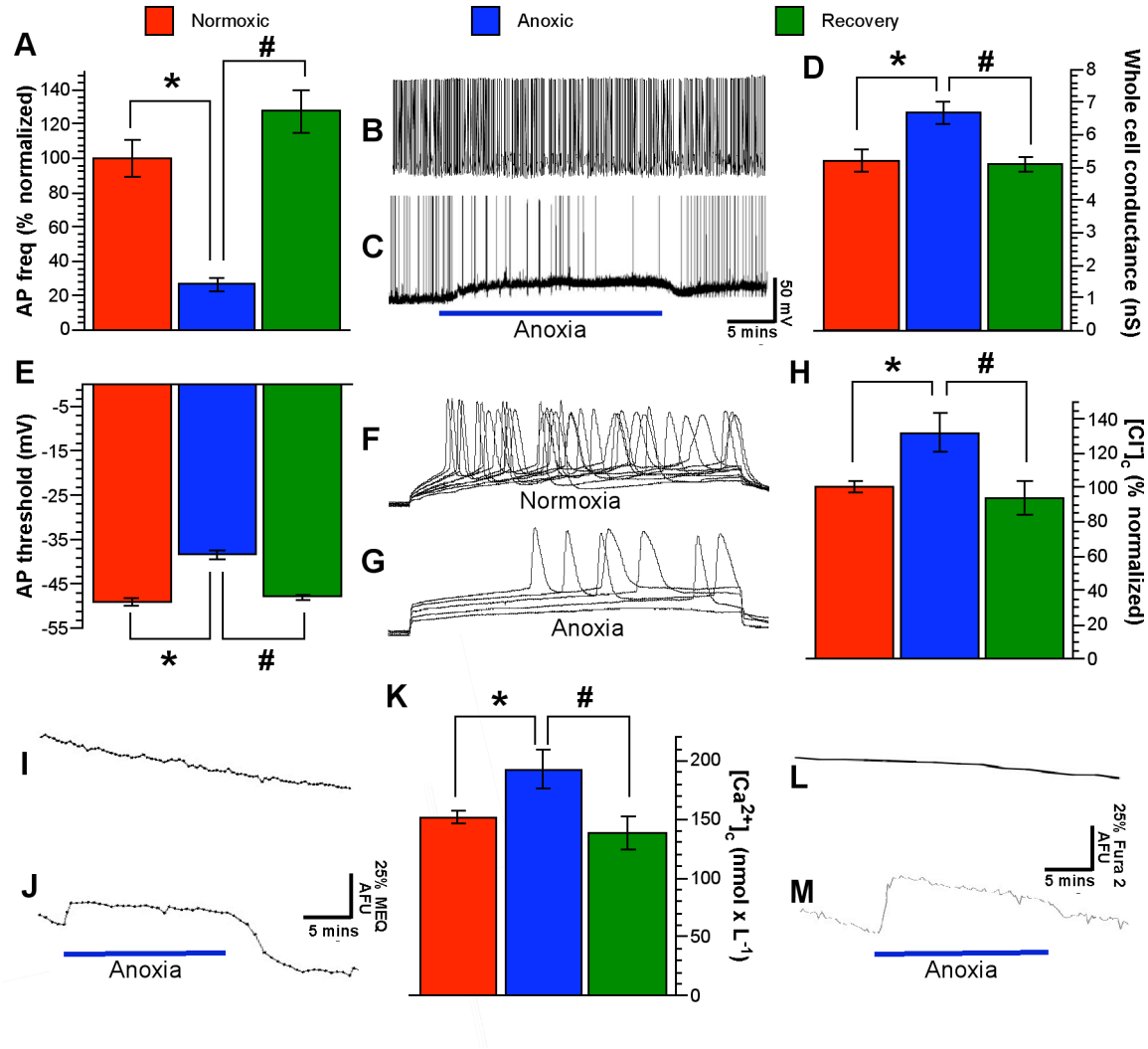

Figure 29. Spike arrest occurs in the anoxic turtle cortex

Anoxic perfusion results in significant electrical depression in turtle cortical neurons. **(A, D-E, H, K)** Summary of anoxic changes of AP_f **(A)**, G_w, **(D)**, AP_{th} **(E)**, $[Cl^-]_c$ **(H)**, and $[Ca^{2+}]_c$ **(K)**. AP_f was normalized to control baseline and was assessed 20 mins following treatment onset. G_w, AP_{th}, $[Ca^{2+}]_c$, and $[Cl^-]_c$ measurements were taken 40 mins following treatment onset. Data are mean ± SEM. Asterisks (*) indicate significant difference from normoxic controls. Pound (#) indicates significant difference anoxic controls. **(B-C)** raw spontaneous electrical activity recordings during normoxia **(B)** or an anoxic transition with recovery **(C)**. **(F-G)** APs elicited by current injected in 1 nA steps during normoxia **(F)** or anoxia **(G)**. **(I-J)** raw MEQ fluorescence recordings from cortical sheets exposed to normoxia **(I)** or an anoxic transition with recovery **(J).** $[Cl^-]_c$ was assessed using a MEQ self-quenching assay, therefore increases in MEQ fluorescence (**Δ**F%) correspond to decreases in $[Cl^-]_c$. **(L-M)** raw fura-2 fluorescence recordings from cortical sheets exposed to normoxia **(L)** or an anoxic transition with recovery **(M)**.

.

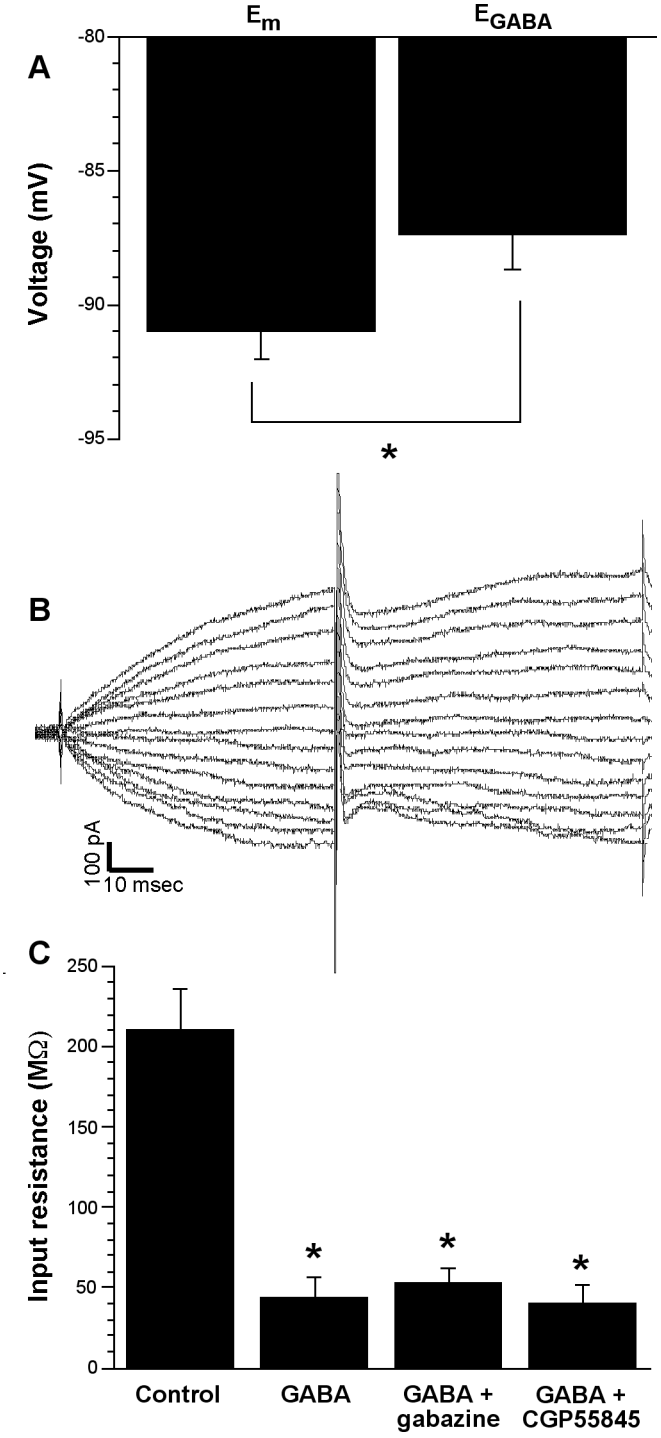

Figure 30. E_{GABA} is slightly depolarizing relative to E_m

(A) Summary of E_m and E_{GABA} measurements from turtle cortical neurons recorded from in the perforated patch configuration with gramicidin. Neurons were co-treated with CNQX to prevent AP generation when determining E_{GABA}. Measurements were taken 20 mins following treatment onset. **(B)** Raw E_{GABA} measurement. **(C)** Summary of R_{in} changes induced by GABA receptor manipulation in gramicidin-patched turtle cortical neurons. Data are mean ± SEM. Asterisks (*) indicate significant difference from normoxic controls.

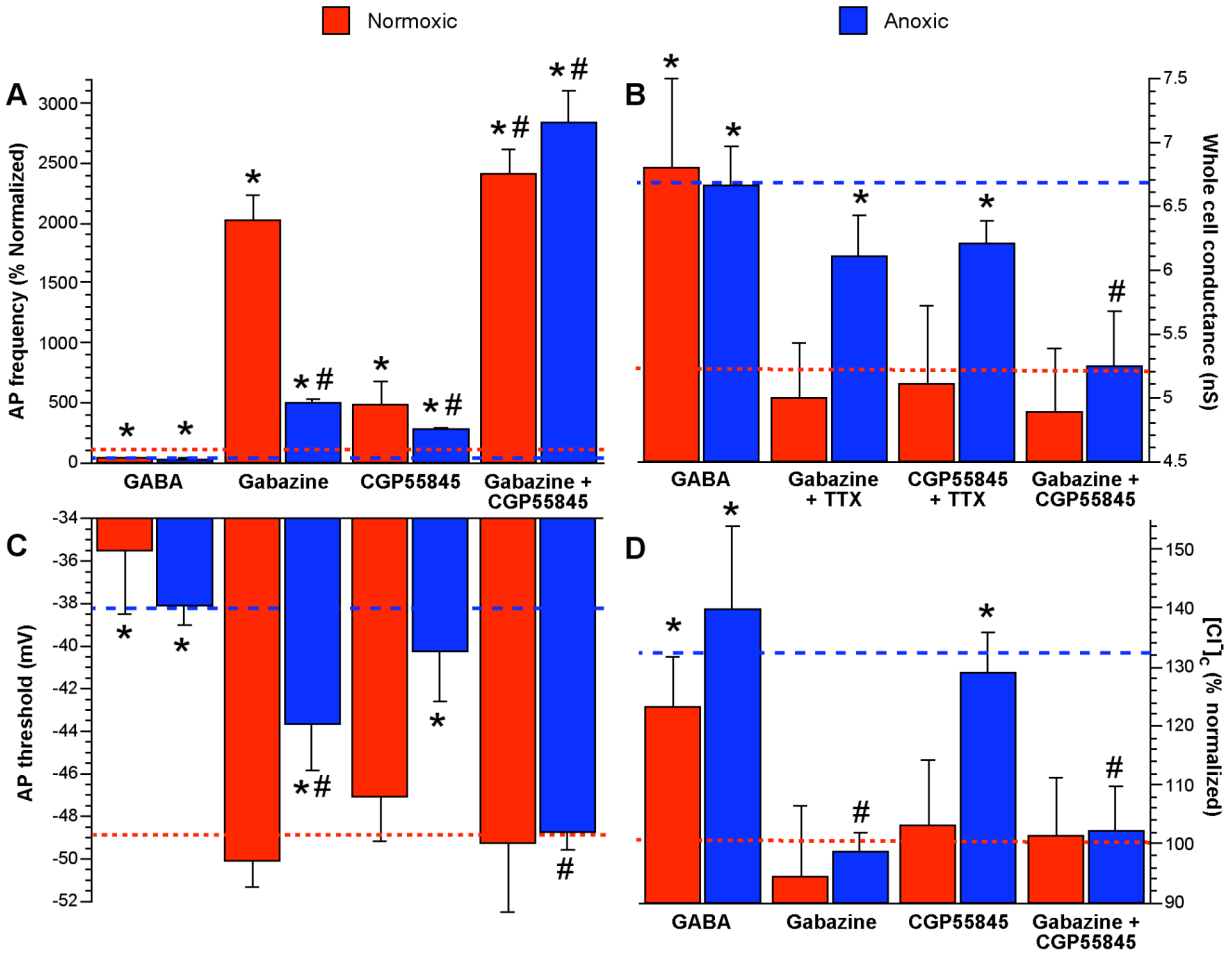

Figure 31. Cortical electrical depression is mediated by GABA

(A-D) Summary of changes of AP_f **(A)**, G_w, **(B)**, AP_{th} **(C)**, and $[Cl^-]_c$ **(D)** in response to GABA receptor manipulation during normoxia and anoxia. Values were assessed as per legend of Fig. 1. G_w was assessed in the presence of TTX to eliminate changes from increased activation of excitatory conductance due to elevated AP_f. Data are mean ± SEM. Asterisks (*) indicate significant difference from normoxic controls. Pound (#) indicates significant difference anoxic controls.

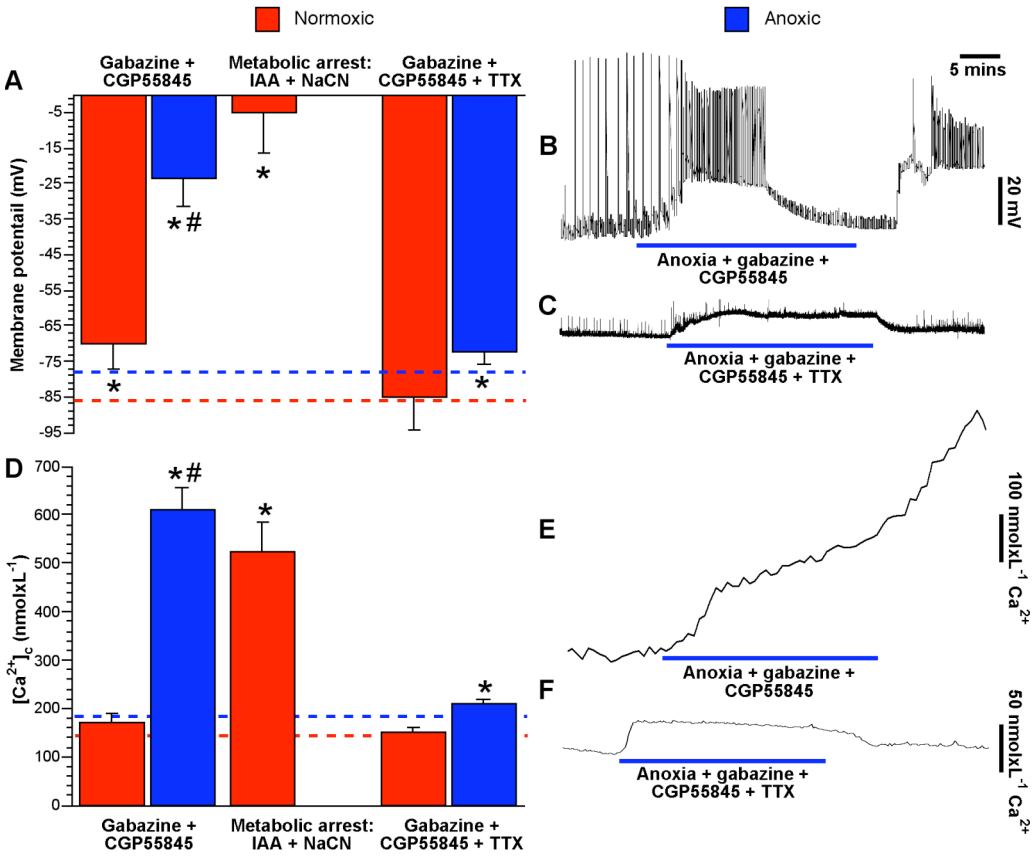

Figure 32. GABA antagonism during anoxia induces anoxic depolarization and $[Ca^{2+}]_c$ elevation.

(A&D) Summary of anoxic changes of E_m **(A)** and $[Ca^{2+}]_c$ **(D)**. E_m and $[Ca^{2+}]_c$ changes were assessed 40 mins following treatment onset. Data are mean ± SEM. Asterisks (*) indicate significant difference from normoxic controls. Pound (#) indicates significant difference anoxic controls. **(B-C)** raw spontaneous electrical activity recordings during a normoxia to anoxia plus $GABA_A$ and $GABA_B$ antagonist co-perfusion with recovery **(B)** and with TTX **(C)**. **(E-F)** raw fura-2 fluorescence recordings from cortical sheets exposed to the same treatment as B-C.

4.4. Discussion: GABA receptor activation is critical to anoxic electrical depression

I demonstrate that turtle cortical neurons undergo profound electrical depression when exposed to anoxic conditions: AP_f decreased ~ 75% and G_w and AP_{th} both increased ~ 25-35%. These inhibitory changes were rapidly reversed by reoxygenation and agree with previous measurements of decreased electrical activity in other regions of the turtle brain (cerebellum), in which depolarization of E_m and AP_{th}, as well as decreased R_{in} and AP_f were observed with anoxia (Perez-Pinzon et al., 1992a). The mechanism underlying anoxic electrical suppression in turtle neurons has not been elucidated, however my results suggest the key component is increased neuronal G_w mediated by activation of GABA receptors, since: (1) normoxic GABA perfusion mimicked the anoxic electrical suppression, (2) synergistic treatment of anoxic neurons with GABA did not increase G_w, AP_f, AP_{th}, or $[Cl^-]_c$ beyond the increases seen with anoxia or GABA perfusion alone, and (3) simultaneous blockade of both $GABA_A$ and $_B$ receptors prevented the anoxic electrical suppression, and neurons entered a highly excited seizure-like state and E_m ran down fully. In addition, $[Ca^{2+}]_c$ was elevated 4-fold from the normoxic baseline, and $\Delta[Ca^{2+}]_c$ was 7-fold higher than in anoxic controls. This depolarization and accumulation of $[Ca^{2+}]_c$ were not reversed by reoxygenation, indeed $[Ca^{2+}]_c$ continued to rise following reoxygenation in hyper-excited turtle neurons, while cell mortality increased 6.5-fold. This phenotype is akin to ECD in mammalian neurons, which is characterized by electrical hyper-excitability, large increases of $[Ca^{2+}]_c$ and AP_f, loss of E_m, and cell death (Lundberg and Oscarsson, 1953; Siesjo, 1989). Thus, it appears that anoxic turtle neurons in which GABA antagonists prevent electrical suppression may undergo ECD akin to ischemic mammalian neurons. The fact that GABA receptor inhibition during anoxia can induce cell death despite a

marked endogenous reduction in [glutamate] and channel arrest of AMPARs and NMDARs in the turtle cortex highlights the critical importance of electrical suppression during anoxic exposure (Bickler et al., 2000; Buck and Bickler, 1995; Milton et al., 2002; Pamenter et al., 2008c).

GABA receptors inhibit electrical activity in a variety of ways: $GABA_A$ receptors are anion channels that are permeable primarily to Cl^- ions and clamp E_m near E_{Cl} (the Cl^- gradient determines E_{Cl}, and $E_{Cl} = E_{GABA}$), whereas $GABA_B$ receptors oppose excitatory electrical events in a similar shunt-like fashion: $GABA_B$ receptors are connected via a G protein to a K^+ channel, whose activation increases neuronal G_K. Since E_K is the primary determinant of E_m in resting neurons, increased G_K opposes neuronal depolarization in a graded fashion similar to increased G_{Cl} (Hille, 1992). Furthermore, when neurons are depolarized due to excitatory events, the driving force on Cl^- or K^+ ions increases as E_m depolarizes away from E_{GABA} and E_K, resulting in greater and greater opposition to further depolarization even as the cell is being depolarized by excitatory events. Here I measure E_{GABA} for the first time in a facultative anaerobe. In my experiments, E_{GABA} was slightly depolarized with regard to E_m and therefore increases in $GABA_A$ receptor activation during anoxia would allow Cl^- ions to leave the neuron, opposing excitatory currents in a shunt-like fashion and reducing AP_f. In my experiments, anoxic or GABA perfusion resulted in increased G_w and an efflux of Cl^-. GABA- or anoxia-mediated Cl^- movement was prevented by $GABA_A$ but not $GABA_B$ blockade, whereas the associated increase in G_w was abolished only when both $GABA_A$ and $GABA_B$ receptors were antagonized simultaneously. Together, these results suggest that in anoxic turtle neurons, increased G_{Cl} and G_K effectively clamp E_m at or near E_{GABA}/E_K, opposing neuronal depolarization due to excitatory events and reducing AP_f.

The increase in G_w due to GABA receptor activation is likely even more profound then reported here. G_w is a global cellular measurement that includes the conductance of all open channels. Previous studies have demonstrated that the turtle employs ion channel arrest as another strategy to reduce ATP demand by ion pumps. During anoxia, AMPA and NMDA receptor activity and K^+ leakage each decrease ~ 50%, while Na^+ channel and NMDA receptor density dip ~ 40% (Buck and Bickler, 1995; Chih et al., 1989b; Pamenter et al., 2008c; Perez-Pinzon et al., 1992c). Anoxic reductions in non-GABAergic ion channel activity would mask the full magnitude of the increase in $GABA_A$-mediated conductance. Thus my measurement of an ~ 30% increase in G_w during anoxia is likely a low estimate of the actual increase in G_w attributable to GABAergic activity. Indeed in perforated-patch recordings from cortical neurons exposed to GABA during normoxia, the decrease in R_{in} is ~ 75%, considerably greater than that observed during anoxic perfusion.

In addition to electrical depression via increased G_K in post-synaptic neurons, activation of $GABA_B$ receptors in pre-synaptic neurons may contribute to spike arrest by reducing glutamate release. In mammalian brain, inhibition of $GABA_B$ receptors depolarizes the pre-synaptic membrane, inducing glutamate release and leading to increased post-synaptic electrical activity (Saint et al., 1990; Travagli et al., 1991). Conversely, activation of $GABA_B$ receptors increases G_K in the pre-synaptic neuron, opposing depolarization and the associated release of glutamate into the synaptic cleft. Elevated [GABA] in the anoxic turtle cortex likely reduces glutamate release via this mechanism. As in mammalian brain, blockade of normoxic $GABA_B$ receptors in turtle brain increased AP_f significantly. However, the large E_m depolarization and increase in G_w observed with CGP55845 are inconsistent with decreased post-synaptic G_K, and

may be due to increased post-synaptic conductance to excitatory ions mediated by increased glutamatergic signaling from pre-synaptic neurons.

In summary, my results suggest GABA-mediated electrical suppression is critical to the anoxic survival of turtle cortex. Activation of GABA receptors increases G_w and considerably more current is required to depolarize E_m to AP_{th}. As a result, AP_f is substantially reduced and neurons become electrically quiet. Inhibition of GABA receptor function during anoxia prevents electrical depression and induces SLEs. These events lead to cytotoxic $[Ca^{2+}]_c$ accumulation, AD and cell death, likely due to the exhaustion of compartmentalized ATP supplies near pumps working to maintain ion gradients in the face of uncontrolled cellular excitation. This conclusion is supported by the fact that cell viability is restored by prevention of excitatory events during anoxia with TTX. Taken together, these results indicate GABA-mediated increases in G_w regulate anoxic depressions in cortical electrical activity and maintain energy supplies in the anoxic turtle cortex. GABA-based interventions against ischemic damage are attractive targets for the clinical treatment of stroke since many of the compounds used to target GABA receptors are already used clinically to treat other disorders (Caramia et al., 2000; Vincent et al., 2005).

5. Anoxia-Induced Changes in Reactive Oxygen Species and cyclic nucleotides in the Painted Turtle

Preface

A modified version of this chapter was published as: Pamenter ME, Richards MD and Buck LT (2007). Anoxia induced changes in reactive oxygen species and cyclic nucleotides in the painted turtle. *Comp. Biochem. Physiol. B.* 177:473-481.

MD Richards and L Buck performed all ROS imaging experiments. I performed all cAMP and cGMP ELISA experiments and wrote the paper with editing by L Buck.

Abstract

The Western Painted turtle survives months without oxygen. A key adaptation is a coordinated reduction of cellular ATP production and utilization that may be signaled by changes in the concentrations of reactive oxygen species (ROS) and cyclic nucleotides (cAMP and cGMP). Little is known about the involvement of cyclic nucleotides in the turtle's metabolic arrest and ROS have not been previously measured in any facultative anaerobes. The present study was designed to measure changes in these second messengers in the anoxic turtle. ROS were measured in isolated turtle brain sheets during a 40-min normoxic to anoxic transition. Changes in cAMP and cGMP were determined in turtle brain, pectoralis muscle, heart and liver throughout 4 hours of forced submergence at 20-22°C. Turtle brain ROS production decreased 25% within 10 mins of cyanide or N_2-induced anoxia and returned to control levels upon reoxygenation. Inhibition of electron transfer from ubiquinol to complex III caused a smaller decrease in [ROS]. Conversely, inhibition of complex I increased [ROS] 15% above controls. In brain, [cAMP] decreased 63%. In liver, [cAMP] doubled after two hours of anoxia before returning to control levels with prolonged anoxia. Conversely, skeletal muscle and heart [cAMP] remained unchanged; however, skeletal muscle [cGMP] became elevated 6-fold after 4 hours of submergence. In liver and heart [cGMP] rose 41% and 127% respectively after two hours of anoxia. Brain [cGMP] did not change significantly during 4 hours of submergence. I conclude that turtle brain ROS production occurs primarily between mitochondrial complexes I and III and decreases during anoxia. Also, cyclic nucleotide concentrations change in a manner suggestive of a role in metabolic suppression in the brain and a role in increasing liver glycogenolysis.

5.1. Introduction: cyclic nucleotides and ROS as signaling molecules

An effective metabolic signaling mechanism must be rapid, reversible, and sensitive to cellular oxygen changes (Hochachka, 1986). Anoxia induces changes in a wide variety of cellular signaling molecules in the freshwater turtle, including glutamate, GABA, PKC and adenosine (Brooks, 1993; Nilsson and Lutz, 1992; Nilsson and Lutz, 1991). However, ROS and cyclic nucleotides are two categories of common second messenger signals that have not been extensively investigated in this organism. Changes in cellular ROS and cyclic-AMP and -GMP in response to anoxia may underlie protective mechanisms in the freshwater turtle and offer clues to extending mammalian tolerance to hypoxic insult.

ROS in particular are well suited to act as cellular low-oxygen signals. ROS modulate signaling cascades by rapidly and reversibly oxidizing cysteine residues on protein kinases and phosphatases, transcription factors, or ion channels (Choi et al., 2001; Cross and Templeton, 2006; Rhee et al., 2003; Wang et al., 1997). Therefore, a ROS-based mechanism provides the required speed and flexibility to be an effective metabolic arrest signal. Furthermore, ROS are primarily produced during mitochondrial respiration, and during anoxia the lack of oxygen slows mitochondrial electron transport and subsequently alters ROS production. This high sensitivity to $[O_2]$ make ROS an excellent candidate to signal changes in O_2 availability and to regulate cellular responses to anoxia. The primary ROS produced by mitochondrial respiration is superoxide ($\cdot O_2^-$), which is converted to hydrogen peroxide (H_2O_2) in the cytosol by superoxide dismutase (Vanden Hoek et al., 1998). This system has received some consideration as a direct cellular oxygen sensor in hypoxic pulmonary vasoconstriction (HPV) and there are conflicting interpretations of the role ROS play in O_2 signaling. Until recently the consensus was that hypoxia regulated HPV via a reduction in mitochondrial ROS generation from the proximal end

of the ETC (Archer et al., 1993; Mohazzab et al., 1995; Mohazzab and Wolin, 1994). However, more recently a paradoxical increase in ROS generation was measured in hypoxic mitochondria (Waypa et al., 2001), leading these authors to suggest an increase in ROS production signals low oxygen and underlies HPV.

Similar to ROS, cyclic nucleotides have received little attention in the study of the turtles anoxia-tolerance but evidence from mammalian studies suggest they may be linked to cytoprotective mechanisms against low oxygen insults. For example in mammalian brain and heart, cAMP has been linked to hypoxic vasodilation in pial and pulmonary arteries, respectively (Barman et al., 2003; Ben-Haim and Armstead, 2000). To date, the role of cAMP in anoxia-tolerance of the turtle has only been examined in liver, where cAMP dependent protein kinase (PKA) activates glycogenolysis to increase available substrates for anaerobic metabolism (Mehrani and Storey, 1995a). There is also evidence to support a role for cGMP in hypoxia-tolerance: inducible cardioprotection in mammals and endogenous cardioprotection in goldfish are mediated by a cGMP/NO pathway that up-regulates ROS production (Chen et al., 2005; Qin et al., 2004). Changes in [cGMP] have not previously been quantified in any turtle tissue.

The aim of this study was to quantify anoxia-induced changes in ROS and the cyclic nucleotides cAMP and cGMP to assess their potential involvement in the turtles' anoxia-tolerance and their potential to serve as signaling messengers of low-oxygen environments to induce neuronal metabolic arrest mechanisms. Furthermore, I attempted to determine the primary ETC site(s) of mitochondrial ROS production.

5.2. Results: anoxic change in ROS and cyclic nucleotides

5.2.1. ROS production decreases in the anoxic turtle cortex

DCFDA fluorescence (an indicator of H_2O_2 production) was unaltered in cortical sheets during normoxic control experiments. Conversely, H_2O_2 production decreased steadily following a normoxic to anoxic transition and increased sharply following normoxic reperfusion, returning to baseline (Fig. 33A). In cortical sheets exposed to repeated transitions between normoxic and anoxic perfusions the change in H_2O_2 production was rapid and repeatable (Fig. 33B, $n = 3$).

To examine the involvement of the ETC in normoxic ROS production, various ETC inhibitors were added to the normoxic perfusate (for ETC inhibitor pathway schematic see Fig. 34). The complex IV inhibitor cyanide decreased H_2O_2 production compared with normoxic controls, and this change was indistinguishable from anoxic (N_2 gassed) controls (Fig. 34E, $n = 5$). However, in addition to blocking complex IV of the ETC, cyanide blocks the antioxidant enzymes catalase and peroxidase required for DCFDA oxidation and may therefore artificially depress fluorescence (Fig. 34). Although cyanide is commonly used to mimic anoxia, and the cyanide-induced changes in ROS in my experiments are similar to the N_2-induced anoxic data, these results should be interpreted with prejudice due to the secondary effects of cyanide on catalase and peroxidase.

To test the involvement of proximal ETC components in normoxic ROS production, the complex III inhibitor myxothiazol was added to the normoxic perfusate (Fig. 33D, $n = 3$). Myxothiazol caused H_2O_2 production in brain sheets to decrease, although the degree to which myxothiazol attenuated H_2O_2 production was significantly less than that caused by anoxic perfusion. Finally, the complex I inhibitor rotenone caused a sustained increase in H_2O_2

production (n = 3, raw data not shown) and the level of H_2O_2 production was significantly higher than anoxic and normoxic.

5.2.2. Changes in cyclic –AMP and –GMP during early anoxia

To determine their potential signaling roles in anoxia-tolerance, changes in concentration of cAMP (Table 2) and cGMP (Table 3) were analyzed in turtle brain, heart, pectoralis muscle, and liver tissues during four hours of forced submergence. Blood pO_2 was measured throughout the four hours of anoxia and the animals were severely hypoxic within 30 mins of submergence and were fully anoxic after one hour (Fig. 35). Endogenous [cAMP] was highest in brain, and tissue [cAMP] scaled as follows: brain > heart > liver > muscle. Brain [cAMP] was reduced within 30 mins of anoxia (n = 5) and remained depressed throughout treatment with a peak reduction of 63% occurring after 60 mins of anoxia. In the liver, [cAMP] increased 2-fold after one hour of anoxic exposure and remained elevated through the first two hours of anoxia (n = 5) before returning to baseline levels after 4 hours. Muscle [cAMP] rose slightly throughout anoxia, but did not become significantly elevated at any point (n = 5). Heart [cAMP] remained unchanged throughout anoxia (n = 5).

Endogenous [cGMP] varied considerably between tissues such that: heart >> brain > liver > muscle. [cGMP] fluctuated but did not change significantly from control in the brain (n = 4). In muscle tissue [cGMP] doubled after two hours of anoxic exposure and increased further to 6-fold above control levels at 4 hours of anoxia (n = 5). In the heart [cGMP] remained constant in the first two hours of anoxia before becoming reduced by 63% at the end of the 4-hour experiment (n = 5). In the liver [cGMP] at 2 hours of anoxia was significantly greater than control groups and one-hour anoxia treatment groups. This increase was temporary and [cGMP] returned to baseline concentrations by 4 hours of anoxia (n = 4).

Table 2. Effect of anoxia on cAMP concentration in turtle tissues.

Tissue and treatment	[cAMP] pmol/gww	% of control
Brain		
Control	2985.8 ± 144.5	-
30 min dive	1618.2 ± 56.9	54%[a]
60 min dive	1103.3 ± 81.5	37%[a]
120 min dive	1346.8 ± 154	45.1%[a]
240 min dive	1227.0 ± 176.6	41.1%[a]
Skeletal Muscle		
Control	159.8 ± 19.3	-
30 min dive	166.7 ± 10.1	104.3%
60 min dive	206.5 ± 8.1	129.3%
120 min dive	204.7 ± 38.7	129.2%
240 min dive	260.6 ± 32.5	163.1%
Heart		
Control	1204.7 ± 115.9	-
30 min dive	1121.1 ± 64.6	93.1%
60 min dive	1062.6 ± 117.8	88.2%
120 min dive	1144.4 ± 186.2	95.0%
240 min dive	1228.1 ± 168.3	101.9%
Liver		
Control	611.3 ± 11.3	-
30 min dive	1023.8 ± 72.0	167.5%[a]
60 min dive	1246.9 ± 148.0	204.0%[a]
120 min dive	1034.8 ± 72.6	169.3%[a]
240 min dive	733.6 ± 20.6	120.0%[b]

Values are mean ± SEM; n = 5 animals in each treatment group and assays were run in duplicate. [a]Significantly different from corresponding control values, [b]significantly different from 1 hour anoxic values. ($p = < 0.05$)

Table 3. Effect of anoxia on cGMP concentration in turtle tissues.

Tissue and treatment	[cGMP] fmol/gww	% of control
Brain		
Control	2748.3 ± 712.9	-
30 min dive	2793.6 ± 423.8	101.6%
60 min dive	1981.3 ± 506.3	71.2%
120 min dive	3592.5 ± 664.0	131.0%
240 min dive	1854.8 ± 655.6	67.5%
Skeletal Muscle		
Control	744.5 ± 64.5	-
30 min dive	806.0 ± 116.3	108.3%
60 min dive	1053.4 ± 233.5	141.5%
120 min dive	1746.1 ± 244.2	234.5%[a]
240 min dive	4533.1 ± 955.6	608.9%[ab]
Heart		
Control	7310.6 ± 1229.4	-
30 min dive	5243.2 ± 1365.7	71.7%
60 min dive	7387.0 ± 2162.3	101.0%
120 min dive	10315.9 ± 1177.7	141.1%[ab]
240 min dive	2740.3 ± 495.2	37.5%[ab]
Liver		
Control	1844.7 ± 452.1	-
30 min dive	2548.7 ± 564.7	138.2%
60 min dive	2163.5 ± 416.9	117.3%
120 min dive	4191.3 ± 605.4	227.2%[ab]
240 min dive	1655.7 ± 447.2	89.8%

Values are mean ± SEM; n = 5 animals in each treatment group and assays were run in duplicate. [a]Significantly different from corresponding control values, [b]significantly different from 1 hour anoxic values. ($p = < 0.05$)

5.3. Figures

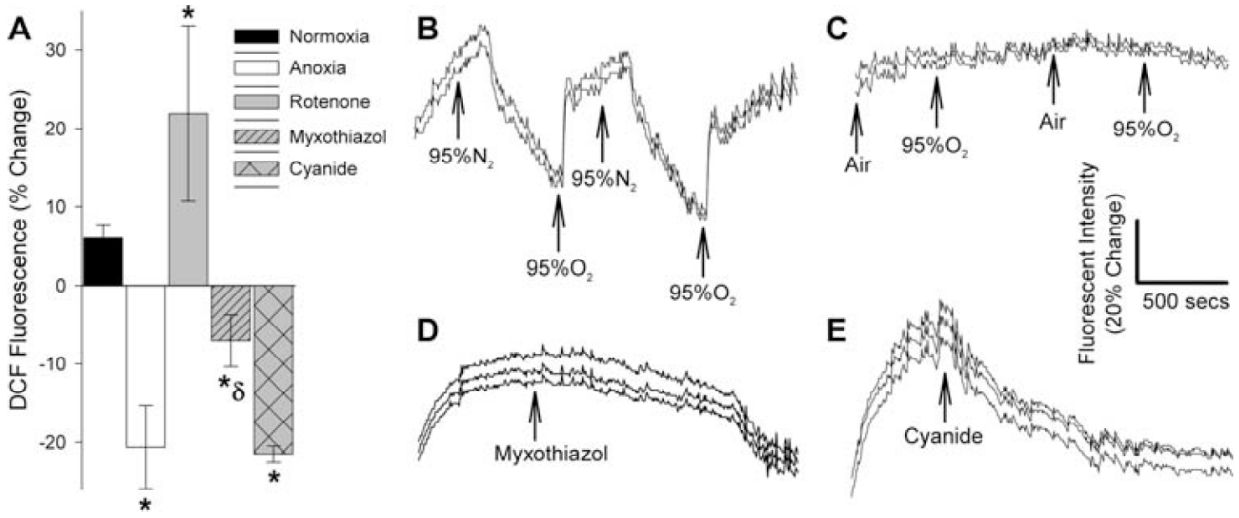

Figure 33. ROS production from turtle cortical sheets decreases with anoxia.

(A) DCFDA fluorescence data normalized to % change in fluorescence taken 15 min after the 10 min equilibration period. Asterisks (*) indicates data are significantly different from normoxic control values, (δ) indicates data are significantly different from anoxic control values ($p < 0.05$). Data are presented as mean ± SEM. (B-E) Representative traces of DCFDA fluorescence in cortical brain sheets: under **(B)** repeated normoxic/anoxic transitions, **(C)** repeated 95% Air/5%CO_2 to 95%O_2/5%CO_2 transitions, **(D)** normoxic/normoxic with myxothiazol, and **(E)** normoxic/normoxic with cyanide. Note: each figure comprises raw data traces from three separate cortical sheet regions. Arrows indicate perfusate switches from normoxic saline to anoxic or normoxic + treatment.

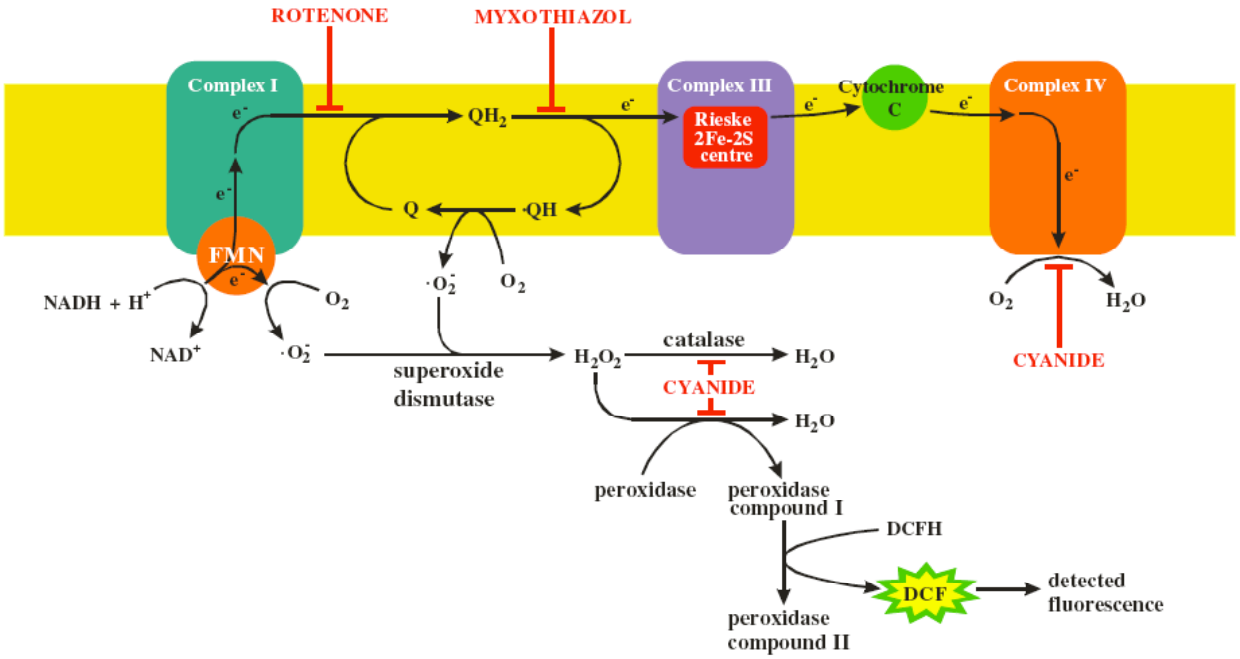

Figure 34. The generalized mitochondrial ETC, its inhibitors, sites of ROS production and detection.

ETC Inhibitors: Rotenone inhibits electron transfer from complex I to ubiquinone (Q). Myxothiazol inhibits electron transfer from ubiquinol (QH_2) to complex III. Cyanide inhibits complex IV cytochrome oxidase as well as the antioxidant enzymes catalase and peroxidase. *ROS Generation*: Superoxide ($\cdot O_2^-$) can be generated at the complex I flavin mononucleotide (FMN) centre and from the ubisemiquinone radical ($\cdot QH$) produced in the Q-cycle. *ROS Detection*: ROS indirectly oxidize CM-H_2DCFDA to fluorescent DCFDA through a peroxidase-mediated reaction.

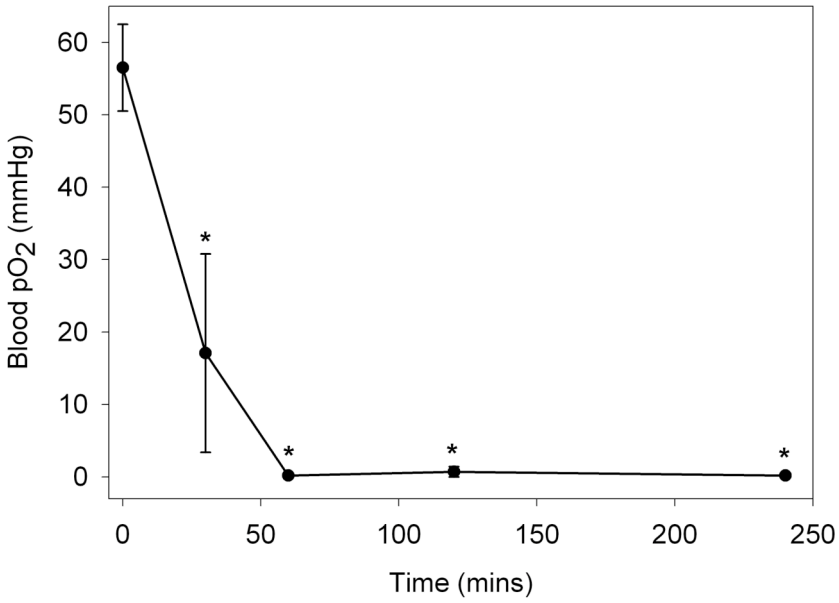

Figure 35. Blood pO2 of submerged dived for 0, 30, 60, 120 and 240 mins.

N = 5 for all groups. Asterisks (*) indicate data significantly different from control groups (*t* = 0) ($p < 0.05$). All data are mean ± SEM.

5.4. Discussion: ROS and cyclic adenylates as anoxic signals

The involvement of ROS and cyclic adenylates in hypoxia-tolerance has been demonstrated in mammals (Giordano, 2005; Palmer, 1985); however, these signaling molecules have received little attention in vertebrate facultative anaerobes. Here I report for the first time measurements of ROS changes in an anoxia-tolerant species. I also present the first comprehensive measurement of cyclic nucleotides during an anoxic dive in the freshwater turtle. ROS have received significant attention as cellular O_2 sensors because mitochondria utilize the majority of cellular O_2, producing ROS in the process (Lopez-Barneo et al., 2004). It has been hypothesized that hypoxic inhibition of mitochondrial oxidative phosphorylation alters ROS production, signaling cellular pO_2 changes (Rounds and McMurtry, 1981). This theory has been challenged by studies showing $[O_2]$-dependent responses are initiated at oxygen tensions above those required to inhibit mitochondrial respiration (Buescher et al., 1991). Indeed, in the anoxic turtle brain ROS production became significantly decreased from controls after 10 mins, whereas anoxia-protective mechanisms such as ion channel arrest may be initiated within a shorter timescale (Bickler et al., 2000; Ghai and Buck, 1999). Therefore, although ROS production is steadily decreasing during this time, I am unable to conclude whether or not changes in ROS act as a cellular oxygen sensor in the anoxic turtle brain.

In HPV models there is debate as to whether ROS production is increased (Waypa et al., 2001) or decreased (Archer et al., 1993) during hypoxia. Waypa *et al*. (2001) observed a burst in DCFH oxidation with the onset of hypoxia and suggested that this burst signaled decreased oxygen availability. In my experiments, H_2O_2 production in turtle cortical sheets was decreased by both anoxia (N_2-anoxia) and by the ETC complex IV inhibitor cyanide (pharmacological anoxia). Turtle cortical sheets exposed to N_2 become hypoxic before they are fully anoxic

following the switch from normoxic to anoxic perfusion and ROS production declined steadily in these tissues without a burst in ROS production as the tissue became hypoxic. ROS production inherently requires the presence of oxygen. Indeed the ROS-dependent HPV response that is initiated by hypoxia in mammals is abolished under true anoxia (Buescher et al., 1991). Measurements taken from whole turtles undergoing forced submergence indicate blood pO_2 effectively reaches 0 torr after one hour of diving. Brain tissue does not have local stores of oxygen and anoxic turtle brain tissue should be incapable of producing ROS under anoxic conditions. Therefore, my data suggests that turtle brain ROS production declines with decreasing oxygen availability and that any cytoprotective mechanisms regulated by ROS in the anoxic turtle brain are activated by decreases in the signaling molecule and not by bursts. ROS production in isolated mammalian brain mitochondria also declines with decreasing oxygen availability, supporting my results (Kudin et al., 2004).

Since ROS production decreases in turtle brain during normoxic to anoxic transitions, it is logical to assume that the normoxic site of ROS production is reduced in activity. Thus we applied specific inhibitors of the ETC under normoxic conditions to determine the site(s) of ROS production. Myxothiazol, a specific inhibitor of electron transfer from ubiquinol to complex III (Fig. 33), significantly decreased DCFDA fluorescence in the turtle cortex. Similarly, Waypa *et al*. (2001) found that myxothiazol attenuated the hypoxic burst in ROS production underlying the HPV response and concluded that complex III was the primary site of ROS production in mammals. In another experiment, the complex I inhibitor rotenone was perfused onto brain sheets. The site of production of ROS from complex I is the flavin mononucleotide moiety (Liu et al., 2002), which is upstream of rotenone's site of action: the transfer of electrons from complex I to the QH cycle. Therefore, if complex I is an important site of ROS production then

rotenone should increase ROS production by forcing electrons through the FMN-mediated pathway which generates ROS. In my experiments, rotenone caused increases in mitochondrial ROS production. Similarly, rotenone increases ROS production in isolated mammalian brain mitochondria (Kudin et al., 2004). Taken together these data indicate that both complex I and complex III are important sites of ROS production in turtle cortical tissue.

Reductions in [ROS] are generally cytoprotective in anoxia-intolerant tissues and perfusion of anti-oxidants blunts hypoxic cell death in mammalian hippocampus (Archer et al., 1993; Jayalakshmi et al., 2005). Similarly, we report a decrease in ROS production with anoxia in turtle cortex. This decrease may allow neurons to utilize redox balance as an intracellular signaling mechanism to regulate anoxic neuroprotective mechanisms. One of the hallmarks of reduced energy metabolism is ion channel arrest, and ROS modulate numerous cellular proteins including ion channels, ion pumps, ion exchangers and ion co-transporters (Kourie, 1998). Therefore, ROS are uniquely positioned as a common signaling molecule that affects numerous ion channels and cellular kinases and phosphatases. A reduction in [ROS] during anoxia could underlie channel arrest and prove to be a fundamental difference in how this facultative anaerobe tolerates anoxic insults that would be lethal to mammalian brain.

Of the cyclic adenylates, liver [cAMP] is the only compound that has been previously studied in freshwater turtles. In *T. scripta,* endogenous normoxic [cAMP] levels were 872 ± 76 pmol/gww, and this concentration became elevated in early anoxia by 57.2% before returning to control levels after 5 hours of anoxic exposure (Mehrani and Storey, 1995b). Concurrently, levels of the active form of PKA rose significantly within the first hour of anoxia and subsequently returned to control levels with prolonged anoxia (Mehrani and Storey, 1995a). These data are in good agreement with my results from *C. picta* showing a baseline liver [cAMP]

of 611.3 ± 11.3 pmol/gww with anoxia-induced increases peaking at one hour of exposure and returning to control values after 4 hours of anoxia. Anoxia-mediated increases in [cAMP] enhance glycogenolysis in turtle liver (Mehrani and Storey, 1995b). Glycolysis is the primary form of anaerobic metabolism in turtles and liver provides the greatest reserve of glycogen (Buck, 2000; Clark and Miller, 1973). Therefore, mobilization of glycogen from liver increases blood glucose levels and provides fuel to tissues with lower glycogen such as the brain; indeed turtle blood [glucose] rises 10-fold after four hours of forced submergence (Ramaglia and Buck, 2004). The fact that liver [cAMP] is elevated only in the first few hours of anoxia suggests that increased glycogenolysis stimulated by cAMP is a short-term response to anoxic exposure that is employed by the turtle to maintain [ATP] while long-term mechanisms of metabolic suppression are initiated, such as removal of proteins from cellular membranes and decreased protein synthesis (Land et al., 1993; Perez-Pinzon et al., 1992c).

[cAMP] did not change in turtle muscle and heart tissue during anoxia, supporting the hypothesis that hepatic glycogenolysis is the primary source of blood glucose during early anoxia and that skeletal muscle and heart reserves are not mobilized by cAMP. The observed decreases in turtle brain [cAMP] may also be related to glycogenolysis. Compared to other tissues, brain has very low endogenous glycogen supplies and the decrease in cAMP may decrease its dependence on local glycogen production during periods of anoxia. In this way the brain would rely on increased blood-borne fuel from the liver, preserving its own glycogen stores.

There is considerably less information available regarding the role of cGMP in the turtles' anoxia-tolerance: [cGMP] has not been previously quantified in any tissue and no studies have been undertaken to examine a potential role for cGMP. However, mammalian data suggests

cGMP plays a significant role in IPC models. In heart, cGMP has been linked to NO in a cardio-protective mechanism such that stimulation of gaunylyl cyclase raises cGMP levels, activating PKG, increasing NO production, and conferring subsequent cardioprotection (Qin et al., 2004). Similar systems have been found in hypoxic cardioprotection in the anoxia-tolerant goldfish (Chen et al., 2005) and in mammalian liver IPC (Carini et al., 2003). We observed increases in [cGMP] in turtle heart and liver at 2 hours of anoxia, with [cGMP] dropping below control levels after 4 hours of exposure. Skeletal muscle [cGMP] rose continuously throughout anoxia to a peak 6-fold increase after 4 hours of anoxia. These increases in [cGMP] may underlie protective mechanisms similar to the cGMP-NOS cardioprotective pathways found in other organisms. Furthermore, the subsequent reduction in cGMP in liver, and particularly in heart where concentrations fell to one third of control levels, may indicate that as the animal undergoes longer-term anoxic exposure, other protective mechanisms are up-regulated and those controlled by [cGMP] are no longer utilized in these tissues.

In summary, ROS and cyclic nucleotides play significant and varied roles in hypoxia-tolerance in mammalian models. Both second messengers are likely involved in tissue-specific anoxia-tolerance responses in the freshwater turtle. The quantification of changes in the concentrations of these molecules is an important first step in assessing their involvement in anoxia-tolerance. Further research is required to elucidate the specific mechanisms of protection that may be regulated by changes in the second messengers measured here. My results show significant changes in all three molecules in anoxia in a variety of tissues and offer numerous potential pathways for future anoxic research.

6. Neuronal membrane potential is mildly depolarized in the anoxic turtle cortex

Preface

A modified version of this chapter was published as: Pamenter ME and Buck LT (2008). Neuronal membrane potential is mildly depolarized in the anoxic turtle cortex. *Comp. Biochem. Physiol. B.* 150(4): 410-414.

I performed all experiments and wrote the paper with editing by L Buck.

Abstract

Neuronal membrane potential (E_m) regulates the activity of excitatory voltage-sensitive channels. Anoxic insults lead to a severe loss of E_m and excitotoxic cell death (ECD) in mammalian neurons. Conversely, anoxia-tolerant freshwater turtle neurons depress energy usage during anoxia by altering ionic conductance to reduce neuronal excitability and ECD is avoided. This wholesale alteration of ion channel and pump activity likely has a significant effect on E_m. Using the whole-cell patch clamp technique we recorded changes in E_m from turtle cortical neurons during a normoxic to anoxic transition in the presence of various ion channel/pump modulators. E_m did not change with normoxic perfusion but underwent a reversible, mild depolarization of 8.1 ± 0.2 mV following anoxic perfusion. This mild anoxic depolarization (MAD) was not prevented by the manipulation of any single ionic conductance, but was partially reduced by pre-treatment with antagonists of $GABA_A$ receptors (5.7 ± 0.5 mV), cellular bicarbonate production (5.3 ± 0.2 mV) or K^+ channels (6.0 ± 0.2 mV), or by perfusion of reactive oxygen species scavengers (5.2 ± 0.3 mV). Furthermore, all of these treatments induced depolarization in normoxic neurons. Together these data suggest that the MAD may be due to the summation of numerous altered ion conductance states during anoxia.

6.1. Introduction to multiple mechanisms that effect E_m are altered by anoxia

Maintenance of E_m during anoxic insults is critical to neuronal function since voltage-dependent ion channels and pumps largely mediate membrane permeability to excitatory ions. For example, $[Ca^{2+}]_c$ is regulated by the voltage-sensitive Na^+/Ca^{2+} exchanger and glutamatergic NMDARs (Courtney et al., 1990; Hoyt et al., 1998). E_m is determined primarily by the activity of the Na^+/K^+ ATPase, which uses 50-60% of the total energy consumed in the normoxic brain (Glitsch, 2001). When neurons from mammalian brain slices are deprived of oxygen they do not produce sufficient energy to maintain pump activity and undergo AD and cytotoxic increases in $[Ca^{2+}]_c$ due to the activation of voltage-sensitive channels (Fung et al., 1999; Lundberg and Oscarsson, 1953; Xie et al., 1995).

While it is accepted that turtle neurons do not suffer AD following anoxic exposure, there are conflicting reports as to the effect of anoxia on E_m (Doll et al., 1993; Perez-Pinzon et al., 1992a). During anoxia, turtle brain relies on glycolytic metabolism and employs a variety of mechanisms to minimize ATP consumption, including decreased: Na^+/K^+ pump activity, K^+, Na^+ and Ca^{2+} leakage, and Ca^{2+} and Na^+ channel density (Bickler et al., 2000; Chih et al., 1989b; Hylland et al., 1997; Pamenter et al., 2008c; Perez-Pinzon et al., 1992c). Furthermore, numerous cellular signals, acid-base state or organelle activity are up- or down-regulated during anoxia, including a mild decrease in pH, mild mitochondrial uncoupling, changes in cellular redox state and elevations of [GABA] and [adenosine] (Buck et al., 1998; Lutz and Kabler, 1997; Milton et al., 2007; Pamenter et al., 2007; Pamenter et al., 2008d). These changes may regulate the activity of membrane proteins that impact E_m. For example: GABA increases substantially with anoxia in turtle brain and activates $GABA_A$ and $GABA_B$ receptors, which increase Cl^- and HCO_3^-, and K^+ permeability, respectively (Kaila et al., 1997; Kaila et al., 1993; Nilsson et al., 1990).

Since numerous ions and receptors that contribute to E_m exhibit activity changes during anoxia, it is unlikely that E_m remains static. Therefore a comprehensive examination of the contribution of various ion conductance states to E_m is warranted. The purpose of this chapter was to examine changes is turtle E_m during anoxic exposure and the potential ion channels/receptors that may underlie any anoxic change. I recorded changes in E_m from cortical pyramidal neurons undergoing a normoxic to anoxic transition in the presence of pharmacological modifiers targeting individual ionic conductance or second messenger systems. Specifically, I manipulated membrane conductance to K^+, Cl^-, Ca^{2+}, Na^+, or HCO_3^- ions, or blocked GABA or adenosine receptors to abrogate any potential contribution of anoxic elevations of GABA or adenosine to E_m. In addition, the roles of decreased pH, ROS reductions or mild mitochondrial uncoupling were examined.

6.2. Results: mild anoxic depolarization

During normoxia, E_m was unchanged throughout 2 hours of recordings, from -81.4 ± 1.5 mV at the start of the experiment to -80.0 ± 1.8 mV at the conclusion of the 2 hour period (Figs. 36A&B). Conversely, anoxic perfusion resulted in a rapid mild anoxic depolarization (MAD) of 8.1 ± 0.2 mV within minutes (Figs. 36A&C, Table 4). This change was reversed following reoxygenation. The recording chamber became anoxic (0% O_2) within 3-4 mins following the switch to anoxic perfusion and MAD was initiated at very hypoxic oxygen levels, reaching a new depolarized steady state at ~ 10 mins (Figs. 36C&D). Oxygen tensions were measured in experiments where the recording electrode was replaced with an O_2 electrode (Fig. 36D). All cells exposed to anoxia underwent MAD and the individual changes in E_m all fell within the range of 7.0 to 10.5 mV. This change was rapid, reversible and repeatable with multiple switches between normoxic and anoxic perfusion (Fig. 36E). Anoxic neurons treated with iodoacetate to block glycolysis underwent a rapid and severe AD (Fig. 36F).

We examined the roles of $GABA_A$ and $GABA_B$ receptors by antagonizing them individually during normoxic to anoxic transitions. Blockade of either receptor during anoxia resulted in excitatory activity that obscured Em, so we co-treated neurons with TTX to prevent excitatory events. $GABA_B$ receptor blockade with CGP55845 had no significant effect on the MAD, however $GABA_A$ antagonism with gabazine resulted in a depolarization of 5.7 ± 0.5 mV, significantly smaller than the control MAD (Table 4). $GABA_A$ receptors are permeable to Cl^- and HCO_3^- ions. To examine the role of Cl^- in the anoxic depolarization we recorded anoxic changes of E_m in cells dialyzed with a wide range of intracellular Cl^- (1-30 mM). These concentrations provide a range of E_{Cl} from ~ -60 mV (at 30 mM) to -120 mV (at 1 mM). Since E_m in these neurons is ~ -80 mV, MAD should reverse and become a mild hyperpolarization in cells patched

with 1 mM $[Cl^-]_c$ if the MAD is Cl^--dependent. In cells clamped with 1 mM $[Cl^-]_c$, the anoxic depolarization was not different from controls (10 mM $[Cl-]_c$), however in cells clamped with 30 mM $[Cl^-]_c$ MAD was enhanced to 11.9 ± 1.7 mV (Table 4). Finally, to examined the role of HCO_3^- in MAD we pre-treated cells with the carbonic anhydrase inhibitor EZA, which abolishes neuronal HCO_3^- production. As in cells treated with gabazine, the anoxic depolarization was significantly reduced to 5.3 ± 0.2 mV with EZA treatment (Table 4).

ROS production inherently requires oxygen, thus with anoxic perfusion, oxygen availability reaches nil and ROS production is abolished in the anoxic turtle cortex (Milton et al., 2007; Pamenter et al., 2007). To mimic this environment we treated normoxic cortical sheets with the free radical scavengers 2-mercaptoproionyl glycine (MPG) or N-acetyl cysteine (NAC). Perfusion of either scavenger resulted in a large depolarization of E_m of 14.4 ± 1.4 and 26.9 ± 3.4 mV, respectively. In cells pre-treated with scavengers and then exposed to anoxia, a further depolarization of 6.0 ± 0.4 and 5.2 ± 0.3 mV were observed with MPG and NAC, respectively (Table 4). Finally, blockade of K^+ channels during normoxia with TEA resulted in a large E_m depolarization; however, a further 6.0 ± 0.2 mV depolarization was observed with subsequent anoxic perfusion that was reversed by reoxygenation (Table 4).

The remainder of the treatments had no effect on the MAD. Blockade of adenosine A_1 receptors with DPCPX, or G_{Na} or G_{Ca} with TTX or CNQX and APV, had no effect on the MAD, nor did chelation of intracellular Ca^{2+} with BAPTA or removal of extracellular Ca^{2+} in the presence of EGTA. Furthermore, modification of pH or mitochondrial respiration did not alter the MAD. In all these experiments, anoxic perfusion induced a significant and reversible MAD in every neuron recorded from. The mean MAD for individual treatment groups fell within the absolute range of 7.2 ± 0.8 to 9.9 ± 1.7 mV. These data are summarized in Table 5.

6.3. Figures

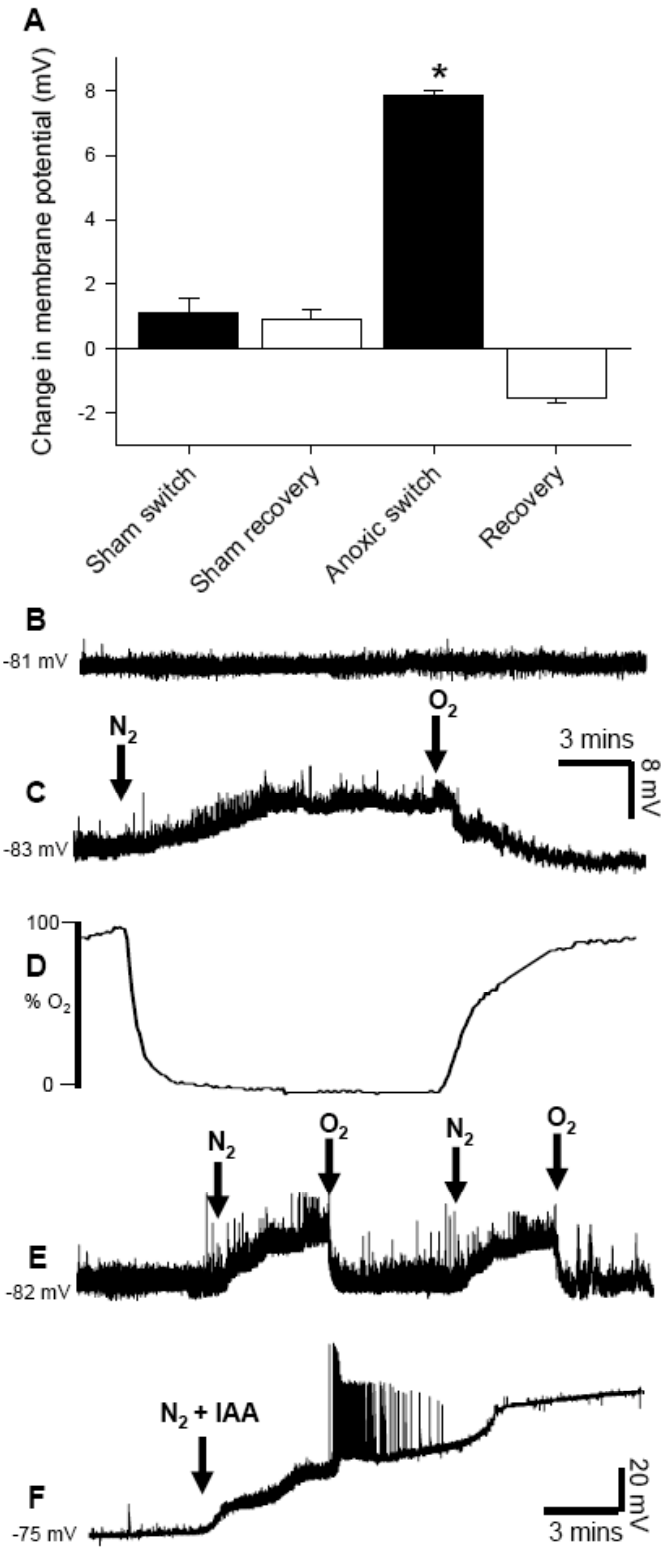
A
Change in membrane potential (mV)
8
6
4
2
0
-2
*
Sham switch
Sham recovery
Anoxic switch
Recovery
B
-81 mV
N2
O2
3 mins
8 mV
C
-83 mV
100
D
% O2
0
N2
O2
N2
O2
E
-82 mV
N2 + IAA
F
-75 mV
20 mV
3 mins

Figure 36. Anoxia-mediated regulation of neuronal resting membrane potential.

(A) Summary of resting membrane potential (E_m) changes during two hours of normoxic or normoxic to anoxic recordings at one hour (black bars) and two hours (recovery, grey bars). (*) different from control values. Data are presented as mean +/- SEM. **(B-C&E)** Raw data traces of E_m changes during a normoxic recording **(B)** a normoxic to anoxic transition and recovery, or **(E)** multiple normoxic-anoxic switches. Arrows indicate switches between normoxic and anoxic saline. **(D)** Raw data trace of recording chamber oxygen levels during the experiment in Fig. 1C. **(F)** Raw data trace of E_m changes during a normoxic to anoxic switch in the presence of the glycolytic inhibitor iodoacetate (IAA).

Table 4. The MAD is the summation of multiple altered ionic conductance states.

Experimental Treatment	Normoxic E_m (mV) 0-10 mins	Anoxic E_m (mV) 40-50 mins	Recovery E_m (mV) 80-90 mins	Anoxic ΔE_m (mV)	Range of ΔE_m (mV)
Normoxia (10)	-81.4 ± 1.5	N/A	-80.0 ± 1.8	1.4 ± 0.5†	0.1 to 2.5
Anoxia (40)	-84.4 ± 1.0	-76.6 ± 0.9*	-87.2 ± 0.7	8.1 ± 0.2†	7.0 to 10.5
GABAergic channels					
CGP55845 (5)	-81.2 ± 1.7	-72.3 ± 1.1*	-83.2 ± 1.4	8.9 ± 1.7†	8.0 to 12.5
Gabazine (10)	-81.2 ± 1.6	-75.5 ± 0.7*	-80.0 ± 1.8	5.7 ± 0.5†‡	5.1 to 6.2
1 mM $[Cl^-]_c$ (6)	-82.6 ± 0.7	-74.7 ± 1.0*	-81.2 ± 1.1	7.9 ± 0.4†	7.1 to 8.3
30 mM $[Cl^-]_c$ (6)	-82.5 ± 1.1	-70.6 ± 1.7*	-80.2 ± 2.4	11.9 ± 1.7†‡	9 to 13.5
EZA (9)	-81.6 ± 2.1	-76.3 ± 1.9*	-80.0 ± 2.9	5.3 ± 0.2†‡	4.6 to 6.1
ROS scavenging					
MPG (5)[a]	-68.3 ± 0.5*	-62.2 ± 0.4*	-69.0 ± 1.1	6.0 ± 0.4†‡	5.1 to 6.7
NAC (5)[a]	-55.0 ± 3.4*	-49.9 ± 1.1*	-54.1 ± 0.7	5.2 ± 0.3†‡	4.2 to 6.0
K^+ channels					
TEA (6)[a]	-47.8 ± 2.5*	-41.8 ± 1.0*	-49.1 ± 1.2*	6.0 ± 0.2†‡	5.2 to 6.5

Summary of E_m changes from pyramidal neurons undergoing normoxic to anoxic transitions alone or co-treated with pharmacological agents. (*) different from control normoxic values. (†) ΔE_m is different from control normoxic ΔE_m change. (‡) ΔE_m is different from the control anoxic ΔE_m change. Average E_m was assessed in the last 10 mins of normoxic, anoxic, or recovery perfusion ($P < 0.05$). Data are presented as mean +/- SEM. Parentheses indicates sample sizes.

Table 5. Summary of treatments that did not abolish the MAD of Em.

Experimental Treatment	Normoxic E_m (mV) 0-10 mins	Anoxic E_m (mV) 40-50 mins	Recovery E_m (mV) 80-90 mins	Anoxic ΔE_m (mV)	Range of ΔE_m (mV)
Na^+/Ca^{2+} Channels					
TTX (6)	-86.6 ± 1.1	-78.9 ± 1.0*	-88.5 ± 2.3	7.7 ± 0.4†	6.5 to 9.6
CNQX (4)	-83.5 ± 5.3	-74.6 ± 6.3*	-85.9 ± 4.3	8.8 ± 1.1†	6.0 to 11.5
APV (4)	-86.9 ± 1.2	-76.2 ± 1.3*	-85.8 ± 1.7	9.9 ± 1.7†	8.2 to 11.9
BAPTA (4)	-86.7 ± 4.4	-76.8 ± 6.1*	-88.7 ± 3.4	9.8 ± 1.7†	7.5 to 14.1
0 $[Ca^{2+}]_e$ + EGTA (5)	-82.1 ± 1.1	-74.5 ± 1.0*	-83.2 ± 2.1	7.6 ± 0.4†	7.1 to 8.2
(-) Mitochondrial uncoupling					
Glyb (4)	-86.5 ± 2.2	-79.8 ± 1.6*	-86.0 ± 6.0	7.7 ± 0.6†	6.6 to 8.1
5HD (5)	-81.6 ± 3.3	-72.8 ± 3.4*	-84.5 ± 3.4	8.8 ± 0.6†	6.1 to 9.5
Cellular acidification					
pH 6.8 (5)	-84.3 ± 1.5	-78.1 ± 2.0*	-83.7 ± 4.8	7.2 ± 0.8†	6.4 to 9.0
Propionate (5)	-83.1 ± 0.8	-74.5 ± 1.1*	-82.2 ± 2.3	8.1 ± 0.4†	7.2 to 9.5
Adenosine receptors					
DPCPX (5)	-82.1 ± 2.1	-74.8 ± 0.9*	-82.7 ± 1.2	7.5 ± 1.0†	7.0 to 9.1

Summary of E_m changes from pyramidal neurons undergoing normoxic to anoxic transitions alone or co-treated with pharmacological agents. (*) different from control normoxic values. (†) ΔE_m is different from control normoxic ΔE_m change. (‡) ΔE_m is different from the control anoxic ΔE_m change. Average E_m was assessed in the last 10 mins of normoxic, anoxic, or recovery perfusion ($P < 0.05$). Data are presented as mean +/- SEM. Parentheses indicates sample sizes.

6.4. Discussion: mechanisms underlying the mild anoxic depolarization

We report that turtle cortical neurons undergo a controlled mild anoxic depolarization of ~ 7-11 mV that is rapidly reversed by reoxygenation. Compared to AD in ischemic mammalian neurons the depolarization in turtle neurons is minor and unlike in mammalian neurons, did not contribute to excitotoxic events (Anderson et al., 2005). E_m remained below -70 mV after the MAD, well below the activation threshold of excitatory voltage-sensitive channels and receptors.

Mammalian neurons exposed to oxygen-glucose deprivation (OGD) suffer AD within minutes of OGD onset, however this effect is ameliorated by temperature reductions, and at 22-24°C rapid AD is not observed in ischemic mammalian neurons (Joshi and Andrew, 2001). Turtles are ectothermic and the avoidance of severe AD in their cortex may be partially temperature-related. In my experiments turtle neurons survived > 1 hour of anoxia at 22°C and 10 mM [glucose] without AD, while others have reported similar results in neurons exposed to 3 hours of anoxia or NaCN exposure at 25°C and 10 mM [glucose] (Doll et al., 1991). Conversely, mammalian neurons exposed to anoxia or NaCN perfusion at 25°C and 11 mM [glucose] maintained E_m for 30-60 mins before the onset of AD. Although this survival was significantly longer than mammalian neurons recorded from at 35°C, which avoided AD onset for only a few minutes of either anoxia or NaCN perfusion, turtle neurons survived 5-6 fold longer than mammalian neurons at 25°C and did so without apparent detriment. Furthermore, turtle neurons survive significantly longer than mammalian neurons when exposed to iodoacetate during anoxia (Doll et al., 1991). Thus, although temperature reductions significantly delay the onset of AD in mammals, the ability of turtle neurons to avoid AD for hours longer than mammalian neurons in the same conditions indicate that turtle neurons are significantly more tolerant to anoxia or ischemia than mammalian neurons.

Although severe AD was not observed in anoxic turtle cortex, the mild repeatable depolarization I report is of interest since it is highly sensitive to oxygen and may underlie, or result from, oxygen-sensing mechanisms in turtle neurons. MAD was not abolished by the antagonism of any individual channel or receptor. Instead, modifications of $GABA_A$ receptors, HCO_3^- production, K^+ channels or cellular redox state each partially reduced it. These data suggest that the MAD is the summation of E_m changes due to altered conductance states of numerous ions during anoxia. Anoxic elevations of [GABA] activate $GABA_A$ receptor-mediated G_{Cl} and G_{HCO3} (Kaila et al., 1993; Nilsson et al., 1990) and MAD was reduced by a $GABA_A$ receptor antagonist or by inhibition of HCO_3^- production, but not by altered $[Cl^-]_c$, suggesting anoxic efflux of cellular HCO_3^- through $GABA_A$ receptors contributes to the MAD. Inhibition of HCO_3^- production may also result in intracellular acidification, but since clamping intracellular pH at 6.8 had no effect on the MAD in my experiments, this effect likely does not underlie the impact of HCO_3^- flux on the MAD.

In addition to $GABA_A$ receptors, GABA increases G_K via $GABA_B$ receptors, however whole cell G_K decreases ~ 50% in the anoxic turtle brain, suggesting most K^+ channels are inhibited by anoxia (Chih et al., 1989b). E_m is largely determined by G_K and perfusion of the general K^+ channel antagonist TEA during normoxia resulted in a large E_m depolarization, and reduced the MAD following subsequent anoxic perfusion. These data support a limited role for K^+ in MAD; however, many K^+ channels have been identified for which there are no known inhibitors or which are not inhibited by TEA. Therefore, the contribution of G_K to MAD may be underestimated in my experiments due to the limited information available on the variety of K^+ channels.

The remainder of the MAD may be due to reduced Na^+/K^+ ATPase activity during anoxia (Hylland et al., 1997). Although this reduction in activity is matched by a 40-50% reduction in G_K and Na^+ channel density compared to normoxic values (Chih et al., 1989b; Perez-Pinzon et al., 1992c), an unequal reduction in the rate of K^+ and Na^+ pumping versus passive leakage could contribute to altered E_m. Indeed, my observation that ROS scavengers reduced the MAD may be due to redox regulation of Na^+/K^+ ATPase activity (Lehotsky et al., 2002).

Previous measurements of turtle E_m during transitions to anoxia have yielded inconsistent results. One study reported a significant change in anoxic transmembrane potential (Perez-Pinzon et al., 1992a). A second study reported an ~ 3.8 mV depolarization in E_m with anoxia that did not reach significance (Buck and Bickler, 1998b). Finally, another study reported no change in E_m with anoxia (Doll et al., 1993). In my experiments the depolarization was observed in all 40 neurons exposed to anoxia and also persisted in almost 100 neurons in which pharmacological treatment failed to abolish the MAD. The MAD was initiated late in the hypoxic period following the switch from normoxic to anoxic perfusate and was maintained throughout the anoxic exposure and rapidly reversed following O_2 reperfusion. This high sensitivity to small amounts of oxygen suggests the MAD may be the result of the summation of several oxygen-conforming mechanisms that are only initiated at very low O_2 levels. The extreme O_2-sensitivity may underlie these conflicting observations if some experiments were hypoxic and not anoxic.

In conclusion, I demonstrate a mild anoxic depolarization of turtle neuronal membrane potential that is reversed by reoxygenation. This depolarization is partially due to $GABA_A$-mediated bicarbonate flux following anoxic GABA release, and also partially due to altered G_K and to depressed ROS production. The remainder of the depolarization may be due to alterations in G_K through unidentified K^+ channels. In addition, I rule out the involvement of other major

excitatory and inhibitory mechanisms commonly affected by anoxia in the freshwater turtle. Since the depolarization is mild, it does not contribute to excitotoxic events, as in mammalian neurons, and may be a byproduct of the rearrangement of ionic homeostasis in the anoxic turtle cortex, rather than a designed response to anoxic insults.

7. Concluding remarks

7.1. Interlocking neuroprotection in the anoxic turtle brain

Building upon the foundation of decades of study into the turtle's anoxia-tolerance, my research has significantly advanced our understanding of the mechanisms that underlie neuroprotection in the anoxic turtle brain and uncovered mechanistic similarities between endogenous neuroprotection in the turtle and inducible neuroprotection in mammals. A complex interplay of complimentary pathways that confer neuroprotection in the turtle brain is beginning to emerge. Below, I will discuss my contributions to these newly elucidated pathways and their relation to mammalian studies (also see Fig. 37).

During the early transition from normoxia to anoxia, turtles experience a prolonged period of graded hypoxia. It is not clear at this stage what the oxygen detection system in the turtle brain is; however, several neuroprotective mechanisms are initiated during this period of hypoxia (Hochachka et al., 1997). [GABA] and [adenosine] increase and [glutamate] decreases, resulting in rapid onset of GABA-mediated spike arrest and decreased glutamatergic stimulation of excitatory AMPARs and NMDARs (Milton et al., 2002; Nilsson and Lutz, 1991). Adenosine potentially initiates early channel arrest of the NMDAR and reduces ROS production and associated redox-mediated injuries (Buck, 2004; Buck and Bickler, 1995; Buck and Bickler, 1998a; Milton et al., 2007; Nilsson and Lutz, 1992; Pamenter et al., 2007).

Adenosine activates the A_1R and its associated G_i protein, which in turn alters [cAMP] and activates mK_{ATP} channels via as yet undetermined signaling pathway (see chapters 3 & 5). Activation of mK_{ATP} channels increases mitochondrial G_K, which is countered by an increase in the activity of the mitochondrial K^+/H^+ exchanger. This futile K^+ cycling depolarizes ψ_m and

thus the driving force on the MCU, which is responsible mitochondrial Ca^{2+} uptake. Decreased mitochondrial Ca^{2+} uptake leads to moderately increased $[Ca^{2+}]_c$, an elevation of which is sustained for at least 6 weeks of anoxia and has been directly correlated to decreased NMDAR activity in the anoxic turtle cortex (Bickler, 1998; Bickler et al., 2000; Pamenter et al., 2008d; Shin et al., 2005). In the first minutes of anoxia, protein phosphatase 1 (PP1) and 2A (PP2A)-dependent dephosphorylation of the NMDAR NR1 subunit reduces NMDAR P_{open} (Bickler et al., 2000; Mulkey et al., 1993). During prolonged anoxia, sustained mild elevations of $[Ca^{2+}]_c$ lead to Ca^{2+}-calmodulin binding and subsequent dissociation of α-actinin-2 from the NR1, leading to decreased NMDAR activity (Bickler et al., 2000; Shin et al., 2005; Zhang et al., 1998). Depressed NMDAR activity also decreases NO production from NOS regulated by NMDAR-mediated Ca^{2+} influx, preventing NO-mediated redox damage (see chapter 3.4). With the onset of anoxia, DOR-based G_i signaling takes over from A_1R-mediated G_i signaling and NMDAR depression is maintained, likely via the same $[Ca^{2+}]_c$-dependent mechanism (see chapter 3.3). Presumably, elevated [enkephalin] stimulates DORs, but this has not been measured in turtle brain.

In addition to reductions in NMDAR activity, AMPAR activity is depressed during anoxia, reducing the incidence of neuronal EPSPs and further suppressing the excitatory tonus of the anoxic turtle brain (see chapter 2). It is not clear what mechanism regulates the depression of AMPAergic activity with anoxia, however this down-regulation is likely mediated by as-yet unidentified intracellular 2^{nd} messenger-based mechanisms. During prolonged anoxia, [GABA] remains elevated and depresses neuronal electrical hyper-excitability by shunting excitatory currents out of the cell via increased G_K and G_{Cl} and also by inhibition of pre-synaptic glutamate release (see chapter 4). Finally, during reoxygenation, each of these effects is reversed in a rapid

and regulated manner and deleterious bursts of ROS or NO are avoided (see chapters 3.4 & 5). Combined, these mechanisms significantly depress the electrical activity of the turtle brain by both enhancing inhibitory signaling and inhibiting excitatory signaling via a variety of overlapping mechanisms. It is important to note that the turtle brain employs channel arrest mechanisms to regulate excitatory channels, but also mechanisms of increased membrane conductance to inhibitory ions to induce spike arrest.

7.2. Turtle and hare, how turtles may help mammals win the race against ischemic insult

Over the past three decades, an intense research effort has focused on elucidating the causes and the prevention of neuronal damage due to ischemic insults. However, despite this concerted effort, neuroprotective therapies against such insults remain elusive and ischemic stroke remains one of the leading causes of mortality in the Western world (Ginsberg, 2008). Facultative anaerobes have been employed as models of anoxia-tolerance, however the volume of research examining these organisms is small relative to mammalian studies and to date has primarily focused on observational studies contrasting their response to anoxia with that of anoxia-sensitive mammals (Bickler and Buck, 2007). There are relatively few vertebrate facultative anaerobes, however there are representatives among fish and reptiles that employ numerous protective mechanisms that are not adaptable to mammalian anoxia-tolerance. These organisms are ectothermic and benefit from Q_{10}-related metabolic savings at low temperatures that are of limited benefit to adult mammals and thus cannot be adopted to protect mammals from damage due to stroke (Hicks and Farrell, 2000; Stecyk and Farrell, 2006). Furthermore, during anoxia, anoxia-tolerant turtles up-regulate CBF, which enables consistent delivery of glycolytic substrate and removal of acidic anaerobic end products from the brain region

(although the challenge of sequestering these acidic products until the end of the anoxic period remains). This situation differs considerably from ischemic insult in stroke-afflicted mammalian brain where CBF ceases and glucose cannot be delivered, nor acidic end products removed. Indeed turtle neurons are not more tolerate to complete metabolic arrest (ischemia) than mammalian neurons (Doll et al., 1991). However, even when maintained at similar temperatures and conditions, turtle neurons are considerably more anoxia-tolerant than mammalian neurons (Doll et al., 1991). As discussed above, the basic make-up of vertebrate neurons is highly conserved (receptor make up, neurotransmitter, etc), therefore the relative lack of susceptibility to anoxia in turtle neurons is likely due to differences in receptor expression or endogenous enhancement of pathways that are otherwise under-expressed or dormant in mammals.

The turtle is indeed a 'model' of anoxia-tolerance and achieves many of the physiological goals that have been identified as key to surviving anoxic insults in mammals. These include regulated metabolic depression without loss of [ATP] or E_m, prevention of excitotoxicity, maintenance of ion gradients and neuronal pump activity and the ability to metabolize or sequester acidic anaerobic end products (Bickler and Buck, 2007). Replication of these changes in mammals is the goal of neuroprotective interventions against ischemic insult; however, it is only recently that the study of anoxia-tolerant organisms has begun to transition from categorization of their differences from mammals, to elucidation of the underlying mechanisms that allow facultative anaerobes to survive prolonged anoxic insults without apparent detriment.

In the meantime, examination of neuroprotective strategies in mammals has proceeded rapidly with a relatively large number of researchers examining the problem. This research has led to the discovery of mammalian IPC and while this field is in its infancy, numerous mediators of IPC have been implicated in the heart and the brain, including mild mitochondrial uncoupling,

altered $[Ca^{2+}]_c$ and ROS signaling and activation of DORs (among numerous other cellular proteins) (Downey et al., 2007; Gidday, 2006). When I commenced my research I was intrigued by the mechanisms of IPC and much of my research was geared towards examining the potential occurrence of these mechanisms in turtle brain. Remarkably, my data suggests that some of the endogenous mechanisms of neuroprotection that characterize the turtles response to anoxia function via pathways similar to those purported to underlie IPC in mammals. Specifically, mild mitochondrial uncoupling, $[Ca^{2+}]_c$ homeostasis, increased DOR activity and expression, altered ROS and NO signaling and increased GABAergic signaling in the turtle brain are all homologous to inducible mechanisms of neuroprotection in mammals (e.g. GABA: Fig. 38). Thus the turtle may naturally, and chronically, express IPC-based mechanisms and pathways that must be upregulated in mammalian brain in order to achieve neuroprotection. These striking similarities underscore the appropriateness of the turtle as a model system in which to examine anoxia-tolerance and suggest that knowledge gained from studies into the mechanisms underlying the adaptations to low oxygen environments utilized by the turtle may be transferred to mammalian neuroprotective models with relative ease.

Interestingly, the most important lesson that can be taken from facultative anaerobes is likely not based on any single mechanism. Facultative anaerobes display a wide variety of adaptations to low-oxygen environments, however most research into mammalian neuroprotective mechanisms has traditionally focused on single point approaches to the problem of ischemic insults. For example, as discussed in the introduction, turtles employ channel and spike arrest, enhanced glycolytic throughput, increased CBF, etc. Conversely, most mammalian researchers tout their preferred singular approach, while collectively the field of study heralds one mechanism as being key and this mechanism changes as clinical trials aimed at these single

mechanisms fail (Ginsberg, 2008). Evolutionary pressures are such that very few cellular responses to a given stress are likely to be incidental or without purpose. Facultative anaerobes are the most tolerant to anoxic insults, and thus it is likely that all changes in response to anoxia are neuroprotective or adaptive to this environmental stress in some way. Indeed my research has highlighted a number of changes that occur in turtle brain that are quite different from the response of unconditioned mammalian brain. With anoxia, turtle brains naturally up-regulate inhibitory GABAergic signaling and co-coordinately depress glutamatergic receptor activity, whereas in unconditioned mammals GABAergic signaling is not invoked and glutamatergic receptors become chronically over-activated, leading to toxic elevations of $[Ca^{2+}]_c$ and $[Ca^{2+}]_m$ (Bickler et al., 2000; Michaels and Rothman, 1990; Pamenter et al., 2008c). Similarly, mammals exhibit cytotoxic bursts of free radical production (ROS and NO) during the reoxygenation stage following an ischemic insult, whereas in turtle cortex ROS and NO production return to normoxic levels and deleterious bursts of ROS and NO production are avoided (Milton et al., 2007; Pamenter et al., 2008a; Pamenter et al., 2007; Scorziello et al., 2004; Waypa et al., 2001).

Abolishment of ROS and NO production, depression of excitatory glutamatergic activity and increased inhibitory GABAergic activity are all likely advantageous to the anoxic turtle brain and opposing changes or a failure to regulate these mechanisms have all been implicated in cell death following ischemic insult in mammalian brain. Since the turtle is the most anoxia-tolerant vertebrate known, it stands to reason that this multi-prong approach to surviving anoxic insults is the maximally adaptive response to anoxia. Therefore, the most important lesson from these studies may be that in order to provide protection from ischemic insults or to reverse damage following stroke in mammals, a combined approach is both appropriate and necessary.

7.3. Discussion Figures

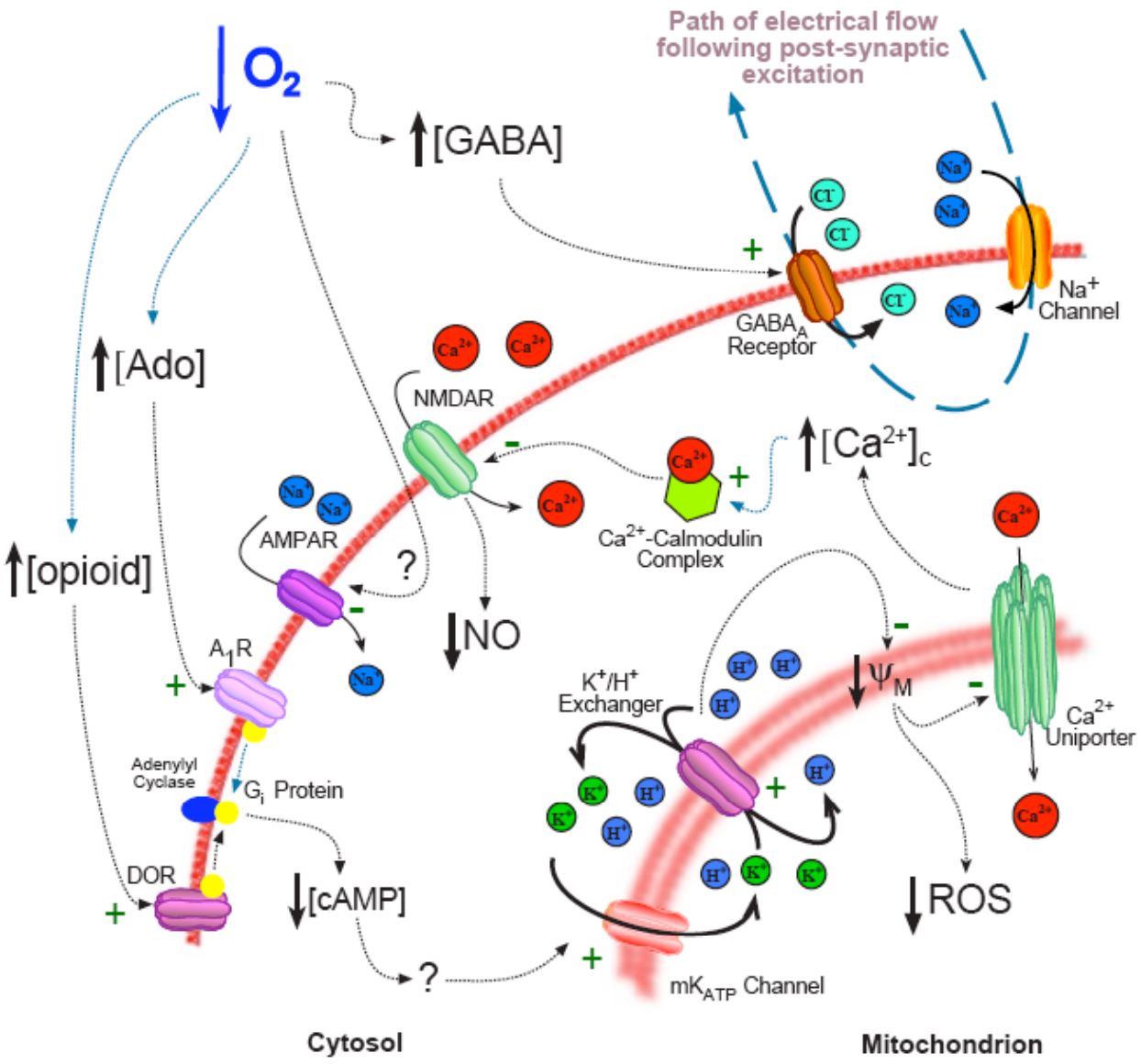

Figure 37. Schematic of endogenous neuroprotective mechanisms in the anoxic turtle brain

Decreasing [O_2] activates numerous downstream neuroprotective mechanisms mediated by adenosine, delta opioid, and GABA receptors and by mild mitochondrial uncoupling. These mechanisms combine to reduce neuronal excitability and free radical generation during hypoxia/anoxia.

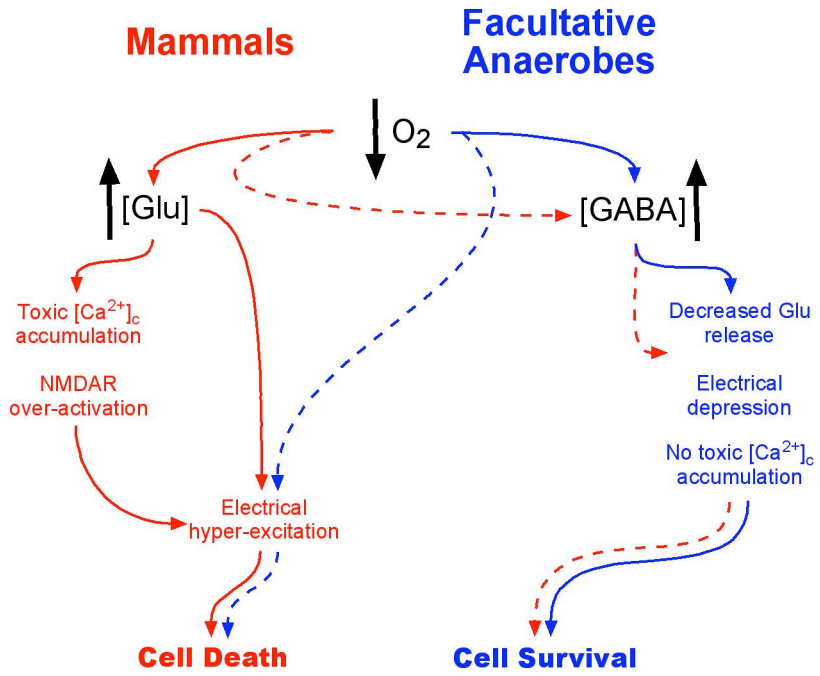

Figure 38. Simple schematic of inhibitory GABAergic mechanisms of neuroprotection in anoxia tolerant facultative anaerobe and preconditioned mammalian neurons.

Ischemic preconditioning (IPC)- or GABA-induced neuroprotective mechanisms resemble endogenous mechanisms in facultative anaerobes: Facultative anaerobes (blue pathway) utilize endogenous GABA-mediated neuroprotective mechanisms (solid blue lines) when exposed to anoxia. Ischemic mammalian neurons (red pathway) undergo excitotoxic cell death (solid red lines) but can be rescued by experimental interventions including IPC, GABA perfusion or $GABA_A$ receptor agonism (dashed red lines). Blockade of $GABA_A$ receptors during anoxic or ischemic insult abolish neuroprotective mechanisms in facultative anaerobes (dashed blue lines) and in IPC- or GABA-pretreated mammalian neurons.

8. Detailed Materials and Methods

8.1. Ethics approval

All studies were approved by the University of Toronto Animal Care committee and conform to the Guide to the Care and Use of Experimental Animals, Volume 2 as determined by the Canadian Council on Animal Care regarding relevant guidelines for the care of experimental animals. Adult turtles (*Chrysemys picta bellii*) collected in spring, summer and autumn were obtained from Niles Biological Inc. (Sacramento, CA, USA) or Lemberger Inc. (Oshkosh, WI). Animals were housed together in a large aquarium with a flow-through dechlorinated freshwater system at 16°C, a basking platform and lamp. Turtle were maintained on a 12L:12D photoperiod and given continuous access to food. All experiments were conducted at room temperature (20-23°C) unless specified otherwise.

8.2. Methods of dissection and tissue preparation

8.2.1. Turtle cortical sheet isolation

Turtle cortical sheets were dissected as described elsewhere (Blanton et al., 1989). Briefly, turtles were decapitated and whole brains were rapidly excised from the cranium within 30 seconds of decapitation. Cortical sheets were isolated from the whole brain in ice-cold artificial turtle cerebrospinal fluid (aCSF; in mM: 107 NaCl, 2.6 KCl, 1.2 $CaCl_2$, 1 $MgCl_2$, 2 NaH_2PO_4, 26.5 $NaHCO_3$, 10 glucose, 5 imidazole, pH 7.4; osmolarity 280-290). Cortical sheets were cut into 2 mm x 1 mm sections and stored at 4°C in aCSF until use.

8.2.2. Isolation of mitochondria

Although my mK_{ATP} experiments were conducted in turtle cortex, turtle heart mitochondria were used for isolated mitochondrial experiments. Turtle heart mitochondria were used due to their abundance in this tissue relative to the comparatively lower abundance and mass of the turtle brain. Although there are tissue-specific difference in mitochondria, mitochondria respond similarly to mK_{ATP} channel modulation in brain, and heart (Bajgar et al., 2001; Holmuhamedov, 1998). For this reason I consider heart mitochondria to be an appropriate model in which to assess the response of turtle mitochondria to mK_{ATP} modulation. Detailed mitochondrial isolation procedures are reported elsewhere (Almeida-Val et al., 1994; Holmuhamedov, 1999). To minimize animal usage, hearts were obtained from those animals sacrificed for cortical tissue. Briefly: mitochondria were suspended in an isolation solution consisting of (in mM: 140 KCl, 20 Na-N-2-hydroxyethylpiperazine-N'-2-ethanesulfonic acid (HEPES), 10 EDTA, and 0.1% bovine serum albumin (BSA) adjusted to pH 7.20 at 20ºC with KOH; osmolarity 295-300 mmol/kg). Mitochondrial pellets were suspended to approximately 1 mg mitochondrial protein/ml. Protein concentrations were analyzed using a spectrophotometer bicinchoninic acid (BCA) endpoint protein assay calibrated to 37ºC at a 562 nm using a Molecular Devices SpectraMax Plus plate spectrophotometer and SoftproMax® software.

8.2.3. Isolation of heart, brain, liver and muscle tissues from dived turtles

For cAMP and cGMP assays, turtles were divided into five treatment groups comprising dive windows of 0, 30, 60, 120 and 240 mins. Animals were placed in dive chambers and submerged at 20-22°C. Following dive-treatment, animals were neck-clamped and decapitated underwater to prevent reoxygenation. Brain tissue was extracted in the same manner as for cortical sheet isolation, except the entire brain was used. A bone saw was used to separate

carapace and plastron and heart, liver and pectoral skeletal muscle tissues were rapidly extracted and all tissues were freeze-clamped in liquid nitrogen in less than 1 min. Blood samples (200 μl) were extracted via aortic puncture from the aortic arch and pO_2 was analyzed with an oxygen meter electrode (OM2000, Cameron Instruments, Port Aransas, TX, USA) to determine the oxygen availability to the tissues of the dived animals. Tissue samples were sonicated and acid-extracted in 7% perchloric acid and then neutralized to pH 7.5 with KOH-TRIS buffer. Samples were frozen with liquid N_2 and stored in an -80°C freezer until use.

8.3. Experimental design

8.3.1. Normoxic and anoxic experimental equipment configurations

All electrophysiological and fluorescent experiments were performed using standard experimental equipment configurations. Isolated cortical sheets were placed in an RC-26 chamber with a P1 platform (Warner Instruments, CT, USA). The chamber was gravity perfused at a rate of 2-3 ml/min with room temperature-equilibrated aCSF. Normoxic aCSF was gassed with 95%O_2/5%CO_2 and a second bottle with 95%N_2/5%CO_2 to achieve an anoxic perfusion. To maintain anoxic conditions, perfusion tubes from IV bottles were double jacketed and the outer jacket gassed with 95%N_2/5%CO_2. The anoxic aCSF reservoir was bubbled for 30 mins before an experiment. A plastic cover with a hole for the recording electrode was placed over the perfusion chamber and the space between the fluid surface and cover was gently gassed with 95%N_2/5%CO_2. Throughout the entire anoxic experiment, aCSF was constantly gassed with N_2/CO_2. The partial pressure of oxygen (PO_2) in the recording chamber was measured with a Clark-type electrode and decreased from approximately 610 mmHg PO_2 (hyperoxia) to 0.5 mmHg PO_2 (anoxia) within 5 min, which is the limit of detection for the PO_2 electrode and not

different from that in the N_2/CO_2 bubbled reservoir. PO_2 levels were maintained at this level for the duration of anoxic experiments (data not shown). For hypoxic experiments, aCSF was gassed with a mixture of $95\%O_2/5\%CO_2$ and $95\%N_2/5\%CO_2$ calibrated to achieve a final $[O_2]$ of 5% O_2. This $[O_2]$ was confirmed using the same O_2 electrode configuration as above.

Turtle cortical sheets are between 600 - 900 microns deep and the vasculature is removed during tissue preparation. As a result the core of these tissues is hypoxic even when the surface of the tissue is exposed to room air containing 21% O_2 (Fujii et al., 1982). To ensure that the entire tissue was oxygenated under normoxic control conditions tissue was perfused with saline gassed with $95\%O_2/5\%CO_2$. The high pO_2 content could lead to hyperoxia in the tissue and subsequent ROS generation. To test for any effects of high O_2 on ROS generation cortical sheets were exposed to repeated transitions between $95\%O_2/5\%CO_2$ and 95% air/$5\%CO_2$. No significant change in ROS was detected (data not shown). Furthermore, control normoxic experiments were repeated with 95% air/$5\%CO_2$ and this gas mixture had no significant effect on whole-cell NMDAR currents, E_m, or spontaneous electrical activity during two hours of recordings (data not shown).

8.3.2. Whole-cell patch-clamp recording overview

Whole-cell recordings were performed using 2-6 MΩ borosilicate glass electrodes containing the following (in mM): 8 NaCl, 0.0001 $CaCl_2$, 10 NaHepes, 130 Kgluconate, 1 $MgCl_2$, 0.3 NaGTP, 2 NaATP, pH adjusted 7.4 with methanesulfonic acid, osmolarity 295-300 mOsM). Cell-attached 5-20 GΩ seals were obtained using the blind-patch technique described elsewhere (Blanton et al., 1989). Whole-cell configuration was achieved by applying a brief suction following seal formation. Typical access resistance (R_a) ranged from 10-30 MΩ and patches were discarded if R_a changed by more than 20% during an experiment. Data were

collected using an Axopatch-1D amplifier, a CV-4 headstage, and a digidata 1200 interface (Axon Instruments) and digitized and stored on computer using Clampex 7 software (Axon Instruments, CA, USA). The bath reference electrode was a silver-silver chloride junction. The liquid junction potential was assessed as ~12 mV and all data have been corrected for this value (raw data traces are unaltered). The liquid junction potential was determined by placing an electrode filled with turtle ICSF in a bath of normoxic aCSF and balancing the junction null, the aCSF bath was then replaced with an ISCF bath and the liquid junction potential was read off the amplifiers' voltage meter.

8.3.3. Perforated-patch recordings

I utilized the gramicidin perforated-patch technique to examine neuronal electrical properties and to determine E_{GABA} without perturbing neuronal Cl^- gradients. For perforated-patch experiments, WPI TW150F-3 thin walled 4-5 MΩ borosilicate glass electrodes were pulled and back-filled with high [Cl^-] ICSF (150 mM KCl) containing 25 μg/ml gramicidin. Slices were visualized using an Olympus BX51W1 microscope (Olympus Canada Inc, Markham, ON) with IR-DIC and stimulated at 0.1 Hz for 100 μsecs duration with an AMPI iso-flex triggered by AMPI master8-stimulating electrode (A.M.P.I., Jerusalem, Is). Data was recorded at a sampling frequency of 5 kHz using an Axon multiclamp 700B amplifier (Axon Instruments, CA, USA).

8.3.4. Evoked current recordings

A fast-step perfusion system (VC-6 perfusion valve controller and SF-77B fast-step perfusion system, Warner Instruments, CT, USA) was used to deliver 50 μM tetrodotoxin (TTX) and either 50-200 AMPA or 300 μM NMDA. The NMDA concentration was selected based on previous experiments in turtle cortex (Shin and Buck, 2003; Shin et al., 2005). At higher

concentrations (100-200 μM), AMPA resulted in large currents that were deleterious to the cell as assessed by loss of E_m and cell death (Fig. 3). All whole-cell AMPA experiments utilized 50 μM AMPA as this concentration resulted in repeatable and consistent currents and did not lead to E_m loss (Fig. 3). Prior to each recording cortical sheets were perfused with TTX for 5 mins to prevent APs or 1 μM TTX was included in the bath perfusate . Cells were voltage clamped at -70 mV and AMPA or NMDA were applied until a current was elicited (3-10 seconds, depending on the proximity of the perfusion system to the patched neuron). This application time was used for all recordings from the same neuron within a single experiment. Evoked current data was recorded at 2 kHz.

The initial peak current was set to 100% and subsequent peak currents were normalized to this value. For anoxic and pharmacological experiments, AMPA or NMDA were initially applied to cortical sheets in normoxic aCSF, and the evoked whole-cell current was set to 100% (t = 0 min). A second control current was obtained after 10 mins and then cortical sheets were exposed to anoxic aCSF or aCSF containing specific receptor modulators for 40 mins. Evoked peak currents were monitored at 20-min intervals following the change in aCSF. Cells were then reperfused with control normoxic aCSF for 40 mins and evoked peak currents were monitored at 20-min intervals following reoxygenation. For evoked AMPAR current experiments, NMDARs were blocked with either high extracellular magnesium (4 mM: hypoxic experiments) or APV (anoxic experiments) to isolate AMPA currents. Current-voltage relationships for turtle NMDARs are unaffected by 1 mM Mg^{2+} but are blocked by 4 mM Mg^{2+} (Shin and Buck, 2003).

8.3.5. Current-voltage relationships

To determine current-voltage relationships of AMPARs, 50 μM AMPA was applied to neurons voltage-clamped in sequential steps at -80, -50, -30, 0 and +30 mV. Cells were treated

with 1 μM TTX and 25 μM APV to prevent spontaneous APs and NMDAR-mediated contamination, respectively. Cells were allowed to recover for 10 mins between each voltage step and all responses were normalized to the current recorded at -80 mV. Current-voltage relationships for turtle NMDARs have been previously reported in single-channel and whole-cell patch clamp studies (Buck and Bickler, 1998a; Shin and Buck, 2003).

8.3.6. Spontaneous activity recordings

EPSC and EPSP activity were recorded for up to two hours at a sampling frequency of 5 kHz. AMPA-mediated EPSC activity was assessed by voltage clamping the cell at -70 mV and recording spontaneous currents. Cells were perfused with APV to prevent NMDA-mediated currents. Spontaneous EPSC and EPSP activities were recorded in cells undergoing the same experimental protocol as the whole-cell current experiments. EPSC and EPSP frequencies and amplitudes were assessed using waveform template analysis in Clampfit 9 software (Axon Instruments, CA, USA). For statistical analysis, spontaneous activity recorded during the final 10 mins of 40-min anoxic exposures or of the corresponding time period (t = 40-50 mins) of normoxic experiments were compared to control recordings from the first 10 mins of the experiment.

8.4. Fluorophore imaging in fixed and live tissues

8.4.1. Fixed tissue Immunohistochemistry and imaging

Turtle brains were dissected and incubated in aCSF containing a K_{ATP}-specific fluorophore (BODIPY-glibenclamide green: 500 nM), and a mitochondria-specific fluorophore (mitotracker deep red: 500 nM). Brains were incubated with the two flourophores for 90 mins and then fixed for 48 hours in 10% formaline and 30% sucrose at 4º C. Fixed brains were then

frozen and the cortex was sliced using a cryostat to a thickness of 20 microns. Cortical slices were mounted on slides with vectashield mounting medium (Vector Laboratories, CA). Samples were imaged with a Zeiss LSM510 META Axioplan2 confocal with 4, 40 and 100x water-immersion lenses. Argon and helium neon lasers were used to excite the probes (ex/em): BODIPY-Green – 504/511, Mitotracker Deep Red – 644/655nm. Data were analyzed using Zeiss LSM410 software.

8.4.2. Live cell fluorescent imaging

Cortical sheets were isolated as described for whole-cell patch clamp experiments and then preloaded in the dark at 4°C with the appropriate fluorophore (see below). Unless specified otherwise, dyes were loaded in two consecutive one-hour incubations, followed by a 15-25 min rinse in dye-free aCSF. Following dye loading, cortical sheets were placed in a flow-through recording chamber equipped with the same perfusion system as the whole-cell patch clamp experiments. A custom cuff was placed around the objective to provide constant N_2 gas across the surface of the bath during anoxic exposure. Unless otherwise specified, probes were excited using a DeltaRam X high-speed random access monochromator and a LPS220B light source (PTI, NJ, USA). Fluorescent measurements were acquired at 10-second intervals using an Olympus BX51W1 microscope and either a QImaging Rolera MGi EMCCD camera (Roper Scientific Inc, Ill, USA), or an Olympus U-CMAD3 camera (Olympus Canada Inc, Markham, ON). Baseline fluorescence was recorded for 10-20 mins and then the tissue was exposed to treatment aCSF for up to 80 mins. Tissues were then reperfused with control aCSF. For each experiment 25-50 neurons were chosen at random and the average change of fluorescence in these neurons was used for statistical comparison. Data were analyzed using EasyRatioPro software. For all dyes, changes in background fluorescence in cortical sheet exposed to each

treatment were assessed in the absence of flourophores. None of the treatments resulted in changes in background fluorescence for the dyes examined (data not shown).

Calcium changes were assessed using fura-2-AM such that an increase in fura-2 fluorescence corresponds to an increase of $[Ca^{2+}]_c$. Fura-2 was excited at 340 and 380 nm in cortical sheets preloaded with fura-2. Fluorescent emissions above 510 nm were isolated using an Olympus DM510 dichroic mirror and fluorescent measurements were acquired (515–530 nm). $[Ca^{2+}]_c$ was calculated as described elsewhere (Buck and Bickler, 1995).

Chloride changes were assessed using 6-methoxy-*N*-ethylquniolinium iodide (MEQ). MEQ is a self-quenching assay, therefore an increase in MEQ fluorescence corresponds to decreased $[Cl^-]_c$. Working stocks of MEQ were prepared daily over nitrogen as described elsewhere (Inglefield and Schwartz-Bloom, 1999). Slices were incubated in 400 μM MEQ for 1 hour and then rinsed in MEQ-free aCSF for 10 mins prior to experimentation. MEQ was calibrated using the Stern-Volmor equation as described elsewhere (Inglefield and Schwartz-Bloom, 1999). MEQ is also sensitive to changes in cell volume, and since cell volume changes are a common result of anoxic insults I measured cell volume changes using a calcein self-quenching assay (Hamann et al., 2002). Cortical sheets were incubated in 5 μM calcein for one hour and then placed in the recording chamber. Calcein was excited at 470-480 nm and emissions were recorded at 510 nm. Cortical sheets were exposed to anoxia or to sequential aCSF solutions with osmolarity adjusted in 25 mOsM steps from 250 to 400 mOsM. The change in osmolarity of aCSF required to match the anoxic change in calcein fluorescence was determined and in a separate set of experiments, cortical sheets incubated in MEQ were treated with a similar osmolarity step. In this manner the change in MEQ fluorescence due to cell

swelling with anoxia could be determined and subtracted from the total change, leaving only the Cl^--mediated change in MEQ fluorescence.

Nitric oxide production was measured using the fluorophore 4-amino-5-methylamino-2′,7′-difluorofluorescein (DAF-FM) such that an increase in DAF-FM fluorescence corresponds to increased NO production. Cortical sheets were incubated in 5 μM DAF-FM. DAF-FM was excited for 0.1 s at 488 nm. Fluorescent emissions above 510 nm were isolated using an Olympus DM510 dichroic mirror and fluorescent measurements were acquired (515–530 nm).

H_2O_2 changes were assessed following 30-mins of loading in the dye 5-(and 6) dichloromethyl-2',7'-dichlorohydrofluorescein diacetate, acetyl ester (CM-H_2DCFDA) such that an increase in CM-H_2DCFDA fluorescence corresponds to increased H_2O_2 production. Following dye loading, cortical sheets were exposed to normoxic or anoxic aCSF, or normoxic aCSF containing either the complex IV inhibitor cyanide, the complex III inhibitor myxothiazol or the complex I inhibitor rotenone. Oxidation of CM-H_2DCFDA to DCFDA was quantified fluorometrically (exc/em: 488/535 nm) using a 40x Zeiss water-immersion lens and an 8-bit non-intensified digital camera. Images and fluorescence data were acquired using Axon Imaging Workbench Version 3. In three anoxic control experiments, cells underwent repeated transitions between normoxic and anoxic perfusions to assess the effect of reoxygenation on ROS generation.

8.4.3. Measurement of mitochondrial O_2 consumption

Rates of O_2 consumption were determined using a Clark-type O_2 electrode attached to a Gilson O_2 chamber. Mitochondria were suspended in incubation medium (in mM: 140 KCl, 20 HEPES, 10 EDTA and 1 Na_2HPO_4) at a 1:8 ratio. Maximum respiratory control rates (RCRs) were achieved with 5 mM α-ketoglutarate (α-kg). Mitochondria exist in state II rates prior to the

addition of ADP or substrate. State II mitochondria are analogous to an engine without fuel. Addition of ADP and substrate induces state III respiration and state IV respiration occurs when the available ADP has been consumed. Since in intact cells the ratio of ATP to ADP is very high, state IV respiration is the closest to in vivo mitochondrial activity. Therefore, I assessed the effects of pharmacological agents during state IV respiration unless noted otherwise. Drug concentrations were the same as those used during whole-cell recordings (see below). Respiration rates were calculated using the LoggerPro v.2.2.1 software (Vernier, OR). Electrodes were calibrated daily.

8.4.4. Cyclic Adenylate Enzyme immunoassay

Concentrations of cyclic adenylates were determined using cAMP and cGMP competitive Biotrak enzyme immunoassay kits from Amersham Biosciences (Piscataway, NJ). Tissue cAMP and cGMP competed with cAMP/cGMP-conjugated horseradish peroxidase for binding sites on a rabbit anti-cAMP/cGMP plate. Reactions were acid-stopped with HCl and plates were read at 450nM to determine cyclic adenylate concentrations.

8.5. Pharmacology

For all experiments cortical sheets were perfused with pharmacological modifiers in the bulk perfusate as specified in the appropriate results section unless noted otherwise below. For ATP dialysis experiments, a recording electrode solution containing 0 [ATP] was used to dialyze ATP from the cytosol as elsewhere (Muller et al., 2002). For experiments with varied $[Cl^-]_c$, changes in Cl^- concentration were compensated for with equimolar replacement of NaCl with Na-gluconate to maintain osmalarity. pH-sensitive ion channels were activated by intracellular

recording solution pH-adjusted to 6.8. To chelate Ca^{2+}, 1,2-bis(o-aminophenoxy)ethane-N,N,N',N'-tetraacetic acid (BAPTA, 5 mM) was included in the recording electrode solution.

Table 6. Working concentrations of pharmacological modifiers.

Chemical	Concentration used	Comment
5HD	100 μM	mK_{ATP} antagonist[a]
Adenosine	250 μM	Cellular metabolite
AMPA	50-200 μM	AMPAR agonist
APV	25 μM	NMDAR antagonist
BAPTA	5 mM	Calcium chelator[b]
Cesium	1.2 mM	General K^+ channel antagonist
CGP55845	5 μM	$GABA_B$ receptor antagonist
CNQX	30 μM	AMPAR antagonist
CPA	100 nM	Adenosine A_1R agonist
Cyanide	100 – 500 μM	Oxidative phosphorylation inhibitor
Diazoxide	10-350 μM	mK_{ATP} agonist[c]
Dinitrophenol	10 mM	protonophore
DPCPX	70 nM	Adenosine A_1R antagonist
EGTA	5 mM	Ca^{2+} chelator
EZA	50 μM	Carbonic anhydrase inhibitor
Furosemide	100 μM	NKCC1/KCC2 antagonist
GABA	10-2000 μM	Cellular metabolite
Glibenclamide	50-100 μM	K_{ATP} antagonist
Iodoacetate	3.5 mM	Glycolytic metabolism inhibitor
L-NAME	0.5-5 mM	Nitric oxide synthase inhibitor
Levcromakalim	100 μM	K_{ATP} agonist
Malonate	5 mM	SDH inhibitor

[a] 5HD has little effect on pK_{ATP} but is a potent inhibitor of mK_{ATP} activity **Garlid, K. D., Paucek, P., Yarov-Yarovoy, V., Murray, H. N., Darbenzio, R. B., D'alonzo, A. J., Lodge, N. J., Smith, M. A. and Grover, G. J.** (1997). Cardioprotective effect of diazoxide and its interaction with mitochondrial ATP-sensitive K+ channels. Possible mechanism of cardioprotection. *Circ Res* **81**, 1072-1082, **Mccullough, J. R., Normandin, D. E., Conder, M. L., Sleph, P. G., Dzwonczyk, S. and Grover, G. J.** (1991). Specific block of the anti-ischemic actions of cromakalim by sodium 5-hydroxydecanoate. *Circ Res* **69**, 949-958..

[b] BAPTA was included in the recording electrode solution **Shin, D. S., Wilkie, M. P., Pamenter, M. E. and Buck, L. T.** (2005). Calcium and protein phosphatase 1/2A attenuate N-methyl-D-aspartate receptor activity in the anoxic turtle cortex. *Comp Biochem Physiol A Mol Integr Physiol* **142**, 50-57..

[c] Diazoxide is known to be 1000-2000x more selectively potent for mK_{ATP} then for plasmalemmal K_{ATP} channels (pK_{ATP}) and is not an effective activator of pK_{ATP} at the concentrations used in this study ($K_{1/2}$: 855 μM) **Garlid, K. D., Paucek, P., Yarov-Yarovoy, V., Murray, H. N., Darbenzio, R. B., D'alonzo, A. J., Lodge, N. J., Smith, M. A. and Grover, G. J.** (1997). Cardioprotective effect of diazoxide and its interaction with mitochondrial ATP-sensitive K+ channels. Possible mechanism of cardioprotection. *Circ Res* **81**, 1072-1082, **Garlid, K. D., Paucek, P., Yarov-Yarovoy, V., Sun, X. and Schindler, P. A.** (1996). The mitochondrial KATP channel as a receptor for potassium channel openers. *J Biol Chem* **271**, 8796-8799..

Mastoparan-7	1 μM	G_i protein agonist
MPG	0.5-5 mM	ROS scavenger
Myxothiazol	200 nM	Mitochondrial complex III inhibitor
NAC	0.5-5 mM	ROS scavenger
Naltrindole	1-10 μM	DOR antagonist
NMDA	300 μM	NMDAR agonist
NS-1619	50 μM	mK_{Ca} agonist
Paxilline	1 μM	mK_{Ca} antagonist
Pertussis Toxin	400 nM	G_i protein inhibitor[d]
Propionate	10 mM	Membrane-permeable weak acid
Rotenone	50 μM	Mitochondrial complex I inhibitor
Ruthenium red	40 nM	Mitochondrial Ca^{2+}-uniporter antagonist
Ryanodine	10 μM	ER ryanodine receptor antagonist[e]
SNP	1–50 mM	Nitric oxide donator
Spermine	500 μM	Mitochondrial Ca^{2+}-uniporter agonist
SR-95531 (gabazine)	25 μM	$GABA_A$ receptor antagonist
TEA	40 μM	General K^+ channel antagonist
Thapsigargin	1 μM	ER Ca^{2+}-ATPase antagonist
Tetrodotoxin	1 μM	Voltage-gated Na^+ channel antagonist
Valinomycin	5 μM	Potassium ionophore

8.5.1. Chemicals

All chemicals were obtained from Sigma Chemical Co. (Oakville, ON, Canada). CPA, Diazoxide, DPCPX, EZA, glibenclamide, levcromakalim, NS1619, paxilline and thapsigargin were initially dissolved in dimethylsulfonic acid (DMSO), and then placed in aCSF not exceeding 1%v/v. Vehicle application alone did not affect NMDA evoked currents, mitochondrial respiration or spontaneous electrical activity (data not shown). Fluorescent probes were obtained from Molecular Probes (Eugene, OR, USA).

8.6. Statistical Analysis

Raw fluorescence data were normalized to the 10-min normoxic baseline value. Results were analyzed using a repeated measures two-way ANOVA with a Holm-Sidak multiple

[d] Cortical sheets were incubated in normoxic saline containing 400 nM PTX for 18 hours prior to experimentation.
[e] Ryanodine is antagonistic at this concentration but activates ryanodine receptors at nM concentrations.

comparisons test. AMPAR and NMDAR whole-cell current, and EPSP and EPSC data were analyzed following root arcsine transformation using two-way ANOVA with a Student-Newman-Keuls (all pairwise) post-hoc test to compare within and against treatment and normoxic values. Cyclic adenylate and mitochondrial respiration data was analyzed using paired t-tests and one-way ANOVA. Significance was determined at $P<0.05$ unless otherwise indicated in results, and all data are expressed as the mean ± SEM (standard error of mean).

References

Abele, A. E. and Miller, R. J. (1990). Potassium channel activators abolish excitotoxicity in cultured hippocampal pyramidal neurons. *Neurosci Lett* **115**, 195-200.

Abele, A. E., Scholz, K. P., Scholz, W. K. and Miller, R. J. (1990). Excitotoxicity induced by enhanced excitatory neurotransmission in cultured hippocampal pyramidal neurons. *Neuron* **4**, 413-419.

Aguilar-Bryan, L. and Bryan, J. (1999). Molecular biology of adenosine triphosphate-sensitive potassium channels. *Endocr Rev* **20**, 101-135.

Ainscow, E. K. and Brand, M. D. (1999). Top-down control analysis of ATP turnover, glycolysis and oxidative phosphorylation in rat hepatocytes. *Eur J Biochem* **263**, 671-685.

Albin, R. L. and Gilman, S. (1992). GABAA, GABAB, and benzodiazepine binding sites in the cerebellar cortex of the red-eared turtle (Pseudemys scripta). *Brain Res* **595**, 164-166.

Allen, T. J., Mikala, G., Wu, X. and Dolphin, A. C. (1998). Effects of 2,3-butanedione monoxime (BDM) on calcium channels expressed in Xenopus oocytes. *J Physiol* **508 (Pt 1)**, 1-14.

Almeida-Val, V. M., Buck, L. T. and Hochachka, P. W. (1994). Substrate and acute temperature effects on turtle heart and liver mitochondria. *Am J Physiol* **266**, R858-862.

Anderson, T. R., Jarvis, C. R., Biedermann, A. J., Molnar, C. and Andrew, R. D. (2005). Blocking the anoxic depolarization protects without functional compromise following simulated stroke in cortical brain slices. *J Neurophysiol* **93**, 963-979.

Andine, P., Orwar, O., Jacobson, I., Sandberg, M. and Hagberg, H. (1991). Changes in extracellular amino acids and spontaneous neuronal activity during ischemia and extended reflow in the CA1 of the rat hippocampus. *J Neurochem* **57**, 222-229.

Arai, A., Kessler, M. and Lynch, G. (1990). The effects of adenosine on the development of long-term potentiation. *Neurosci Lett* **119**, 41-44.

Archer, S. L., Huang, J., Henry, T., Peterson, D. and Weir, E. K. (1993). A redox-based O2 sensor in rat pulmonary vasculature. *Circ Res* **73**, 1100-1112.

Ariel, M. (2006). Modulation of visual inputs to accessory optic system by theophylline during hypoxia. *Exp Brain Res* **172**, 351-360.

Arundine, M. and Tymianski, M. (2003). Molecular mechanisms of calcium-dependent neurodegeneration in excitotoxicity. *Cell Calcium* **34**, 325-337.

Auchampach, J. A., Maruyama, M., Cavero, I. and Gross, G. J. (1991). The new K+ channel opener Aprikalim (RP 52891) reduces experimental infarct size in dogs in the absence of hemodynamic changes. *J Pharmacol Exp Ther* **259**, 961-967.

Audinat, E., Gahwiler, B. H. and Knopfel, T. (1992). Excitatory synaptic potentials in neurons of the deep nuclei in olivo-cerebellar slice cultures. *Neuroscience* **49**, 903-911.

Babenko, A., P., Aguilar-Bryan, L. and Bryan, J. (1998). A view of sur/KIR6.X, KATP channels. *Annu Rev Physiol* **60**, 667-687.

Bai, D., Muller, R. U. and Roder, J. C. (2002). Non-ionotropic cross-talk between AMPA and NMDA receptors in rodent hippocampal neurones. *J Physiol* **543**, 23-33.

Bajgar, R., Seetharaman, S., Kowalowski, A. J., Garlid, K. D. and Paucek, P. (2001). Identification and properties of a novel intracellular (mitochondrial) ATP-sensitive potassium channel in brain. *J Biol Chem* **276**, 33369-33374.

Banerjee, R., Saravanan, K. S., Thomas, B., Sindhu, K. M. and Mohanakumar, K. P. (2007). Evidence for Hydroxyl Radical Scavenging Action of Nitric Oxide Donors in the Protection Against 1-Methyl-4-phenylpyridinium-induced Neurotoxicity in Rats. *Neurochem Res*.

Barman, S. A., Zhu, S., Han, G. and White, R. E. (2003). cAMP activates BKCa channels in pulmonary arterial smooth muscle via cGMP-dependent protein kinase. *Am J Physiol Lung Cell Mol Physiol* **284**, L1004-1011.

Ben-Ari, Y. (2002). Excitatory actions of gaba during development: the nature of the nurture. *Nat Rev Neurosci* **3**, 728-739.

Ben-Ari, Y., Gaiarsa, J. L., Tyzio, R. and Khazipov, R. (2007). GABA: a pioneer transmitter that excites immature neurons and generates primitive oscillations. *Physiol Rev* **87**, 1215-1284.

Ben-Haim, G. and Armstead, W. M. (2000). Stimulus duration-dependent contribution of k(ca) channel activation and cAMP to hypoxic cerebrovasodilation. *Brain Res* **853**, 330-337.

Bickler, P. E. (1992a). Cerebral anoxia tolerance in turtles: regulation of intracellular calcium and pH. *Am J Physiol* **263**, R1298-1302.

Bickler, P. E. (1992b). Effects of temperature and anoxia on regional cerebral blood flow in turtles. *Am J Physiol* **262**, R538-541.

Bickler, P. E. (1998). Reduction of NMDA receptor activity in cerebrocortex of turtles (Chrysemys picta) during 6 wk of anoxia. *Am J Physiol* **275**, R86-91.

Bickler, P. E. and Buck, L. T. (1998). Adaptations of vertebrate neurons to hypoxia and anoxia: maintaining critical Ca2+ concentrations. *J Exp Biol* **201**, 1141-1152.

Bickler, P. E. and Buck, L. T. (2007). Hypoxia tolerance in reptiles, amphibians, and fishes: life with variable oxygen availability. *Annu Rev Physiol* **69**, 145-170.

Bickler, P. E., Donohoe, P. H. and Buck, L. T. (2000). Hypoxia-induced silencing of NMDA receptors in turtle neurons. *J Neurosci* **20**, 3522-3528.

Bickler, P. E. and Fahlman, C. S. (2004). Moderate increases in intracellular calcium activate neuroprotective signals in hippocampal neurons. *Neuroscience* **127**, 673-683.

Bickler, P. E., Fahlman, C. S. and Ferriero, D. M. (2004). Hypoxia increases calcium flux through cortical neuron glutamate receptors via protein kinase C. *J Neurochem* **88**, 878-884.

Bickler, P. E. and Hansen, B. M. (1994). Causes of calcium accumulation in rat cortical brain slices during hypoxia and ischemia: role of ion channels and membrane damage. *Brain Res* **665**, 269-276.

Blanton, M. G., Lo Turco, J. J. and Kriegstein, A. R. (1989). Whole cell recording from neurons in slices of reptilian and mammalian cerebral cortex. *J Neurosci Methods* **30**, 203-210.

Bonfoco, E., Krainc, D., Ankarcrona, M., Nicotera, P. and Lipton, S. A. (1995). Apoptosis and necrosis: two distinct events induced, respectively, by mild and intense insults with N-methyl-D-aspartate or nitric oxide/superoxide in cortical cell cultures. *Proc Natl Acad Sci U S A* **92**, 7162-7166.

Bosley, T. M., Woodhams, P. L., Gordon, R. D. and Balazs, R. (1983). Effects of anoxia on the stimulated release of amino acid neurotransmitters in the cerebellum in vitro. *J Neurochem* **40**, 189-201.

Brightman, T., Ye, J. H., Ortiz-Jimenez, E., Flynn, E. J., Wu, W. H. and Mcardle, J. J. (1995). 2,3-Butanedione monoxime protects mice against the convulsant effect of picrotoxin by facilitating GABA-activated currents. *Brain Res* **678**, 110-116.

Brooks, S. P. J., Storey, K.B. (1993). Protein kinase C in turtle brain: changes in enzyme activity during anoxia. *J. Comp. Physiol. B*. **163**, 84-88.

Buck, L., Espanol, M., Litt, L. and Bickler, P. (1998). Reversible decreases in ATP and PCr concentrations in anoxic turtle brain. *Comp Biochem Physiol A Mol Integr Physiol* **120**, 633-639.

Buck, L. T. (2000). Succinate and alanine as anaerobic end-products in the diving turtle (Chrysemys picta bellii). *Comp Biochem Physiol B Biochem Mol Biol* **126**, 409-413.

Buck, L. T. (2004). Adenosine as a signal for ion channel arrest in anoxia-tolerant organisms. *Comp Biochem Physiol B Biochem Mol Biol* **139**, 401-414.

Buck, L. T. and Bickler, P. (1995). Role of adenosine in NMDA receptor modulation in the cerebral cortex of an anoxia-tolerant turtle (Chrysemys picta belli). *J Exp Biol* **198**, 1621-1628.

Buck, L. T. and Bickler, P. (1998a). Adenosine and anoxia reduce N-methyl-D-aspartate receptor open probability in turtle cerebrocortex. *J Exp Biol* **201**, 289-297.

Buck, L. T. and Bickler, P. E. (1998b). Adenosine and anoxia reduce N-methyl-D-aspartate receptor open probability in turtle cerebrocortex. *J Exp Biol* **201**, 289-297.

Buck, L. T., Espanol, M., Litt, L., Bickler, P. (1998). Reversible decreases in ATP and PCr concentrations in anoxic turtle brain. *Comparative Biochemistry and Physiology Part A* **120**, 633-639.

Buck, L. T. and Hochachka, P. W. (1993). Anoxic suppression of Na(+)-K(+)-ATPase and constant membrane potential in hepatocytes: support for channel arrest. *Am J Physiol* **265**, R1020-1025.

Buck, L. T., Land, S. C. and Hochachka, P. W. (1993). Anoxia-tolerant hepatocytes: model system for study of reversible metabolic suppression. *Am J Physiol Regul Integr Comp Physiol* **265**.

Buck, L. T. and Pamenter, M. E. (2006). Adaptive responses of vertebrate neurons to anoxia-Matching supply to demand. *Respir Physiol Neurobiol* **154**, 226-240.

Buescher, P. C., Pearse, D. B., Pillai, R. P., Litt, M. C., Mitchell, M. C. and Sylvester, J. T. (1991). Energy state and vasomotor tone in hypoxic pig lungs. *J Appl Physiol* **70**, 1874-1881.

Busija, D. W., Katakam, P., Rajapakse, N. C., Kis, B., Grover, G., Domoki, F. and Bari, F. (2005). Effects of ATP-sensitive potassium channel activators diazoxide and BMS-191095 on membrane potential and reactive oxygen species production in isolated piglet mitochondria. *Brain Res Bull* **66**, 85-90.

Cao, C. M., Xia, Q., Gao, Q., Chen, M. and Wong, T. M. (2005). Calcium-activated potassium channel triggers cardioprotection of ischemic preconditioning. *J Pharmacol Exp Ther* **312**, 644-650.

Cao, Y. J., Bian, J. T. and Bhargava, H. N. (1997). Effects of NMDA receptor antagonists on delta1- and delta2-opioid receptor agonists-induced changes in the mouse brain [3H]DPDPE binding. *Eur J Pharmacol* **335**, 161-166.

Caramia, M. D., Palmieri, M. G., Desiato, M. T., Iani, C., Scalise, A., Telera, S. and Bernardi, G. (2000). Pharmacologic reversal of cortical hyperexcitability in patients with ALS. *Neurology* **54**, 58-64.

Carini, R., Grazia De Cesaris, M., Splendore, R., Domenicotti, C., Nitti, M. P., Pronzato, M. A. and Albano, E. (2003). Signal pathway responsible for hepatocyte preconditioning by nitric oxide. *Free Radic Biol Med* **34**, 1047-1055.

Chao, D., Bazzy-Asaad, A., Balboni, G. and Xia, Y. (2007a). delta-, but not mu-, opioid receptor stabilizes K(+) homeostasis by reducing Ca(2+) influx in the cortex during acute hypoxia. *J Cell Physiol* **212**, 60-67.

Chao, D., Donnelly, D. F., Feng, Y., Bazzy-Asaad, A. and Xia, Y. (2007b). Cortical delta-opioid receptors potentiate K+ homeostasis during anoxia and oxygen-glucose deprivation. *J Cereb Blood Flow Metab* **27**, 356-368.

Chen, J., Zhu, J. X., Wilson, I. and Cameron, J. S. (2005). Cardioprotective effects of K ATP channel activation during hypoxia in goldfish Carassius auratus. *J Exp Biol* **208**, 2765-2772.

Cheung, U., Moghaddasi, M., Hall, H. L., Smith, J. J., Buck, L. T. and Woodin, M. A. (2006). Excitatory actions of GABA mediate severe-hypoxia-induced depression of neuronal activity in the pond snail (Lymnaea stagnalis). *J Exp Biol* **209**, 4429-4435.

Chih, C. P., Feng, Z. C., Rosenthal, M., Lutz, P. L. and Sick, T. J. (1989a). Energy metabolism, ion homeostasis, and evoked potentials in anoxic turtle brain. *Am J Physiol* **257**, R854-860.

Chih, C. P., Rosenthal, M. and Sick, T. J. (1989b). Ion leakage is reduced during anoxia in turtle brain: a potential survival strategy. *Am J Physiol* **257**, R1562-1564.

Choi, D. W. (1994). Calcium and excitotoxic neuronal injury. *Ann N Y Acad Sci* **747**, 162-171.

Choi, Y., Chen, H. V. and Lipton, S. A. (2001). Three pairs of cysteine residues mediate both redox and zn2+ modulation of the nmda receptor. *J Neurosci* **21**, 392-400.

Clark, V. M., and Miller, A.T. (1973). Studies of anaerobic metabolism in the fresh-water turtle (Pseudemys scripta elegans). *Comp Biochem Physiol A Mol Integr Physiol* **44**, 55-62.

Clark, V. M. and Miller, A. T., Jr. (1973). Studies on anaerobic metabolism in the fresh-water turtle (Pseudemys scripta elegans). *Comp Biochem Physiol A Mol Integr Physiol* **44**, 55-62.

Collis, M. G. (1989). The vasodilator role of adenosine. *Pharmacol Ther* **41**, 143-162.

Conti, F. and Weinberg, R. J. (1999). Shaping excitation at glutamatergic synapses. *Trends Neurosci* **22**, 451-458.

Costa, A. D., Garlid, K. D., West, I. C., Lincoln, T. M., Downey, J. M., Cohen, M. V. and Critz, S. D. (2005). Protein kinase G transmits the cardioprotective signal from cytosol to mitochondria. *Circ Res* **97**, 329-336.

Costanzo, J. P., Jones, E. E. and Lee, R. E., Jr. (2001). Physiological responses to supercooling and hypoxia in the hatchling painted turtle, Chrysemys picta. *J Comp Physiol [B]* **171**, 335-340.

Coulter, D. A., Sombati, S. and Delorenzo, R. J. (1992). Electrophysiology of glutamate neurotoxicity in vitro: induction of a calcium-dependent extended neuronal depolarization. *J Neurophysiol* **68**, 362-373.

Courtney, M. J., Lambert, J. J. and Nicholls, D. G. (1990). The interactions between plasma membrane depolarization and glutamate receptor activation in the regulation of cytoplasmic free calcium in cultured cerebellar granule cells. *J Neurosci* **10**, 3873-3879.

Crepel, F., Dupont, J. L. and Gardette, R. (1983). Voltage clamp analysis of the effect of excitatory amino acids and derivatives on Purkinje cell dendrites in rat cerebellar slices maintained in vitro. *Brain Res* **279**, 311-315.

Crepel, V., Hammond, C., Chinestra, P., Diabira, D. and Ben-Ari, Y. (1993a). A selective LTP of NMDA receptor-mediated currents induced by anoxia in CA1 hippocampal neurons. *J Neurophysiol* **70**, 2045-2055.

Crepel, V., Rovira, C. and Ben-Ari, Y. (1993b). The K+ channel opener diazoxide enhances glutamatergic currents and reduces GABAergic currents in hippocampal neurons. *J Neurophysiol* **69**, 494-503.

Crompton, M. (2000). Mitochondrial intermembrane junctional complexes and their role in cell death. *J Physiol* **529 Pt 1**, 11-21.

Cross, J. V. and Templeton, D. J. (2006). Regulation of signal transduction through protein cysteine oxidation. *Antioxid Redox Signal* **8**, 1819-1827.

Dave, K. R., Lange-Asschenfeldt, C., Raval, A. P., Prado, R., Busto, R., Saul, I. and Perez-Pinzon, M. A. (2005). Ischemic preconditioning ameliorates excitotoxicity by shifting glutamate/gamma-aminobutyric acid release and biosynthesis. *J Neurosci Res* **82**, 665-673.

Davies, D. G. (1989). Distribution of systemic blood flow during anoxia in the turtle, Chrysemys scripta. *Respir Physiol* **78**, 383-389.

Delpire, E. (2000). Cation-Chloride Cotransporters in Neuronal Communication. *News Physiol Sci* **15**, 309-312.

Diemer, N. H., Jorgensen, M. B., Johansen, F. F., Sheardown, M. and Honore, T. (1992). Protection against ischemic hippocampal CA1 damage in the rat with a new non-NMDA antagonist, NBQX. *Acta Neurol Scand* **86**, 45-49.

Doll, C., Hochachka, P. and Hand, S. (1994). A microcalorimetric study of turtle cortical slices: insights into brain metabolic depression. *J Exp Biol* **191**, 141-153.

Doll, C. J., Hochachka, P. W. and Reiner, P. B. (1991). Effects of anoxia and metabolic arrest on turtle and rat cortical neurons. *Am J Physiol Regul Integr Comp Physiol* **260**, R747-R755.

Doll, C. J., Hochachka, P. W. and Reiner, P. B. (1993). Reduced ionic conductance in turtle brain. *Am J Physiol* **265**, R929-933.

Domanska-Janik, K., Pylowa, S. and Zalewska, T. (1993). Coupling of adenosine receptors to adenylate cyclase in postischemic rat brain. *Cell Signal* **5**, 337-343.

Downey, J. M., Davis, A. M. and Cohen, M. V. (2007). Signaling pathways in ischemic preconditioning. *Heart Fail Rev* **12**, 181-188.

Edwards, R. A., Lutz, P.L., Baden, D.G. (1989). Relationship between energy expenditure and ion channel density in the turtle and rat brain. *Am J Physiol Regul Integr Comp Physiol* **26**, R1354-R1358.

Erecinska, M. and Silver, I. A. (1989). ATP and brain function. *J Cereb Blood Flow Metab* **9**, 2-19.

Fang, S. Y., Tseng, C. C., Yang, Y. L., Lee, E. J., Chen, H. Y., Bhardwaj, A. and Chen, T. Y. (2006). Nitric oxide scavenger carboxy-PTIO reduces infarct volume following permanent focal ischemia. *Acta Anaesthesiol Taiwan* **44**, 141-146.

Feng, Z.-C., Rosenthal, M. and Sick, T. J. (1988). Suppression of evoked potentials with continued ion transport during anoxia in turtle brain. *American Journal of Physiology, (Regulatory Integrative Comparative Physiology)* **24**, R478-R484.

Fernandes, J. A., Lutz, P. L., Tannenbaum, A., Todorov, A. T., Liebovitch, L. and Vertes, R. (1997). Electroencephalogram activity in the anoxic turtle brain. *Am J Physiol* **273**, R911-919.

Fernandez, N., Garcia, J. L., Garcia-Villalon, A. L., Monge, L., Gomez, B. and Dieguez, G. (1993). Cerebral blood flow and cerebrovascular reactivity after inhibition of nitric oxide synthesis in conscious goats. *Br J Pharmacol* **110**, 428-434.

Fujii, T., Baumgartl, H. and Lubbers, D. W. (1982). Limiting section thickness of guinea pig olfactory cortical slices studied from tissue pO2 values and electrical activities. *Pflugers Arch* **393**, 83-87.

Fung, M. L., Croning, M. D. and Haddad, G. G. (1999). Sodium homeostasis in rat hippocampal slices during oxygen and glucose deprivation: role of voltage-sensitive sodium channels. *Neurosci Lett* **275**, 41-44.

Garlid, K. D., Paucek, P., Yarov-Yarovoy, V., Murray, H. N., Darbenzio, R. B., D'alonzo, A. J., Lodge, N. J., Smith, M. A. and Grover, G. J. (1997). Cardioprotective effect of diazoxide and its interaction with mitochondrial ATP-sensitive K+ channels. Possible mechanism of cardioprotection. *Circ Res* **81**, 1072-1082.

Garlid, K. D., Paucek, P., Yarov-Yarovoy, V., Sun, X. and Schindler, P. A. (1996). The mitochondrial KATP channel as a receptor for potassium channel openers. *J Biol Chem* **271**, 8796-8799.

Garthwaite, G. and Garthwaite, J. (1986). Amino acid neurotoxicity: intracellular sites of calcium accumulation associated with the onset of irreversible damage to rat cerebellar neurones in vitro. *Neurosci Lett* **71**, 53-58.

Garthwaite, J., Charles, S. L. and Chess-Williams, R. (1988). Endothelium-derived relaxing factor release on activation of NMDA receptors suggests role as intercellular messenger in the brain. *Nature* **336**, 385-388.

Garthwaite, J., Garthwaite, G. and Hajos, F. (1986). Amino acid neurotoxicity: relationship to neuronal depolarization in rat cerebellar slices. *Neuroscience* **18**, 449-460.

Ghai, H. S. and Buck, L. T. (1999). Acute reduction in whole cell conductance in anoxic turtle brain. *Am J Physiol* **277**, R887-893.

Gidday, J. M. (2006). Cerebral preconditioning and ischaemic tolerance. *Nat Rev Neurosci* **7**, 437-448.

Ginsberg, M. D. (2008). Neuroprotection for ischemic stroke: Past, present and future. *Neuropharmacology*.

Giordano, F. J. (2005). Oxygen, oxidative stress, hypoxia, and heart failure. *J Clin Invest* **115**, 500-508.

Glitsch, H. G. (2001). Electrophysiology of the sodium-potassium-ATPase in cardiac cells. *Physiol Rev* **81**, 1791-1826.

Grabb, M. C., Lobner, D., Turetsky, D. M. and Choi, D. W. (2002). Preconditioned resistance to oxygen-glucose deprivation-induced cortical neuronal death: alterations in vesicular GABA and glutamate release. *Neuroscience* **115**, 173-183.

Grover, G. J. (1997). Pharmacology of ATP-sensitive potassium channel (KATP) openers in models of myocardial ischemia and reperfusion. *Can J Physiol Pharmacol* **75**, 309-315.

Gu, X. Q., Siemen, D., Parvez, S., Cheng, Y., Xue, J., Zhou, D., Sun, X., Jonas, E. A. and Haddad, G. G. (2007). Hypoxia increases BK channel activity in the inner mitochondrial membrane. *Biochem Biophys Res Commun* **358**, 311-316.

Gunter, T. E., Buntinas, L., Sparagna, G. C. and Gunter, K. K. (1998). The Ca2+ transport mechanisms of mitochondria and Ca2+ uptake from physiological-type Ca2+ transients. *Biochim Biophys Acta* **1366**, 5-15.

Haga, K. K., Gregory, L. J., Hicks, C. A., Ward, M. A., Beech, J. S., Bath, P. W., Williams, S. C. and O'neill, M. J. (2003). The neuronal nitric oxide synthase inhibitor, TRIM, as a neuroprotective agent: effects in models of cerebral ischaemia using histological and magnetic resonance imaging techniques. *Brain Res* **993**, 42-53.

Hall, E. D., Andrus, P. K., Fleck, T. J., Oostveen, J. A., Carter, D. B. and Jacobsen, E. J. (1997). Neuroprotective properties of the benzodiazepine receptor, partial agonist PNU-101017 in the gerbil forebrain ischemia model. *J Cereb Blood Flow Metab* **17**, 875-883.

Hall, E. D., Fleck, T. J. and Oostveen, J. A. (1998). Comparative neuroprotective properties of the benzodiazepine receptor full agonist diazepam and the partial agonist PNU-101017 in the gerbil forebrain ischemia model. *Brain Res* **798**, 325-329.

Hamann, S., Kiilgaard, J., Litmann, T., Alverez-Leefmans, F., Winther, B. and Zeuthen, T. (2002). Measurement of cell volume changes by fluorescence self-quenching. *J Fluorescence* **12**, 139-145.

Heurteaux, C., Lauritzen, I., Widmann, C. and Lazdunski, M. (1995). Essential role of adenosine, adenosine A1 receptors, and ATP-sensitive K+ channels in cerebral ischemic preconditioning. *Proc Natl Acad Sci U S A* **92**, 4666-4670.

Hicks, J. M. and Farrell, A. P. (2000). The cardiovascular responses of the red-eared slider (Trachemys scripta) acclimated to either 22 or 5 degrees C. I. Effects of anoxic exposure on in vivo cardiac performance. *J Exp Biol* **203**, 3765-3774.

Hicks, J. W. and Wang, T. (1999). Hypoxic hypometabolism in the anesthetized turtle, Trachemys scripta. *Am J Physiol* **277**, R18-23.

Hille, B. (1992). Ionic Channels of Excitable Membranes, Second Edition. *Sinauer Associates, Inc. Sunderland, Massachusetts*.

Hitzig, B. M., Kneussl, M. P., Shih, V., Brandstetter, R. D. and Kazemi, H. (1985). Brain amino acid concentrations during diving and acid-base stress in turtles. *J Appl Physiol* **58**, 1751-1754.

Hochachka, P. W. (1986). Defense strategies against hypoxia and hypothermia. *Science* **231**, 234-241.

Hochachka, P. W., Buck, L. T., Doll, C. J. and Land, S. C. (1996). Unifying theory of hypoxia tolerance: molecular/metabolic defense and rescue mechanisms for surviving oxygen lack. *Proc Natl Acad Sci U S A* **93**, 9493-9498.

Hochachka, P. W. and Dunn, J. F. (1983). Metabolic arrest: the most effective means of protecting tissues against hypoxia. *Prog Clin Biol Res* **136**, 297-309.

Hochachka, P. W., Land, S. C. and Buck, L. T. (1997). Oxygen sensing and signal transduction in metabolic defense against hypoxia: lessons from vertebrate facultative anaerobes. *Comp Biochem Physiol A Mol Integr Physiol* **118**, 23-29.

Holmuhamedov, E. L., Jovanovic, S., Dzeja, P.P., Jovanovic, A., and Terzic, A. (1998). Mitochondrial ATP-sensitive K+ channels modulate cardiac mitochondrial function. *Am J Physiol Heart Circ Physiol* **44**, H1567-H1576.

Holmuhamedov, E. L., Wang, L., Terzic, A. (1999). ATP-sensitive K+ channel openers prevent Ca2+ overload in rat cardiac mitochondria. *J Physiol* **519.2**, 347-360.

Hoyt, K. R., Arden, S. R., Aizenman, E. and Reynolds, I. J. (1998). Reverse Na+/Ca2+ exchange contributes to glutamate-induced intracellular Ca2+ concentration increases in cultured rat forebrain neurons. *Mol Pharmacol* **53**, 742-749.

Hylland, P., Milton, S., Pek, M., Nilsson, G. E. and Lutz, P. L. (1997). Brain Na+/K+-ATPase activity in two anoxia tolerant vertebrates: crucian carp and freshwater turtle. *Neurosci Lett* **235**, 89-92.

Hylland, P. and Nilsson, G. E. (1999). Extracellular levels of amino acid neurotransmitters during anoxia and forced energy deficiency in crucian carp brain. *Brain Res* **823**, 49-58.

Hylland, P., Nilsson, G. E. and Lutz, P. L. (1994). Time course of anoxia-induced increase in cerebral blood flow rate in turtles: evidence for a role of adenosine. *J Cereb Blood Flow Metab* **14**, 877-881.

Iadecola, C. (1997). Bright and dark sides of nitric oxide in ischemic brain injury. *Trends Neurosci* **20**, 132-139.

Iadecola, C., Xu, X., Zhang, F., El-Fakahany, E. E. and Ross, M. E. (1995). Marked induction of calcium-independent nitric oxide synthase activity after focal cerebral ischemia. *J Cereb Blood Flow Metab* **15**, 52-59.

Ikonomidou, C. and Turski, L. (2002). Why did NMDA receptor antagonists fail clinical trials for stroke and traumatic brain injury? *Lancet Neurol* **1**, 383-386.

Inglefield, J. R., Perry, J. M. and Schwartz, R. D. (1995). Postischemic inhibition of GABA reuptake by tiagabine slows neuronal death in the gerbil hippocampus. *Hippocampus* **5**, 460-468.

Inglefield, J. R. and Schwartz-Bloom, R. D. (1999). Fluorescence imaging of changes in intracellular chloride in living brain slices. *Methods* **18**, 197-203.

Ioroi, T., Yonetani, M. and Nakamura, H. (1998). Effects of hypoxia and reoxygenation on nitric oxide production and cerebral blood flow in developing rat striatum. *Pediatr Res* **43**, 733-737.

Ishida, H., Hirota, Y., Genka, C., Nakazawa, H., Nakaya, H., Sato, T. (2001). Opening of mitochondrial KATP channels attenuates the ouabain-induced calcium overload in mitochondria. *Am J Physiol Heart Circ Physiol* **89**, 856-858.

Ishii, H., Shibuya, K., Ohta, Y., Mukai, H., Uchino, S., Takata, N., Rose, J. A. and Kawato, S. (2006). Enhancement of nitric oxide production by association of nitric oxide synthase with N-methyl-D-aspartate receptors via postsynaptic density 95 in genetically engineered Chinese hamster ovary cells: real-time fluorescence imaging using nitric oxide sensitive dye. *J Neurochem* **96**, 1531-1539.

Iwasaki, K., Chung, E. H., Egashira, N., Hatip-Al-Khatib, I., Mishima, K., Egawa, T., Irie, K. and Fujiwara, M. (2004). Non-NMDA mechanism in the inhibition of cellular apoptosis and memory impairment induced by repeated ischemia in rats. *Brain Res* **995**, 131-139.

Jackson, D. C. (1968). Metabolic depression and oxygen depletion in the diving turtle. *J Appl Physiol* **24**, 503-509.

Jackson, D. C., Crocker, C. E. and Ultsch, G. R. (2000a). Bone and shell contribution to lactic acid buffering of submerged turtles Chrysemys picta bellii at 3 degrees C. *Am J Physiol Regul Integr Comp Physiol* **278**, R1564-1571.

Jackson, D. C., Heisler, N. (1983). Intracellular and extracellular acid-base and electrolyte status of submerged anoxic turtles at 3C. *Respir Physiol* **53**, 187-201.

Jackson, D. C., Ramsey, A. L., Paulson, J. M., Crocker, C. E. and Ultsch, G. R. (2000b). Lactic acid buffering by bone and shell in anoxic softshell and painted turtles. *Physiol Biochem Zool* **73**, 290-297.

Jarvis, C. R., Anderson, T. R. and Andrew, R. D. (2001). Anoxic depolarization mediates acute damage independent of glutamate in neocortical brain slices. *Cereb Cortex* **11**, 249-259.

Jayalakshmi, K., Sairam, M., Singh, S. B., Sharma, S. K., Ilavazhagan, G. and Banerjee, P. K. (2005). Neuroprotective effect of N-acetyl cysteine on hypoxia-induced oxidative stress in primary hippocampal culture. *Brain Res* **1046**, 97-104.

Jensen, F. E. (1995). An animal model of hypoxia-induced perinatal seizures. *Ital J Neurol Sci* **16**, 59-68.

Jensen, F. E., Blume, H., Alvarado, S., Firkusny, I. and Geary, C. (1995). NBQX blocks acute and late epileptogenic effects of perinatal hypoxia. *Epilepsia* **36**, 966-972.

Jiang, C., Xia, Y. and Haddad, G. G. (1992). Role of ATP-sensitive K+ channels during anoxia: major differences between rat (newborn and adult) and turtle neurons. *J Physiol* **448**, 599-612.

Johansson, D. and Nilsson, G. (1995). Roles of energy status, KATP channels and channel arrest in fish brain K+ gradient dissipation during anoxia. *J Exp Biol* **198**, 2575-2580.

Johansson, D., Nilsson, G., Ouml and Rnblom, E. (1995). Effects of anoxia on energy metabolism in crucian carp brain slices studied with microcalorimetry. *J Exp Biol* **198**, 853-859.

Johns, L., Sinclair, A. J. and Davies, J. A. (2000). Hypoxia/hypoglycemia-induced amino acid release is decreased in vitro by preconditioning. *Biochem Biophys Res Commun* **276**, 134-136.

Joshi, I. and Andrew, R. D. (2001). Imaging anoxic depolarization during ischemia-like conditions in the mouse hemi-brain slice. *J Neurophysiol* **85**, 414-424.

Jourdain, P., Nikonenko, I., Alberi, S. and Muller, D. (2002). Remodeling of hippocampal synaptic networks by a brief anoxia-hypoglycemia. *J Neurosci* **22**, 3108-3116.

Kader, A., Frazzini, V. I., Solomon, R. A. and Trifiletti, R. R. (1993). Nitric oxide production during focal cerebral ischemia in rats. *Stroke* **24**, 1709-1716.

Kaila, K. (1994). Ionic basis of GABAA receptor channel function in the nervous system. *Prog Neurobiol* **42**, 489-537.

Kaila, K., Lamsa, K., Smirnov, S., Taira, T. and Voipio, J. (1997). Long-lasting GABA-mediated depolarization evoked by high-frequency stimulation in pyramidal neurons of rat hippocampal slice is attributable to a network-driven, bicarbonate-dependent K+ transient. *J Neurosci* **17**, 7662-7672.

Kaila, K., Voipio, J., Paalasmaa, P., Pasternack, M. and Deisz, R. A. (1993). The role of bicarbonate in GABAA receptor-mediated IPSPs of rat neocortical neurones. *J Physiol* **464**, 273-289.

Kakizawa, H., Matsui, F., Tokita, Y., Hirano, K., Ida, M., Nakanishi, K., Watanabe, M., Sato, Y., Okumura, A., Kojima, S. et al. (2007). Neuroprotective effect of nipradilol, an NO donor, on hypoxic-ischemic brain injury of neonatal rats. *Early Hum Dev* **83**, 535-540.

Kannurpatti, S. S., Joshi, P.G., and Joshi, N.B. (2000). Calcium sequestering ability of mitochondria modulates influx of calcium through glutamte receptor channel. *Neurochem Res* **25**, 1527-1536.

Kannurpatti, S. S., Sanganahalli, B. G., Mishra, S., Joshi, P. G. and Joshi, N. B. (2004). Glutamate-induced differential mitochondrial response in young and adult rats. *Neurochem Int* **44**, 361-369.

Karschin, A., Brockhaus, J. and Ballanyi, K. (1998). KATP channel formation by the sulphonylurea receptors SUR1 with Kir6.2 subunits in rat dorsal vagal neurons in situ. *J Physiol* **509 (Pt 2)**, 339-346.

Katchman, A. N. and Hershkowitz, N. (1997). Nitric oxide modulates synaptic glutamate release during anoxia. *Neurosci Lett* **228**, 50-54.

Kelly, D. A. and Storey, K. B. (1988). Organ-specific control of glycolysis in anoxic turtles. *Am J Physiol* **255**, R774-779.

Kirichok, Y., Krapivinsky, G. and Clapham, D. E. (2004). The mitochondrial calcium uniporter is a highly selective ion channel. *Nature* **427**, 360-364.

Kis, B., Nagy, K., Snipes, J. A., Rajapakse, N. C., Horiguchi, T., Grover, G. J. and Busija, D. W. (2004). The mitochondrial K(ATP) channel opener BMS-191095 induces neuronal preconditioning. *Neuroreport* **15**, 345-349.

Kis, B., Rajapakse, N. C., Snipes, J. A., Nagy, K., Horiguchi, T. and Busija, D. W. (2003). Diazoxide induces delayed pre-conditioning in cultured rat cortical neurons. *J Neurochem* **87**, 969-980.

Klockgether, T., Turski, L., Honore, T., Zhang, Z. M., Gash, D. M., Kurlan, R. and Greenamyre, J. T. (1991). The AMPA receptor antagonist NBQX has antiparkinsonian effects in monoamine-depleted rats and MPTP-treated monkeys. *Ann Neurol* **30**, 717-723.

Koh, S. and Jensen, F. E. (2001). Topiramate blocks perinatal hypoxia-induced seizures in rat pups. *Ann Neurol* **50**, 366-372.

Kojima, H., Hirotani, M., Nakatsubo, N., Kikuchi, K., Urano, Y., Higuchi, T., Hirata, Y. and Nagano, T. (2001). Bioimaging of nitric oxide with fluorescent indicators based on the rhodamine chromophore. *Anal Chem* **73**, 1967-1973.

Kopp, S. J., Krieglstein, J., Freidank, A., Rachman, A., Seibert, A. and Cohen, M. M. (1984). P-31 nuclear magnetic resonance analysis of brain: II. Effects of oxygen deprivation on isolated perfused and nonperfused rat brain. *J Neurochem* **43**, 1716-1731.

Korge, P., Honda, H.M., Weiss, J.N. (2002). Protection of cardiac mitochondria by diazoxide and protein kinase C: Implications for ischemic preconditioning. *Proc Natl Acad Sci U S A* **99**, 3312-3317.

Kourie, J. I. (1998). Interaction of reactive oxygen species with ion transport mechanisms. *Am J Physiol* **275**, C1-24.

Krnjevic, K. (1997). Role of GABA in cerebral cortex. *Can J Physiol Pharmacol* **75**, 439-451.

Kudin, A. P., Bimpong-Buta, N. Y., Vielhaber, S., Elger, C. E. and Kunz, W. S. (2004). Characterization of superoxide-producing sites in isolated brain mitochondria. *J Biol Chem* **279**, 4127-4135.

Land, S. C., Buck, L. T. and Hochachka, P. W. (1993). Response of protein synthesis to anoxia and recovery in anoxia-tolerant hepatocytes. *Am J Physiol Regul Integr Comp Physiol* **34**, R41-R48.

Le, D., Das, S., Wang, Y. F., Yoshizawa, T., Sasaki, Y. F., Takasu, M., Nemes, A., Mendelsohn, M., Dikkes, P., Lipton, S. A. et al. (1997). Enhanced neuronal death from focal ischemia in AMPA-receptor transgenic mice. *Brain Res Mol Brain Res* **52**, 235-241.

Lehotsky, J., Kaplan, P., Matejovicova, M., Murin, R., Racay, P. and Raeymaekers, L. (2002). Ion transport systems as targets of free radicals during ischemia reperfusion injury. *Gen Physiol Biophys* **21**, 31-37.

Li, D. Q., Duan, Y. L., Bao, Y. M., Liu, C. P., Liu, Y. and An, L. J. (2004). Neuroprotection of catalpol in transient global ischemia in gerbils. *Neurosci Res* **50**, 169-177.

Lim, Y. J., Zheng, S. and Zuo, Z. (2004). Morphine preconditions Purkinje cells against cell death under in vitro simulated ischemia-reperfusion conditions. *Anesthesiology* **100**, 562-568.

Limbrick, D. D., Jr., Sombati, S. and Delorenzo, R. J. (2003). Calcium influx constitutes the ionic basis for the maintenance of glutamate-induced extended neuronal depolarization associated with hippocampal neuronal death. *Cell Calcium* **33**, 69-81.

Lin, S. Z., Chiou, A. L. and Wang, Y. (1996). Ketamine antagonizes nitric oxide release from cerebral cortex after middle cerebral artery ligation in rats. *Stroke* **27**, 747-752.

Liu, Y. and Downey, J. M. (1992). Ischemic preconditioning protects against infarction in rat heart. *Am J Physiol* **263**, H1107-1112.

Liu, Y., Fiskum, G. and Schubert, D. (2002). Generation of reactive oxygen species by the mitochondrial electron transport chain. *J Neurochem* **80**, 780-787.

Lopatin, A. N. and Nichols, C. G. (1993). 2,3-Butanedione monoxime (BDM) inhibition of delayed rectifier DRK1 (Kv2.1) potassium channels expressed in Xenopus oocytes. *J Pharmacol Exp Ther* **265**, 1011-1016.

Lopez-Barneo, J., Del Toro, R., Levitsky, K. L., Chiara, M. D. and Ortega-Saenz, P. (2004). Regulation of oxygen sensing by ion channels. *J Appl Physiol* **96**, 1187-1195; discussion 1170-1182.

Lundberg, A. and Oscarsson, O. (1953). Anoxic depolarization of mammalian nerve fibres. *Acta Physiol Scand Suppl* **111**, 99-110.

Lutz, P. L. and Kabler, S. (1997). Release of adenosine and ATP in the brain of the freshwater turtle during long-term anoxia. *Brain Res* **769**, 281-286.

Lutz, P. L. and Manuel, L. (1999). Maintenance of adenosine A1 receptor function during long-term anoxia in the turtle brain. *Am J Physiol* **276**, R633-636.

Lutz, P. L., Mcmahon, P., Rosenthal, M., Sick, T.J. (1984). Relationships between aerobic and anaerobic energy production in turtle brain in situ. *Am J Physiol Regul Integr Comp Physiol* **16**, R740-R744.

Lutz, P. L. and Milton, S. L. (2004). Negotiating brain anoxia survival in the turtle. *J Exp Biol* **207**, 3141-3147.

Lyubkin, M., Durand, D. M. and Haxhiu, M. A. (1997). Interaction between tetanus long-term potentiation and hypoxia-induced potentiation in the rat hippocampus. *J Neurophysiol* **78**, 2475-2482.

Martinez-Murillo, R., Fernandez, A. P., Serrano, J., Rodrigo, J., Salas, E., Mourelle, M. and Martinez, A. (2007). The nitric oxide donor LA 419 decreases brain damage in a focal ischemia model. *Neurosci Lett* **415**, 149-153.

Martyniuk, C. J., Crawford, A. B., Hogan, N. S. and Trudeau, V. L. (2005). GABAergic modulation of the expression of genes involved in GABA synaptic transmission and stress in the hypothalamus and telencephalon of the female goldfish (Carassius auratus). *J Neuroendocrinol* **17**, 269-275.

Maruo, K., Yamamoto, S., Kanno, T., Yaguchi, T., Maruo, S., Yashiya, S. and Nishizaki, T. (2006). Tunicamycin decreases the probability of single-channel openings for N-methyl-D-aspartate and alpha-amino-3-hydroxy-5-methyl-4-isoxazole propionic acid receptors. *Neuroreport* **17**, 313-317.

Materi, L. M., Rasmusson, D. D. and Semba, K. (2000). Inhibition of synaptically evoked cortical acetylcholine release by adenosine: an in vivo microdialysis study in the rat. *Neurosci* **97**, 219-226.

Matsuo, M., Kimura, Y. and Ueda, K. (2005). KATP channel interaction with adenine nucleotides. *J Mol Cell Cardiol* **38**, 907-916.

Mccullough, J. R., Normandin, D. E., Conder, M. L., Sleph, P. G., Dzwonczyk, S. and Grover, G. J. (1991). Specific block of the anti-ischemic actions of cromakalim by sodium 5-hydroxydecanoate. *Circ Res* **69**, 949-958.

Mehrani, H. and Storey, K. B. (1995a). cAMP-dependent protein kinase and anoxia survival in turtles: purification and properties of liver PKA. *Mol Cell Biochem* **145**, 81-88.

Mehrani, H. and Storey, K. B. (1995b). Enzymatic control of glycogenolysis during anoxic submergence in the freshwater turtle Trachemys scripta. *Int J Biochem Cell Biol* **27**, 821-830.

Mei, Y. A., Vaudry, H. and Cazin, L. (1994). Inhibitory effect of adenosine on electrical activity of frog melanotrophs mediated through A1 purinergic receptors. *J Physiol* **481 (Pt 2)**, 349-355.

Michaels, R. L. and Rothman, S. M. (1990). Glutamate neurotoxicity in vitro: antagonist pharmacology and intracellular calcium concentrations. *J Neurosci* **10**, 283-292.

Milton, S. L. and Lutz, P. L. (1998). Low extracellular dopamine levels are maintained in the anoxic turtle (Trachemys scripta) striatum. *J Cereb Blood Flow Metab* **18**, 803-807.

Milton, S. L. and Lutz, P. L. (2005). Adenosine and ATP-sensitive potassium channels modulate dopamine release in the anoxic turtle (Trachemys scripta) striatum. *Am J Physiol Regul Integr Comp Physiol* **289**, R77-83.

Milton, S. L., Nayak, G., Kesaraju, S., Kara, L. and Prentice, H. M. (2007). Suppression of reactive oxygen species production enhances neuronal survival in vitro and in vivo in the anoxia-tolerant turtle Trachemys scripta. *J Neurochem* **101**, 993-1001.

Milton, S. L., Nayak, G., Lutz, P. L. and Prentice, H. M. (2006). Gene transcription of neuroglobin is upregulated by hypoxia and anoxia in the brain of the anoxia-tolerant turtle Trachemys scripta. *J Biomed Sci* **13**, 509-514.

Milton, S. L., Thompson, J. W. and Lutz, P. L. (2002). Mechanisms for maintaining extracellular glutamate levels in the anoxic turtle striatum. *Am J Physiol Regul Integr Comp Physiol* **282**, R1317-1323.

Mohazzab, K. M., Fayngersh, R. P., Kaminski, P. M. and Wolin, M. S. (1995). Potential role of NADH oxidoreductase-derived reactive O2 species in calf pulmonary arterial PO2-elicited responses. *Am J Physiol* **269**, L637-644.

Mohazzab, K. M. and Wolin, M. S. (1994). Sites of superoxide anion production detected by lucigenin in calf pulmonary artery smooth muscle. *Am J Physiol* **267**, L815-822.

Montague, P. R., Gancayco, C. D., Winn, M. J., Marchase, R. B. and Friedlander, M. J. (1994). Role of NO production in NMDA receptor-mediated neurotransmitter release in cerebral cortex. *Science* **263**, 973-977.

Moroney, P. M., Scholes, T. A. and Hinkle, P. C. (1984). Effect of membrane potential and pH gradient on electron transfer in cytochrome oxidase. *Biochemistry* **23**, 4991-4997.

Mulkey, R. M., Herron, C. E. and Malenka, R. C. (1993). An essential role for protein phosphatases in hippocampal long-term depression. *Science* **261**, 1051-1055.

Muller, M., Brockhaus, J. and Ballanyi, K. (2002). ATP-independent anoxic activation of ATP-sensitive K+ channels in dorsal vagal neurons of juvenile mice in situ. *Neuroscience* **109**, 313-328.

Murata, M., Akao, M., O'rourke, B., Marban, E. (2001). Miochondrial ATP-sensitive potassium channels attenuate matrix Ca2+ overload during stimulated ischemia and reperfusion. *Circulation Research* **89**, 891-898.

Murry, C. E., Jennings, R. B. and Reimer, K. A. (1986). Preconditioning with ischemia: a delay of lethal cell injury in ischemic myocardium. *Circulation* **74**, 1124-1136.

Musacchia, X. J. (1959). The viability of Chrysemys picta submerged at various temperatures. *Physiol Zoo 1* **32**, 57-50.

Namiranian, K., Koehler, R. C., Sapirstein, A. and Dore, S. (2005). Stroke outcomes in mice lacking the genes for neuronal heme oxygenase-2 and nitric oxide synthase. *Curr Neurovasc Res* **2**, 23-27.

Nilsson, G. and Lutz, P. (1992). Adenosine release in the anoxic turtle brain: a possible mechanism for anoxic survival. *J Exp Biol* **162**, 345-351.

Nilsson, G. E. (2001). Surviving anoxia with the brain turned on. *News Physiol Sci* **16**, 217-221.

Nilsson, G. E., Alfaro, A. A. and Lutz, P. L. (1990). Changes in turtle brain neurotransmitters and related substances during anoxia. *Am J Physiol* **259**, R376-384.

Nilsson, G. E. and Lutz, P. L. (1991). Release of inhibitory neurotransmitters in response to anoxia in turtle brain. *Am J Physiol* **261**, R32-37.

Nilsson, G. E. and Renshaw, G. M. (2004). Hypoxic survival strategies in two fishes: extreme anoxia tolerance in the North European crucian carp and natural hypoxic preconditioning in a coral-reef shark. *J Exp Biol* **207**, 3131-3139.

Nilsson, G. E. and Winberg, S. (1993). Changes in the brain levels of GABA and related amino acids in anoxic shore crab (Carcinus maenas). *Am J Physiol* **264**, R733-737.

Nowak, L., Bregestovski, P., Ascher, P., Herbet, A. and Prochiantz, A. (1984). Magnesium gates glutamate-activated channels in mouse central neurones. *Nature* **307**, 462-465.

O'rourke, B. (2000). Pathophysiological and protective roles of mitochondrial ion channels. *J Physiol* **529 Pt 1**, 23-36.

O'rourke, B. (2007). Mitochondrial ion channels. *Annu Rev Physiol* **69**, 19-49.

Obrietan, K., Belousov, A. B., Heller, H. C. and Van Den Pol, A. N. (1995). Adenosine pre- and postsynaptic modulation of glutamate-dependent calcium activity in hypothalamic neurons. *J Neurophysiol* **74**, 2150-2162.

Ohmori, J., Sakamoto, S., Kubota, H., Shimizu-Sasamata, M., Okada, M., Kawasaki, S., Hidaka, K., Togami, J., Furuya, T. and Murase, K. (1994). 6-(1H-imidazol-1-yl)-7-nitro-2,3(1H,4H)-quinoxalinedione hydrochloride (YM90K) and related compounds: structure-activity relationships for the AMPA-type non-NMDA receptor. *J Med Chem* **37**, 467-475.

Oldenburg, O., Cohen, M. V. and Downey, J. M. (2003). Mitochondrial K(ATP) channels in preconditioning. *J Mol Cell Cardiol* **35**, 569-575.

Pagonopoulou, O., Efthimiadou, A., Asimakopoulos, B. and Nikolettos, N. K. (2006). Modulatory role of adenosine and its receptors in epilepsy: possible therapeutic approaches. *Neurosci Res* **56**, 14-20.

Palmer, G. C. (1985). Cyclic nucleotides in stroke and related cerebrovascular disorders. *Life Sci* **36**, 1995-2006.

Pamenter, M. E. and Buck, L. T. (2008). Neuronal membrane potential is mildly depolarized in the anoxic turtle cortex. *Comp Biochem Physiol A Mol Integr Physiol* **150**, 410-414.

Pamenter, M. E., Hogg, D. W. and Buck, L. T. (2008a). Endogenous reductions in N-methyl-d-aspartate receptor activity inhibit nitric oxide production in the anoxic freshwater turtle cortex. *FEBS Lett* **582**, 1738-1742.

Pamenter, M. E., Richards, M. D. and Buck, L. T. (2007). Anoxia-induced changes in reactive oxygen species and cyclic nucleotides in the painted turtle. *J Comp Physiol [B]* **177**, 473-481.

Pamenter, M. E., Shin, D. S. and Buck, L. (2008b). Adenosine A1 receptor activation mediates NMDA receptor activity in a pertussis toxin-sensitive manner during normoxia but not anoxia in turtle cortical neurons. *Brain Res* **1213C**, 27-34.

Pamenter, M. E., Shin, D. S. and Buck, L. T. (2008c). AMPA receptors undergo channel arrest in the anoxic turtle cortex. *Am J Physiol Regul Integr Comp Physiol* **294**, R606-613.

Pamenter, M. E., Shin, D. S., Cooray, M. and Buck, L. T. (2008d). Mitochondrial ATP-sensitive K+ channels regulate NMDAR activity in the cortex of the anoxic western painted turtle. *J Physiol* **586**, 1043-1058.

Patel, H. H., Ludwig, L. M., Fryer, R. M., Hsu, A. K., Warltier, D. C. and Gross, G. J. (2002). Delta opioid agonists and volatile anesthetics facilitate cardioprotection via potentiation of K(ATP) channel opening. *Faseb J* **16**, 1468-1470.

Peeters-Scholte, C., Koster, J., Veldhuis, W., Van Den Tweel, E., Zhu, C., Kops, N., Blomgren, K., Bar, D., Van Buul-Offers, S., Hagberg, H. et al. (2002). Neuroprotection by selective nitric oxide synthase inhibition at 24 hours after perinatal hypoxia-ischemia. *Stroke* **33**, 2304-2310.

Pek, M. and Lutz, P. L. (1997). Role for adenosine in channel arrest in the anoxic turtle brain. *J Exp Biol* **200**, 1913-1917.

Pek-Scott, M. and Lutz, P. L. (1998). ATP-sensitive K+ channel activation provides transient protection to the anoxic turtle brain. *Am J Physiol* **275**, R2023-2027.

Perez-Pinzon, M. A., Chan, C. Y., Rosenthal, M. and Sick, T. J. (1992a). Membrane and synaptic activity during anoxia in the isolated turtle cerebellum. *Am J Physiol Regul Integr Comp Physiol* **263**, R1057-R1063.

Perez-Pinzon, M. A., Lutz, P. L., Sick, T. J. and Rosenthal, M. (1993). Adenosine, a "retaliatory" metabolite, promotes anoxia tolerance in turtle brain. *J Cereb Blood Flow Metab* **13**, 728-732.

Perez-Pinzon, M. A., Rosenthal, M., Lutz, P. W. and Sick, T. J. (1992b). Anoxic Survival of the isolated cerebellum of the turtle pseudemis scripta elegans. *J. Comp. Physiol. B.* **162**, 68-73.

Perez-Pinzon, M. A., Rosenthal, M., Sick, T. J., Lutz, P. L., Pablo, J. and Mash, D. (1992c). Downregulation of sodium channels during anoxia: a putative survival strategy of turtle brain. *Am J Physiol Regul Integr Comp Physiol* **262**, R712-R715.

Perkel, D. J., Hestrin, S., Sah, P. and Nicoll, R. A. (1990). Excitatory synaptic currents in Purkinje cells. *Proc Biol Sci* **241**, 116-121.

Podrabsky, J. E., Lopez, J. P., Fan, T. W., Higashi, R. and Somero, G. N. (2007). Extreme anoxia tolerance in embryos of the annual killifish Austrofundulus limnaeus: insights from a metabolomics analysis. *J Exp Biol* **210**, 2253-2266.

Qin, Q., Yang, X. M., Cui, L., Critz, S. D., Cohen, M. V., Browner, N. C., Lincoln, T. M. and Downey, J. M. (2004). Exogenous NO triggers preconditioning via a cGMP- and mitoKATP-dependent mechanism. *Am J Physiol Heart Circ Physiol* **287**, H712-718.

Quintana, P., Alberi, S., Hakkoum, D. and Muller, D. (2006). Glutamate receptor changes associated with transient anoxia/hypoglycaemia in hippocampal slice cultures. *Eur J Neurosci* **23**, 975-983.

Rader, R. K. and Lanthorn, T. H. (1989). Experimental ischemia induces a persistent depolarization blocked by decreased calcium and NMDA antagonists. *Neurosci Lett* **99**, 125-130.

Ramaglia, V. and Buck, L. T. (2004). Time-dependent expression of heat shock proteins 70 and 90 in tissues of the anoxic western painted turtle. *J Exp Biol* **207**, 3775-3784.

Rees, D. D., Palmer, R. M., Schulz, R., Hodson, H. F. and Moncada, S. (1990). Characterization of three inhibitors of endothelial nitric oxide synthase in vitro and in vivo. *Br J Pharmacol* **101**, 746-752.

Reshef, A., Sperling, O. and Zoref-Shani, E. (2000a). Opening of K(ATP) channels is mandatory for acquisition of ischemic tolerance by adenosine. *Neuroreport* **11**, 463-465.

Reshef, A., Sperling, O. and Zoref-Shani, E. (2000b). Role of K(ATP) channels in the induction of ischemic tolerance by the 'adenosine mechanism' in neuronal cultures. *Adv Exp Med Biol* **486**, 217-221.

Rezvani, M. E., Mirnajafi-Zadeh, J., Fathollahi, Y. and Palizvan, M. R. (2007). Anticonvulsant effect of A1 but not A2A adenosine receptors of piriform cortex in amygdala-kindled rats. *Can J Physiol Pharmacol* **85**, 606-612.

Rhee, S., Chang, T., Bae, Y., Lee, S. and Kang, S. (2003). Cellular regulation by hydrogen peroxide. *J am Soc Nephrol* **14**, s211-s215.

Rossi, D. J., Oshima, T. and Attwell, D. (2000). Glutamate release in severe brain ischaemia is mainly by reversed uptake. *Nature* **403**, 316-321.

Rounds, S. and Mcmurtry, I. F. (1981). Inhibitors of oxidative ATP production cause transient vasoconstriction and block subsequent pressor responses in rat lungs. *Circ Res* **48**, 393-400.

Rousou, A. J., Ericsson, M., Federman, M., Levitsky, S. and Mccully, J. D. (2004). Opening of mitochondrial KATP channels enhances cardioprotection through the modulation of mitochondrial matrix volume, calcium accumulation, and respiration. *Am J Physiol Heart Circ Physiol* **287**, H1967-1976.

Saint, D. A., Thomas, T. and Gage, P. W. (1990). GABAB agonists modulate a transient potassium current in cultured mammalian hippocampal neurons. *Neurosci Lett* **118**, 9-13.

Santos, M. S., Moreno, A. J. and Carvalho, A. P. (1996). Relationships between ATP depletion, membrane potential, and the release of neurotransmitters in rat nerve terminals. An in vitro study under conditions that mimic anoxia, hypoglycemia, and ischemia. *Stroke* **27**, 941-950.

Saotome, M., Katoh, H., Satoh, H., Nagasaka, S., Yoshihara, S., Terada, H. and Hayashi, H. (2005). Mitochondrial membrane potential modulates regulation of mitochondrial Ca2+ in rat ventricular myocytes. *Am J Physiol Heart Circ Physiol* **288**, H1820-1828.

Sasaki, N., Sato, T., Ohler, A., O'rourke, B. and Marban, E. (2000). Activation of mitochondrial ATP-dependent potassium channels by nitric oxide. *Circulation* **101**, 439-445.

Sato, T., Saito, T., Saegusa, N. and Nakaya, H. (2005). Mitochondrial Ca2+-activated K+ channels in cardiac myocytes: a mechanism of the cardioprotective effect and modulation by protein kinase A. *Circulation* **111**, 198-203.

Sattler, R. and Tymianski, M. (2000). Molecular mechanisms of calcium-dependent excitotoxicity. *J Mol Med* **78**, 3-13.

Schafer, G., Wegener, C., Portenhauser, R. and Bojanovski, D. (1969). Diazoxide, an inhibitor of succinate oxidation. *Biochem Pharmacol* **18**, 2678-2681.

Schmidt-Nielson, K. (1984). Scaling: Why is animal size so important?: Cambridge University Press.

Schurr, A., Reid, K. H., Tseng, M. T., West, C. and Rigor, B. M. (1986). Adaptation of adult brain tissue to anoxia and hypoxia in vitro. *Brain Res* **374**, 244-248.

Schwartz-Bloom, R. D., Mcdonough, K. J., Chase, P. J., Chadwick, L. E., Inglefield, J. R. and Levin, E. D. (1998). Long-term neuroprotection by benzodiazepine full versus partial agonists after transient cerebral ischemia in the gerbil [corrected]. *J Cereb Blood Flow Metab* **18**, 548-558.

Schwartz-Bloom, R. D., Miller, K. A., Evenson, D. A., Crain, B. J. and Nadler, J. V. (2000). Benzodiazepines protect hippocampal neurons from degeneration after transient cerebral ischemia: an ultrastructural study. *Neuroscience* **98**, 471-484.

Scorziello, A., Pellegrini, C., Secondo, A., Sirabella, R., Formisano, L., Sibaud, L., Amoroso, S., Canzoniero, L. M., Annunziato, L. and Di Renzo, G. F. (2004). Neuronal NOS activation during oxygen and glucose deprivation triggers cerebellar granule cell death in the later reoxygenation phase. *J Neurosci Res* **76**, 812-821.

Semenov, D. G., Samoilov, M.O., Zielonka, P., Lazarewiscz. (2000). Responses to reversible anoxia of intracellular free and bound Ca2+ in rat cortical slices. *Resuscitation* **44**, 207-214.

Serrano, J., Fernandez, A. P., Martinez-Murillo, R., Alonso, D., Rodrigo, J., Salas, E., Mourelle, M. and Martinez, A. (2007). The nitric oxide donor LA 419 decreases ischemic brain damage. *Int J Mol Med* **19**, 229-236.

Sheardown, M. J., Nielsen, E. O., Hansen, A. J., Jacobsen, P. and Honore, T. (1990). 2,3-Dihydroxy-6-nitro-7-sulfamoyl-benzo(F)quinoxaline: a neuroprotectant for cerebral ischemia. *Science* **247**, 571-574.

Sheardown, M. J., Suzdak, P. D. and Nordholm, L. (1993). AMPA, but not NMDA, receptor antagonism is neuroprotective in gerbil global ischaemia, even when delayed 24 h. *Eur J Pharmacol* **236**, 347-353.

Shimizu, K., Lacza, Z., Rajapakse, N., Horiguchi, T., Snipes, J. and Busija, D. W. (2002). MitoK(ATP) opener, diazoxide, reduces neuronal damage after middle cerebral artery occlusion in the rat. *Am J Physiol Heart Circ Physiol* **283**, H1005-1011.

Shin, D. S. and Buck, L. T. (2003). Effect of anoxia and pharmacological anoxia on whole-cell NMDA receptor currents in cortical neurons from the western painted turtle. *Physiol Biochem Zool* **76**, 41-51.

Shin, D. S., Wilkie, M. P., Pamenter, M. E. and Buck, L. T. (2005). Calcium and protein phosphatase 1/2A attenuate N-methyl-D-aspartate receptor activity in the anoxic turtle cortex. *Comp Biochem Physiol A Mol Integr Physiol* **142**, 50-57.

Sick, T. J., Rosenthal, M. and Lutz, P. L. (1984). Mechanisms of brain survival in anoxia: mitochondrial activity and ion homeostasis in turtle and rat. *Adv Exp Med Biol* **180**, 221-231.

Siemen, D., Loupatatzis, C., Borecky, J., Gulbins, E. and Lang, F. (1999). Ca2+-Activated K Channel of the BK-type in the inner mitochondrial membrane of a human glioma cell line. *Biochem Biophys Res Commun* **257**, 549-554.

Siesjo, B. K. (1988). Mechanisms of ischemic brain damage. *Crit Care Med* **16**, 954-963.

Siesjo, B. K. (1989). Calcium and cell death. *Magnesium* **8**, 223-237.

Siesjo, B. K., Memezawa, H. and Smith, M. L. (1991). Neurocytotoxicity: pharmacological implications. *Fundam Clin Pharmacol* **5**, 755-767.

Sommer, C., Fahrner, A. and Kiessling, M. (2002). [3H]muscimol binding to gamma-aminobutyric acid(A) receptors is upregulated in CA1 neurons of the gerbil hippocampus in the ischemia-tolerant state. *Stroke* **33**, 1698-1705.

Sommer, C., Fahrner, A. and Kiessling, M. (2003). Postischemic neuroprotection in the ischemia-tolerant state gerbil hippocampus is associated with increased ligand binding to inhibitory GABA(A) receptors. *Acta Neuropathol* **105**, 197-202.

Sparagna, G. C., Gunter, K. K., Sheu, S. S. and Gunter, T. E. (1995). Mitochondrial calcium uptake from physiological-type pulses of calcium. A description of the rapid uptake mode. *J Biol Chem* **270**, 27510-27515.

St-Pierre, J., Buckingham, J. A., Roebuck, S. J. and Brand, M. D. (2002). Topology of Superoxide Production from different sites in the mitochondrial electron transport chain. *J. Biol. Chem.* **277**, 44784-44790.

Stecyk, J. A. and Farrell, A. P. (2006). Regulation of the cardiorespiratory system of common carp (Cyprinus carpio) during severe hypoxia at three seasonal acclimation temperatures. *Physiol Biochem Zool* **79**, 614-627.

Stenslokken, K. O., Sundin, L., Renshaw, G. M. and Nilsson, G. E. (2004). Adenosinergic and cholinergic control mechanisms during hypoxia in the epaulette shark (Hemiscyllium ocellatum), with emphasis on branchial circulation. *J Exp Biol* **207**, 4451-4461.

Sternau, L. L., Lust, W. D., Ricci, A. J. and Ratcheson, R. (1989). Role for gamma-aminobutyric acid in selective vulnerability in gerbils. *Stroke* **20**, 281-287.

Takano, K., Ogura, M., Nakamura, Y. and Yoneda, Y. (2005). Neuronal and glial responses to polyamines in the ischemic brain. *Curr Neurovasc Res* **2**, 213-223.

Takashi, E., Wang, Y. and Ashraf, M. (1999). Activation of mitochondrial K(ATP) channel elicits late preconditioning against myocardial infarction via protein kinase C signaling pathway. *Circ Res* **85**, 1146-1153.

Thompson, J. W., Prentice, H. M. and Lutz, P. L. (2007). Regulation of extracellular glutamate levels in the long-term anoxic turtle striatum: coordinated activity of glutamate transporters, adenosine, K (ATP) (+) channels and GABA. *J Biomed Sci* **14**, 809-817.

Travagli, R. A., Ulivi, M. and Wojcik, W. J. (1991). gamma-Aminobutyric acid-B receptors inhibit glutamate release from cerebellar granule cells: consequences of inhibiting cyclic AMP formation and calcium influx. *J Pharmacol Exp Ther* **258**, 903-909.

Turner, A. J. and Whittle, S. R. (1983). Biochemical dissection of the gamma-aminobutyrate synapse. *Biochem J* **209**, 29-41.

Ultsch, G. R. (2006). The ecology of overwintering among turtles: where turtles overwinter and its consequences. *Biol Rev Camb Philos Soc* **81**, 339-367.

Ultsch, G. R., Carwile, M. E., Crocker, C. E. and Jackson, D. C. (1999). The physiology of hibernation among painted turtles: the Eastern painted turtle Chrysemys picta picta. *Physiol Biochem Zool* **72**, 493-501.

Ultsch, G. R. and Jackson, D. C. (1982). Long-term submergence at 3C of the turtle *chrysemys picta bellii* in normoxic and severely hypoxic water
I. Survival, gas exchange and acid-base status. *J Exp Biol* **96**, 11-28.

Van Den Tweel, E. R., Van Bel, F., Kavelaars, A., Peeters-Scholte, C. M., Haumann, J., Nijboer, C. H., Heijnen, C. J. and Groenendaal, F. (2005). Long-term neuroprotection with 2-iminobiotin, an inhibitor of neuronal and inducible nitric oxide synthase, after cerebral hypoxia-ischemia in neonatal rats. *J Cereb Blood Flow Metab* **25**, 67-74.

Van Mil, A. H., Spilt, A., Van Buchem, M. A., Bollen, E. L., Teppema, L., Westendorp, R. G. and Blauw, G. J. (2002). Nitric oxide mediates hypoxia-induced cerebral vasodilation in humans. *J Appl Physiol* **92**, 962-966.

Vanden Hoek, T. L., Becker, L. B., Shao, Z., Li, C. and Schumacker, P. T. (1998). Reactive oxygen species released from mitochondria during brief hypoxia induce preconditioning in cardiomyocytes. *J Biol Chem* **273**, 18092-18098.

Vincent, A. M., Backus, C., Taubman, A. A. and Feldman, E. L. (2005). Identification of candidate drugs for the treatment of ALS. *Amyotroph Lateral Scler Other Motor Neuron Disord* **6**, 29-36.

Wada, Y., Yamashita, T., Imai, K., Miura, R., Takao, K., Nishi, M., Takeshima, H., Asano, T., Morishita, R., Nishizawa, K. et al. (2000). A region of the sulfonylurea receptor critical for a modulation of ATP-sensitive K(+) channels by G-protein betagamma-subunits. *Embo J* **19**, 4915-4925.

Wang, L., Cherednichenko, G., Hernandez, L., Halow, J., Camacho, S. A., Figueredo, V. and Schaefer, S. (2001). Preconditioning limits mitochondrial Ca(2+) during ischemia in rat hearts: role of K(ATP) channels. *Am J Physiol Heart Circ Physiol* **280**, H2321-2328.

Wang, L., Cherednichenko, G., Hernandez, L., Halow, J., Camacho, S.A., Figueredo, V., Schaefer, S. (2001). Preconditioning limits mitochondrial Ca2+ during ischemia in rat hearts: role of KATP channels. *Am J Physiol Heart Circ Physiol* **280**, H2321-H2328.

Wang, X. M. and Mokha, S. S. (1996). Opioids modulate N-methyl-D-aspartic acid (NMDA)-evoked responses of trigeminothalamic neurons. *J Neurophysiol* **76**, 2093-2096.

Wang, Z. W., Nara, M., Wang, Y. X. and Kotlikoff, M. I. (1997). Redox regulation of large conductance Ca(2+)-activated K+ channels in smooth muscle cells. *J Gen Physiol* **110**, 35-44.

Waypa, G. B., Chandel, N. S. and Schumacker, P. T. (2001). Model for hypoxic pulmonary vasoconstriction involving mitochondrial oxygen sensing. *Circ Res* **88**, 1259-1266.

Wilkie, M. P., Pamenter, M. E., Alkabie, S., Carapic, D., Shin, D. S. and Buck, L. T. (2008). Evidence of anoxia-induced channel arrest in the brain of the goldfish (Carassius auratus). *Comp Biochem Physiol C Toxicol Pharmacol*.

Wink, D. A., Hanbauer, I., Laval, F., Cook, J. A., Krishna, M. C. and Mitchell, J. B. (1994). Nitric oxide protects against the cytotoxic effects of reactive oxygen species. *Ann N Y Acad Sci* **738**, 265-278.

Wise, G., Mulvey, J. M. and Renshaw, G. M. C. (1998). Hypoxia tolerance in the epaulette shark (Hemiscyllium ocellatum). *J Exp Zool* **281**, 1-5.

Xia, Y. and Haddad, G. G. (2001). Major difference in the expression of delta- and mu-opioid receptors between turtle and rat brain. *J Comp Neurol* **436**, 202-210.

Xie, Y., Zacharias, E., Hoff, P. and Tegtmeier, F. (1995). Ion channel involvement in anoxic depolarization induced by cardiac arrest in rat brain. *J Cereb Blood Flow Metab* **15**, 587-594.

Xu, M., Wang, Y., Ayub, A. and Ashraf, M. (2001). Mitochondrial K(ATP) channel activation reduces anoxic injury by restoring mitochondrial membrane potential. *Am J Physiol Heart Circ Physiol* **281**, H1295-1303.

Xu, W., Liu, Y., Wang, S., Mcdonald, T., Van Eyk, J., Sidor, A. and O'rourke, B. (2002). Cytoprotective Role of Ca2+-activated K+ channels in the cardiac inner mitochondrial membrane. *Science* **298**, 1029-1033.

Yao, H., Sun, X., Gu, X., Wang, J. and Haddad, G. G. (2007). Cell death in an ischemic infarct rim model. *J Neurochem* **103**, 1644-1653.

Ye, J. H. and Mcardle, J. J. (1996). 2,3-Butanedione monoxime modifies the glycine-gated chloride current of acutely isolated murine hypothalamic neurons. *Brain Res* **735**, 20-29.

Yoshida, M., Nakakimura, K., Cui, Y. J., Matsumoto, M. and Sakabe, T. (2004). Adenosine A(1) receptor antagonist and mitochondrial ATP-sensitive potassium channel blocker attenuate the tolerance to focal cerebral ischemia in rats. *J Cereb Blood Flow Metab* **24**, 771-779.

Zhang, D. X., Chen, Y. F., Campbell, W. B., Zou, A. P., Gross, G. J. and Li, P. L. (2001). Characteristics and superoxide-induced activation of reconstituted myocardial mitochondrial ATP-sensitive potassium channels. *Circ Res* **89**, 1177-1183.

Zhang, J., Gibney, G. T., Zhao, P. and Xia, Y. (2002). Neuroprotective role of delta-opioid receptors in cortical neurons. *Am J Physiol Cell Physiol* **282**, C1225-1234.

Zhang, J., Haddad, G. G. and Xia, Y. (2000). delta-, but not mu- and kappa-, opioid receptor activation protects neocortical neurons from glutamate-induced excitotoxic injury. *Brain Res* **885**, 143-153.

Zhang, J., Price, J. O., Graham, D. G. and Montine, T. J. (1998). Secondary excitotoxicity contributes to dopamine-induced apoptosis of dopaminergic neuronal cultures. *Biochem Biophys Res Commun* **248**, 812-816.

Zhang, S. Z., Gao, Q., Cao, C. M., Bruce, I. C. and Xia, Q. (2006). Involvement of the mitochondrial calcium uniporter in cardioprotection by ischemic preconditioning. *Life Sci* **78**, 738-745.

Zubrow, A. B., Delivoria-Papadopoulos, M., Ashraf, Q. M., Ballesteros, J. R., Fritz, K. I. and Mishra, O. P. (2002). Nitric oxide-mediated expression of Bax protein and DNA fragmentation during hypoxia in neuronal nuclei from newborn piglets. *Brain Res* **954**, 60-67.